# Intense NIR Absorbing Porphyrin based Dyes with BODIPY as Acceptor: Potential Photosensitizers for Dye Sensitized Solar Cells

# A Thesis Submitted for the Degree of DOCTOR OF PHILOSOPHY



By Jyotsna Bania

School of Chemistry University of Hyderabad Hyderabad-500 046 INDIA

September 2023

# Dedicated to Maa, Baba, Swapna and Nanda

#### **TABLE OF CONTENTS**

Declarat	ion		I
Certifica	te		III
Preface	,		V
	Acknowledgement List of abbreviations		VII IX
Lisi oj ai	oreviai	tions	IA
Chapter	1 Intro	duction	1-27
1.1	Porph	yrins-Background and Nomenclature	2
1.2	Synth	esis of porphyrins	4
	1.2.1	From pyrrole tetramerization	4
	1.2.2	From Dipyrrolic intermediate: The [2+2] Route	5
		1.2.2.1 Using Dipyrromethenes	6
		1.2.2.2 Using Dipyrromethanes	6
	1.2.3	From tripyrromethane intermediates: The [3+1] Route	7
	1.2.4	From open-chain tetrapyrrolic intermediates	7
1.3	Struct	ture and properties	8
1.4	Appli	cation of Porphyrin	11
	1.4.1	Photodynamic Therapy (PDT)	11
	1.4.2	Nonlinear optics (NLO)	13
	1.4.3	Sensors	15
	1.4.4	Artificial photosynthetic systems	17
	1.4.5	Solar cells	19
1.5	Scope	e of the present work	21
1.6	Refer	rences	22
Chapter	2 Mate	rials and Methods	28-44
2.1	Gener	ral Experimental	29
	2.1.1	Solvents	29
		2.1.1.1 Solvent for reactions	29
		2.1.1.2 NMR solvents	29
		2.1.1.3 Solvents for optical measurement	29
	2.1.2	Reagents	29
2.2	Chron	natography	30

2.3	Characterization and instrumentation	30
2.4	Computational Details	31
2.5	Preparation of starting materials	31
	2.5.1 Synthesis of porphyrin precursor	31
	2.5.2 Synthesis of Donors	34
	2.5.3 Synthesis of BODIPY precursor	39
2.6	Summary	41
2.7	References	42
2.8	<sup>1</sup> H NMR, <sup>13</sup> C NMR, and HRMS spectra	43
Chapter Conjugo	r 3 Diarylamine Donor Appended Porphyrin-BO ates	DIPY 45-97
3.1	Introduction	46
3.2	Research goal	50
3.3	Results and discussion	51
	3.3.1 Synthesis	51
	3.3.2 UV-Vis-NIR and fluorescence studies	52
	3.3.3 DFT studies	58
	3.3.4 Electrochemical studies	62
3.4	Conclusion	63
3.5	Experimental details	64
3.6	References	69
3.7	<sup>1</sup> H NMR, <sup>13</sup> C NMR, IR and HRMS spectra	74
3.8	Computational Studies	88
-	r 4 Carbazole and Phenothiazine Donor based Po Y Conjugates	orphyrin- 98-134
4.1	Introduction	99
4.2	Research goal	102
4.3	Results and discussion	103
	4.3.1 Synthesis	103
	4.3.2 UV-Vis-NIR and fluorescence studies	104

	4.3.3	DFT studies	108
	4.3.4	Electrochemical studies	112
4.4	Conclu	sion	113
4.5	Experi	114	
4.6	Referen	117	
4.7	<sup>1</sup> H NM	119	
4.8	Comp	utational Studies	126
Chapter	5 Conc	lusion	135-141
5.1	Summa	ary	136
	5.1.1	Introduction	136
	5.1.2	Synthetic and characterization	136
	5.1.3	Photophysical properties	137
	5.1.4	Electrochemical studies	139
	5.1.5	DFT calculations	139
5.2	Referen	nces	141
Pub	lications	s and Presentations	142

#### DECLARATION

I hereby declare that the matter embodied in the thesis entitled "Intense NIR Absorbing Porphyrin based Dyes with BODIPY as Acceptor: Potential Photosensitizers for Dye Sensitized Solar Cells" is the result of investigations carried out by me in the School of Chemistry, University of Hyderabad, Hyderabad, India under the supervision of Prof. Pradeepta K. Panda and it has not been submitted elsewhere for the award of any degree or diploma or membership, etc. This work is also free from plagiarism. I hereby agree that my thesis can be deposited in Shodhganga/INFLIBNET.

In keeping with the general practice of reporting scientific investigations, due acknowledgements have been made wherever the work described is based on the findings of other investigators. Any omission or error that might have occurred by oversight or error is sincerely regretted.

September 2023

Jyotsna Bania

Prof. Pradeepta K. Panda School of Chemistry University of Hyderabad Central University P. O. Hyderabad 500 046



Phones: +91-40-23134818(O)
Fax : +91-40-23012460
E-Mail : pkpsc@uohyd.ernet.in
pradeepta.panda@uohyd.ac.in

#### CERTIFICATE

This is to certify that the work described in this thesis entitled "Intense NIR Absorbing Porphyrin based Dyes with BODIPY as Acceptor: Potential Photosensitizers for Dye Sensitized Solar Cells" has been carried out by Ms. Jyotsna Bania, holding the Reg. No. 16CHPH13 under my supervision, for partial fulfilment for the award of Doctor of Philosophy in Chemistry and the same has not been submitted elsewhere for any degree, which is a plagiarism free thesis.

#### Part of thesis have been:

#### Published in following journals

- Bania, J.; Sahoo, S. S.; Kishore, M. V. N.; Panda, P. K. Porphyrin-BODIPY Conjugates as Photosensitizers with Absorption up to Near Infrared Region for Dye-Sensitized Solar Cells (DSSC). Indian Patent Application No.: 202341027215; April 12, 2023.
- Bania, J.; Sahoo, S. S.; Kishore, M. V. N.; Panda, P. K. Intense NIR Absorbing Porphyrin based Dyes with BODIPY as Acceptor. New J. Chem. 2023, 47, 16327-16331. https://doi.org/10.1039/D3NJ02995F

#### Presented in the following conferences

- Poster presentation on "A Panchromatic Porphyrin-BODIPY Conjugate for DSSC", CHEMFEST-2020, School of Chemistry, University of Hyderabad, Hyderabad, 27-28<sup>th</sup> February, 2020.
- Oral presentation on "A Novel Porphyrin-BODIPY Conjugate with Panchromatic Absorption for DSSC" in Virtual Conference Recent Advances in Bis and Tetra-Pyrrolic Molecular Materials, Department of Chemistry, Central University of Kerala, Kerala, 24-26<sup>th</sup> August, 2020.
- 3. Oral presentation on "Novel Porphyrin-Bodipy Conjugate with Panchromatic Absorption for Dye Sensitized Solar Cell Application", National Seminar on

- 4. Recent Advances in Materials Chemistry (RAMC-2021), P. G. Department of Chemistry & Centre of Excellence in Advanced Materials and Applications, Utkal University, Bhubaneswar, 8-9th March, 2021.
- 5. Oral presentation on "A Panchromatic Porphyrin-BODIPY Conjugate for DSC Application", CHEMFEST-2021, School of Chemistry, University of Hyderabad, Hyderabad, 19-20th March, 2021.
- 6. Poster presentation on "Novel Panchromatic Porphyrin BODIPY Conjugates for Application in Dye Sensitized Solar Cells", ACS CRSI poster session (online), 27th CRSI National Symposium Chemistry, Kolkata, 26-29th September, 2021.

Further the student has passed the following courses towards fulfilment of course work requirement for the Ph.D. degree.

Name of the course		Credits			
P	ass/I	fail			
65	1)	CY-801 Research Proposal	3		Pass
	2)	CY-802 Chemistry Pedagogy	3		Pass
	3)	CY-805 Instrumental Methods-A	3		Pass
	4)	CY-806 Instrumental Methods-B	3		Pass

Dean

School of Chemistry

Dean SCHOOL OF CHEMISTRY University of Hyderabad

Hyderabad-500 046.

adeepta K. I

(Thesis Supervisor)

Prof. Pradeepta K. Panda School of Chemistry University of Hyderabad Hyderabad - 500 046.

#### **PREFACE**

The present thesis entitled "Intense NIR Absorbing Porphyrin based Dyes with BODIPY as Acceptor: Potential Photosensitizers for Dye Sensitized Solar Cells" is divided into five chapters. Basically, it describes the synthesis, photophysical properties, DFT and electrochemical studies of the porphyrin-BODIPY conjugates. Although different kinds of porphyrin based sensitizers have been developed with benchmark efficiency of 13% such as SM315, these porphyrins lack absorption in the NIR region where there is a significant flux of solar photons. For harvesting maximum solar flux from sunlight we have designed and synthesized four novel porphyrin-BODIPY conjugates with the introduction of diarylamine, carbazole and phenothiazine moieties as donors on to the porphyrin core and employing the napthobipyrrole based BODIPY as the acceptor for the first time for their application in dye sensitized solar cells. The brief content included in the thesis is presented below.

In **chapter 1**, a brief description about various synthetic routes, structural features, photophysical properties along with application of porphyrins has been reported. **Chapter 2** provides the information about the materials and methods used in the course of the investigation. In **chapter 3**, we have demonstrated a novel strategy for harvesting NIR flux of photons by synthesizing two new diarylamine donor based porphyrin-BODIPY conjugates which displays a panchromatic absorption from 300 to 800 nm with an intense lowest energy band which is significantly red-shifted when compared to previously reported dye **YD2-o-C8**. DFT calculations revealed a well separated electron density in frontier orbitals which may facilitate the charge injection. These dyes display a workable dye regeneration and electron injection along with good photostability making them potential photosensitizers for DSSC application. In **chapter 4**, we have successfully incorporated carbazole and phenothiazine as donors by replacing the diarylamine in the previously reported porphyrin-BODIPY conjugates. As expected, these dyes also show a significantly red-shifted absorption along with fulfilling the other requirements required for a dye to be used in DSSC application. Finally, the **chapter 5** summarizes the findings of the present investigation.

September 2023

Jyotsna Bania

#### Acknowledgement

I would like to acknowledge all the people who has helped me directly or indirectly to carry out my Ph.D. work in University of Hyderabad.

At first, I would like to express my sincere and special gratitude to my supervisor **Prof. Pradeepta K. Panda** for his kind guidance, and encouragement. Especially his patience and way of logical thinking and analysis helped me in all the time of research work. Even during my health issues, he encouraged me and never allowed me to give up and supported me to continue my work.

I would like to thank the former and present Deans, School of Chemistry, for their constant support and for allowing me to use the available facilities. I am extremely thankful individually to all the faculty members including doctoral committee members Prof. R. Chandrasekar and Prof. Tushar Jana of the School for their kind help and suggestions whenever I needed.

University of Hyderabad, SERB and DST-CERI India is gratefully acknowledged for providing me the fellowship.

I would also like to express my heartiest gratitude to the person, Dr. M. V. Nanda Kishore who has always been with me not only as a senior but also as a life partner throughout this journey and has helped and motivated me through thick and thin. Without his support I wouldn't have overcome all the difficulties that surpassed me.

Also to my labmate Dr. Sipra Sucharita Sahoo, I am extremely grateful for her contribution in synthesis of BODIPY and in computational studies. I am thankful to Dr. Majji Shankar for his help towards accomplishment of the C–N coupling reaction.

I am deeply thankful to technicians, without them, this thesis would have not been possible, Mr, Durgesh Kumar Singh, Mr. G. Mahender and Mrs. Vijaylakshmi for their help in the NMR facility. Mrs. Asia Pervez and specially Dr. Manasi Dalai who always supported me as an elder sister are deeply acknowledged for their help in availing HRMS facilities.

A special thanks goes to all my seniors where I have been lucky enough to work with help of their intelligence and strategies to thrive in lab like family members- Dr. Narendra Nath Pati, Dr. B. Sathish Kumar, Dr. P. Obaiah, Dr. Vikranth, Dr. Kurumurthy, Dr. Chandrashekhar, Dr.

Yadagiri and Dr. Sudhakar. They have never failed to enlighten me with their insightful mind and brilliance. I am greatly thankful to Dr. J. Nagamaiah and Dr. Rahul Soman in making the lab environment friendly and being always helpful senior. Dr. Sameeta, Dr. Sipra and Dr. Ishfaq for always being cordial and extending a helping hand whenever needed. Shanmugapriya, Srinath, Jiji, Vijay, Arnab, Chitrak, Jeladhara, Shalini, Deepak, Narmada, Mahendra, Raghuvaran, Soumoshree, Alka, Fasna, Laila, Swati, Kalyani, Pankaj, Swetha, Sadiya, Shuvankar, Haseeba, Hizana, Dr. Subhalaxmi Panda and Aishwarya, all their contributions in their own way are highly appreciated.

I would like to thank all my super seniors, Dr. Sanjeev, Dr. Tridib, Dr. Ritwik, Dr. Brijesh, Dr. Anup for providing guidance whenever I have needed their advice and expertise.

My pleasant association with some friends in my B.Sc., M.Sc. and Ph.D. tenure inside and outside UOH such as Kiran, Shikha, Manas, Geeta, Karishma, Juriti, Soumya, Mamina, Suman, Narasimha, Gorachand, Shanti, Laxman, Sarada, Kalyani, Pritam, Prachi, Mou, Syed Basha, Reena, Arun, Anju, Jishu, Daradi, Manash, Junu, Dr. M. Ashwin and Mrs. M. Hema is unforgettable.

I would like to thank all teachers in different educational levels, Mrs. Pushpa Sharma, Mrs. Dipika Sandhu, Mr. Ashok Sharma, Mrs. Asha Pathania, Dr. Jagmohan Singh Bains, Mr. Diganta Das, Dr. Pankaj Hazarika, Dr. Pranil Bora, Dr. Palashmoni Saikia, Mrs. Tumpa Paul, Dr. J. Ganguli and Mr. Diganta Das.

Last but not the least I would like to take this opportunity to express my heartfelt gratitude to my father (Mr. Nirmal Chandra Bania) and mother (Mrs. Nizora Bania) who has always supported my dreams with all their blessings and always believing on me. Also separate thanks to my sister, Ms. Swapna Bania for her constant support and upliftment. I am greatly thankful to my in-laws for their support Bava garu (Mr. Sesha Phani Sarma), akka (Mrs. M. Vasudha Bhargavi), Mr. M. V. Kowsik, Mr. M. V. Muni Sankar, Mrs. M. Neelima, Neelesh, Chinmai and Ananya. Apart from the above mentioned people there are many other people whom I would like to express my thankfulness, all my uncles, aunties, brothers and sisters.

September 2023

Jyotsna Bania

University of Hyderabad

#### **LIST OF ABBREVIATIONS**

abs	absorbance
aq.	aqueous
atm	atmosphere
Å	Angstrom
a.u.	arbitrary unit
BF <sub>3</sub> .OEt <sub>2</sub>	Boron trifluoride diethyl etherate
BLA	bond length alternation
bp	boiling point
B <sub>2</sub> Pin <sub>2</sub>	Bis(pinacolato)diboron
t-Bu	tertiary-butyl
СВ	Conduction band
CMSD	Centre for Modelling, Simulation & Design
cm	Centimeter (s)
conc.	Concentrated
CuI	Copper(I)iodode
CV	Cyclic voltammetry
d	Doublet
dd	Double doublet
δ	chemical shift in parts per million
0	Degree
°C	Degree Celsius
DCE	1,2-dichloroethane
DCM	Dichloromethane
DDQ	2,3-Dichloro-5,6-dicyano-1,4-benzoquinone
DFT	Density Functional Theory
DMF	Dimethylformamide
DMSO	Dimethyl sulphoxide
DPV	Differential pulse voltammetry
DPPF	1,1'-Bis(diphenylphosphino)ferrocene
DPEPhos	Bis[(2-diphenylphosphino)phenyl]ether

DSSCs	Dye sensitized solar cells
dtbpy	4,4'-Di- <i>tert</i> -butyl-2,2'-dipyridyl
Е	Energy
ε	Epsilon (molar extinction coefficient)
e.g.	For example
eq.	Equivalent
eV	Electron volt
ESI	Electrospray Ionization
et al.	and others
etc	et cetera (and other similar things)
EtOH	Ethanol
fl	fluorescence
FT	Fourier transform
FTO	Fluorine doped tin oxide
g	gram
h	Hour (s)
H-bond	hydrogen bond
HCl	Hydrochloric acid
HOMA	Harmonic oscillator model of aromaticity
НОМО	Highest occupied molecular orbital
HRMS	High resolution-mass spectrometry
Hz	Hertz
i.e.	that is
IPCE	Incident photon to current efficiency
IR	Infrared
J	coupling constant (in NMR spectrum)
K <sub>2</sub> CO <sub>3</sub>	Potassium carbonate
КОН	Potassium hydroxide
L	Liter
lit.	Literature
log	Logarithm

LUMO	Lowest unoccupied molecular orbital
μ	micro
M	moles per litre
m	meta (structure); multiplet (NMR); milli (unit)
mA	milli Ampere
МеОН	Methanol
mg	milligram
MgSO <sub>4</sub>	Magnesium sulfate
MHz	megahertz
min	Minute (s)
mL	milliLitre
mp	melting point
MS	mass spectrometry
m/z	mass to charge ratio (in mass spectrometry)
NaOAc	Sodium acetate
NaCl	Sodium chloride
Na <sub>2</sub> CO <sub>3</sub>	Sodium carbonate
NaH	Sodium hydride
Na <sub>2</sub> SO <sub>4</sub>	Sodium sulfate
NBS	N-bromosuccinimide
NH <sub>4</sub> Cl	Ammonium chloride
NICS	Nucleus independent chemical shift
NIR	Near IR
NLO	Nonlinear optical
nm	nano meter (s)
NMR	Nuclear magnetic resonance
ns	nano second (s)
0	ortho
p	para
<i>i</i> -Pr	isopropyl
ppm	parts per million

p-TSA	<i>p</i> -Toluenesulfonic acid
q	quartet
rt	room temperature
S	singlet
sat.	saturated
t	triplet
TBAF	Tetra-n-butylammonium fluoride
TD-DFT	Time dependent density functional theory
TEA	triethylamine
TFA	Trifluoroacetic acid
THF	Tetrahydrofuran
TIPS	Triisopropylsilane
TLC	Thin layer chromatography
TMEDA	Tetramethyl ethylenediamine
TPP	Tetraphenylporphyrin
UV-vis-NIR	Ultraviolet-visible-near infrared
via	going through
viz.	namely
VOC	Volatile organic compounds
vs	versus (against)
w.r.t.	with respect to
Zn	Zinc

## **CHAPTER 1**

## Introduction

#### 1.1 Porphyrins - Background and Nomenclature

The name "porphyrin" was taken from Greek word "porphyros (πορφύρα)" meaning purple. Evolution of photosynthetic bacteria long time ago changed the earth's reduced atmosphere to oxidisable condition through "the great oxygenation event" and paved the way for the sustenance of eukaryotic organisms and higher life forms containing porphyrin-based pigments. The history of porphyrin generally emanates from chemical-medical aspects in the early 1840s. Berzelius (1840) and other groups have isolated iron free hematin - red colored water solution, thus proving that iron is not responsible for the red coloration of blood. Later, in 1879, Hoppe-Seyler proposed the name "porphyrin" with prefix "haemato" and "phyllo" while studying phylloporphyrin, a chlorophyll derived red fluorescence pigment. In 1883, a sharp and intense transition around near UV-region was attributed to hemoglobin by Soret and subsequently named it Soret band. Porphyrin structure was first presented by Küster in 1912, though it was not believed at that time. First synthesis of general porphyrin was performed by Milroy. Later the synthesis of chlorohemin by Fischer explained the porphyrin structure, proving the Küster theory, and got honoring him with Nobel Prize in 1930, leading towards the new age of synthetic porphyrin chemistry.

Most of the proteins which constitute porphyrin or its derivatives play a pivotal role in biological processes, such as chlorophyll containing a reduced Mg(II)-porphyrin responsible for the conversion of light energy into chemical energy, producing life surviving oxygen. The oxygen thus produced during the photosynthesis is widely utilized in various forms by heme containing proteins viz. hemoglobin, myoglobin, hemerythrin etc. Additionally, catalase, peroxidase and the other heme containing proteins also have significant role in catalytic oxidation processes. Vitamin B<sub>12</sub> (Figure 1.1) is responsible for the formation of blood, functioning of brain and nervous system. Hence this naturally occurring tetrapyrrolic macrocycles for their ubiquitous nature supported by their attractive colours, has led Battersby to call this tetrapyrrolic macrocycles as the "pigments of life". 6 Photophysical, optical, chemical and biological properties of porphyrins involve wide variety of fields such as optoelectronics, material chemistry, catalysis, as photosensitizers in photodynamic therapy etc. This vital role in different fields led to a new research area in developing more synthetic systems such as contracted, isomeric, expanded, inverted, confused and core modified porphyrins that bear similar resemblance to naturally occurring macrocycles but being chemically quite different.<sup>7</sup>

**Figure 1.1** Structures of some biologically important porphyrins

In general, 2,5-positions of a five membered heterocyclic ring (e.g., pyrrole **1.1** in Figure 1.2) are named as α-positions and 3,4-positions are named as β-positions, whereas "*meso*" has been used for the bridging carbon atoms. Four pyrrole subunits and four methine bridges connect to α-carbon atoms in a coplanar fashion to give porphyrin skeleton a square planar geometry (Figure 1.2).<sup>7</sup> Due to complexity in applying IUPAC nomenclature, creators have coined trivial names based on their color or structural features. The suffix "phyrin" or "rin" has been used generally at the end which was started initially by R. B. Woodward by naming an expanded porphyrin with five heterocyclic rings as "Sapphyrin" due to its blue color in the solid state.<sup>8</sup> Different groups led by Sessler also followed this trend by naming porphyrins in a similar fashion such as rubyrin, amethyrin, orangarin, platyrin etc.<sup>9</sup>

In this modern era Franck's approach is generally applied for the nomenclature of porphyrinoids. <sup>10</sup> It has been divided into three parts. The first part, consists of a square-bracketed prefix shows the number of  $\pi$  electrons in conjugation pathway followed by second part, a core name indicating the number of heterocyclic subunits and the third part, a round-bracketed suffix which indicates the number of meso carbon bridge between the heterocyclic subunits beginning from the largest unit. According to this approach, porphyrin **1.2** should be named as [18]porphyrin-(1.1.1.1) with an  $18\pi$ -electronic system where four pyrroles are bridged through single meso carbon atoms.

Figure 1.2 Nomenclature of few macrocycles by Franck's approach.

Similarly, corrole **1.3** named as [18]porphyrin-(1.1.1.0), porphycene **1.4** as [18]porphyrin-(2.0.2.0), pentapyrrolic macrocycle, sapphyrin **1.5** as [22]pentaphyrin-(1.1.1.1.0) and hexaphyrin **1.8** as [26]hexaphyrin-(1.1.1.1.1).

#### 1.2 Synthesis of Porphyrins

Porphyrins can be synthesized in four different ways.

#### 1.2.1 From pyrrole tetramerization

The most famous route of pyrrole polymerization to porphyrin involves the synthesis of tetraarylporphyrins such as 5,10,15,20-tetraphenylporphyrin **1.9** (Scheme 1) from pyrrole and benzaldehyde. This reaction was first developed by Rothemund,<sup>11</sup> modified by Alder, Longo and colleagues<sup>12</sup> and later optimized by Lindsey's group.<sup>13</sup>

Scheme 1. Synthesis of tetraphenyl porphyrin 1.9.

This approach to octa-alkyl type porphyrin by tetramerization of pyrroles can also be achieved provided that  $\beta$ -substituents in the pyrrole are identical and the self-condensation of pyrrole bearing a suitable 2-substituent should provide the corresponding meso carbons, followed by aerial oxidation leads to the synthesis of porphyrin. For example, reduction of **1.10** gives pyrrole-2-carbinol **1.11**, which was then tetramerized using acid catalysis to afford porphyrin **1.12** in good yield (Scheme 2). <sup>14,15</sup>

Scheme 2. Synthesis of  $\beta$ -octaethylporphyrin **1.12**.

Asymmetric porphyrin with one regiochemically pure isomer from two different pyrroles can be synthesized under neutral conditions using ferricyanide (in MeOH) followed by DDQ oxidation. Here in this case, one of the pyrrole moieties should possess the future meso carbon atoms while the other pyrrole should be  $\alpha$ -free. Scheme 3 describes the synthesis of exclusively one regiochemically pure isomer 1.15 from cyclohexyl-fused pyrrole 1.13 and diethylpyrrole 1.14.

\

Scheme 3. Synthesis of regiochemically pure porphyrin 1.15.

#### 1.2.2 From Dipyrrolic intermediates: The [2 + 2] Route

The most commonly used dipyrrolic intermediates for porphyrin are dipyrromethenes and dipyrromethanes.

#### 1.2.2.1 Using Dipyrromethenes

Dipyrromethene precursors for the synthesis of porphyrins were developed by Hans Fischer's group. To reasonable self-condensation of 1-bromo-9-methyldipyrromethene **1.16** in boiling formic acid or tartaric acid at temperatures upto 200 °C produce centrosymmetrically substituted porphyrin **1.17** in good yields. Heating of 1-bromo-9-bromodipyrromethene **1.18**, 1-bromo-9-methyldipyrromethene **1.19** or mixture of both in formic acid gives excellent yield of the same porphyrin **1.17** (Scheme 4).

Scheme 4. Synthesis of centrosymmetrically substituted porphyrin 1.17.

#### 1.2.2.2 Using Dipyrromethanes

Compared to dipyrromethenes, dipyrromethanes were unstable toward acidic reagents (atleast those used by Fischer) to be useful as porphyrin precursors. MacDonald's discovery<sup>18</sup> play a pivotal role in porphyrin synthesis from dipyrromethane, in which an acid catalyst (ptoluenesulfonic acid) was employed in condensing 1,9-diformyldipyrromethane 1.20 with 1,9-di-unsubstituted dipyrromethane or its 1,9-dicarboxylic acid 1.21 to afford pure uroporphyrin III octamethylester 1.22) with an yield of 60% (Scheme 5).

Scheme 5. Synthesis of uroporphyrin III octamethylester 1.22.

#### 1.2.3 From Tripyrromethane intermediates: The [3 + 1] Route

Macrocyclization of a 2,5-difunctionalized pyrrole with a "linear" tripyrrolic species is also one of the important methods to produce a porphyrin. The tripyrrolic species is a tripyrrane i.e. a tripyrrole connected by methylene groups. Boudif and Momenteau used the [3 + 1] approach to prepare porphyrin 1.25<sup>19</sup>, in which they used a 2,5-diformylpyrrole 1.23 and a tripyrrane dicarboxylic acid 1.24 (Scheme 6).

Scheme 6. Synthesis of porphyrin 1.25.

The "one-pot" synthesis of porphyrins bearing identical opposite rings<sup>16</sup> was extended by the U. C. Davis group, using a [3 + 1] protocol in absence of acid catalysis, and therefore definitively protects the core of tripyrrane against pyrrole redistribution reactions. Thus reaction of tripyrrane 1.26 with 2,5-bis(N,N-dimethylaminomethyl) pyrrole 1.27 in presence of ferricyanide/methanol afforded porphyrin 1.28 in 27% yield (Scheme 7).

Scheme 7. Synthesis of porphyrin 1.28.

#### 1.2.4 From open-chain tetrapyrrolic intermediates

Asymmetric porphyrins with completely different array of substituents can be prepared sequentially from pyrrole through discrete open chain tetrapyrrolic intermediates. Such open chain tetrapyrroles with different forms are known as bilanes, bilenes, and biladienes.

In 1952, Corwin and Coolidge<sup>21</sup> initially achieved porphyrin synthesis using an open chain tetrapyrrole as an intermediate. 1,19-dicarboxylic acid **1.29** was cyclized in formic acid to give 36% yield of etioporphyrin II **1.30** (Scheme 8).

Scheme 8. Synthesis of etioporphyrin II 1.30.

Porphyrin synthesis using b-bilenes was summarized by Clezy.<sup>22</sup> The b-bilene **1.31** with 1-and 19- methyl groups can be immediately cyclized oxidatively by utilizing copper(II) salts in DMF to afford copper (II) porphyrin **1.32**. Metal-free porphyrin can be obtained by reaction of conc. H<sub>2</sub>SO<sub>4</sub> or better with conc. H<sub>2</sub>SO<sub>4</sub> in TFA (Scheme 9).<sup>23</sup>

Scheme 9. Synthesis of porphyrin 1.33.

#### 1.3 Structure and properties

The porphine (freebase) **1.34** has a total of 11 double bonds with 9 bonds in conjugation and a metalloporphyrin **1.35** can be obtained by replacing two inner hydrogens of pyrrole with a metal ion. A porphyrin diacid species **1.36** can also be obtained with the addition of two protons to imine nitrogens of freebase porphyrin.<sup>24</sup>

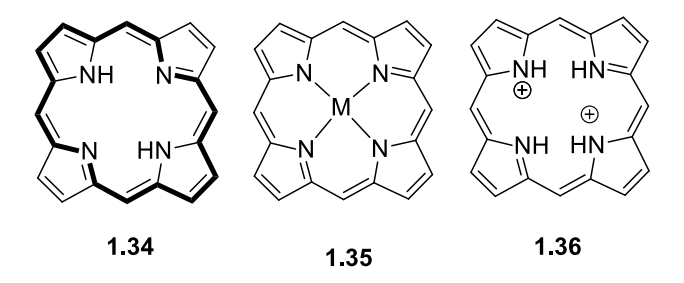


Figure 1.3 Skeletal structures of freebase 1.34, metalloporphyrin 1.35 and diacid 1.36.

Naturally occurring porphyrins can be studied by employing suitable synthetic models such as *meso*-tetraphenylporphyrin **1.9**. For the better understanding of physical properties i.e., UV-visible absorption spectra, solubility and magnetic properties one should have a good knowledge of structure of the porphyrin molecule. Structural properties also define chemical properties like the rates and mechanism of metalloporphyrins formation and decomposition, substitution reaction on the ring and oxidation-reductions reactions of the porphyrin and metalloporphyrin system.<sup>24</sup>

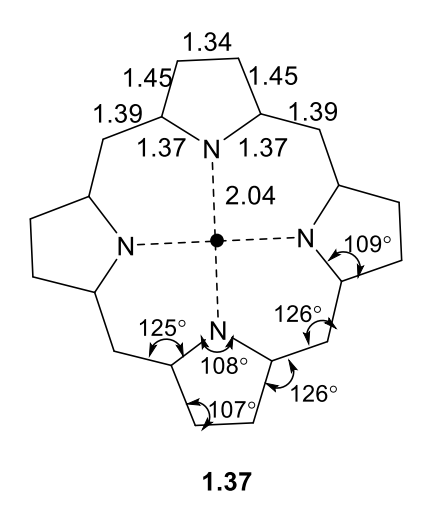


Figure 1.4 Structure parameters of porphyrin skeletal.

A porphyrin has a fourfold axis of symmetry with respect to the bond distances and angles, 1.37 (Figure 1.4) Effect of different substituents on the porphine skeleton is usually very small and almost comparable with the estimated errors in bond parameters. Only the metal-nitrogen bond distance in case of metalloporphyrins change appreciably, and the distance varied significantly from 2.10 Å to 1.95 Å in case of ferric porphyrins to porphyrins with nickel at the metal centre whereas the average distance between the two opposite pyrrolic nitrogen via the centre of the ring porphyrin is 2.04 Å. The structure of porphyrin is not completely rigid, as it shows almost planarity in porphine to very ruffled in TPP series. The freebase form of TPP crystallizes in two forms with varied conformations of the porphine skeleton. Generally,

porphyrin has a near-planar conformation in a "free" environment probably having a little energy barrier w.r.t. deviations from planarity and thus leads to conformational adaptability which make it difficult to predict the structure under various circumstances.<sup>24</sup>

One of the reasons porphyrins have been majorly explored is due to their fundamental property of aromaticity. Originally aromaticity was described in flat, cyclic systems with conjugated 4n+2  $\pi$ -electrons such as benzene, naphthalene and anthracene etc., but it can be readily applicable to porphyrins also.<sup>25</sup> Porphyrin macrocycle consist of 22  $\pi$ -electrons out of which only  $18 \pi$ -electrons form a conjugated aromatic ring following Huckle's  $(4n+2)\pi$  rule. Aromatic character of porphyrins is supported by the kind of reactions it undergoes i.e., electrophilic substitution reactions. To distinguish between aromatic and antiaromatic systems different experimental techniques have been employed, such as <sup>1</sup>H NMR spectroscopy, analysis of NICS calculations, <sup>26</sup> HOMA<sup>27</sup> and BLA<sup>28</sup>. Among these, <sup>1</sup>H NMR spectroscopy is considered to be one of the most important tools. The inner protons of a delocalized aromatic system are generally resonated in the upfield region of -3 to 0 ppm, while the perimeter protons are shifted to the downfield region upto 10 ppm. Porphyrin displays strong aromatic ring current with the conjugation pathway going through β-pyrrole carbons in two pyrrole moieties making the other β- β-pyrrolic bonds purely double bond in nature. The β- β-pyrrolic bond distance is found to be 1.37 Å which is close to the C-C bond distance in ethylene (1.34 Å). But in case of the expanded macrocycles (sapphyrins, pentaphyrins, hexaphyrins etc.), the criterion of planarity is not absolutely necessary because of their conformational flexibility.<sup>29</sup> In few cases they exhibit three-dimensional (3D) structure with a topology of Möbius strip and in these kinds of molecules, aromaticity was predicted for  $4n\pi$ - and antiaromatic for  $(4n+2) \pi$ .

Porphyrins due to their highly conjugated  $\pi$ -system display a very characteristic UV-visible absorption spectra with bands in two distinct regions, the first an intense band in the range of 380-500 nm, called Soret or B-band and the other comparatively weak bands called Q-bands in the region of 500-650 nm. It is observed that change in symmetry and conjugation pathway will influence its UV-visible absorption spectrum. In 1959, Gouterman explained the absorption spectrum of porphyrins, by his famous "four-orbital (two highest occupied  $\pi$  orbitals and two lowest unoccupied  $\pi$  orbitals) model", in which he explained the importance of charge localization on electronic spectroscopic properties.<sup>31</sup>

This model proposes the absorption bands in porphyrins correspond to the transitions between HOMOs consisting of  $a_{1u}$  and  $a_{2u}$  orbitals and LUMOs, a degenerate set of  $e_g$  orbitals, giving rise to two excited states - a higher energy state with good oscillator strength (leading to Soret band) and lower energy state with weak oscillator strength (giving rise to Q bands).

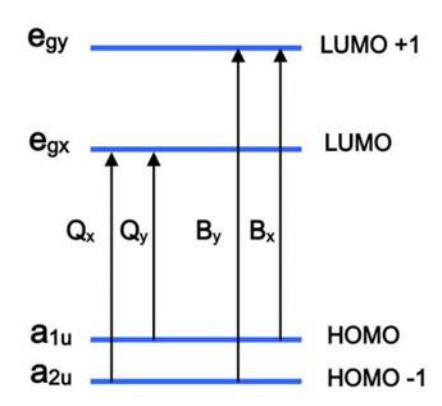


**Figure 1.5** Transitions in frontier orbitals.

Therefore, the transition in the range of 380-500 nm correspond to the excitation from ground to second excited state ( $S_0$  to  $S_2$ ) which is intense and the weak transitions in the range between 500-750 nm correspond to the first excited state ( $S_0$  to  $S_1$ ).

Peripheral substitution of porphyrin ring causes only minor variations to the intensity and wavelength of absorption spectrum. But protonation or metallation will lead to a strong change in the visible range of the absorption spectrum because of change of symmetry from  $D_{2h}$  to  $D_{4h}$ .

#### 1.4 Applications of Porphyrin

Porphyrins, because of their tunable structural and photophysical properties are highly suitable for different applications. Since the structure of porphyrin comprises four pyrrole subunits connected by four methane bridges, it has the capability to generate coordination complex with almost all metal ions, which often enhances its properties. The research on porphyrin is not limited to synthetic organic chemist but further expanded to multiple disciplines such as medicine, physics, engineering and theoretical studies. Some of its important applications are detailed below:

#### 1.4.1 Photodynamic Therapy (PDT)

PDT, with a fundamental goal of controlled and selective destruction of malignant cells while leaving normal tissue unaffected is a new tool of cancer treatment. The PDT procedure involves

combination of an oxidizing agent (molecular oxygen, O<sub>2</sub>), light (of an appropriate wavelength) and a photosensitizer (PS) to produce lethal cytotoxic singlet oxygen which inactivate tumour cells. The mechanism of this procedure can be explained by Jablonski diagram (Figure 1.6).

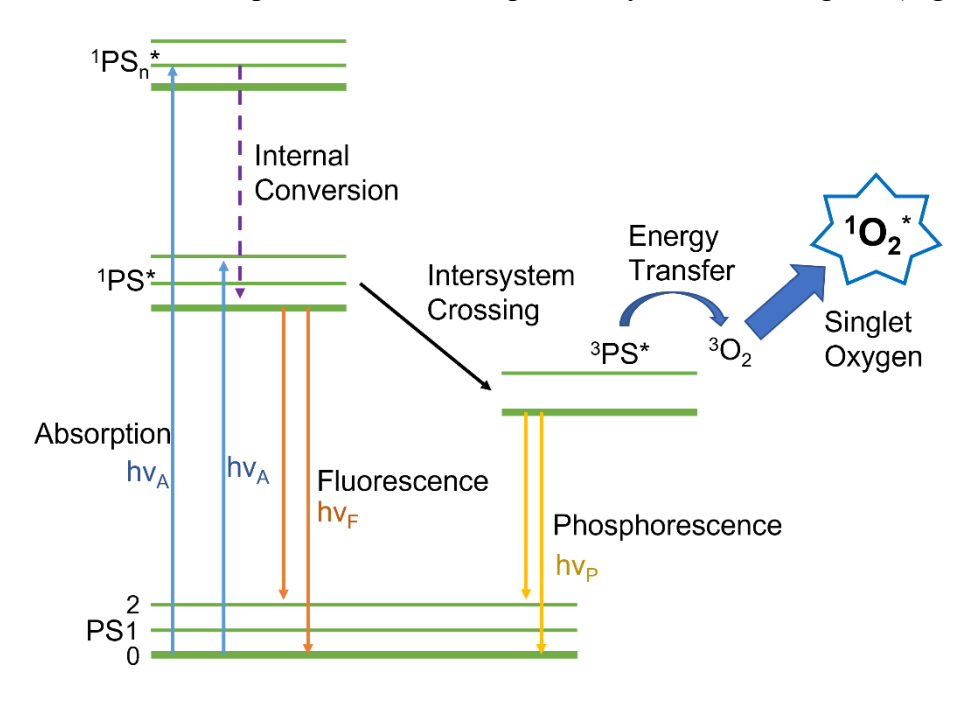


Figure 1.6 Jablonski diagram explaining the mechanism of PDT.

On absorption of light, the photosensitizer (PS) is excited from the ground state S<sub>0</sub> to the first excited state S<sub>1</sub>, followed by intersystem crossing (ISC) to triplet state T<sub>1</sub>. The triplet state lifetime is longer than the singlet state which enables the PS to interact with the surrounding molecules. The excited triplet state can go through two types of reactions: type I and type II mechanisms. The type I mechanism involves the direct reaction of the PS with a biological substrate via radical formation. In type II process, the triplet state PS interacts with the stable ground state triplet oxygen ( ${}^{3}O_{2}$ ) to produce highly reactive  ${}^{1}O_{2}$  (singlet oxygen), which attacks tumour cells. Generally, type II process is considered as most relevant PDT practice.  ${}^{33}$ 

Porphyrins display distinct photophysical properties, a characteristic optical spectrum which involves strong  $\pi$ - $\pi$ \* transition around 400 nm (Soret band) and four Q bands in the visible region. Absorption of light results transfer of electron from ground state to an excited state, which can dissipate its energy either by fluorescence, phosphorescence, or through ISC into an excited triplet state, thus enabling their use as diagnostic tool. Their capability to undergo ISC to excited triplet state (results in the production of singlet oxygen) allows their use in therapeutic application such as PDT.

Photofrin **1.38** is the first approved porphyrin photosensitizer drug by US FDA in the treatment of different types of cancers and skin diseases.<sup>34</sup> Photofrin absorption band ends at 630 nm and has very little intensity in the red region. Since penetration of light in the tissue increases with increasing wavelength, second generation PS has been developed to overcome the disadvantages. A second-generation PS Verteporfin (benzo-porphyrin derivative monoacid ring) **1.39** has been developed, which is now under Phase III clinical trials for its use in macular degeneration.<sup>35</sup>

**Figure 1.7** Structures of porphyrins synthesized for PDT: Photofrin **1.38**, Verteporfin **1.39** and Temoporfin **1.40**.

Verteporfin has intense absorption in the red region (690 nm) when compared to photofrin at 630 nm where tissue penetration of light is 50% greater. Temoporfin (**1.40**) or tetra(m-hydroxyphenyl)chlorine (m-THPC) under the trade name of Foscan<sup>TM</sup> is a new second-generation PS for PDT, which is under Phase III trials.<sup>36</sup>

#### 1.4.2 Nonlinear optics (NLO)

The nonlinear optics is defined as the phenomena in which a strong oscillating electromagnetic field or high light intensity (e.g. laser light) interacts with matter or molecules, to give an emission of new electromagnetic fields with a change in frequency/phase or other optical properties. Materials having good NLO properties are thoroughly investigated because of their potential applications for optical communication, data storage, computers and optical signal processing. When a molecule is interacted with a laser beam, the change in total polarization is calculated with the following expression:

$$P_i = P_i + \alpha_{ii}E_i + \beta_{iik}E_iE_k + \gamma_{iikl}E_iE_kE_l + \dots$$

Where  $P_i$  corresponds to the dipole moment of perturbing optical field E,  $\alpha_{ij}$  is the linear polarizability, while  $\beta_{iik}$  and  $\gamma_{iikl}$  are the quadratic and cubic hyperpolarizabilities, respectively. Initially, research work on NLO was focused on inorganic materials, such as quartzs, lithium niobate, potassium dihydrogen phosphate, cadmium telluride and cadmium germanium arsenide. Eventually organic and organometallic molecules got wide attention compared to traditional inorganic solids as NLO materials. Organic NLO materials can be modified through molecular structure to play a pivotal role in simultaneously controlling various primary and secondary NLO properties.<sup>37</sup> In this case, highly delocalized 18π-aromatic system of porphyrins have attracted great attention because such systems may exhibit large ultrafast nonresonant NLO responses.<sup>38</sup> Porphyrins exhibit architectural flexibility as different substituents can be fixed at the meso- or β- positions of a metalloporphyrin making them superior to other NLO chromophores as optical materials. Optical properties of porphyrins can be tuned with different metal centres, axial ligands, its oxidation state or various peripheral substituents. Different porphyrins have been reported with a good second and third order NLO properties.<sup>36</sup> In 1985, 5,10,15,20-tetraphenylporphyrin **1.9** was studied for its optical properties. Later NLO studies have been done on numerous S4 symmetric porphyrins. The studies indicated the change in NLO response with different metals by using different techniques like Z-scan and DFWM. 37

Permanent dipole moment is essential to increase the efficacy of porphyrins for their application in optical materials.<sup>39</sup> Therefore asymmetric porphyrins are expected to show greater potential for NLO application than symmetric ones. In this scenario Suslick's group demonstrated a series of push-pull porphyrins (**1.41a-d**) for NLO application.<sup>40</sup>

Figure 1.8 Push-Pull porphyrins designed by Suslick's group.

Conjugated porphyrin oligomers with an extended  $\pi$ -systems display a strong NLO behaviour. In this context, Anderson reported first soluble conjugated porphyrin polymers **1.42** employing Glasser-Hay coupling reaction.<sup>37a</sup>

$$R = 0$$

Figure 1.9 Structure of soluble conjugated porphyrin polymers by Anderson's group.

Porphyrin arrays are one of the new promising materials for NLO applications, where individual porphyrin units are linked to extend the  $\pi$ -systems. Herein, the example given below show fused porphyrin **1.43** and **1.44** systems with different meso/ $\beta$ - linkages to give extended  $\pi$ -systems with good NLO properties.<sup>37,38</sup>

Figure 1.10 Structures of fused porphyrin for NLO studies.

#### 1.4.3 Sensors

Chemical sensors are the devices in which a chemical signal such as change in concentration of a particular component to the absolute concentration is converted into a measurable signal.<sup>41</sup> Technological advance in electronics is a must for sensor development because information of the sensed analyte is in the form of electronic signal which can be transmitted, stored and used efficiently. The parameters of a chemical sensor depend on the chemical interaction with the

environment it come in contact. As a result, a chemical sensor is composed of two components viz. a receptor and transducer. Interaction of the receptor with chemical environment causes some changes in the properties of the interacting analyte, that measurement of interaction can be converted to an electronic signal by transducer. Porphyrins because of their rich properties such as stability, distinctive optical and coordination properties emerged as versatile candidate as receptors in chemical sensors compared to metal oxides or polymers.<sup>42</sup> The exploration of porphyrins as sensors got attraction mainly because the interaction of the target analyte by porphyrin sensing material mimic the role of porphyrin in biological systems e.g. reversible binding of gaseous compounds and can undergo photophysical or redox reactions mediated by the target analyte.<sup>43</sup>

The use of porphyrin-based sensors for the detection of gases e.g.,  $O_2$  is mainly due to quality of heme to bind various gases such as  $O_2$  and  $CO_2$ . The detection of the analyte (gas molecule) by the porphyrin metal centre leads to detectable optical change. The detection of  $O_2$  by using metalloporphyrin based sensors is generally performed through phosphorescence quenching process by  $O_2$ . Eastwood and Gouterman suggested that because of high phosphorescence and long triplet lifetimes, platinum and palladium porphyrins can be employed as sensing materials for  $O_2^{44}$  for example Hans and coworkers design Pt and Pd porphyrins **1.45** and **1.46**.

Figure 1.11 Pt and Pd porphyrins design by Hans and coworkers.

Moncada and co-workers have employed polymeric film of Ni(II) tetrakis(3-methoxy-4-hydroxy-phenyl) porphyrin **1.47** deposited on a carbon electrode as a NO microsensor using differential pulse voltammetry. Using this approach, they were able to find that human platelets on aggregation releases NO.<sup>46</sup> Meso-tetra(4-sulphonatophenyl) porphyrin (TPPS) **1.48** as an optical based sensor was utilized by Awawdeh et al. by immobilizing it on a cellulose film for

detecting amino acids such as arginine, glycine, histidine and serine in a concentration level of nanomolar.<sup>47</sup>

Figure 1.12 Structures for porphyrins for sensors.

Recently, Ze Gu group have prepared multifunctional wearable sensing devices using four kinds of porphyrin (TPP(NH<sub>2</sub>)<sub>4</sub>, CuTPP, ZnTPP and CoTPP) **1.49** and **1.50-1.52** modified reduced graphene oxide films in sensing VOC vapours with high precession.<sup>48</sup>

$$H_2N$$

NH<sub>2</sub>

NH<sub>2</sub>

NH<sub>2</sub>

NH<sub>2</sub>

M= Cu, Zn, Co

1.49

1.50-1.52

Figure 1.13 Structures of freebase and metalloporphyrin by Ze Gu group for sensors.

#### 1.4.4 Artificial photosynthetic systems

The sun produces enormous amount of energy out of which a small portion is absorbed by plants and bacteria, this light harvesting action from sunlight and conversion of it to the biochemical energy is termed as photosynthesis.<sup>49</sup> Artificial photosynthesis is a replication of natural photosynthesis in which artificial photosynthetic systems, consist of an energy donor and acceptor component linked to a chromophore or light harvesting unit, similar to the natural systems. The binding of components to proteins employs covalent bond instead of weak H-

bonds or van der Waal interaction, which results efficient electron transfer process between the two components i.e., donor and acceptor and ultimately leads to higher quantum yield. <sup>50</sup> Upon irradiation, donor absorbs light and transfers the energy to acceptor, this electron transfer process generate a charge separated state. Artificial photosynthetic systems are aimed at achieving a long lifetime of charge separated state, to inhibit back reactions. It was further studied that components of the reaction centre i.e., donor and acceptor can undergo more controlled electron transfer process by linking the two to form a molecular dyad, in which it is possible to achieved a charge separated state with longer lifetime by altering the length and type of their linkages. 51 Because of their resemblance to the light harvesting antenna systems, porphyrins, among all chromophores, have been employed in synthesizing artificial photosynthetic complexes. Due to the excellent properties of porphyrins such as photo- and thermal stability, strong absorbance, rich redox features and tunable electronic properties by structural modifications make them ideal choice for this kind of systems.<sup>52</sup> Similar to natural photosynthetic systems, Gust, Moore and co-workers designed a covalently connected triad, 1.53 comprising tetraarylporphyrin (chromophore), carotenoid (donor) and quinone (acceptor), displaying an excellent lifetime of 55 µs with 83% quantum yield.<sup>53</sup>

Figure 1.14 Artificial Photosynthetic system designed by Gust, Moore and co-workers.

Imahori et al. achieved a charge separated state with an extremely longer lifetime of 0.38 s, close to bacterial photosynthetic systems, using a ferrocene-Zn(II)porphyrin-freebase porphyrin-fullerene tetrad, **1.54** through intramolecular charge transfer.<sup>54</sup>

Figure 1.15 Ferrocene-Zn(II)porphyrin-freebase porphyrin-fullerene tetrad by Imahori et al.

#### 1.4.5 Solar cells

The ever-growing human population causes increase in energy consumption which accelerated the depletion of non-renewable energy sources such as coal, petroleum and natural gas. These carbons based non-renewable sources inflicts many environmental hazards such as global warming. Therefore, the renewable sources of energy such as solar, wind, hydroelectric and biomass (which are abundant in earth) attracts the scientists to focus on it. Among all renewable sources of energy, solar energy is the most abundant, cheap, safe and cleanest energy source and can play a pivotal role in replacing fossil fuels in solar energy technology or generating electric current from sunlight, also known as photovoltaic effect.<sup>55</sup> Solar energy is a substantially infinite energy source and effective conversion of solar energy into electricity has been developed as an essential strategy for sustainable development. It is dominated for decades by the silicon-based devices, which covers about 90% of the PV market. But due to the high cost of the silicon based material the second-generation solar cells became another competitive class of PVs, which are built on thin film technologies, for example, amorphous silicon, CdTe and CIGS. The thin film solar cells have the advantage of easy manufacturing, allowing a reduction of the production cost and a broad range of applications with interesting appearance and flexible substrate. Amorphous silicon (a-Si) is the most established thin film technology but having lower efficiencies than c-Si. The first- and second-generation solar cells are built on single junction solar cells.<sup>56a</sup> In a single junction solar cell, the calculated thermodynamic efficiency limit is 31% by the assumption that a single electron-hole pair formed by the absorption of an individual photon and all the excess photon energy of the energy gap is lost as heat. This is known as Shockley-Queisser limit, which can be mitigated by the use of various third-generation solar cell devices. There are several schemes to accomplish the efficiencies more than 31% including tandem cells, multiband cells, hot carrier cells, and

thermophotovoltaics etc.<sup>56b</sup> Dye-sensitized solar cells (DSSCs) technology can be positioned between the second and third generation solar cells. By using the nanoscale properties of the device, it has the potential to become a third-generation solar cell. In the present stage DSSC emerged as a low-cost alternative owing to its ease of fabrication, a short-energy pay-back time, low sensitivity to temperature changes and eco-friendliness. A conventional DSSC consists of a working electrode which is made of FTO containing mesoporous TiO<sub>2</sub> nanoparticles onto which a monolayer of dye will be adsorbed and a thin layer of the platinum catalyst coated on a FTO is acts as a counter electrode. With the use of a polymer sealant the two electrodes are sealed together and a liquid electrolyte, containing a redox mediator and additives filled the space between the electrodes. When the light transmitted through the transparent FTO and TiO<sub>2</sub> semiconductor, molecules of the dye absorbed the light and excited dye molecules inject the electrons into the TiO<sub>2</sub> CB. The redox mediator subsequently regenerates the oxidized dye and get restored by counter electrode. 56c In 1991, Grätzel and coworkers were the first to develop the DSSC, also known as Grätzel cell.<sup>57</sup> Though different dyes are designed for DSSC, porphyrins got the major attraction due to their strong light harvesting ability, tunable electronic and photophysical properties by molecular modifications and having thermal-, chemical- and photo stability. First example of a porphyrin sensitized solar cell was prepared in 1993 using copper chlorophyll derivative 1.55 by Kay and Grätzel giving 2.6% efficiency. 58 Further, Yeh and Diau on collaboration with Grätzel able to achieve 11% efficiency by co-sensitizing YD2 (1.56) with another complementary dye.<sup>59</sup>

$$C_6H_{13}$$
 $C_6H_{13}$ 
 $C_6H_{13}$ 

Figure 1.15 Structures of first porphyrin sensitizer for solar cell 1.55 and YD2 (1.56).

Efficiency surpassed 12% when t-butyl groups of YD2 were replaced with octyloxy groups YD2-o-C8 (1.57) and using cobalt based redox electrolyte.<sup>60</sup> Now a record efficiency of 13% was again achieved by Grätzel et al., using sensitizer SM315 (1.58).<sup>61</sup>

Figure 1.16 Structures of YD2-o-C8 (1.57) and SM315 (1.58).

#### 1.5 Scope of the present work

As it can be seen from the above discussion, one can understand the importance of porphyrins, since porphyrins exhibits intense absorption in the visible region, good thermal and photostability, high molar absorption coefficient and their tunable structural and electrochemical properties, which make them a prominent candidate for DSSC applications. Though tremendous work has been done by Grätzel and coworkers in developing novel D- $\pi$ -A architectures reaching an efficiency of 13%, most of the dyes lack significant absorption in the NIR region which contains significant flux of solar photons. To overcome this deficiency, we envisaged of utilizing a very efficient NIR active naphthobipyrrole derived BODIPY dye recently developed by our group. <sup>62</sup> For this, we thought of linking porphyrin and BODIPY to form the desired porphyrin-BODIPY conjugate and explore its photophysical, and electrochemical properties. The present work also enlists the usage of computational calculations for better understanding of these porphyrin-BODIPY conjugates.

#### 1.6 References

- 1. Olson, J. M. Photosynthesis in the Archean Era. *Photosynth. Res.* **2006**, *88*, 109.
- 2. (a) With, T. K. A short history of porphyrins and the porphyrias *Int. J. Biochem.*, **1980**, *11*, 189; (b) Dolphin, D. *The Porphyrins, Structure and Synthesis Part A*, **1978**, *1*, 29.
- 3. Warren, M. J.; Smith, A. G. Tetrapyrroles: Birth, Life and Death, 2009, 5.
- 4. Milroy, J. A. Observations on some Metallic Compounds of *Haematoporphyrin Biochem. J.* **1918**, *12*, 318.
- 5. Fischer, H.; Zeile, K. Justus Liebigs Ann. Chem., 1929, 468, 98.
- 6. Battersby, A. R.; Fookes, C. J. R.; Matcham, G. W. J.; McDonald, E. Biosynthesis of the pigments of life: formation of the macrocycle. *Nature*, **1980**, *285*, 17.
- 7. (a) *The Porphyrin Handbook* (Eds.: K. M. Kadish; K. M. Smith; R. Guilard) Academic Press, San Diego, **2000**. (b) *Handbook of Porphyrin Science* (Eds.: K. M. Kadish; K. M. Smith; R. Guilard) World Scientific Publishing, Singapore, **2010**.
- 8. Bauer, V. J.; Clive, D. L. J.; Dolphin, D.; Paine III, J. B. P.; Harris, F. L.; King, M. M.; Loder, J.; Wang, S.-W. C.; Woodward, R. B. Sapphyrins: novel aromatic pentapyrrolic macrocycles. *J. Am. Chem. Soc.* **1983**, *105*, 6429.
- 9. Sessler, J. L.; Weghorn, S. J. Expanded, Contracted and Isomeric Porphyrins Pergamon, New York, 1997.
- 10. Franck, B.; Nonn, A. Novel Porphyrinoids for Chemistry and Medicine by Biomimetic Syntheses. *Angew. Chem., Int. Ed. Engl.* **1995**, *34*, 1795.
- 11. (a) Rothemund, P. Formation of Porphyrins from Pyrrole and Aledehydes. *J. Am. Chem. Soc.* **1935,** *57,* 2010; (b) Rothemund, P.; Menotti, A. R. Porphyrin Studies. IV The Synthesis of a,0,7,5-Tetraphenylporphine. *J. Am. Chem. Soc.*, **1941,** *63*, 267.
- 12. Adler, A. D.; Longo, F.R.; Finarelli, J. D.; Goldmacher, J.; Assour, J.; Korsakoff, L. A simplified synthesis for meso-tetraphenylporphine. *J. Org. Chem.*, **1967**, *32*, 476.
- 13. Lindsey, J. S.; Schreiman. I. C.; Hsu, H. C.; Kearney, P. C.; Marguerettaz, A. M. Rothemund and Adler-Longo reactions revisited: synthesis of tetraphenylporphyrins under equilibrium conditions. *J. Org. Chem.*, **1987**, *52*, 827.
- 14. Ono, N.; Kawamura, H.; Bougauchi, M.; Maruyama, L. Porphyrin synthesis from nitrocompounds. *Tetrahedron*, **1990**, *46*, 7483.

- 15. Aoyagi, K.; Haga, T.; Toi, H.; Aoyama, Y.; Mizutani, T.; Ogoshi, H. Electron Deficient Porphyrins III. Facile Syntheses of Perfluoroalkylporphyrins Including Water Soluble Porphyrin. *Bull. Chem. Soc. Jpn.* **1997**, *70*, 937.
- 16. Ngugen, L. T.; Senge, M. O.; Smith, K. M One-pot synthesis of regiochemically pure Porphyrins from two different pyrroles. *Tetrahedron Lett.*, **1994**, *35*, 7581.
- 17. Fischer, H.; Klarer, J. Ann. Chem., 1926, 448, 178.
- 18. Arsenault, G. P.; Bullock, E.; MacDonald, S. F. Pyrromethanes and Porphyrins Therefrom. *J. Am. Chem. Soc.*, **1960**, *82*, 4384.
- 19. Boudif, A.; Momenteau, M. J. Chem. Soc. Chem. Commun. 1994, 2096.
- 20. Ngugen, L. T.; Senge, M. O.; Smith, K. M. Simple Methodology for Syntheses of Porphyrins Possessing Multiple Peripheral Substituents with an Element of Symmetry J. Org. Chem. 1996, 61, 998.
- 21. Kämpfen, U.; Eschenmoser, A. Porphyrin synthesis by ring transplantation. *Tetrahedron Lett.* **1985**, *26*, 5899.
- 22. Clezy, P. S. Studies in Porphyrin Chemistry: A Synthetic Approach. *Aust. J. Chem.*, 1991, 44, 1163.
- 23. (a) Almeida, J. A. P. B.; Kenner, G. W.; Rimmer, J.; Smith, K. M. Pyrroles and related compounds—XXXV: A stepwise, general synthesis of unsymmetrically substituted porphyrins. *Tetrahedron*, **1976**, *32*, 1793. (b) Smith, K. M.; Craig, G. W. Porphyrin Synthesis through Tripyrrins: An Alternate Approach. *J. Org. Chem.* **1983**, *48*, 4302.
- 24. Fleischer, E. B. Structure of porphyrins and metalloporphyrins. *Acc. Chem. Res.* **1970**, *3*, 105.
- 25. Aromaticity in Heterocyclic Compounds (Eds. T. M. Kryogowski, M. K. Cyrański) Springer, Verlag-Berlin Heidelberg, **2009.**
- 26. Chen, Z.; Wannere, C. S.; Corminboeuf, C.; Puchta, R.; Schleyer, P. v. R. Nucleus-Independent Chemical Shifts (NICS) as an Aromaticity Criterion. *Chem. Rev.*, **2005**, *105*, 3842.

- 27. Krygowski, T. M. Crystallographic studies of inter- and intramolecular interactions reflected in aromatic character of. pi. -electron systems. *Chem. Inf. Comput. Sci.* **1993**, 33, 70.
- 28. Schleyer, P. v. R.; Freeman, P.; Jiao, H.; Goldfuss, B. Aromaticity and Antiaromaticity in Five-Membered C<sub>4</sub>H<sub>4</sub>X Ring Systems: "Classical" and "Magnetic" Concepts May Not Be "Orthogonal". *Angew. Chem. Int. Ed.* **1995**, *34*, 337.
- 29. (a) Stępień, M.; Latos-Grażyński, L.; Sprutta, N.; Chwalisz, P.; Szterenberg, L. Expanded Porphyrin with a Split Personality: A Hückel-Möbius Aromaticity Switch. Angew. Chem., Int. Ed. 2007, 46, 7869. (b) Rachlewicz, K.; Sprutta, N.; Latos-Grażyński, L.; Chmielewski, P. J.; Szterenberg, L. Protonation of 5,10,15,20tetraphenylsapphyrin—identification of inverted and planar dicationic forms. J. Chem. Soc., Perkin Trans. 2 1998, 959. (c) Sarma, T.; Anusha, P. T.; Pabbathi, A.; Rao, S. V.; K. Naphthobipyrrole-Derived Sapphyrins: Rational Characterization, Nonlinear Optical Properties, and Excited-State Dynamics. Chem. Eur. J. **2010**, 20, 15561. (d) Shetti, V. S.; Kee, S.-Y.; Lee, C. H. Core-Modified Analogues of Expanded Porphyrins Containing Rigid β,β'-Linked o-Phenylene Bridges. Chem. Asian J. 2014, 9, 734. (e) Shimizu, S.; Taniguchi, R.; Osuka, A. meso-Aryl-Substituted [26]Hexaphyrin(1.1.0.1.1.0) and [38] Nonaphyrin(1.1.0.1.1.0.1.1.0) from Oxidative Coupling of a Tripyrrane, Angew. Chem., Int. Ed. 2005, 44, 2225.
- 30. (a) Yoon, Z. S.; Osuka, A.; Kim, D. Möbius aromaticity and antiaromaticity in expanded porphyrins. *Nat. Chem.* **2009**, *1*, 113. (b) Tanaka, T.; Osuka, A. Chemistry of *meso*-Aryl-Substituted Expanded Porphyrins: Aromaticity and Molecular Twist . *Chem. Rev.*, **2017**, *117*, 2584.
- 31. Gouterman, M. Spectra of porphyrins. J. Mol. Spectrosc., 1961, 6, 138.
- 32. Macro to Nano Spectroscopy (Ed. R. Giovannetti) Intechopen, Rijeka, 2012.
- 33. MacDonald, I. J.; Dougherty, T. J. Basic principles of photodynamic therapy. *J. Porphyrins Pthalocyanines*, **2001**, *5*, 105.
- 34. Sharman, W. M.; Allen, C. M.; Van Lier, J. E. Photodynamic therapeutics: basic principles and clinical applications. *Drug Discovery Today*, **1999**, *4*, 507.

- 35. Ethirajan, M.; Chen, Y.; Joshi, P.; Pandey, R. K. The role of porphyrin chemistry in tumor imaging and photodynamic therapy. *Chem. Soc. Rev.*, **2011**, *40*, 340.
- 36. Tessore, F.; Orbelli Biroli, A.; D Carlo, G.; Pizzotti, M. Porphyrins for Second Order Nonlinear Optics (NLO): An Intriguing History. *Inorganics*, **2018**, *6*, 81.
- 37. (a) Senge, M.; Fazekas, M.; Notaras, E.; Blau, W.; Zawadzka, M.; Locos, O.; Ni Mhuircheartaigh, E. Adv. Mater., 2009, 19, 2737. (b) a) Aratani, N.; Osuka, A.; Kim, Y. H.; Jeong, D. H.; Kim, D. Extremely Long, Discrete meso meso-Coupled Porphyrin Arrays. Angew. Chem. Int. Ed. 2000, 39, 1458. c) Tsuda, A.; Furuta, H.; Osuka, A. Completely Fused Diporphyrins and Triporphyrin. Angew. Chem. Int. Ed., 2000, 39, 2549. d) Tsuda, A.; Furuta, H.; Osuka, A. J. Am. Chem. Soc. 2001,123, 10, 304. e) Jin, L.-M.; Chen, L.; Yin, J.-J.; Guo, C.-C.; Chen, Q.-Y. A Facile and Potent Synthesis of meso,meso-Linked Porphyrin Arrays Using Iodine(III) Reagents. Eur. J. Org. Chem. 2005, 3994. f) Kim, D.; Osuka, A. Photophysical Properties of Directly Linked Linear Porphyrin Arrays. J. Phys. Chem. A., 2003, 107, 8791.
- 38. a) Tsuda, A.; Nakano, A.; Furuta, H.; Yamochi, H.; Osuka, A. Doubly meso-beta-Linked Diporphyrins from Oxidation of 5,10,15-Triaryl-Substituted Ni(II)- and Pd(II) Porphyrins. *Angew.Chem. Int. Ed.* **2000**, *39*, 558. b) Tsuda, A.; Osuka, A. Discrete Conjugated Porphyrin Tapes with an Exceptionally Small Bandgap. *Adv. Mater.* **2002**, 14, 75. c) Senge, M. O.; Rössler, B.; Gersdorff, J. v.; Schäfer, A.; Kurreck, H. The meso-b-linkage as structural motif in porphyrin-based donor–acceptor compounds. *Tetrahedron Lett.*, **2004**, *45*, 3363.
- 39. S. R. Marder; J. E. Sohn.; G. D. Stucky, *Materials for Nonlinear Optics, Chemical Perspective*, ACS, Washington DC, **1991**.
- 40. K. S. Suslick, C. T. Chen, G. R. Meredith, L. T. Cheng. The nature of bonding and stability of beryllium carbonyl (CO)2Be-Be(CO)2: a molecule with a beryllium-beryllium double bond. *J. Am. Chem. Soc.*, **1992**, *114*, 6928.
- 41. Hulanicki, A.; Glab, S.; Ingman, F.; Chemical sensors: definitions and classification. *Pure Appl. Chem.*, **1991**, *63*, 1247.
- 42. Paolesse, R.; Nardis, S.; Monti, D.; Stefanelli, M.; Natale, C. D. Porphyrinoids for Chemical Sensor Applications. *Chem. Rev.*, **2017**, *117*, 2517.

- 43. Paolesse, R.; Nardis, Sara.; Monti, D.; Stefanelli, M.; Natale, C. D. Porphyrinoids for Chemical Sensor Applications. *Chem. Rev.*, **2017**, *117*, 2517.
- 44. Eastwood, D.; Gouterman, M. Porphyrins: XVIII. Luminescence of (Co), (Ni), Pd, Pt complexes. *J. Mol. Spec.* **1970**, *35*, 359.
- 45. Han, B. H.; Manners, I.; Winnik, M. A. Oxygen Sensors Based on Mesoporous Silica Particles on Layer-by-Layer Self-assembled Films. *Chem. Mater.* **2005**, *17*, 3160.
- 46. Malinski, K.; Radomski, M. W.; Taha, Z.; Moncada, S. Direct electrochemical measurement of nitric oxide release from human platlets. *Biochem. Biophys. Res. Commun.*, **1993**, *194*, 960.
- 47. Awawdeh, M. A.; Legako, A. J.; Harmon, J. H. Solid-state optical detection of amino acids. *Sensors Actuat.*, **2003**, *91*, 227.
- 48. Xu, H.; Xiang, J. X.; Lu, Y. F.; Zhang, M. K.; Li, J. J.; Gao, B. B.; Zhao, Y. J.; Gu, Z. Z. Multifunctional Wearable Sensing Devices Based on Functionalized Graphene Films for Simultaneous Monitoring of Physiological Signals and Volatile Organic Compound Biomarkers. *ACS Appl. Mater. Interfaces*, **2018**, *10*, 11785.
- 49. Tachibana, Y.; Vayssieres, L.; Durrant, J. R. Artificial photosynthesis for solar watersplitting *Nat. Photonics*, **2012**, *6*, 511.
- 50. Nikolaou, V.; Charisiadis, A.; Stangel, C.; Charalambidis, G.; Coutsolelos, A. G. C. J. Cabon Res., 2019, 5, 57.
- 51. Stangel, C.; Schubert, C.; Kuhri, S.; Rotas, G.; Margraf, J. T.; Regulska, E.; Clark, T.; Torres, T.; Tagmatarchis, N.; Coutsolelos, A. G.; Guldi, D. M Tuning the reorganization energy of electron transfer in supramolecular ensembles metalloporphyrin, oligophenylenevinylenes, and fullerene and the impact on electron transfer kinetics. *Nanoscale*, **2015**, *7*, 2597.
- 52. Hiroto, S.; Miyake, Y.; Shinokubo, H. Synthesis and Functionalization of Porphyrins through Organometallic Methodologies. *Chem. Rev.*, **2017**, *117*, 2910.
- 53. Moore, T. A.; Gust, D.; Mathis, P.; Mialocq, J. C.; Chachaty, C.; Bensasson, R. V.; Land, E. J.; Doisi, D.; Liddell, P. A.; Lehman, W. R.; Nemeth, G. A.; Moore, A. L.

- Photodriven charge separation in a carotenoporphyrin–quinone triad. *Nature*, **1984**, 307, 630.
- 54. Imahoi, H.; Guldi, D. M.; Tamaki, K.; Yoshida, Y.; Luo, C.; Sakata, Y.; Fukuzumi, S. Charge Separation in a Novel Artificial Photosynthetic Reaction Center Lives 380 ms *J. Am. Chem. Soc.*, **2001**, *123*, 6617.
- 55. Birel, Ö.; Nadeem, S.; Duman, H. Porphyrin-Based Dye-Sensitized Solar Cells (DSSCs): a Review *J Fluoresc.*, **2017**, *27*, 1075.
- 56. (a) Hagfeldt, A.; Boschloo, G.; Sun, G.; Kloo, L.; Pettersson, H. Dye-Sensitized Solar Cells. Chem. Rev. 2010, 110, 6595 (b) Green, M. A. Third Generation PhotoVoltaics: Advanced Solar Energy Conversion; Springer-Verlag: Berlin, Heidelberg, 2003. (c) Zhang, Y.; Higashino, T.; Imahori, H. J. Mater. Chem., A. DOI: 10.1039/d2ta09264f.
- 57. O'Regan, B.; Grätzel, M. A low-cost, high-efficiency solar cell based on dye-sensitized colloidal TiO<sub>2</sub> films. *Nature*, **1991**, *353*, 737.
- 58. Kay, A.; Grätzel, M. Artificial Photosynthesis. 1. Photosensitization of 2 Solar Cells with Chlorophyll Derivatives and Related Natural Porphyrins. *J. Phys. Chem.*, **1993**, 97, 6272.
- 59. Lee, C.-W.; Lu, H.-P.; Lan, C.-M.; Huang, Y.-L.; Liang, Y.-R.; Yen, W.-N.; Liu, Y.-C.; Lin, Y.-S.; Diau, E. W.-G.; Yeh, C.-Y. Novel zinc porphyrin sensitizers for dyesensitized solar cells: synthesis and spectral, electrochemical, and photovoltaic properties. *Chem. Eur. J.*, **2009**, *15*, 1403.
- 60. Yella, A.; Lee, H.-W.; Tsao, H. N.; Yi, C.; Chandiran, A. K.; Nazeeruddin, M. K.; Diau, E. W.-G.; Yeh, C.-Y.; Grätzel, M. Porphyrin-Sensitized Solar Cells with Cobalt (II/III)—Based Redox Electrolyte Exceed 12 Percent Efficiency *Science* **2011**, *334*, 629.
- 61. Mathew, S.; Yella, A.; Gao, P.; Humphry-Baker, R.; Curchod, B. F. E.; Ashari-Astani, N.; Tavernelli, I.; Rothlisberger, U.; Nazeeruddin, M. K.; Grätzel, M. Dye-sensitized solar cells with 13% efficiency achieved through the molecular engineering of porphyrin sensitizers *Nature Chem.*, **2014**, *6*, 242.
- 62. Sarma, T.; Panda, P. K.; Setsune, J.-i. Bis-naphthobipyrrolylmethene derived BODIPY complex: an intense near-infrared fluorescent dye. *Chem. Commun.*, **2013**, *49*, 9806.

# **CHAPTER 2 Materials and Methods**

#### **General Experimental Methods and Techniques**

This chapter provides a detailed account of the chemicals used, instrumentation and methods followed for various studies. Also, the procedures used for the purification of solvents and chemicals are described. Further, we have elaborated about the synthetic procedures of known compounds employed during the course of our investigations.

#### 2.1 General experimental

#### **2.1.1 Solvents**

#### 2.1.1.1 Solvent for reactions<sup>1</sup>

Chloroform, DCM, DCE and DMF were dried by distillation over calcium hydride. THF was dried by passing through column of activated alumina, followed by distillation over sodium metal, in presence of benzophenone as indicator. Toluene, hexane and octane were refluxed with sodium and benzophenone until blue colour persists and distilled before use. Pyridine and triethylamine were dried over KOH pellets and distilled before use. Methanol was dried by refluxing with sodium and then distilling or refluxing with magnesium activated with iodine followed by distillation.

#### 2.1.1.2 NMR solvents

Chloroform-d, DMSO- $d_6$  and THF- $d_8$ , were purchased from Sigma Aldrich/ SYNMR private limited and directly used for spectroscopic purpose.

#### 2.1.1.3 Solvents for optical measurement

DCM (spectroscopy grade) were purchased from Merck and dry THF used.

#### 2.1.2 Reagents

B<sub>2</sub>Pin<sub>2</sub>, dtbpy, PdCl<sub>2</sub>(PPh<sub>3</sub>)<sub>2</sub>, CuI, NaH, CaH<sub>2</sub>, BF<sub>3</sub>.OEt<sub>2</sub>, benzophenone, 4-hexyloxyaniline, 4hexylaniline, 1-bromo-4-hexylbenzene, 1-bromo-4-hexyloxybenzene, 4-iodobenzaldehyde, AsPh<sub>3</sub>, DPEPhos, DPPF, Na<sup>t</sup>OBu, DDQ, TIPSAcetylene, Pd<sub>2</sub>(dba)<sub>3</sub>, Pd(PPh<sub>3</sub>)<sub>4</sub>, TBAF and Pd(OAc)<sub>2</sub> were bought from Sigma-Aldrich® and used as such. THF and Et<sub>3</sub>N was purchased from Finar chemicals. Pyridine, toluene, DCE, NBS, DMF, DCM, CHCl<sub>3</sub>, DMSO, MeOH, TMEDA, TFA, InCl<sub>3</sub>, ethylene glycol, and pyrrole were purchased Merck/SRL/Finar/Avra/TCI. PPh3 and sodium were purchased from Finar chemicals. All the inorganic salts, mineral acids, NaOH, MgSO<sub>4</sub>.7H<sub>2</sub>O, K<sub>2</sub>CO<sub>3</sub>, Na<sub>2</sub>SO<sub>4</sub>, KOH, anhydrous MgSO<sub>4</sub>, KOH, Na<sub>2</sub>S<sub>2</sub>O<sub>3</sub>.5H<sub>2</sub>O, NaHCO<sub>3</sub>, Zn(OAc)<sub>2</sub>.2H<sub>2</sub>O and solvents used for the routine laboratory work, were purchased from Merck, India.

#### 2.2 Chromatography

Thin layer chromatography was performed on pre-coated TLC Silica gel 60 F<sub>254</sub> on aluminium sheet, purchased from Merck. Column chromatography was carried out on silica gel (100-200 mesh) purchased from Merck/SRL/Dessica, India.

#### 2.3 Characterization and instrumentation

All the instrumentation facilities have been provided by School of Chemistry, University of Hyderabad, Hyderabad, India for the thesis work. Nuclear magnetic resonance (NMR) spectra were recorded on Bruker 400 MHz and 500 MHz. In CDCl<sub>3</sub>, TMS ( $\delta$  = 0 ppm) was used as internal standard for <sup>1</sup>H NMR spectra and for other deuterated solvents, solvent residual peak was taken as standard. Similarly, for <sup>13</sup>C NMR spectra solvent peak was taken as standard for all deuterated solvent for calibration purpose. Mass spectral data were collected by Bruker Maxis HRMS by ESI techniques and LCMS were recorded by Shimadzu-LCMS-2010 mass spectrometer both by positive and negative ionization method. IR spectra were recorded on NICOLET Is5 FT-IR spectrometer by either using KBr pellet or neat sample.

UV-vis spectra were recorded on Perkin Elmer Lambda 35 spectrophotometer. Fluorescence spectra were recorded in JASCO FP-8500 and Fluorolog-3-221 spectrofluorometer.<sup>2</sup>

The standard approach of time-correlated single-photon counting (TCSPC) was used to study time resolved photoluminescence (TRPL). Using a picosecond pulsed diode laser with an output of 405 nm, TCSPC experiments were carried out. Dilute Ludox solution, a light scattering solution was used to measure the instrument response function (IRF). To estimate emission lifetimes, TRPL curves were fitted by mono-exponential fitting parameters using the deconvolution method accompanying with the IRF. The residual calculations ( $\chi^{(2)}$ ) were used to estimate the fit's reliability. As the decay profile was multiexponential for both the dyes average lifetime was calculated using following equation<sup>3</sup>

$$\tau_{\rm av} = \sum c_i \tau_i$$

where  $\tau_i$  lifetime of the  $i^{th}$  component and  $c_i$  is the fractional contribution of the  $i^{th}$  component to the total steady state intensity which was estimated via the following equation

$$c_i = \alpha_i \tau_i / \sum \alpha_i \tau_i$$

 $\alpha_i$  is amplitude of the  $i^{th}$  component.

All steady-state measurements were carried out by using a quartz cuvette with a path length of 1 cm at ambient temperature.

Cyclic voltammetric and differential pulse voltammetric measurements were performed using CH instruments electrochemical workstation and electrodes were purchased from CH

Instruments Inc. All measurements were done in dichloromethane under the flow of nitrogen, and 0.1 M tetrabutylammonium hexafluorophosphate (TBAPF<sub>6</sub>) used as a supporting electrolyte, glassy carbon as a working electrode, platinum wire as a counter electrode and Ag/AgCl as a reference electrode were used. The redox potential was calibrated with external reference ferrocenium/ferrocene couple (0.48 V vs SCE). The redox potentials were referenced vs. saturated calomel electrode. All cyclic voltammetric data were recorded at 50 mV/sec scan rate.

#### 2.4 Computational Details

We have carried out quantum mechanical calculations using Gaussian 09 program provided by CMSD facility of the University of Hyderabad.<sup>4</sup> All calculations were carried out by DFT with Becke's three-parameter hybrid exchange functional and the Lee-Yang-Parr correlation functional (B3LYP) was used. LANL2DZ basis set was used for Zn and 6-31G(d) basis set was used for all other atoms in calculations and the molecular orbitals were visualized using Gauss view 5. Electronic spectra were calculated using TD-DFT in THF solvent using PCM model. The result of TD-DFT was analysed using GaussSum programme.<sup>5</sup>

#### 2.5 Preparation of starting materials

#### 2.5.1 Synthesis of porphyrin precursor<sup>6a</sup>

Scheme 1 Synthesis of 2.2.6b

To prepare Compound **2.2**, a mixture of paraformaldehyde (600 mg, 20 mmol) and pyrrole (28 ml, 400 mmol) was degassed with a stream of nitrogen for 10 min. The mixture was heated at 55 °C for about 10 min under nitrogen to obtain a clear solution. InCl<sub>3</sub> was then added and stirred the mixture at 55 °C for 2.5 h. The heat source was removed and triethylamine was added. The mixture was stirred for 1 h and then filtered. The filtrate was concentrated and the pyrrole was recovered. The crude product obtained after removing pyrrole was subjected to Kugelrohr distillation to give compound **2.2** (1 g, 36.6%).

Reported yield = 41%

Obtained yield = 36.6%

#### Scheme 2 Synthesis of 2.9<sup>6a</sup>

Scheme 2 Synthesis of 2.9.

Synthesis of 1,3-bis(octyloxy)benzene (2.4): A mixture of resorcinol (11 g, 0.1 mol), 1-bromooctane (69.6 mL, 0.4 mol) and K<sub>2</sub>CO<sub>3</sub> (69 g, 0.5 mol) was refluxed for 4 days in dry acetone (500 mL). The solvent was removed under reduced pressure and extracted with EtOAc (3 × 100 mL). The combined extracts were washed with water and dried over anhydrous MgSO<sub>4</sub>. After removal of solvent under reduced pressure, the product was purified by column chromatography by eluting with hexanes to give 1,3-di(octyloxy)benzene (26.5 g).

Reported yield = 79%

Obtained yield = 79%

Synthesis of 2,6-bis(octyloxy)benzaldehyde (2.5): A three-neck flask was equipped with an addition funnel and charged with compound 2.4 (10 g, 0.03 mol) and TMEDA (1.15 mL) in tetrahydrofuran (84 mL). The solution was degassed with dinitrogen for 15 min and cooled to 0 °C, and then *n*-butyllithium (22.4 mL, 1.6 M solution in hexanes 0.036 mol) was added dropwise over 20 min and allowed to stir for 3 h. After warming to room temperature, DMF (4.38 mL, 0.06 mol) was added dropwise, and the reaction mixture was stirred for an additional 2 h. The reaction was quenched with water, and the product was extracted with ether (3 × 80

mL), dried over anhydrous MgSO<sub>4</sub>, and the solvent was removed under reduced pressure. The product was recrystallized from hexanes to yield a white solid (8.67 g).

Reported yield = 80%

Obtained yield = 80%

Synthesis of 5,15-bis(2,6-bis(octyloxy)phenyl) porphyrin (2.6): Compound 2.6 was prepared by addition of trifluoroacetic acid (0.47 mL, 6.14 mmol) to a degassed solution of dipyrromethene 2.2 (1 g, 6.84 mmol) and compound 2.5 (2.5 g, 6.84 mmol) in DCM (1 L). After the solution was stirred at room temperature under dinitrogen atmosphere for 4 h, DDQ (2.33 g, 10.26 mmol) was added and the mixture was stirred for an additional 1 h. The mixture was basified with Et<sub>3</sub>N (1.16 mL) and filtered through neutral alumina. The solvent was removed under reduced pressure and the residue was purified by recrystallization from MeOH/CH<sub>2</sub>Cl<sub>2</sub> to give the product 2.6 (1.14 g) as a purple powder.

Reported yield = 30.7%

Obtained yield = 34.3%

Synthesis of [5-Bromo-10,20-bis(2,6-di-octoxyphenyl)porphinato] zinc(II) (2.7): To a stirred solution of porphyrin 2.6 (0.5 g, 0.51 mmol) in DCM (214 mL) was slowly added a solution of NBS (0.095g, 0.53 mmol) in DCM (57 mL) in a period of 6 h at 0 °C under dinitrogen. After the reaction was quenched with acetone (4 mL), the solvent was removed under reduced pressure. The residue was purified by column chromatography (silica gel) using 30% DCM/hexanes as eluent. Recrystallization from MeOH/hexane gave the product (343 mg, 63%) as a purple powder, followed by addition of bromo-porphyrin (500 mg, 0.48 mmol) and Zn(OAc)<sub>2</sub>.2H<sub>2</sub>O (1 g, 4.75 mmol) in a mixture of DCM (97 mL) and MeOH (47 mL) was stirred at room temperature for 3 h. The reaction was quenched with water (100 mL), and the mixture was extracted with DCM (2 × 100 mL). The combined extracts were washed with water and dried over anhydrous Na<sub>2</sub>SO<sub>4</sub>. The solvent was removed under reduce pressure to give the product (490 mg).

Reported yield = 98%

Obtained yield = 98%

Synthesis of [5,15-Bis(2,6-di-octoxyphenyl)-10-(triisopropylsilyl)ethynyl-porphinato] zinc(II) (2.8): A mixture of 2.7 (500 mg, 0.447 mmol), triisopropylacetylene (520 μL, 2.23

mmol), Pd(PPh<sub>3</sub>)<sub>2</sub>Cl<sub>2</sub> (63 mg, 0.089 mmol), CuI (25 mg, 0.134 mmol) and THF (25 mL) and NEt<sub>3</sub> (3 mL) taken in a Schlenk tube and gently refluxed for 2 h under dinitrogen. The solvent was removed under vacuum. The residue was purified by column chromatography (silica gel) using 30% DCM/hexanes as eluent to give the product (545 mg) as a purple solid.

Reported yield = 83%

Obtained yield = 80%

Synthesis of [5-Bromo-15-(triisopropylsilyl)ethynyl-10,20-bis(2,6-dioctoxyphenyl)porphyrinato] zinc(II) (2.9): To a stirred solution of 2.8 (600 mg, 0.493 mmol) in DCM (180 mL) and pyridine (7 mL) was added NBS (118 mg, 0.665 mmol) at 0 °C. After stirring for 1 h, the reaction was quenched with acetone (18 mL). The solvent was removed under reduced pressure. The residue was purified by column chromatography (silica gel) using 25% DCM/hexanes as eluent to give the product (478 mg, 85%).

Reported yield = 85%

Obtained yield = 85%

#### 2.5.2 Synthesis of donors

#### Scheme 3 Synthesis of 2.10 and 2.11

Synthesis of compound bis(4-hexylphenyl)amine (2.10): To a 25 ml Schlenk flask containing 4-n-hexyl-bromobenzene (297 mg, 1.22 mmol), 4-hexylaniline (200 mg, 1.12 mmol), Pd<sub>2</sub>(dba)<sub>3</sub> (51.6 mg, 0.056 mmol), 1,1'- Bis(diphenylphosphino)ferrocene (62 mg, 0.112 mmol), sodium t-butoxide (325 mg, 3.38 mmol) and anhydrous toluene (10 mL) were added under nitrogen atmosphere. The suspension was refluxed for 24 h. The mixture was concentrated under reduced pressure. The crude product was purified by silica column chromatography by eluting with 5% ethyl acetate/hexane to give a yellow liquid. (274 mg, 71.9 %).

Reported yield = 69%

Obtained yield = 71.9%

Synthesis of compound bis(4-(hexyloxy)phenyl)amine (2.11)<sup>7</sup>: To a 25 mL Schlenk tube containing 4-n-hexyloxy-bromobenzene (275 mg, 1.06 mmol), 4-nhexyloxyaniline (187.8 mg, 0.97 mmol), Pd<sub>2</sub>(dba)<sub>3</sub> (10.9 mg, 0.049 mmol), 1,1'- Bis( diphenylphosphino) ferrocene (53.9 mg, 0.097 mmol), sodium t-butoxide (280 mg, 2.916 mmol) and 10 mL of anhydrous toluene were added under nitrogen atmosphere. The suspension was refluxed for 24 h. The mixture was concentrated under reduced pressure. The crude product was purified by silica column chromatography eluted with 10% ethyl acetate/hexane to give a white fluffy solid. (232 mg, 63%)

Reported yield = 67%

Obtained yield = 63%

#### Scheme 4 Synthesis of 2.15

Synthesis of 9-hexyl-9H-carbazole (2.13): 2.13 is synthesized by using modified procedure in literature. H-carbazole (2.12, 1 g, 0.0059 mmol) and NaOt-Bu (1.7 g, 0.0179 mmol, 3 eq.) were dissolved at 0 °C in THF (100 mL). After the mixture had been stirred at 0 °C for 1 h, 1-bromohexane (0.9 mL, 0.0065 mmol, 1.1 eq) was added, and the mixture was stirred for another 3 h.  $H_2O$  (50 mL) was added, and the organic layer was removed under reduced pressure. The residue was dissolved in  $CH_2Cl_2$  (50 mL), and the aq. layer was extracted with  $CH_2Cl_2$  (2 × 50 mL). The combined organic layers were dried over  $Na_2SO_4$ , and the solvent was removed under reduced pressure. The residue was purified by column chromatography using hexane as eluent yielding 9-hexyl-9*H*-carbazole (2.13, 1.4 g) was obtained as a yellow oil.

Reported yield = 92%

Obtained yield = 92%

Synthesis of 3-bromo-9-hexyl-9H-carbazole (2.14)<sup>9</sup>: A solution of 9-hexyl-9H-carbazole (2.13) (0.5 g, 1.99 mmol, 1eq) in dry DMF (120 mL) was stirred in an ice-water bath for about 15 min and N-bromosuccinimide (318 mg, 1.791 mmol, 0.9 eq) was added to the solution

portion-wise over 1.5 h under dark. The resulting mixture was stirred at room temperature overnight. After diluted with water (100 mL), the mixture was extracted with dichloromethane and the organic phase was dried with anhydrous Na<sub>2</sub>SO<sub>4</sub>. After the removal of the solvent under reduced pressure, the crude product was purified by column chromatography on silica gel using hexane as eluent yielding **2.14** as a light-yellow oil (532 mg).

Reported yield = 81 %

Obtained yield = 81%

Synthesis of 9-hexyl-3-(4,4,5,5-tetramethyl-1,3,2-dioxaborolan-2-yl)-9H-carbazole (jb-2.15)<sup>8</sup>: Bis(pinacolato) diboron (92 mg, 0.363 mmol, 1.2eq), potassium acetate (89 mg, 0.908 mmol, 3 eq) and dichlorobis(triphenylphosphine)palladium(II) (21 mg, 0.0302 mmol, 0.1 eq) catalyst were added to a 3-bromo-N-hexylcarbazole (100 mg, 0.302 mmol) solution in toluene (3 mL). The reaction mixture was heated at 90 °C for 24 h under a nitrogen atmosphere. The crude product was extracted with dichloromethane (3 × 20 mL), and the combined extracts were dried over anhydrous sodium sulfate and concentrated under reduced pressure, excess reagents were recrystallized out from the desired product with hexane. Pure product 2.15 (82 mg) was obtained as a yellow liquid.

Reported yield = 73%

Obtained yield = 72%

#### Scheme 5 Synthesis of 2.19

1-Bromohexane, Nat/OBu DMF, Reflux DMF, Reflux 
$$C_6H_{13}$$
 DMF DMF  $C_6H_{13}$   $C_6H_{13}$ 

Synthesis of 10-hexyl-10H-phenothiazine (2.17)<sup>8</sup>: 10H-Phenothiazine (2.16, 1 g, 0.005 mmol) and NaOt-Bu (1.4 g, 0.015 mmol, 3 eq.) were dissolved at 0 °C in DMF (120 mL). After the mixture had been stirred at 0 °C for 1 h, 1-bromohexane (0.9 mL, 0.0055 mmol, 1.1 eq) was added, and the mixture was stirred for 1 h at rt. The mixture was warmed to rt and stirred for another 2 h. H<sub>2</sub>O (50 mL) was added, and the organic layer was removed under reduced pressure. The residue was dissolved in CH<sub>2</sub>Cl<sub>2</sub> (50 mL), and the aq. layer was extracted with

CHAPTER 2

 $CH_2Cl_2$  (2 × 50 mL). The combined organic layers were dried over anhydrous  $Na_2SO_4$ , and the solvent was removed under reduced pressure. The residue was purified by column chromatography on silica gel using hexane as eluent yielding 10-hexyl-10*H*-phenothiazine (2.17, 1.25 g) as a yellow oil.

Reported yield = 90%

Obtained yield = 88%

Synthesis of 3-bromo-10-hexyl-10H-phenothiazine (2.18)<sup>9</sup>: A solution of 10-hexyl-10H-phenothiazine (2.17) (0.5 g, 1.765 mmol) in dry DMF (25 mL) was stirred in an ice-water bath for about 15 min and N-bromosuccinimide (282 mg, 1.589 mmol, 0.9 eq) was added to the solution portion-wise over 1.5 h under dark. The resulting mixture was stirred at room temperature overnight. After diluted with water (100 mL), the mixture was extracted with dichloromethane and the organic phase was dried with anhydrous Na<sub>2</sub>SO<sub>4</sub>. After the removal of the solvent under reduced pressure, the crude product was purified by column chromatography on silica gel using hexane as eluent, yielding 2.18 as a light-yellow oil (514 mg).

Reported yield = 80%

Obtained yield = 78%

Synthesis of 10-hexyl-3-(4,4,5,5-tetramethyl-1,3,2-dioxaborolan-2-yl)-10H-phenothiazine (2.19)<sup>10</sup>: Bis(pinacolato)diboron (84 mg, 0.331 mmol, 1.2 eq), potassium acetate (81.2 mg, 0.827 mmol, 3 eq), **DPPF** (18 0.033 mmol, 0.12 mg, eq) and dichlorobis(triphenylphosphine)palladium(II) (23 mg, 0.0331 mmol, 0.12 eq) catalyst were added to a 3-bromo-N-hexylcarbazole (100 mg, 0.275 mmol) solution in toluene (3 mL). The reaction mixture was heated at 90 °C for 24 h under nitrogen atmosphere. The crude product was extracted with dichloromethane (3 × 20 mL), and the combined extracts were dried over anhydrous sodium sulfate and then filtered. Upon concentration under reduced pressure, excess reagents were recrystallized out from the desired product with hexane. Pure product 2.19 (80 mg, 69%) was obtained as a yellow liquid.

Reported yield = 71%

Obtained yield = 69%

#### Scheme 6 Synthesis of 2.22 and 2.23.

Synthesis of compound [5-Bis(4-hexylphenyl)amino-15-(Triisopropylsilyl)ethynyl-10,20-bis(2,6-di-octoxyphenyl)porphyrinato] Zinc(II) (2.20)<sup>6</sup>: A mixture of bis(4-hexylphenyl)amine 2.10 (0.046 g, 0.135 mmol), and 60 % NaH (0.0062g, 1.54 mmol), taken in a Schlenk tube in toluene (10 mL) and heated for 15 min. Heat source was removed and after coming to room temperature porphyrin 2.9 (0.050 g, 0.038 mmol), DPEPhos (0.0075 g, 0.014 mmol) and Pd(OAc)<sub>2</sub> (0.002 g, 0.00093 mmol) added to the reaction mixture and was gently refluxed for 4 h under nitrogen atmosphere. The solvent was removed under vacuum. The residue was purified by column chromatography (silica gel) using 20% DCM/hexanes as eluent to give the product 2.20 (0.041 g) as green solid.

Reported yield = 71%

Obtained yield = 69%

Synthesis of compound [5-Bis(4-hexylphenyl)amino-15-ethynyl-10,20-bis(2,6-bis(octyloxy)phenyl)porphyrinato] Zinc (II) (2.22): To a solution of porphyrin 2.20 (20 mg, 0.013 mmol) in dry THF (3 mL) was added TBAF (65 μL, 1M in THF). The solution was stirred at 25 °C for 30 min under nitrogen atmosphere. The mixture was quenched with water and then extracted with DCM. The organic layer was dried over anhydrous Na<sub>2</sub>SO<sub>4</sub> and the solvent was removed under reduced pressure and used as it is.

Synthesis of compound [5-Bis(4-hexyloxyphenyl)amino-15-(Triisopropylsilyl)ethynyl-10,20-bis(2,6-di-octoxyphenyl)porphyrinato] Zinc(II) (2.21): A mixture of bis(4-hexyloxyphenyl) amine 2.11 (0.050 g, 0.135 mmol), and 60 % NaH (6.17 mg, 0.154 mmol), taken in a Schlenk tube in toluene (10 mL) and heated for 15 min. Heat source was removed and after coming to room temperature followed by addition of porphyrin 2.9 (0.050 g, 0.038 mmol), DPEPhos (0.0075 g, 0.014 mmol) and Pd(OAc)<sub>2</sub> (0.0002 g, 0.0093 mmol) added to the reaction mixture and was gently refluxed for 4 h under nitrogen atmosphere. The solvent was removed under

vacuum. The residue was purified by column chromatography (silica gel) using 20% DCM/hexanes as eluent to give the product **2.21** (0.037 g, 60%) as green solid.

Melting point >300 °C; FTIR data: 2921, 1457, 1275, 1260 cm<sup>-1</sup>; <sup>1</sup>H NMR (CDCl<sub>3</sub>, 500 MHz)  $\delta_{\rm H}$  9.63 (d, J=4.5 Hz, 2H), 9.16 (d, J=4.5 Hz, 2H), 8.83 (d, J=4.5 Hz, 2H), 8.67 (d, J=4.5 Hz, 2H), 7.63 (t, J=8.5 Hz, 2H), 7.20 (d, J=8.4 Hz, 4H), 6.94 (d, J=8.5 Hz, 4H), 6.68 (d, J=8.8 Hz, 4H), 3.80 (t, J=6.5 Hz, 12H), 1.43 (m, 18H), 1.28-1.25 (m, 18H), 0.98-0.95 (m, 8H), 0.88-0.76 (m, 20H), 0.63-0.46 (m, 44H). <sup>13</sup>C NMR (CDCl<sub>3</sub>, 100 MHz)  $\delta_{\rm C}$  160.0, 152.9, 152.6, 152.0, 150.6, 150.1, 147.0, 132.1, 131.9, 130.6, 130.4, 129.8, 123.2, 121.0, 115.0, 114.2, 105.2, 99.2, 96.2, 96.1, 68.7, 68.3, 31.7, 31.4, 30.4, 29.8, 29.5, 28.6, 28.5, 25.8, 25.2, 22.7, 22.3, 19.2, 14.1, 13.9, 12.1. HRMS: m/z calcd for [M] C<sub>99</sub>H<sub>137</sub>N<sub>5</sub>O<sub>6</sub>SiZn: 1583.9624, found 1583.9627.

Synthesis of compound [5-Bis(4-hexyloxyphenyl)amino-15-ethynyl-10,20-bis(2,6-bis(octyloxy)phenyl)porphyrinato] Zinc (II) (2.23): To a solution of porphyrin 2.21 (20 mg, 0.013 mmol) in dry THF (3 mL) was added TBAF (65 μL, 1M in THF). The solution was stirred at room temperature for 30 min under nitrogen atmosphere. The mixture was quenched with water and then extracted with DCM. The organic layer was dried over anhydrous Na<sub>2</sub>SO<sub>4</sub> and the solvent was removed under reduced pressure and used as it is.

#### 2.5.3 Synthesis of BODIPY precursor<sup>12</sup>

Scheme 7 Synthesis of 2.28.

*Synthesis of 2,3-dihydrazineylnaphthalene 2.25*: To a suspension of 2,3-dihydroxynapthalene (10 g, 62.5 mmol), and hydrazine sulphate (3.3 g, 25.7 mmol) in ethanol (5 mL), hydrazine hydrate (10 mL, 206 mmol) was added, and the reaction mixture was refluxed till the product

CHAPTER 2

has precipitated out. The product was filtered under suction and further washed with ethanol to obtain the compound as white solid.

Reported yield=61%

Obtained yield= 66%

Synthesis of ethyl 4-methyl-2-oxopentanoate 2.26: Magnesium turnings (20 g, 833 mmol) and catalytic amount of iodine were taken in a dry 3-necked RB and stirred for some time under N<sub>2</sub> atmosphere till it looks brown colored indicating Mg is activated. To this, dry THF (150 mL), was added followed by slow addition of isobutyl bromide (26 mL, 206 mmol). Addition is done maintaining low temperature by keeping it in ice bath. It was stirred for 2 h. Then this mixture was added through cannula to solution of diethyl oxalate (28 mL, 206 mmol) in THF (105 mL) at -78 °C. It was further stirred for 3 h. Then reaction was quenched with dil. HCl. Organic layer was extracted with EtOAc and dried under reduced pressure. Crude mixture was distilled under reduced pressure to get pure yellow colored liquid.

Reported yield= 80%

Obtained yield= 83%

Synthesis of diethyl 2,2'-(naphthalene-2,3-diylbis(hydrazin-2-yl-1-ylidene))(2E,2'E)-bis(4-methylpentanoate) 2.27: To a suspension of 2.25 (1 g, 5.3 mmol) in ethanol (35 mL), 2.26 (2.5 g, 16 mmol) was added and stirred continuously under N<sub>2</sub> atmosphere at room temperature for 24 h. Then it was dried under reduced pressure. Excess of 2.26 was distilled out under reduced pressure. The red dense liquid thus obtained was extracted with ethyl acetate followed by a filter column over silica gel with 20% ethyl acetate in hexane as the eluent, to obtain the product as a mixture of isomers and used for next step reaction without further purification.

Synthesis of diethyl 3,8-diisopropyl-1,10-dihydrobenzo[e]pyrrolo[3,2-g]indole-2,9-dicarboxylate, 2.28: p-TSA (10 equiv.) was dried properly under vacuum till it becomes powdery. Then it was dissolved with ethanol under N<sub>2</sub> atmosphere. Then to this 2.27 (1 equiv.) was added and stirred at reflux condition for 24 h. Then it was cooled to room temperature and poured to ice bath. Then the mixture was washed with EtOAc and dried under reduced pressure. Crude mixture was purified in silica gel column chromatography using 10% ethyl acetate in hexane as the eluent to get pure off-white colored solid product.

Reported yield= 26%

Obtained yield= 30%

#### 2.6 Summary

A brief account of various solvents and chemicals used in the synthesis and different techniques and other physical and computational methods employed for characterization in our investigation, is given in this chapter. All reported compounds are synthesized and characterized by following reported procedure, which are employed as starting materials for the dissertation work, were also described here.

#### 2.7 References

- 1. Armarego, W. L. F.; Chai, C. In *Purification of laboratory chemicals*, sixth edition, Elsevier, Burlington, **2003**.
- 2. Williams, A. T. R.; Winfield, S. A.; Miller, J. N. Analyst 1983, 108, 1067.
- 3. Paul, S.; Ahmed, T.; Das, S.; Samanta, A. Effect of Lead: Halide Precursor Ratio on the Photoluminescence and Carrier Dynamics of Violet- and Blue-Emitting Lead Halide Perovskite. Nanocrystals. *J. Phys. Chem. C.*, **2021**, *125*, 23539.
- 4. Gaussian 09, (Revision C.01), Frisch, M. J. et al. Gaussian, Inc., Wallingford CT, 2010.
- 5. O'Boyle, N. M.; Tenderholt A. L.; Langner, K. M. cclib: A library for package-independent computational chemistry algorithms. *J. Comp. Chem.*, **2008**, *29*, 839
- 6. (a)Yella, A.; Lee, H.-W.; Tsao, H. N.; Yi, C.; Chandiran, A. K.; Nazeeruddin, M. K.; Diau, W.-G.; Yeh, E. C.-Y.; Grätzel, M. Porphyrin-Sensitized Solar Cells with Cobalt (II/III)—Based Redox Electrolyte Exceed 12 Percent Efficiency. *Science*, 2011, 334, 629. (b) Laha, J. K.; Dhanalekshmi, S.; Taniguchi, M.; Ambroise, A.; Lindsey, J. S. A Scalable synthesis of meso-substituted dipyrromethanes. *Org. Proc. Res. Dev.*, 2003, 7, 799.
- Kang, S. H.; Choi, I, T.; Kang, M. S.; Eom, Y. K.; Ju, M. J.; Hong, J. Y.; Kang, H. S.; Kim, H. K. Novel D–π–A structured porphyrin dyes with diphenylamine derived electron-donating substituents for highly efficient dye-sensitized solar cells *J. Mater. Chem. A.*, 2013, 1, 3977.
- 8. Reddy, M. A.; Kumar, CH. P.; Ashok, A.; Sharma, A.; Sharma, G. D.; Chandrasekharam, M. Hetero aromatic donors as effective terminal groups for DPP based organic solar cells. *RSC Adv.*, **2016**, *6*, 9023.
- 9. Bao, L. Q.; Ho, P.; Chitumalla, R. K.; Jang, J.; Thogiti, S.; Kim, J. H. Single and double branched organic dyes based on carbazole and red-absorbing cationic indolium for ptype dye sensitized solar cells: A combined experimental and theoretical investigation. *Dyes Pigm*, **2018**, *149*, 25.
- Aghazada, S.; Ren, Y.; Wang, P.; Nazeeruddin, M. K. Effect of Donor Groups on the Performance of Cyclometalated Ruthenium Sensitizers in Dye-Sensitized Solar Cells. *Inorg. Chem.* 2017, 56, 13437.
- 11. Sarma, T.; Panda, P. K.; Anusha, P. T.; Rao, S. V. Dinaphthoporphycenes: Synthesis and Nonlinear Optical Studies. *Org. Lett.*, **2011**, *13*, 188.

#### 2.8 $^{1}\text{H}$ NMR, $^{13}\text{C}$ NMR and HRMS spectra

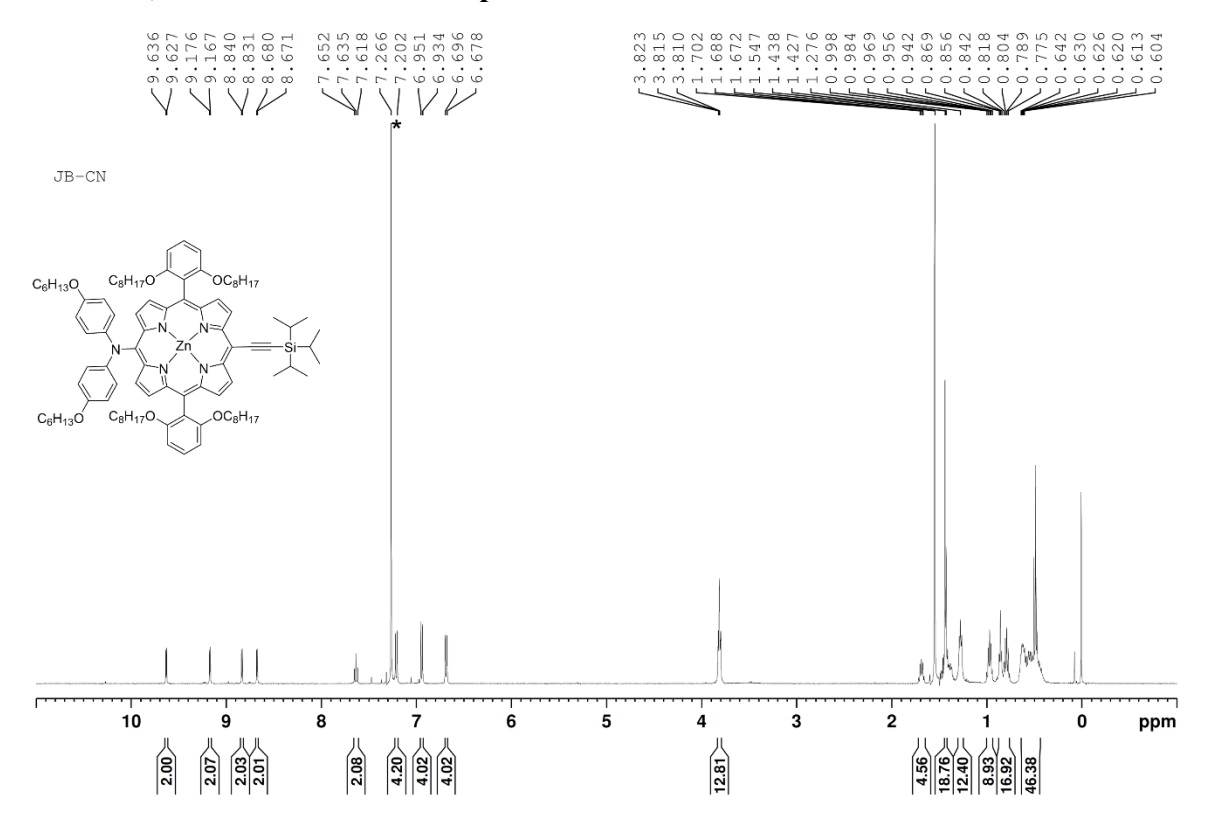


Figure 2.1 <sup>1</sup>H NMR spectrum of 2.21 in CDCl<sub>3</sub>.

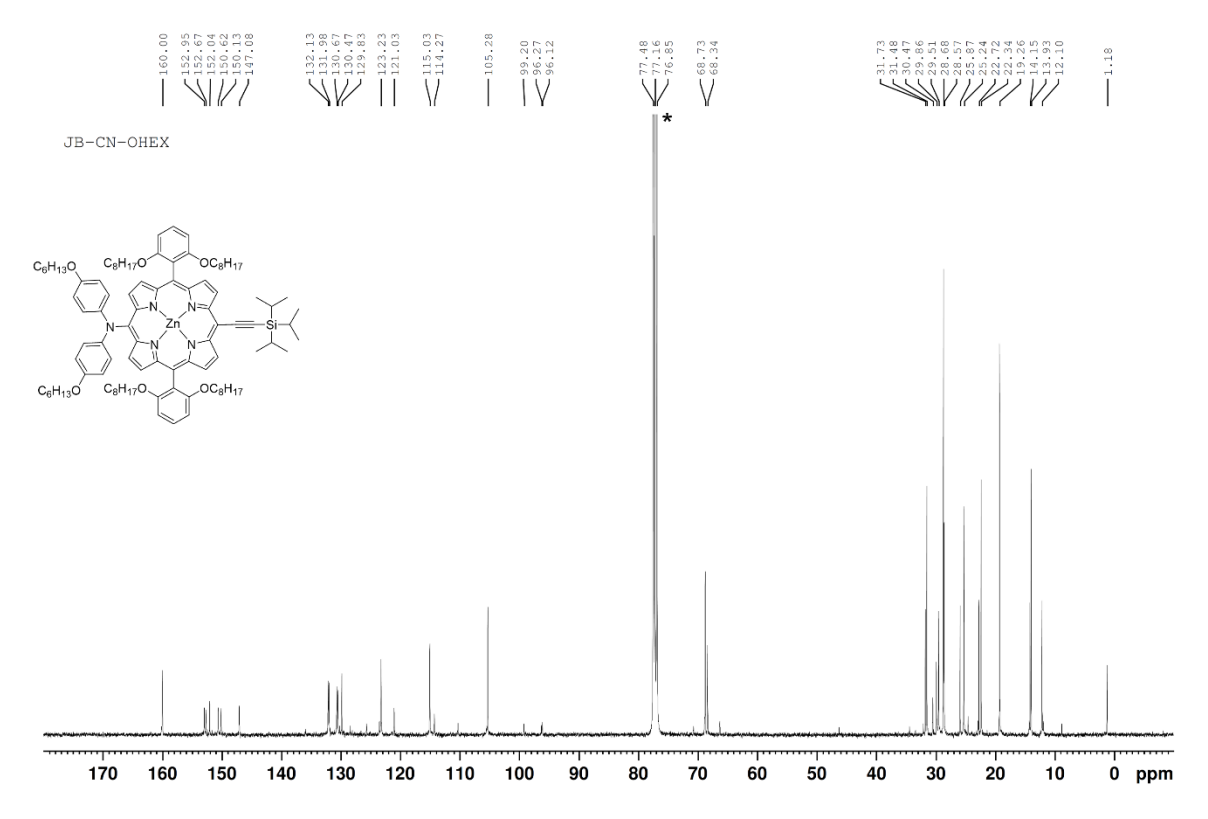
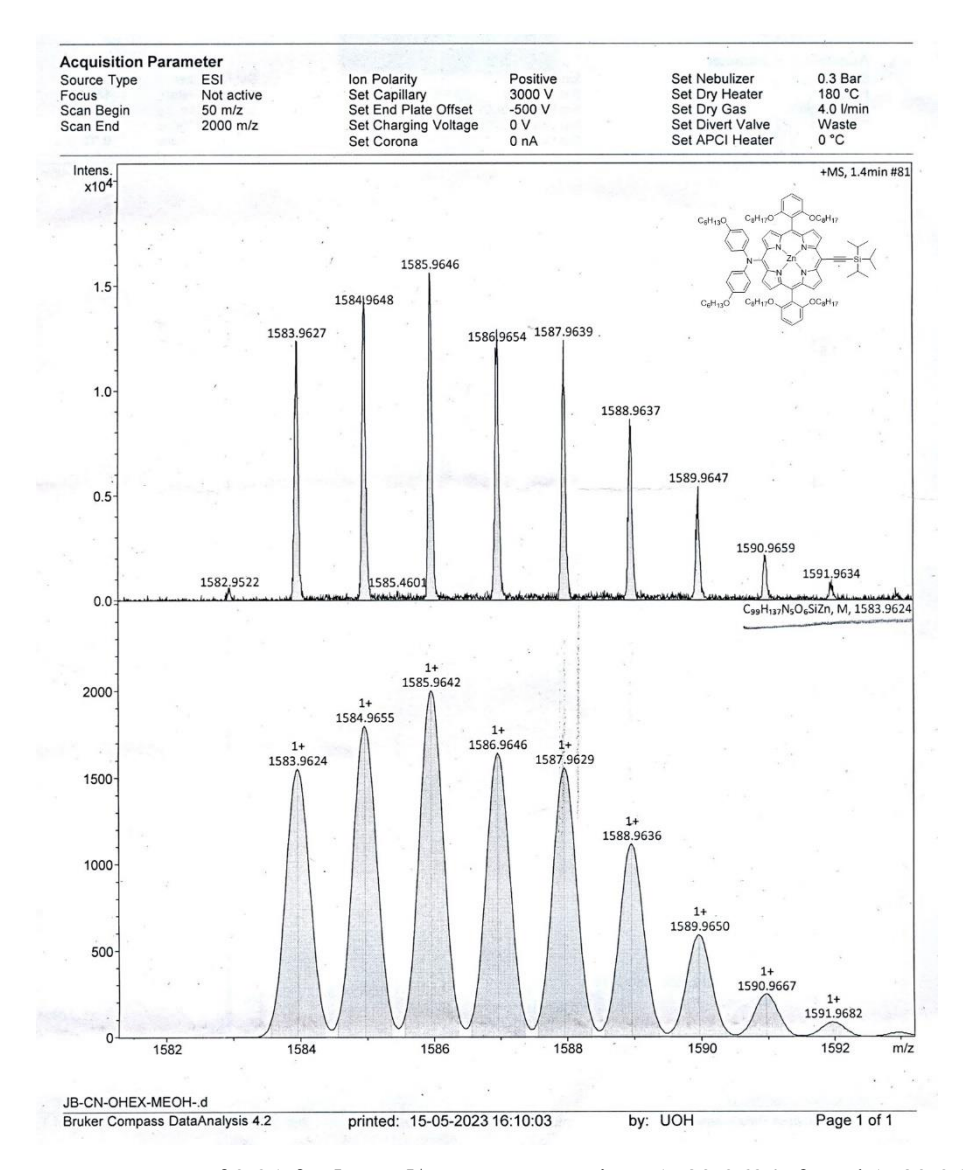


Figure 2.2 <sup>13</sup>C NMR spectrum of 2.21 in CDCl<sub>3</sub>.



**Figure 2.3** HRMS spectrum of **2.21** for  $[M+H]^+$   $C_{99}H_{138}N_5O_6SiZn$ : 1583.9624, found 1583.9627.

### **CHAPTER 3**

## Diarylamine substituted porphyrin-BODIPY conjugates

#### 3.1 Introduction

The massive growth in population, increases the consumption of fossil fuels. Thus, it is essential to develop an alternative renewable source of energy. In comparison to geothermal energy, wind energy, tidal energy and biomass energy, solar energy is the most abundant, clean and powerful source of renewable energy. Solar energy is a substantially infinite energy source and effective conversion of solar energy into electricity has been developed as an essential strategy for sustainable development. It is dominated for decades by the silicon-based devices, which covers around 90% of the PV market. In the present stage DSSC emerged as a low-cost alternative owing to its ease of fabrication, a short-energy pay-back time, low sensitivity to temperature changes and eco-friendliness after the pioneering report of Grätzel and coworkers in 1991. Although ruthenium-based dyes, 4 (e.g., N719, N3 dye) as shown in Figure 3.1 exhibit efficiencies higher than 11%, but its low abundance and high cost are major drawbacks.

Figure 3.1 Structures of ruthenium-based dyes.

Hence, scientist turn their attention towards ruthenium-free dyes. As a result, organic sensitizers,<sup>5-7</sup> in particular porphyrins, with their intense absorption in the visible region, high molar extinction coefficients and tunable electrochemical properties have enriched their presence in DSSCs, offering promising features in thin film generation.<sup>8-14</sup> Grätzel and Kay introduced chlorophyll derivatives and porphyrins as DSSC sensitizers and achieved an efficiency of 2.6% leading to the development of porphyrin based dyes.<sup>15</sup> The incorporation of a push-pull structure that are based on the donor- $\pi$ -acceptor (D- $\pi$ -A) approach are effective technique to enhance the light harvesting properties. Benchmark dyes comprising the donor- $\pi$ -bridge-acceptor (D- $\pi$ -A) structured porphyrins such as **YD2-\sigma-C8**, **SM315** and **XW73** achieved a device efficiency up to 13% (Figure 3.2).<sup>16-19</sup>

(a) (b) 
$$C_{e}H_{13}O$$
  $C_{e}H_{17}O$   $OC_{e}H_{17}$   $C_{e}H_{13}O$   $C_{e}H_{17}O$   $OC_{e}H_{17}$   $C_{e}H_{13}O$   $C_{e}H_{17}O$   $OC_{e}H_{17}$   $C_{e}H_{13}O$   $C_{e}H_{17}O$   $OC_{e}H_{17}$   $C_{e}H_{13}O$   $C_{e}H_{17}O$   $OC_{e}H_{17}$   $OC_{e}H_{17}O$   $OC_$ 

Figure 3.2 (a) YD2-o-C8, (b) SM315, and (c) XW73.

In general, the absorption properties of porphyrin and BODIPY are complementary to each other with BODIPY absorbing strongly at ~500 nm and porphyrins with intense absorption in the region of 400 nm and weaker absorption in 500-700 nm region. Thus, covalently or non-covalently linked porphyrin-BODIPY conjugates, with porphyrin and BODIPY having complementary absorption, found to cover the entire visible range of solar spectrum, with BODIPY acting as a donor and the porphyrin as an acceptor.<sup>20</sup> The first porphyrin-BODIPY conjugate as shown in **Figure 3.3(a)** was reported by Lindsey and co-workers in 1998.<sup>21</sup> The studies supported an efficient energy transfer (>90 %) from BODIPY unit to porphyrin unit in the dyad.

(a) (b) 
$$C_{12}H_{25}O$$
  $OC_{12}H_{25}$   $OC_{12}H_{25}$   $OC_{12}H_{25}$   $OC_{12}H_{25}$   $OC_{12}H_{25}$ 

Figure 3.3 Porphyrin-BODIPY Conjugate reported by (a) Lindsey group and (b) Hupp group.

Hupp and co-workers synthesised a dyad containing porphyrin fragment conjugated to a BODIPY moiety through a triple bond with benzoic acid as an acceptor.<sup>22</sup> The dye displayed an intense absorption band centred around 530 nm which is clearly coming from the BODIPY moiety and intense peaks at 450 and 650 nm from the porphyrin unit. The dyad exhibits greater solar spectroscopic coverage based on IPCE, and an improved power conversion efficiency ( $\eta = 1.55\%$ ) compared with its counterpart without the BODIPY fragment ( $\eta = 0.84\%$ ). The enhanced efficiency of BODIPY-Zn(II)porphyrin dyad (**Figure 3.3 (b)**) was primarily attributed largely to the achievement in spectroscopic absorbance provided by the BODIPY fragment in the dyad.

Galateia and co-workers applied another strategy and appended two BODIPY moieties to a porphyrin and synthesized a triad, where two BODIPY chromophores covalently bridge a metal-free porphyrin unit via a 1,3,5-triazine moiety (**PorCOOH(BDP)**<sub>2</sub>) as shown in **Figure 3.5(a)**.<sup>23</sup> The dye display intense absorption around 500 nm, which corresponds to the absorption of the BODIPY. Using pristine TiO<sub>2</sub> (device A) yielded a PCE of 5.17%, and using rGO/TiO<sub>2</sub> (device B) photoanodes sensitised by the porphyrin-BODIPY triad yielded a PCE of 6.20%.

Odobel and co-workers further covalently linked a squaraine unit (SQT) to a porphyrin linked BODIPY as an acceptor. They have synthesized trichromophoric supramolecular sensitizer (Figure 3.5 (b)), based on the antenna effect, for DSSCs. In this trichromophore, the light harvesting agent are BODIPY and ZnP, whereas the squaraine unit acts as acceptor and it will inject electron injection into TiO<sub>2</sub>. Because of the high molar extinction coefficients squaraine unit was chosen as sensitizer along with that the low-lying excited state which will benefit it both as final energy acceptor and as electron injector. Three chromophoric subunits viz SQT (Squaraine unit), D (Porphyrin unit linked to squarine moiety) and T (Figure 3.4 (d)) have shown absorption spectra complementary to each other and thus cover a wide window of the solar spectrum (Figure 3.5 (b)). The cell achieved an overall PCE of 3.9%.<sup>24</sup>

**Figure 3.4** Porphyrin-BODIPY Conjugates reported by (a) Galateia group and (b) Odobel group.

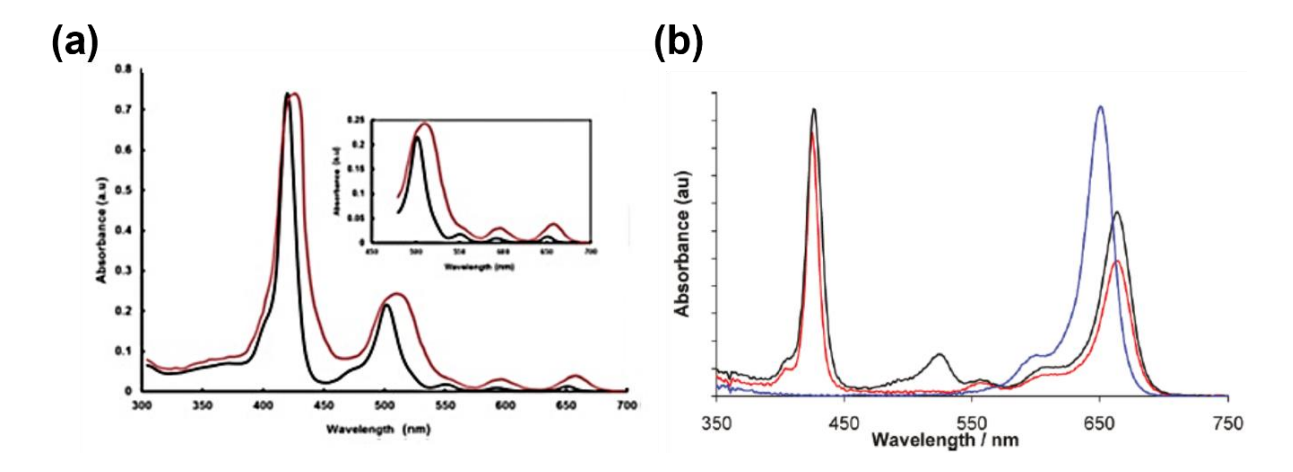


**Figure 3.5** (a) Normalized UV-visible absorption spectra of **PorCOOH-(BDP)**<sup>2</sup> in THF solution (black line) and adsorbed onto TiO<sub>2</sub> film (red line). (b) Absorption spectra of **SQI** (blue solid line), **D** (red solid line), and **T** (black solid line) recorded in THF.

#### 3.2 Research goal

In the examples cited above, most of them lack even reasonable absorption in the NIR region where the solar flux of photons is quite significant, thus limiting further enhancement of their efficiency in order to realize highly-efficient devices. BODIPY acts as a donor and porphyrin is playing the role of acceptor. So, in order to capitalize the NIR region of the spectrum, we intended to utilize our photo-stable and intensely absorbing naphthobipyrrole-derived BODIPY dye, <sup>25,26</sup> which, because of its unique photophysical properties in the NIR region, should make an ideal acceptor when attached with the porphyrin dyes. As the porphyrin dyes with D- $\pi$ -A structure have shown higher efficiencies, we have opted for the hexyloxy and hexyl groups appended diarylamine as donor, because of their stronger electron donating capability as well as the long alkyl and alkoxy chains suppressing dye aggregation.<sup>27,28</sup> The alkoxy chains endowed on the periphery of the diarylamine donor may also enhance electron-donating ability.<sup>29,30</sup> Diarylamine donor is expected to be more stable in its excited state due to the delocalization of the excited radical in the π-system. Bis(octyloxy)phenyl groups substituted on the porphyrin  $\pi$ -bridge may reduce the charge recombination process between iodine/triiodide moieties and the oxidized dye.<sup>31</sup> The BODIPY unit, incorporated with two acid groups for better anchoring, was conjugated with the donor substituted porphyrin moiety to design the novel porphyrin-BODIPY conjugates JB-1 and JB-2 as shown in Figure 3.6. To our knowledge, this is the first example of porphyrin-BODIPY conjugate, where the substituted porphyrin acts as a donor and the BODIPY moiety enacting as the role of an acceptor. These new dyes JB-1 and JB-2 provide a novel strategy for designing efficient porphyrin-BODIPY conjugates and are expected to cover the entire visible portion of the solar spectrum along with NIR region. This should result in much higher solar energy-to-electricity conversion efficiency  $(\eta)$  and help make efficient solar cell.

Figure 3.6 Porphyrin-BODIPY Conjugates, JB-1 and JB-2.

#### 3.3 Results and discussion

#### 3.3.1 Synthesis

Naphthobipyrrole diester **2.27**, the starting material for the acceptor BODIPY unit, was prepared according to our previously reported method.<sup>32</sup> The diester was partially hydrolysed in presence of sodium hydroxide and ethanol to synthesize the ester-acid derivative of naphthobipyrrole **JB-3.1** in 55% yield, which was in turn decarboxylated by refluxing in ethylene glycol to afford naphthobipyrrole monoester **JB-3.2** in 97% yield (**Scheme 1**). Subsequently, the monoester **JB-3.2** was condensed with 4-iodobenzaldehyde to obtain the dipyrromethane derivative **JB-3.3** in 42% yield, which was further oxidized with DDQ and treated with BF<sub>3</sub>.OEt<sub>2</sub> to obtain the naphthobipyrrole-derived BODIPY **JB-3.4**.

Scheme 1 Synthesis of Porphyrin-BODIPY Conjugates JB-1 and JB-2.

Subsequently, BODIPY diester **JB-3.4** was subjected to Sonogashira coupling with porphyrin **2.23** to synthesize the porphyrin-BODIPY conjugate **JB-3.6** in 60% yield. Though the hydrolysis of ester groups of **JB-3.6** resulted in the formation of the desired product, the TLC profile was complicated to isolate the clean product.

Therefore, we performed the hydrolysis of the BODIPY diester **JB-3.4** with aq. KOH in a mixture of THF and ethanol to yield the diacid-anchoring groups appended bisnaphthobipyrrole-derived BODIPY acceptor **JB-3.5** in 78% yield. Finally, the diacid **JB-3.5** was successfully attached to the donor appended porphyrin moieties **2.22** and **2.23** via Sonogashira coupling in presence of Pd<sub>2</sub>(dba)<sub>3</sub>, AsPh<sub>3</sub> and Et<sub>3</sub>N in THF leading to the formation of the desired porphyrin-BODIPY conjugates **JB-1** and **JB-2** in 42 and 60 % yield, respectively as shown in **Scheme 1**.<sup>33</sup> We have also synthesized the reported **YD2-***o***-C8** as per the literature method for reference.<sup>4</sup>

#### 3.3.2 UV-Vis-NIR and fluorescence studies

The photophysical properties of the porphyrin-BODIPY conjugates **JB-1** and **JB-2** were studied in THF solvent at room temperature as shown in **Figure 3.7**. The absorption spectra show the Soret band of these two dyes at 448 and 442 nm, respectively, which is similar to that of sensitizer **YD2-o-C8** (fwhm: 1758.3 cm<sup>-1</sup>), however they are much broader with fwhm of 2410.8 and 2599.63 cm<sup>-1</sup> for **JB-1** and **JB-2**, respectively. On the other hand, the introduction of the BODIPY acceptor unit had a significant impact on the absorption spectra of the dyes, most evident being the lowest energy bands, for example, absorbance of both the dyes shows an enhancement from 500 nm onwards. While **JB-1** shows two bands at 648 and 675 nm, **JB-2** exhibits a band at 670 nm, those are more intense than the corresponding donor porphyrins Q-bands (**Table 3.1**).

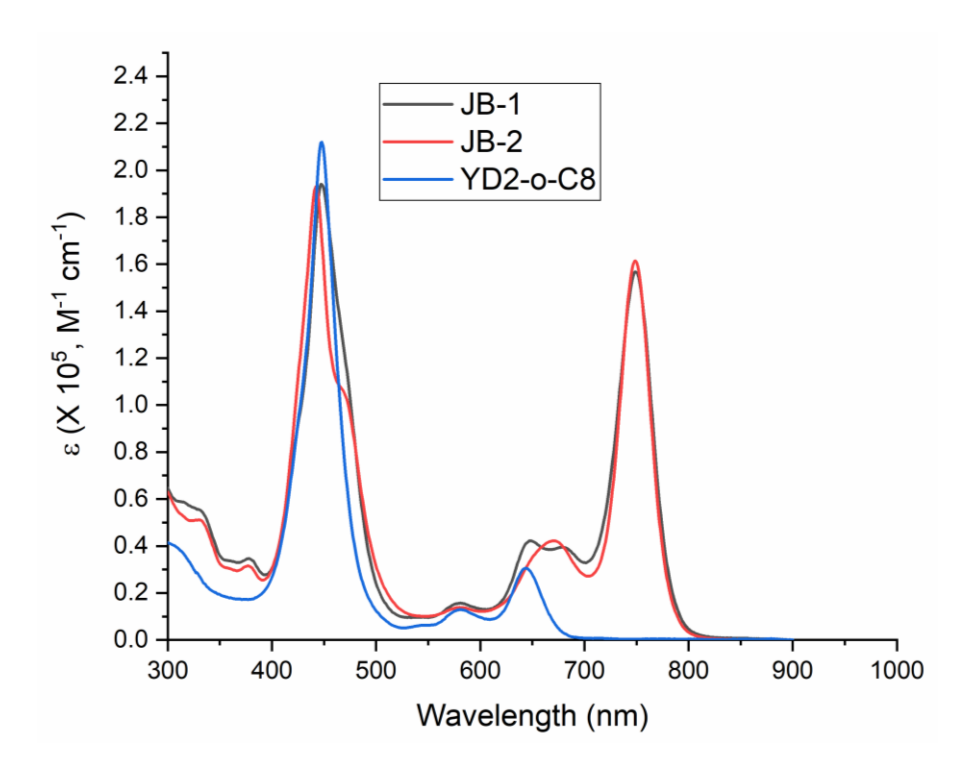


Figure 3.7 Absorption spectra of JB-1 and JB-2 in comparison with YD2-*σ*-C8 in THF.

In addition, both the dyes display a large intensified lowest energy band with maxima at 750 nm, which is significantly red-shifted compared to **YD2-σ-C8**. This band is almost 80% as intense as the Soret band with the tail extending beyond 800 nm region of the absorption spectra. These new dyes exhibit non-zero absorption in the entire range of 300-800 nm. Thus, they fall into a unique class of dyes which are not only panchromatic but in addition absorb a good amount of solar flux in the NIR region. The shift in the absorption spectra of sensitizers **JB-1** and **JB-2** is mainly due to the presence of extended π-conjugation in its molecular structure. This can be realized from the comparison of UV-Vis spectra of donor appended porphyrin with the porphyrin-BODIPY Conjugates, **JB-1** and **JB-2**.

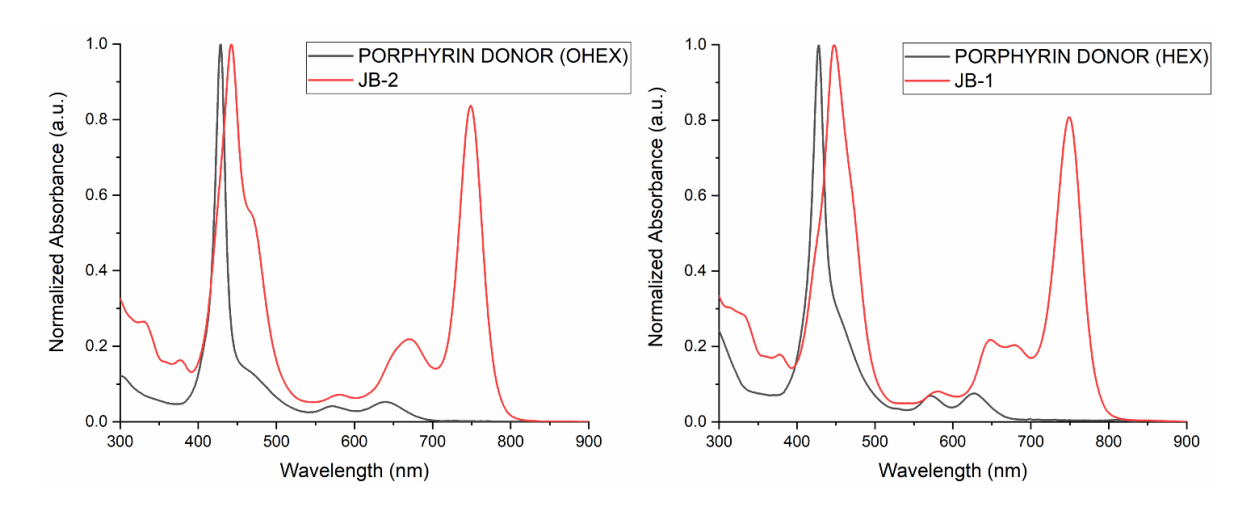


Figure 3.8 Absorption spectra of JB-1 and JB-2 in comparison with donor appended porphyrin in THF.

As it can be seen clearly that after the attachment of NIR absorbing BODIPY moiety there is a bathochromic shift in the absorption with lowest energy band extending up to 800 nm with respect to w.r.t. donor appended porphyrin **2.12** and **2.13**.

**Table 3.1** Absorption data for different porphyrin **2.6**, **2.12**, **2.13** and Meso-free BODIPY in DCM and acceptor BODIPY, **JB-1** and **JB-2** in THF.

Dye	Absorption peaks (nm)
5,15-diaryl porphyrin ( <b>2.6</b> )	412 (λ <sub>max</sub> ), 502, 535, 576, 631
Porphyrin donor (hexyl) (2.12)	428 (λ <sub>max</sub> ), 572, 627
Porphyrin donor (hexyloxy) (2.13)	429 (λ <sub>max</sub> ), 571, 640
Meso-free BODIPY [3]	727 (λ <sub>max</sub> )
Acceptor BODIPY (3.6)	746 (λ <sub>max</sub> )
JB-1	448 (λ <sub>max</sub> ), 648, 750
JB-2	442 (λ <sub>max</sub> ), 670, 749

To understand the emission properties of the conjugates, first the emission of the individual moieties i.e., two donors (2.10 and 2.11) and BODIPY acceptor (JB-3.5) were checked in a polar solvent (THF) and a nonpolar solvent (toluene). The fluorescence spectra of the three units as shown in **Figure 3.9** have no significant change in their emission pattern in two different solvents.

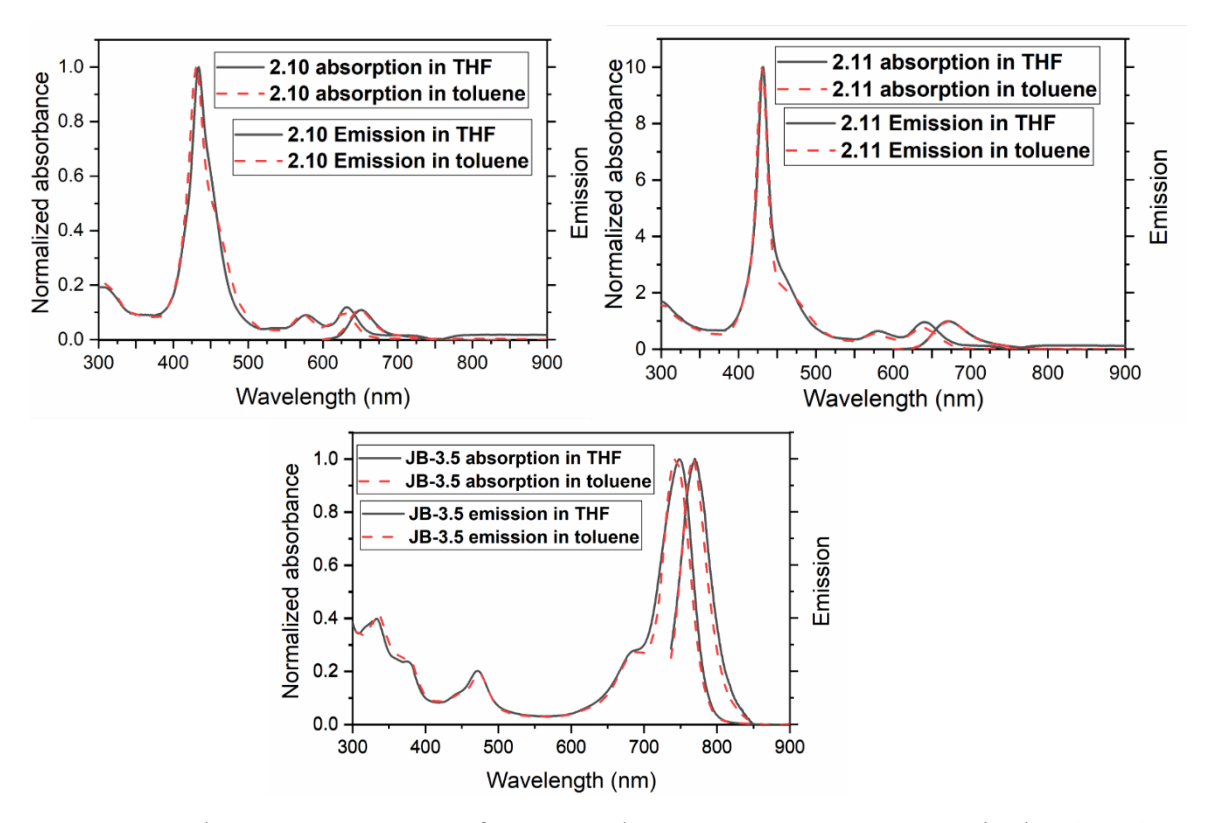


**Figure 3.9.** Fluorescence spectra of compounds **2.10**, **2.11** and **JB-3.5** excited at 433, 432 and 748 nm, respectively in THF (black solid line) and in toluene (dash red line).

But emission properties of the dyes **JB-1** and **JB-2** measured in THF solvent at room temperature by exciting at their respective Soret bands as shown in **Figure 3.10** (a) exhibits dual bands. The first band is corresponding to the emission from the porphyrin moiety and the second band is from the BODIPY acceptor indicating that probably in THF the molecule is behaving like independent moieties. The quantum yields of **JB-1** and **JB-2** in THF were found to be ( $\phi_f = 0.0043$ ) for **JB-1** and ( $\phi_f = 0.0030$ ) for **JB-2**. Interestingly, in toluene as shown in **Figure 3.10** (b), the emission band corresponding to the porphyrin is quenched with a major band coming from the BODIPY acceptor with high intensity and an increased quantum yield ( $\phi_f = 0.025$ ) for **JB-1** and ( $\phi_f = 0.016$ ) for **JB-2**. This type of phenomena with an altered emission in different solvents is probably due to the intramolecular charge transfer transition process occurring from donor appended porphyrin to BODIPY acceptor moiety.

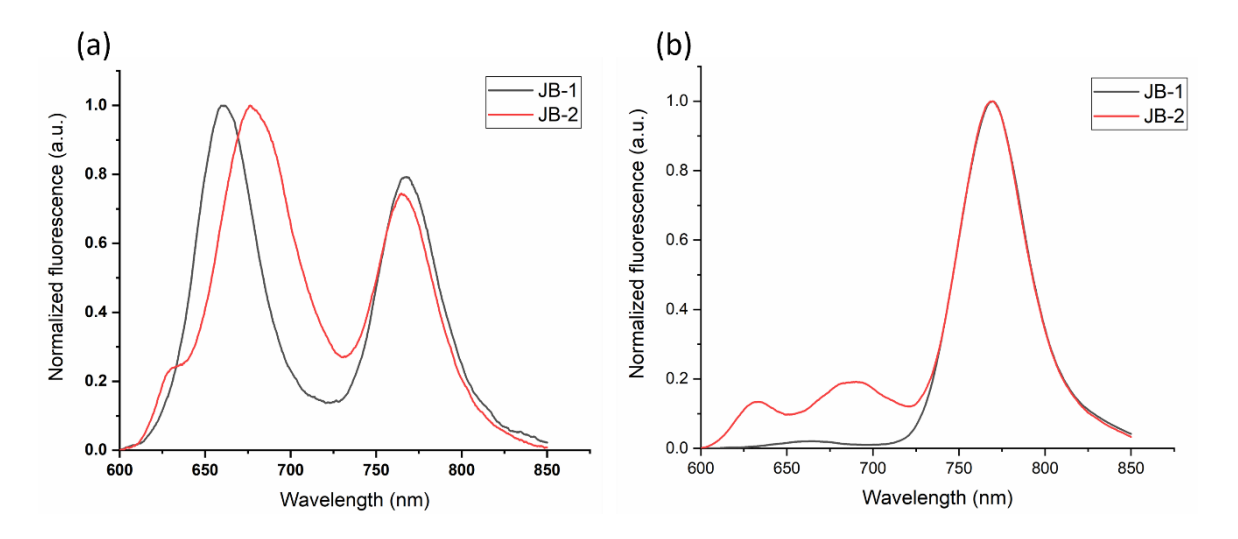
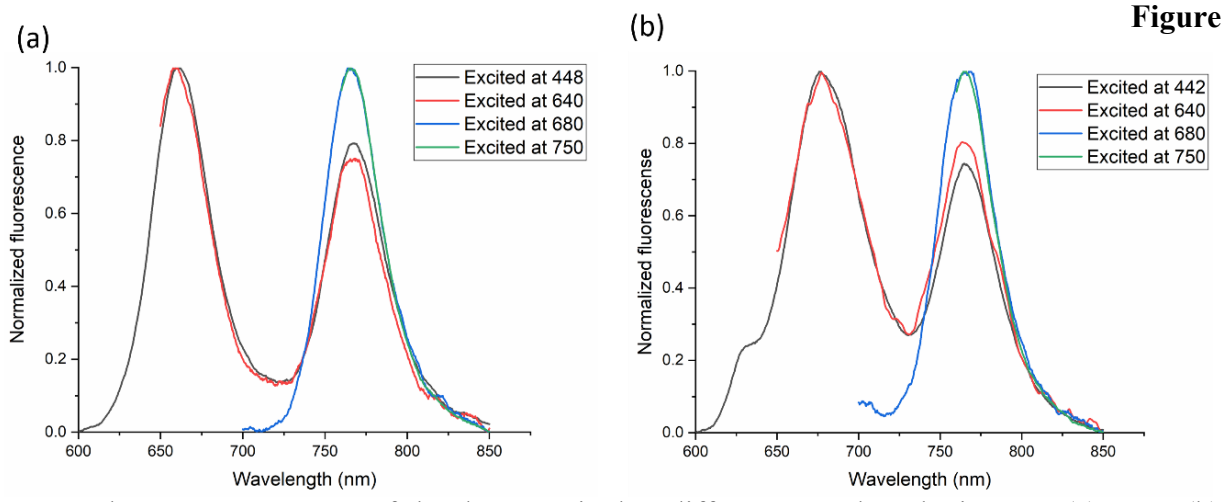


Figure 3.10. Fluorescence spectra of dyes JB-1 and JB-2, excited at their respective Soret bands at 448 and 442 nm, respectively. (a) in THF (b) in toluene.

Fluorescence studies of the porphyrin-BODIPY conjugates excited at different wavelengths including BODIPY absorption band in THF and toluene leads to the same emission pattern, further confirming the role of BODIPY as acceptor, as shown in **Figure 3.11** and **3.12**.



**3.11**. Fluorescence spectra of the dyes, excited at different wavelengths in THF (a) **JB-1** (b) **JB-2**.

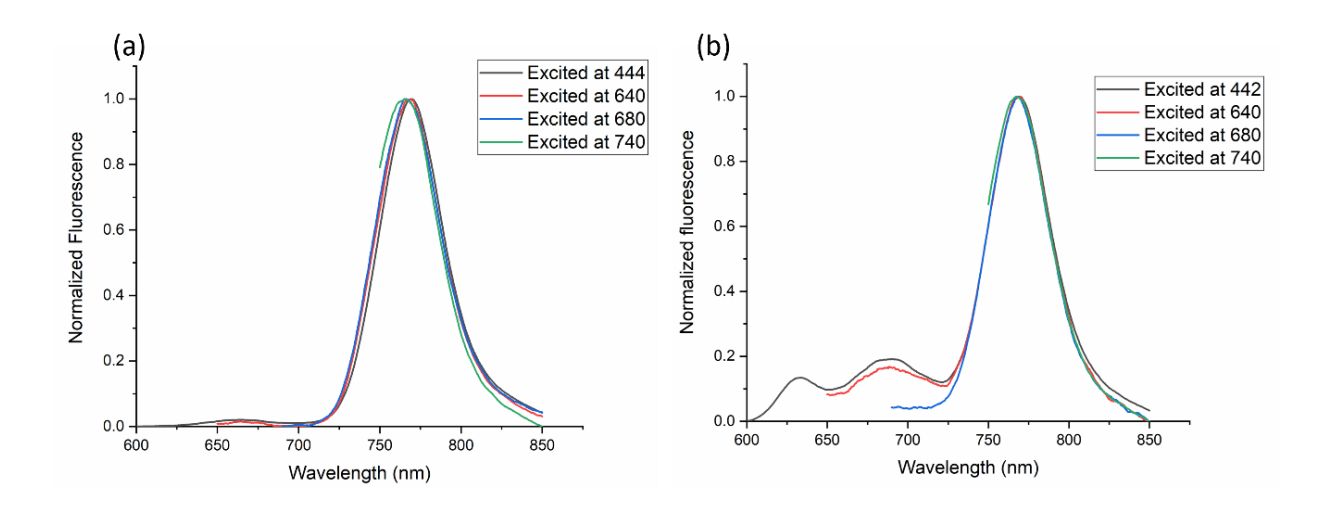
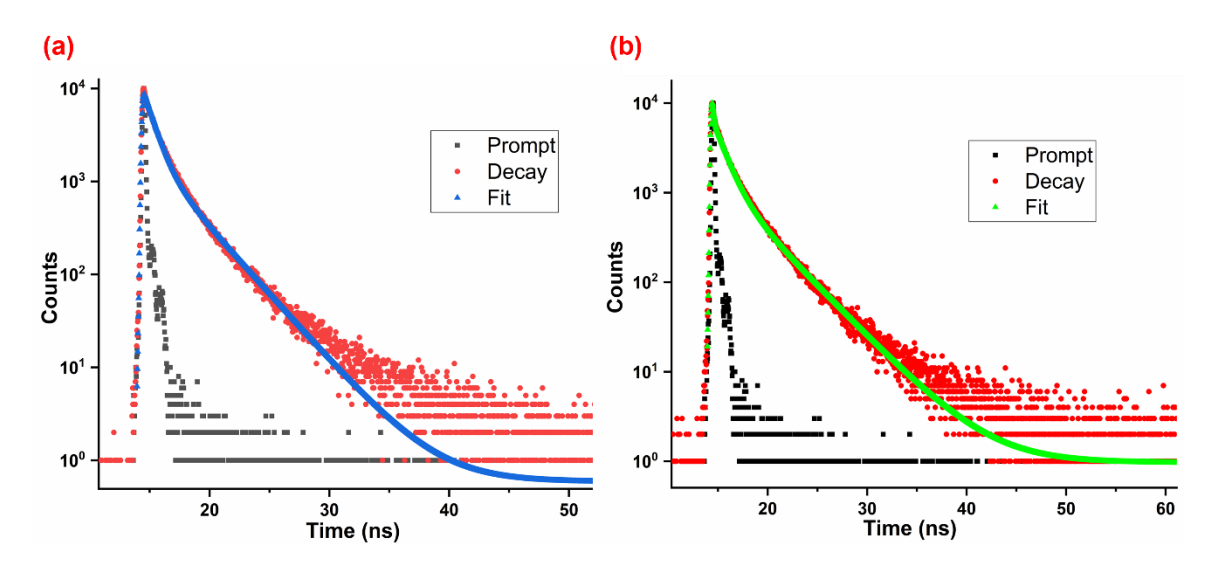


Figure 3.12. Fluorescence spectra of the dyes, excited at different wavelengths in toluene (a) JB-1 (b) JB-2.

Photoluminescence decay as shown in **Figure 3.10** was measured using time-correlated single-photon counting with a picosecond pulsed diode laser ( $\lambda_{exc}$ =405 nm). Decay profile of **JB-1** and **JB-2** were found to be bi- and tri- exponential, respectively with an average lifetime of 1.8 and 2.1 ns, respectively.



**Figure 3.13.** Fluorescence decay profile of: a) **JB-1**; b) **JB-2** recorded in chloroform ( $\lambda_{exc}$ = 405 nm).

## 3.3.3 DFT studies

We have carried out quantum mechanical calculations using Gaussian 09 program provided by CMSD facility of University of Hyderabad.<sup>34</sup> All calculations were carried out by density functional theory (DFT) with Becke's three-parameter hybrid exchange functional and the Lee-Yang-Parr correlation functional (B3LYP) was used. LANL2DZ basis set was used for Zn and 6-31G(d) basis set was used for all other atoms in calculations and the molecular orbitals were visualized using Gauss view 5. Electronic spectra were calculated using TD-DFT in THF solvent using PCM model. The result of TD-DFT was analyzed using GaussSum programme.<sup>35</sup> The **Figure 3.11** clearly depicts that the porphyrin and BODIPY units of the dyes **JB-1** and **JB-2** are not in the same plane, which is advantageous for reducing dye aggregation. Porphyrin and BODIPY exhibit a dihedral angle of 85.31° for **JB-1** and 80.83° for **JB-2**, which is advantageous for reducing dye aggregation (**Figure 3.12**). This makes our designed dyes more promising compared to well-studied planar phthalocyanine-based dyes,<sup>36,37</sup> which although display similar intense lowest energy absorption bands like naturally occurring chlorophylls and bacteriochlorophylls, albeit much blue-shifted (λ<sub>max</sub> ~ 680-700 nm).<sup>38,39</sup>

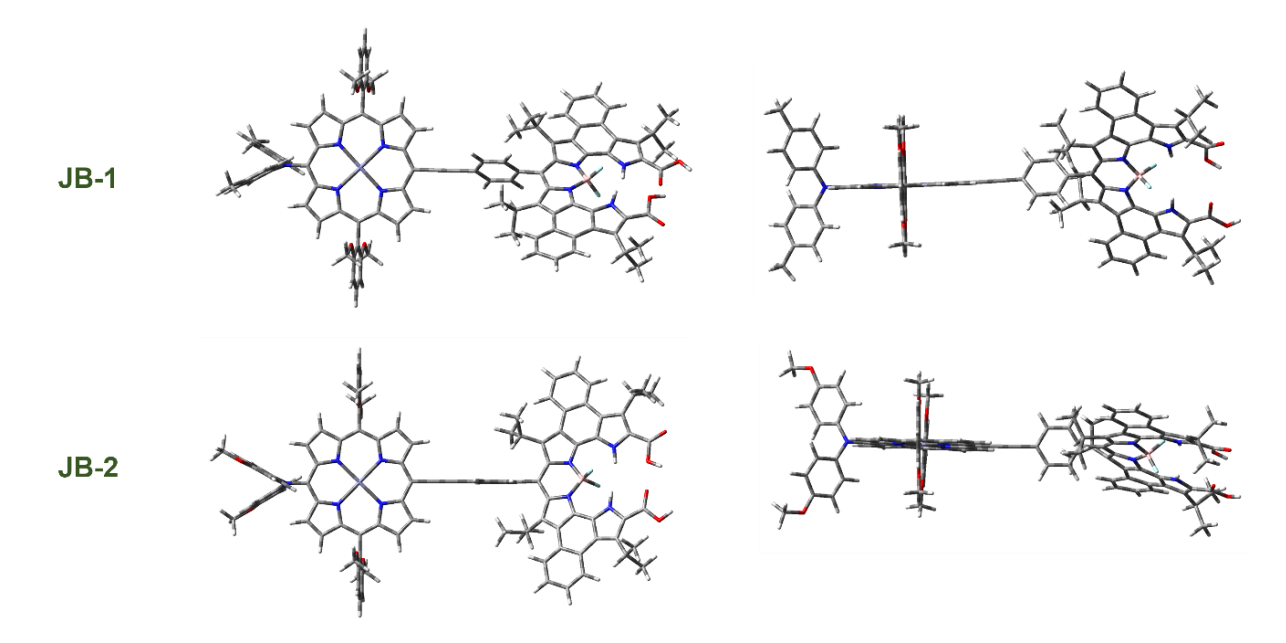


Figure 3.14. DFT optimized structures of dyes JB-1 and JB-2.

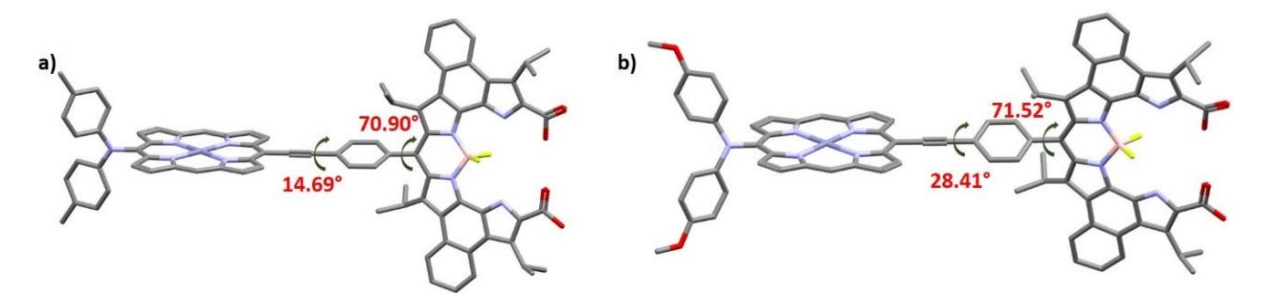
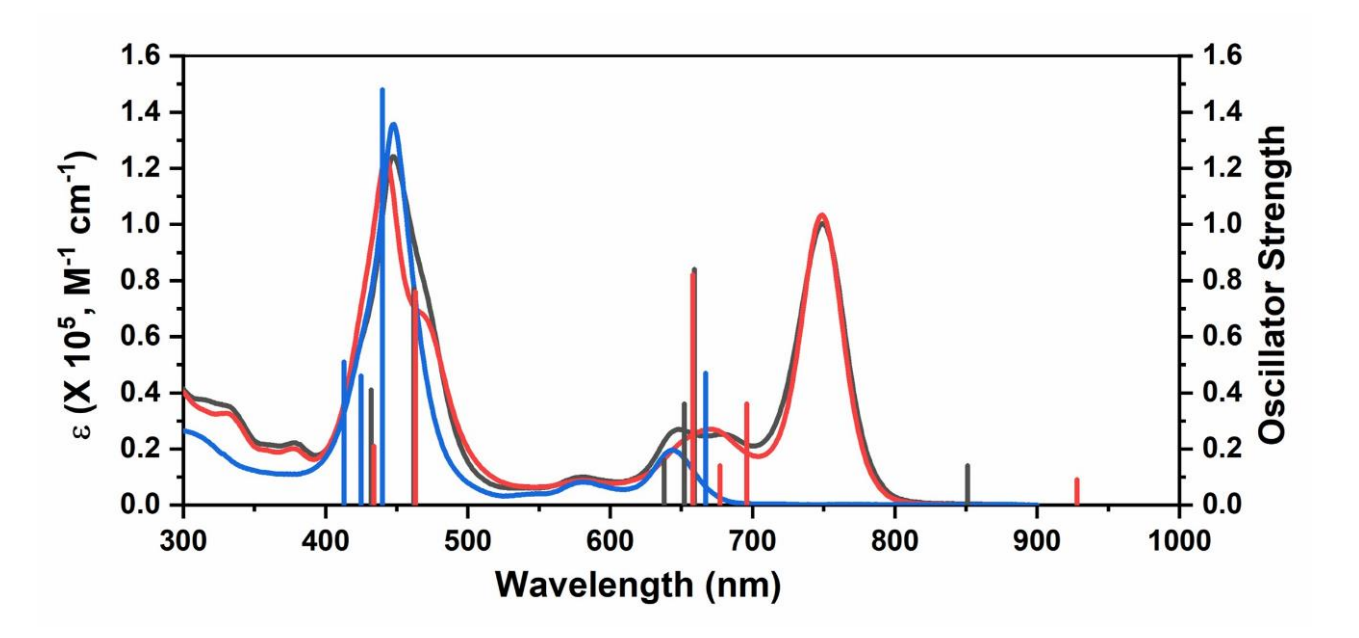


Figure 3.15. DFT optimized structures of dyes (a) JB-1 and (b) JB-2 with dihedral angle between porphyrin, phenyl and BODIPY planes.

We have run TD-DFT computations and stimulated theoretical absorption spectra for the **JB-1** and **JB-2** in order to acquire more understanding and compared with the previously reported **YD2-***o***-C8**. It was found that the steady state absorption spectra and vertical electronic transitions are comparable. (**Figure 3.13**).



**Figure 3.16** Theoretical (vertical bars) and experimental (continuous lines) UV-Vis-NIR absorption spectra of **JB-1** (black), **JB-2** (red) and **YD2-0-C8** (blue) in THF.

The frontier orbital diagrams as shown in **Figure 3.14 and 3.15** further revealed that HOMO levels are primarily localized over diarylamine donor moieties and extending up to the porphyrin segment implying the significant contribution of diarylamine substituted porphyrin as a donor. LUMO coefficient is completely absent on porphyrin, which was not observed in the case of previously reported much accomplished porphyrin dyes such as **YD2-o-C8** and **SM315**. <sup>16,17</sup> On the other hand, LUMO lies completely on the acceptor BODIPY unit, which implies HOMO to LUMO photoexcitation will involve charge transfer from aryl amine substituted porphyrin to BODIPY unit. A well separated electron density distribution of HOMO

and LUMO levels may indicate smooth electron transfers from the donor substituted porphyrin to the BODIPY acceptor via the porphyrin bridge, which will facilitate the efficient electron injection into TiO<sub>2</sub> conduction band. Computational HOMO-LUMO energy gap was found to be 1.52 and 1.69 eV for the sensitizers **JB-1** and **JB-2**, respectively.

**Table 3.2:** Selected transitions, oscillator strength, symmetry calculated (H = HOMO, L = LUMO) from DFT analysis for **JB-1**, **JB-2** and **YD2-***o***-C8**.

Dye	Wavelength (nm)	Oscillator Strength	Major Contribution
JB-1	851	0.14	H→L (98%)
	659	0.84	H-1→L (100%)
	652	0.36	H→L+1 (87%)
	638	0.16	H-3→L (93%)
	462	0.77	H-8→L (64%), H-9→L (13%)
	432	0.41	H-13→L (22%), H-13→L (15%), H- 11→L (28%)
JB-2	928	0.09	H→L (98%)
	696	0.36	H→L+1 (94%)
	658	0.82	H-2→L (99%)
	463	0.76	H-9→L (49%), H-11→L (19%), H-10→ L (17%)
	434	0.21	H-12→L (41%). H-14→ L (19%), H- 13→ L (15%)
YD2-o-C8	667	0.47	H→L (91%)
	440	1.48	H-1→L+1 (43%), H→L+2 (39%)
	425	0.76	H-2→L+1 (45%), H-1→L (34%)
	413	0.51	H→L+2 (54%), H-1→L+1 (23%)

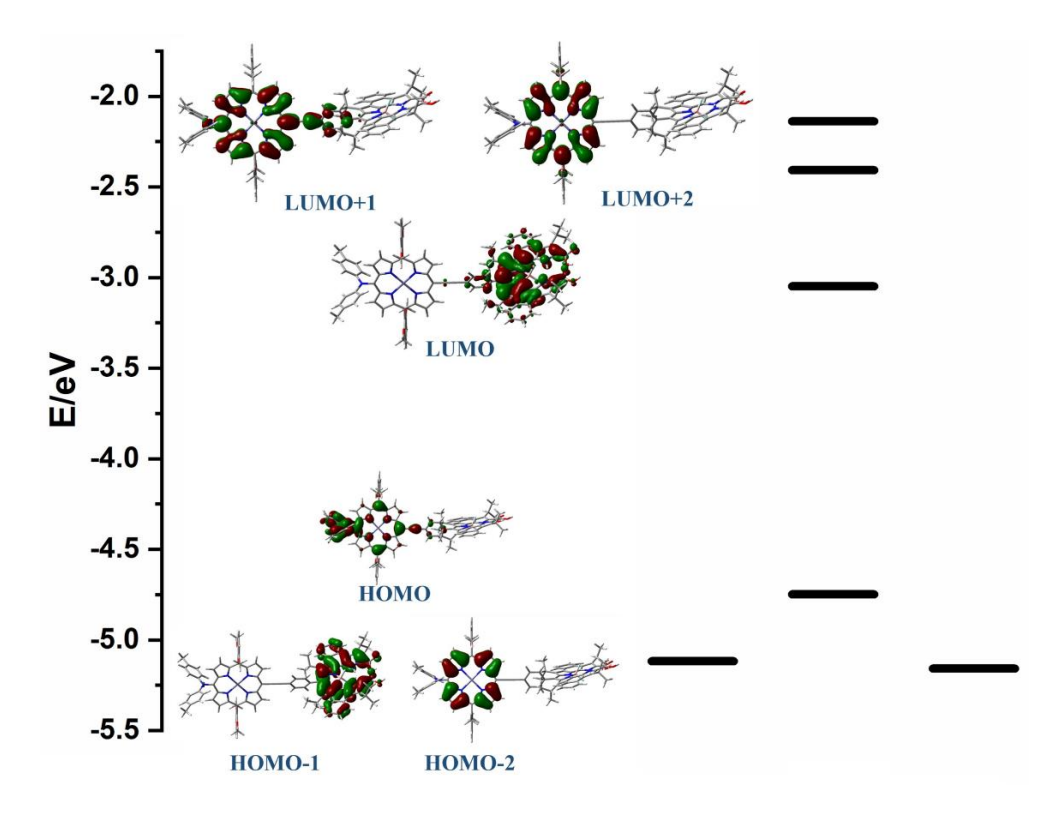


Figure 3.17 Delocalized electron densities of selected MOs of JB-1 with energy level diagram.

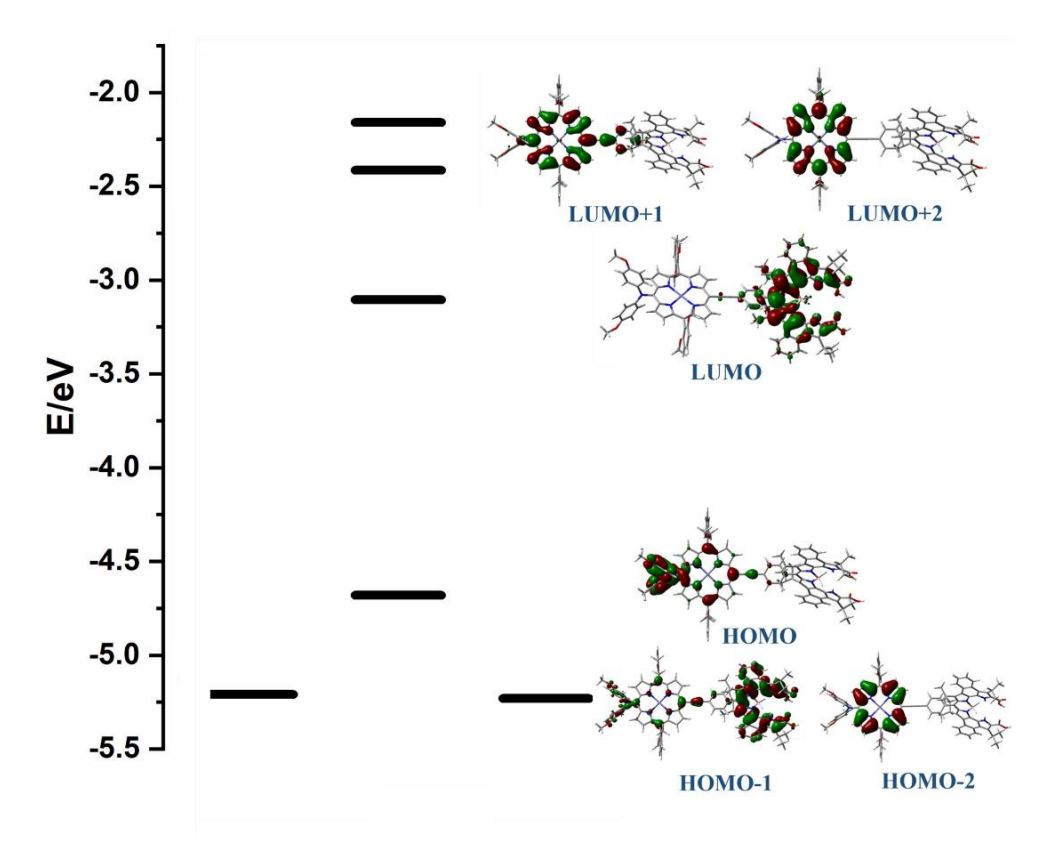


Figure 3.18 Delocalized electron densities of selected MOs of JB-2 with energy level diagram.

## 3.3.4 Electrochemical studies

The redox properties of Porphyrin-BODIPY Conjugates, **JB-1** and **JB-2** were evaluated by CV and DPV in THF solvent using tetrabutylammonium hexafluorophosphate as supporting electrolyte, a glassy carbon working electrode, an Ag/AgCl reference electrode and Pt wire auxiliary electrode and the corresponding data was shown in **Figure 3.16** with potential details in **Table 3.3**. The first oxidations for the formation of the porphyrin cation radical  $E_{ox}$  (or HOMO level) of **JB-1** and **JB-2** are quasi-reversible with values of 1.02 V and +0.98 (vs NHE), respectively. Both the dyes exhibit more positive potentials than the redox potential of the  $I^r/I_3^-$  couple, demonstrating the feasibility of the dye regeneration. In addition, energy level of LUMO, ( $E_{LUMO}$ ) calculated from the equation  $E_{LUMO} = E_{ox} - E_{0-0}$  for **JB-1** and **JB-2** are found to be -0.67 and -0.64 V, respectively, which are higher than that of conduction band edge ( $E_{CB}$ ) of TiO<sub>2</sub> indicating the workable electron injection from the excited sensitizer to the conduction band of TiO<sub>2</sub> as shown in **Figure 3.17**.

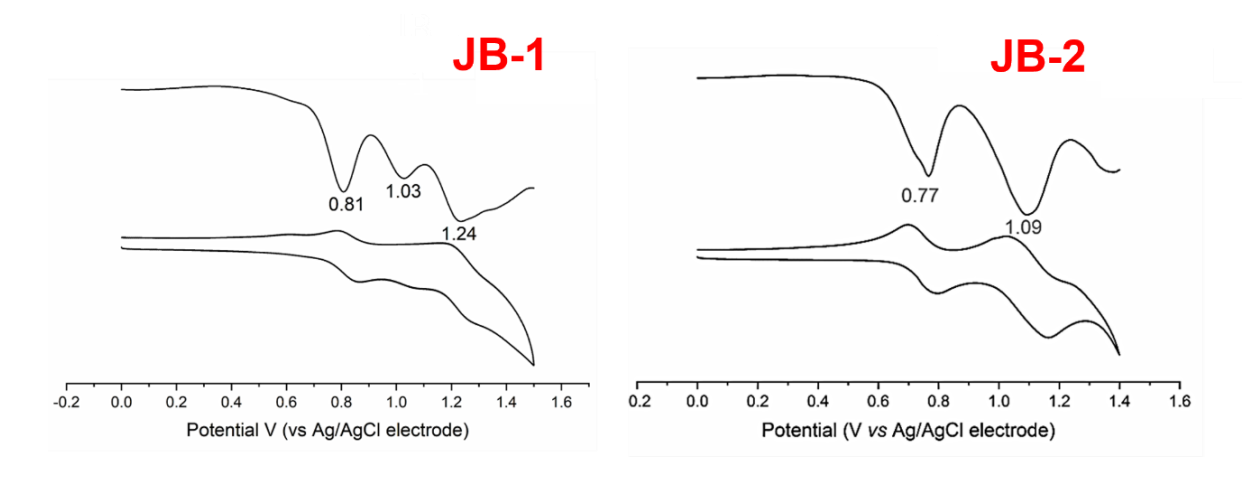


Figure 3.19 CV (below) and DPV (above) of JB-1 and JB-2 in THF measured at 298K.

**Table 3.3:** Absorption spectral and electrochemical data for **JB-1** and **JB-2**.

Dye	Absorption	Emission	$E_{0-0}$	Oxidation	Reduction	$E_{LUMO}=E_{0-0}$ -	Eec
	$\lambda_{max}/nm$	in nm	in	E <sub>ox</sub> (from	E <sub>red</sub> (from	$E_{HOMO}$	in V
	$(\epsilon/10^5 \text{ M}^{-1})$		eV	DPV) vs.	DPV) vs.	in V	
	cm <sup>-1</sup> )			NHE in V	NHE in V		
JB-1	448 (1.94),	661, 767	1.64	1.02	-0.4	-0.62	1.42
	649 (0.41),						
	753 (1.64)						
JB-2	443 (1.93),	682, 770	1.64	0.98	-0.55	-0.66	1.53
	670 (0.43),						
	750 (1.53)						

## 3.4 Conclusion

In conclusion, we have successfully designed a novel strategy for harvesting the NIR flux of photons from the sunlight by synthesizing two new porphyrin-BODIPY conjugates, **JB-1** and **JB-2**, with the highly conjugated BODIPY group acting as an acceptor for the

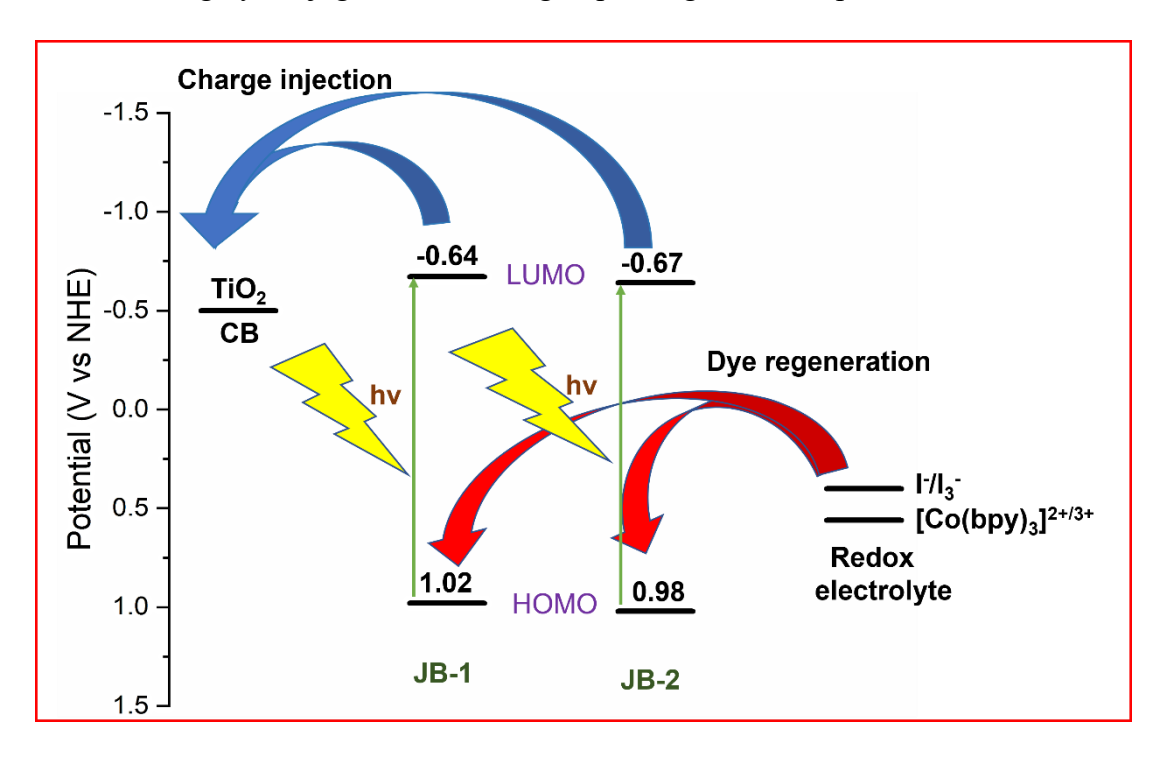


Figure 3.20 The electron transfer processes in DSSC.

first time. These dyes display a significant red shifted and intense lowest energy bands having non-zero absorption beyond 800 nm which was mostly absent in case of previously reported dyes. The DFT calculations revealed a promising feature of LUMO with electron density fully located on acceptor moiety and anchoring group, which may facilitate the charge separation processes while the energy levels of HOMO and LUMO have shown a facile dye regeneration and charge injection abilities, respectively.

## 3.5 Experimental details

The synthetic details regarding donor groups 2.10 and 2.11 along with donor appended porphyrin, 2.14 and 2.15 and napthobipyrrole diester 2.27 were discussed in the materials and methods section.

Synthesis of 9-(Ethoxycarbonyl)-3,8-diisopropyl-1,10-dihydrobenzo[e]pyrrolo[3,2-g]indole-2-carboxylic acid (JB-3.1): Compound 2.27 (400 mg, 0.92 mmol, 1eq) was taken in a 50 mL two-necked round-bottom flask with a reflux condenser and a nitrogen inlet. It was dissolved in ethanol (20 mL) and aq. NaOH (37 mg, 0.92 mmol in 3.5 mL water, 1eq) and refluxed for 48 h. The reaction was quenched with addition of dil. HCl, and the precipitate formed was filtered, and washed properly with water. The residue was purified by column chromatography (silica gel) using EtOAc/hexane:30/70 to give napthobipyrrole monoester acid, JB-3.1 (205 mg, 55%) as white solid.

Melting point: >300°C; FTIR: 3473, 3357, 2924, 2123 cm<sup>-1</sup>. <sup>1</sup>H NMR (DMSO- $d_6$ , 500 MHz)  $\delta_H$  12.98 (s, br, 1H), 11.99 (s, 1H), 11.89 (s, 1H), 8.49-8.44 (m, 2H), 7.53-7.48 (m, 2H), 4.52-4.36 (m, 4H), 1.54 (dd, J=7.2 Hz, 1.05 Hz, 12H), 1.42 (t, J=7 Hz, 3H). <sup>13</sup>C NMR (DMSO  $d_6$ , 100 MHz)  $\delta_C$  160.7, 160.9, 145.6, 133.6, 132.8, 131.6, 131.2, 127.9, 127.1, 125.4, 123.6, 121.2, 120.2, 118.6, 118.4, 102.8, 63.4, 60, 24.8, 20.7, 14.4. HRMS: m/z calcd for [M+H]<sup>+</sup>  $C_{24}H_{27}N_2O_4$ : 407.1971, found 407.1974.

Synthesis of Ethyl 3,8-diisopropyl-1,10-dihydrobenzo[e]pyrrolo[3,2-g]indole-2-carboxylate (JB-3.2): Compound JB-3.1 (200 mg, 0.49 mmol,) was taken in a 10 mL two-necked round-bottom flask equipped with a condenser, dissolved in dry ethylene glycol (4 mL) and kept in vacuum for 0.5 h. The reaction mixture was refluxed for 3 h in a pre-heated oil bath. Heat source was removed and after cooling to room temperature the reaction mixture was poured in ice bath to give precipitate. Compound was filtered through a Buchner funnel and dried in desiccator to obtain napthobipyrrole monoester, JB-3.2 (173 mg, 97%) as white solid.

Melting point: >300°C; FTIR: 3364, 2958, 1631, 1461 cm<sup>-1</sup>; <sup>1</sup>H NMR (CDCl<sub>3</sub>, 500 MHz)  $\delta_{\rm H}$  12.36 (s, 1H), 9.86 (s, 1H), 8.61 (m, 1H), 8.49 (m, 1H), 7.55-7.48 (m, 2H), 7.0 (d, J=1.8 Hz, 1H), 4.63-4.49 (m, 3H), 3.79-3.70 (m, 1H), 1.65 (d, J=7.5 Hz, 6H), 1.57 (t, J=7 Hz, 3H), 1.48 (d, J=6.5 Hz, 6H). <sup>13</sup>C NMR (CDCl<sub>3</sub>, 125 MHz)  $\delta_{\rm C}$  164.5, 136.1, 128.6, 128.2, 126.9, 124.7, 123.7, 123.0, 122.3, 119.4, 119.3, 118.4, 117.1, 96.2, 61.4, 34.8, 31.7, 26.8, 26.0, 23.7, 21.3, 14.6, 14.3, 14.2. HRMS: m/z calcd for [M+H]<sup>+</sup> C<sub>23</sub>H<sub>27</sub>N<sub>2</sub>O<sub>2</sub>: 363.2073, found 363.2074.

Synthesis of Diethyl 9,9'-((4-iodophenyl)methylene)bis(3,8-diisopropyl-1,10-dihydrobenzo[e]pyrrolo[3,2-g]indole-2-carboxylate) (JB-3.3): Compound JB-3.2 (100 mg, 0.27 mmol, 1.9 eq) and 4-iodobenzaldehyde (32 mg, 0.14 mmol, 1 eq) were taken in a two-necked round-bottom flask and kept under nitrogen atmosphere. DCM (10 mL) was added to it and stirred for 15 min to dissolve the solids, followed by addition of TFA (10 μL, 0.13 mmol, 0.9 eq). Reaction was monitored by checking TLC. After the consumption of all the starting material, the solvent was removed under reduced pressure and the residue was purified by column chromatography (silica gel) using EtOAc/heaxane: 20/80 as eluent. Recrystallization from hexane yielded the napthobipyrrole based dipyrromethane, JB-3.3 (10 mg, 42%) as a white solid.

Melting point: >300°C; FTIR: 3349, 2958, 1702, 1666 cm<sup>-1</sup>; <sup>1</sup>H NMR (CDCl<sub>3</sub>, 400 MHz)  $\delta_{\rm H}$  11.75 (s, 2H), 10.57 (s, 2H), 8.49-8.47 (m, 4H), 7.78 (d, J= 8.4 Hz), 7.47 (t, J= 3.8 Hz, 4H), 7.03 (d, J= 8.4 Hz, 2H), 6.48 (s, 1H), 4.47-4.34 (s, br, 2H), 4.35-4.31 (m, 4H), 1.55-1.54 (m, 12H), 1.44-1.40 (m, 12 H), 1.38-1.33 (m, 9H), 1.31-1.18 (m, 4H). <sup>13</sup>C NMR (CDCl<sub>3</sub>, 125 MHz)  $\delta_{\rm C}$  171.4, 138.5, 138.0, 134.0, 131.3, 130.9, 130.6, 128.7, 127.1, 126.1, 124.7, 123.3, 118.2, 96.2, 92.9, 64.6, 60.6, 31.0, 30.7, 29.8, 26.6, 25.4, 21.2, 14.3. HRMS: m/z calcd for [M+H]<sup>+</sup> C<sub>53</sub>H<sub>56</sub>IN<sub>4</sub>O<sub>4</sub>: 939.3346, found 939.3346.

Synthesis of Napthobipyrrole derived BODIPY Diester (JB-3.4): Compound JB-3.3 (100 mg, 0.11 mmol, 1 eq) was dissolved in DCM (10 ml) and DDQ (24 mg, 0.11 mmol, 1 eq) was added to it and stirred. Reaction was monitored by checking TLC and after all starting material consumed, solvent was reduced and a filter column is performed and kept for boron complexation by dissolving in DCM (5 mL) and Et<sub>3</sub>N (0.5 mL, 3.52 mmol). After stirring for 10 min, BF<sub>3</sub>.OEt<sub>2</sub> (0.6 mL, 5.28 mmol) was added and stirred for 4 h at rt. Solvent was removed under reduced pressure and the residue was purified by column chromatography (silica gel) using EtOAc/hexane: 20/80 as eluent. Recrystallization from hexane provided napthobipyrrole based BODIPY diester JB-3.4 (67.6 mg, 65%) as a green solid.

Melting point: >300°C; FTIR: 3429, 2957, 1719, 1684 cm<sup>-1</sup>; <sup>1</sup>H NMR (CDCl<sub>3</sub>, 500 MHz)  $\delta_{\rm H}$  11.02 (t, J=7 Hz, 2H), 8.40 (dd, J=8 Hz, 1 Hz 1H), 7.97 (d, J=8.3 Hz, 2H), 7.51-7.46 (m, 2H), 7.45-7.39 (m, 4H), 4.55 (q, J=7.1 Hz, 4H), 4.36 (t, J=7.1 Hz, 2H), 2.81-2.72 (m, 2H), 1.62 (d, J=7.2 Hz, 12H), 1.47 (t, J=7.1 Hz, 6H), 1.26 (d, J=7.3 Hz, 12H). <sup>13</sup>C NMR (CDCl<sub>3</sub>, 100 MHz)  $\delta_{\rm C}$  161.4, 149.7, 140.7, 140.5, 137.9, 136.0, 135.8, 134.2, 131.2, 129.3, 128.9, 128.0, 126.6,

126.2, 125.8, 124.4, 122.2, 95.1, 61.3, 25.7, 24.6, 21.1, 20.3, 14.5. HRMS: m/z calcd for [M+H]<sup>+</sup> C<sub>53</sub>H<sub>53</sub>BF<sub>2</sub>IN<sub>4</sub>O<sub>4</sub>: 985.3173, found 985.3172.

Synthesis of Napthobipyrrole derived BODIPY Diacid (JB-3.5): Compound JB-3.4 (15 mg, 0.02 mmol) was taken in a mixture of EtOH:THF (1:1, 6 mL) and KOH (170 mg, 3.04 mmol, 202 eq) in H<sub>2</sub>O (0.8 mL) was added and stirred for 12 h at 80 °C. After cooling to room temperature, the mixture was poured into dil. HCl, extracted with CH<sub>2</sub>Cl<sub>2</sub>, dried over anhydrous Na<sub>2</sub>SO<sub>4</sub> and then the residue was purified by recrystallization from DCM/hexane to afford the compound JB-3.5 (11 mg, 78%) as green solid.

Melting point: >300°C; FTIR: 2959, 2856, 1599, 1459, 1065 cm<sup>-1</sup>; <sup>1</sup>H NMR (THF- $d_8$ , 500 MHz)  $\delta_H$  10.88 (s, 2H), 8.40 (d, J= 7.7 Hz, 2H), 8.35 (d, J=7.9 Hz, 2H), 8.06 (d, J =7.8 Hz, 2H), 7.69 (d, J=8.1 Hz, 2H), 7.63-7.53 (m, 4H), 4.35 (s, 2H), 3.59 (t, J=6.5 Hz, 2H), 1.56 (d, J=7.1 Hz, 12H), 1.21 (t, J=7.2 Hz, 12H). <sup>13</sup>C NMR (THF- $d_8$ , 125 MHz)  $\delta_C$  150.4, 141.3, 139.0, 137.0, 136.6, 132.7, 130.7, 130.3, 130.0, 128.5, 127.2, 127.0, 126.6, 125.1, 96.1, 33.0, 30.7, 30.4, 26.6, 25.9, 25.8, 23.7, 21.4, 20.5, 14.5. HRMS: m/z calcd for [M+H]<sup>+</sup> C<sub>49</sub>H<sub>45</sub>BF<sub>2</sub>IN<sub>4</sub>O<sub>4</sub>: 929.2547, found 929.2546.

Synthesis of Porphyrin-BODIPY Conjugate (Diester) (JB-3.6): Compound 2.23 (15 mg, 0.0105 mmol, 1 eq) and BODIPY (JB-3.4) (12.4 mg, 0.0125 mmol, 1.2 eq) were taken in a 10 mL Schlenk tube and dissolved in a mixture of dry THF (5 mL) and Et3N (0.4 mL) and the solution was degassed with dinitrogen for 10 min, Pd<sub>2</sub>(dba)<sub>3</sub> (2.8 mg, 0.0031 mmol, 0.3 eq) and AsPh<sub>3</sub> (6.5 mg, 0.021 mmol, 2 eq) were added to the mixture. The solution was refluxed for 4 h under nitrogen atmosphere. The solvent was removed under reduced pressure. The residue was purified by recrystallization from hexane to give JB-3.6 (10 mg, 42%) as a green solid.

Melting point: >250°C (decomp); FTIR: 2957, 2922, 2859, 1718, 1461 cm-1; 1H NMR (CDCl3, 500 MHz)  $\delta$ H 11.08(t, J= 7.0 Hz, 2H), 9.75(d, J= 4.5 Hz, 2H), 9.19 (d, J= 4.6 Hz, 2H), 8.92 (d, J= 4.6 Hz, 2H), 8.69 (d, J= 4.7 Hz, 2H), 8.42 (d, J= 8.9 Hz, 2H), 8.25 (d, J= 8.0 Hz, 2H), 7.85 (d, J= 8.1 Hz, 2H), 7.67 (t, J= 8.5 Hz, 2H), 7.49-7.41 (m, 4H), 7.21 (d, J= 9.2 Hz, 4H), 6.97 (d, J= 8.5 Hz, 4H), 6.70 (d, J= 9.2 Hz, 4H), 4.58-4.54 (m, 4H), 4.39-4.37 (m, 2H), 3.85-3.82 (m, 8H), 3.06-3.02 (m, 2H), 1.71-1.68 (m, 4H), 1.64 (d, J= 7.2 Hz, 12H), 1.53 (s, 18H), 1.48 (t, J= 7.1 Hz, 8H), 1.38 (d, J= 7.3 Hz, 16H), 1.29-1.25 (m, 14H), 1.02-1.00(m, 8H), 0.87-0.84 (m, 16H), 0.70-0.47(m, 50H); HRMS: m/z calcd for [M+H]+ C143H170BF2N9O10Zn: 2286.2379, found 2286.2325.

## 2.1.3 Synthetic routes for JB-1 and JB-2:

Synthesis of JB-1 dye: Compound 2.22 (20 mg, 0.0203 mmol, 1.8 eq) and BODIPY-Diacid JB-3.5 (10 mg, 0.0107 mmol, 1 eq) were taken in a 25 mL Schlenk tube and dissolved in a mixture of dry THF (5 mL) and Et<sub>3</sub>N (0.4 mL) and the solution was degassed with dinitrogen for 10 min, Pd<sub>2</sub>(dba)<sub>3</sub> (2.8 mg, 0.003 mmol, 0.3 eq) and AsPh<sub>3</sub> (6.2 mg, 0.020 mmol, 2eq) were added to the mixture. The solution was refluxed for 4 h. The solvent was removed under reduced pressure. The residue was purified by recrystallization from CH<sub>3</sub>OH/hexane to isolate JB-1 (16.8 mg, 60%) as a green solid.

Melting point: >250°C (decomp); FTIR: 2925, 2853, 1595, 1457 cm<sup>-1</sup>. H NMR (THF  $d_8$ , 500 MHz)  $\delta_H$  11.55 (s br, 2H), 9.73 (s, 2H), 9.73 (s, 2H), 9.07 (s, 2H), 8.83 (s, 2H), 8.58 (s, 2H), 8.46 (s, 2H), 8.35 (d, J= 6.5 Hz, 4H), 8.05 (s, 2H), 7.67 (s, 2H), 7.40 (s br, 4H), 7.22 (d, J= 7.5 Hz, 4H), 7.04 (t, J= 4.0 Hz, 4H), 6.94 (d, J= 7.5 Hz, 4H), 3.89 (s br, 8H), 3.50 (s br, 4H), 3.17 (s br, 4H), 2.48 (s br, 4H), 2.04 (s, 2H), 1.57 (s br, 8H), 1.44 (s br, 8H), 1.10-1.03 (m, 12H), 0.96-0.85 (m, 44H), 0.75-0.63 (m, 33H).  $^{13}$ C NMR (THF- $d_8$ , 125 MHz)  $\delta_C$  161.1, 152.3, 152.6, 151.9, 151.5, 151.3, 141.1, 136.2, 132.7, 132.5, 132.1, 131.3, 130.7, 130.6, 130.3, 129.5, 129.2, 127.7, 127.2, 126.1, 124.3, 123.8, 122.7, 121.8, 115.3, 105.5, 98.3, 95.3, 69.1, 36.2, 33.0, 32.8, 32.8, 32.7, 30.8, 30.5, 30.4(4), 30.4(0), 30.2, 29.9, 29.8, 29.7, 28.1, 27.1, 24.3, 25.9, 23.7, 23.6, 23.4, 21.9, 20.8, 14.5. HRMS: m/z calcd for [M+H]<sup>+</sup> C<sub>139</sub>H<sub>161</sub>BF<sub>2</sub>N<sub>9</sub>O<sub>8</sub>Zn: 2199.1857, found 2199.1836.

Synthesis of JB-2 dye: Compound 2.23 (22.6 mg, 0.016 mmol, 1.8 eq) and BODIPY JB-3.5 (10 mg, 0.0107 mmol, 1eq) were taken in a 25 mL Schlenk tube and dissolved in a mixture of dry THF (5 mL) and Et<sub>3</sub>N (0.4 mL) and the solution was degassed with dinitrogen for 10 min, Pd<sub>2</sub>(dba)<sub>3</sub> (3 mg, 0.0032 mmol, 0.3 eq) and AsPh<sub>3</sub> (6.6 mg, 0.022 mmol, 2 eq) were added to the mixture. The solution was refluxed for 4 h under nitrogen atmosphere. The solvent was removed under reduced pressure. The residue was purified by recrystallization from CH<sub>3</sub>OH/hexane to obtain JB-2 (10 mg, 42%) as a green solid.

Melting point: >280°C (decomp); FTIR: 2924, 2854, 1595, 1457 cm<sup>-1</sup>; <sup>1</sup>H NMR (THF- $d_8$ , 500 MHz)  $\delta_H$  11.59 (s, br, 2H), 10.83 (s, 2H), 9.69 (d, J= 4.5 Hz, 2H), 9.07 (d, J=4.5 Hz, 2H), 8.80 (d, J=4.5 Hz, 2H), 8.55 (d, J=4.5 Hz, 2H), 8.46 (s, 4H), 8.33 (d, J= 7.2 Hz, 2H), 7.66 (t, J=8.5 Hz, 2H), 7.44-7.38 (m, 4H), 7.19-7.17 (m, 4H), 7.03 (d, J=8.5 Hz, 4H), 6.67 (d, J=9.5 Hz, 4H), 3.86-3.83 (m, 12H), 1.85 (s, 4H), 1.68-1.65 (m, 11H), 1.59 (s, 4H), 1.43-1.42 (m, 11H), 1.31-

1.29 (m, 11H), 1.06-1.01 (m, 8H), 0.93-0.90 (m, 11H), 0.89-0.86 (m, 12H), 0.82-0.79 (m, 8H), 0.71-0.63 (m, 30H).  $^{13}$ C NMR (THF- $d_8$ , 125 MHz)  $\delta_C$  161.1, 154.1, 152.9, 151.4, 149.3, 148.1, 141.0, 138.8, 136.1, 133.1, 132.7, 132.3, 132.0, 130.7, 130.5, 129.2, 127.6, 127.1, 124.5, 124.3, 123.7, 121.8, 115.6, 115.2, 108.0, 105.5, 98.1, 95.3, 69.0, 33.0, 32.7, 32.5, 30.9, 30.7, 30.6, 30.5, 30.4, 29.9, 29.8, 29.7, 28.1, 26.8, 26.5, 26.4, 26.3, 25.9, 23.7, 23.6, 23.4, 21.9, 20.8, 14.5. HRMS: m/z calcd for [M+H] $^+$  C<sub>139</sub>H<sub>160</sub>BF<sub>2</sub>N<sub>9</sub>O<sub>10</sub>Zn: 2230.1677, found 2230.1613.

## 3.6 References

- 1. Zhou, W.; Cao, Z.; Jiang, S.; Huang, H.; Deng, L.; Liu, Y.; Shen, P.; Zhao, B.; Tan, S.; Zhang, X Porphyrins modified with a low-band-gap chromophore for dye-sensitized solar cells. *Organic Electronics*, **2012**, *13*, 560.
- 2. O'Regan, B.; Grätzel, M. A low-cost, high-efficiency solar cell based on dye-sensitized colloidal TiO<sub>2</sub> films. **1991**, *353*, 737.
- 3. Nazeeruddin, M. K.; Kay, I. R.; Humphry-Baker, R.; Müller, E. Liska, P.; Vlachopoulos, N.; Grätzel, M. Conversion of Light to Electricity by c/j-X2Bis(2,2'-bipyridyl-4,4/-dicarboxylate) ruthenium(II) Charge-Transfer Sensitizers (X = Cl", Br", I", CN", and SCN~) on Nanocrystalline TiO<sub>2</sub> Electrodes. *J. Am. Chem. Soc.*, **1993**, *115*, 6382.
- Nazeeruddin, M.; Angelis, F. D.; Fantacci, S.; Selloni, A.; Viscardi, G.; Liska, P.; Ito, S.; Takeru, B.; Grätzel, M. Combined Experimental and DFT-TDDFT Computational Study of Photoelectrochemical Cell Ruthenium Sensitizers. *J. Am. Chem. Soc.*, 2005, 127, 16835.
- Zhou, N.; Prabakaran, K.; Lee, B.; Chang, S. H.; Harutyunyan, B.; Guo, P.; Butler, M. R.; Timalsina, A.; Bedzyk, M. J.; Ratner, M. A.; Vegiraju, S.; Yau, S.; Wu, C. G.; Chang, R. P. H.; Facchetti, A.; Chen, M. C.; Marks, T Metal-Free Tetrathienoacene Sensitizers for High-Performance Dye-Sensitized Solar Cells. *J. Am. Chem. Soc.*, 2015, 137, 4414.
- 6. Zhang, L.; Yang, X.; Wang, W.; Gurzadyan, G. G.; Li, J.; Li, X.; An, J.; Yu, Z.; Wang, H.; Cai, B.; Hagfeldt, A.; Sun, L. 13.6% Efficient Organic Dye-Sensitized Solar Cells by Minimizing Energy Losses of the Excited State. *ACS Energy Lett.* **2019**, *4*, 943.
- 7. Devadiga, D.; Selvakumar, M.; Shetty, P.; Santosh, M.; Chandrabose, R. S.; Karazhanov, S. Recent developments in metal-free organic sensitizers derived from carbazole, triphenylamine, and phenothiazine for dye-sensitized solar cells. *Int. J. Energy Res.* **2021**, *45*, 6584.
- 8. Zeng, K.; Chen, Y.; Zhu, W-H.; He, T.; Xie, Y. Efficient Solar Cells Based on Concerted Companion Dyes Containing Two Complementary Components: An Alternative Approach for Cosensitization. *J. Am. Chem. Soc.*, **2020**, *142*, 5154.

- (a) Krishna, N. V.; Krishna, J. S. V.; Singh, S. P.; Han, L.; Giribabu, L.; Bedja, I. M.; Gupta, R. K.; Islam, A. Donor-π–Acceptor Based Stable Porphyrin Sensitizers for Dye-Sensitized Solar Cells: Effect of π-Conjugated Spacers. *J. Phys. Chem. C.* 2017, *121*, 6464. (b) Krishna, N. V.; Krishna, J. V. S.; Singh, S. P.; Giribabu, L.; Islam, A.; Bedja, I. Bulky Nature Phenanthroimidazole-Based Porphyrin Sensitizers for Dye-Sensitized Solar Cell Applications. *J. Phys. Chem. C.*, 2017, *121*, 25691.
- 10. J. V. S. Krishna, Krishna, N. V.; Chowdhury, T. H.; Singh, S. P.; Bedja, I.; Islam, A.; Giribabu, L. Kinetics of dye regeneration in liquid electrolyte unveils efficiency of 10.5% in dye-sensitized solar cells. *J. Mater. Chem. C.*, **2018**, *6*, 11444.
- 11. Krishna, J. V. S.; Koteshwar, D.; Chowdhury, T. H.; Singh, S. P.; Bedja, I.; Islam, A.; Giribabu, L. Efficient near IR porphyrins containing a triphenylamine-substituted anthryl donating group for dye sensitized solar cells. *J. Mater. Chem. C.*, **2019**, *7*, 13594.
- 12. Koteshwar, D.; Seelam, P.; Singh, S. P.; Chowdhury, T. H.; Bedja, I.; Islam, A.; Giribabu, L. Effects of methoxy group(s) on D-p-A porphyrin based DSSCs: efficiency enhanced by co-sensitization. *Mater. Chem. Front.*, **2022**, *6*, 580.
- 13. Zhou, H.; Ji, J-M.; Kang, S. H.; Kim, M. S.; Lee, H. S.; Kim, C. H.; Kim, H. K. Molecular design and synthesis of D–π–A structured porphyrin dyes with various acceptor units for dye-sensitized solar cells, *J. Mater. Chem. C.*, **2019**, *7*, 2843.
- 14. Chen, C-C.; Chen, J-S.; Nguyen, V. S.; Wei, T-C.; Yeh, C-Y. Double Fence Porphyrins that are Compatible with Cobalt (II/III) Electrolyte for High-Efficiency Dye-Sensitized Solar Cells, *Angew. Chem. Int. Ed.*, **2021**, *60*, 4886.
- 15. Kay, A.; Grätzel, M. Artificial photosynthesis. 1. Photosensitization of titania solar cells with chlorophyll derivatives and related natural porphyrins, *J. Phys. Chem.*, **1993**, 97, 6272.
- 16. Yella, A.; Lee, H.-W.; Tsao, H. N.; Yi, C.; Chandiran, A. K.; Nazeeruddin, M. K.; Diau, E. W.-G.; Yeh, C.-Y.; Grätzel, M. Porphyrin-Sensitized Solar Cells with Cobalt (II/III)—Based Redox Electrolyte Exceed 12 Percent Efficiency. *Science.*, 2011, 334, 629.
- 17. Mathew, S.; Yella, A.; Gao, P.; Humphry-Baker, R.; Curchod, B. F.; Ashari-Astani, N.; Tavernelli, I.; Rothlisberger, U.; Nazeeruddin, M. K.; Grätzel, M. Dye-sensitized solar

- cells with 13% efficiency achieved through the molecular engineering of porphyrin sensitizers, *Nat. Chem.* **2014**, *6*, 242.
- 18. Zou, J.; Tang, Y.; Baryshnikov, G.; Yang, Z.; Mao, R.; Feng, W.; Guan, J.; Li, C.; Xie, Y. Porphyrins containing a tetraphenylethylene substituted phenothiazine donor for fabricating efficient dye sensitized solar cells with high photovoltages, *J. Mater. Chem. A.*, 2022, 10, 1320.
- 19. Hagfeldt, A.; Boschloo, G.; Sun, L.; Kloo, L.; Pettersson, H. Dye-Sensitized Solar Cells. *Chem. Rev.*, **2010**, *110*, 6595.
- 20. Warnan, J.; Pellegrin, Y.; Blart, E.; Odobel, F. Supramolecular light harvesting antennas to enhance absorption cross-section in dye-sensitized solar cells *Chem. Commun.*, **2012**, 48, 675.
- 21. Li, F.; Yang, S. I.; Ciringh, Y.; Seth, J.; Martin, C. H.; Singh, D. L.; Kim, D.; Birge, R. R.; Bocian, D. F.; Holten, D.; Lindsey, J. S. Design, Synthesis, and Photodynamics of Light-Harvesting Arrays Comprised of a Porphyrin and One, Two, or Eight Boron-Dipyrrin Accessory Pigments J. Am. Chem. Soc., 1998, 120, 10001.
- 22. Lee, C. Y.; Hupp, J. T. Dye Sensitized Solar Cells: TiO<sub>2</sub> Sensitization with a Bodipy-Porphyrin Antenna System *Langmuir*, **2010**, *26*, 3760.
- 23. Galateia, Z. E.; Agapi, N.; Vasilis, N.; Sharma, G. D.; Athanassios, C. G. "Scorpion"-shaped mono(carboxy)porphyrin-(BODIPY)2, a novel triazine bridged triad: synthesis, characterization and dye sensitized solar cell (DSSC) applications *J. Mater. Chem. C.*, **2015**, *3*, 56525664
- 24. Warnan, J.; Buchet, F.; Pellegrin, Y.; Blart, E.; Odobel, F. Panchromatic Trichromophoric Sensitizer for Dye-Sensitized Solar Cells Using Antenna Effect, *Org. Lett.*, **2011**, *13*, 3945.
- 25. Sarma, T.; Panda, P. K.; Setsune, J-i. Bis-naphthobipyrrolylmethene derived BODIPY complex: an intense near-infrared fluorescent dye *Chem. Commun.* **2013**, *49*, 9806.
- 26. Sahoo, S. S.; Sarma, T.; Srivishnu, K. S.; Panda, P. K. Tuning the Photophysical Properties and Photostability of Bis(naphthobipyrrolylmethene) derived BODIPY via Functionalization. *Chem. Eur. J.*, **2023**, *29*, e202300942.

- 27. Kroeze, J. E.; Hirata, N.; Koops, S.; Nazeeruddin, M. K.; Schmidt-Mende, L.; Grätzel, M.; Durrant, J. R. Alkyl Chain Barriers for Kinetic Optimization in Dye-Sensitized Solar Cells J. Am. Chem. Soc., 2006, 128, 16376.
- 28. Koumura, N.; Wang, Z.-S.; Mori, S.; Miyashita, M.; Suzuki, E.; Hara, K. Alkyl-Functionalized Organic Dyes for Efficient Molecular Photovoltaics *J. Am. Chem. Soc.*, **2006**, *128*, 14256.
- 29. Kang, S. H.; Choi, I, T.; Kang, M. S.; Eom, Y. K.; Ju, M. J.; Hong, J. Y.; Kang, H. S.; Kim, H. K. Novel D–π–A structured porphyrin dyes with diphenylamine derived electron-donating substituents for highly efficient dye-sensitized solar cells *J. Mater. Chem. A*, **2013**, *1*, 3977.
- 30. Liu, L.; Chen, J.; Ku, Z.; Li, X.; Han, H Unsymmetrical squaraine sensitizers containing auxiliary arylamine donor for NIR-harvesting on dye-sensitized solar cell. *Dyes and Pigments*, **2014**, 106, 128.
- 31. Wang, C. L.; Lan, C. M.; Hong, S. H.; Wang, Y. F.; Pan, T. Y.; Chang, C. W.; Kuo, H. H.; Kuo, M. Y.; Diau. E. W. G.; Lin, C. Y. Enveloping porphyrins for efficient dyesensitized solar cells *Energy Environ. Sci.*, **2012**, *5*, 6933.
- 32. (a) V. Roznyatovskiy, V. Lynch and J. L. Sessler, Dinapthoporphycenes. *Org. Lett.* 2010, **12**, 4424-4427. (b) Sarma, T.; Panda, P. K.; Anusha, P. T.; Rao, S. V. Dinaphthoporphycenes: Synthesis and Nonlinear Optical Studies *Org. Lett.* **2011**, *13*, 188.
- 33. Bania, J.; Sahoo, S. S.; Kishore, M. V. N.; Panda, P. K. Porphyrin-BODIPY Conjugates as photosensitizers with absorption up to near infrared region for dye-sensitized solarcells (DSSC). Indian Patent Application No.: 202341027215; May 05, **2023**.
- 34. Gaussian 09, (Revision C.01), Frisch, M. J. et al. Gaussian, Inc., Wallingford CT, 2010.
- 35. O'Boyle, N. M.; Tenderholt, A. L.; Langner, K. M. A library for package-independent computational chemistry algorithms, *J. Comp. Chem.*, **2008**, *29*, 839.
- 36. Urbani, M.; Ragoussi, M-E.; Nazeeruddin, M. K.; Torres, T. Phthalocyanines for dyesensitized solar cells. *Coord. Chem. Rev.*, **2019**, *381*, 1.

- 37. Brogdon, P.; Cheema, H.; Delcamp, J. H. NIR Absorbing Metal-Free Organic, Porphyrin, and Phthalocyanine Dyes for Panchromatic DSCs. *ChemSusChem*, 10.1002/cssc.201701441.
- 38. Lindsey, J. S.; Mass, O.; Chen, C-Y. Tapping the near-infrared spectral region with bacteriochlorin arrays *New J. Chem.*, **2011**, *35*, 511.
- 39. Harputlu, E.; Ocakoglu, K.; Yakuphanoglu, F.; Tarnowska, A.; Gryko, D. T. Physical properties of self-assembled zinc chlorin nanowires for artificial light-harvesting materials. *Nano-Structures & Nano-Objects*. **2017**, *10*, 9.

# 3.7 <sup>1</sup>H NMR, <sup>13</sup>C NMR and HRMS spectra

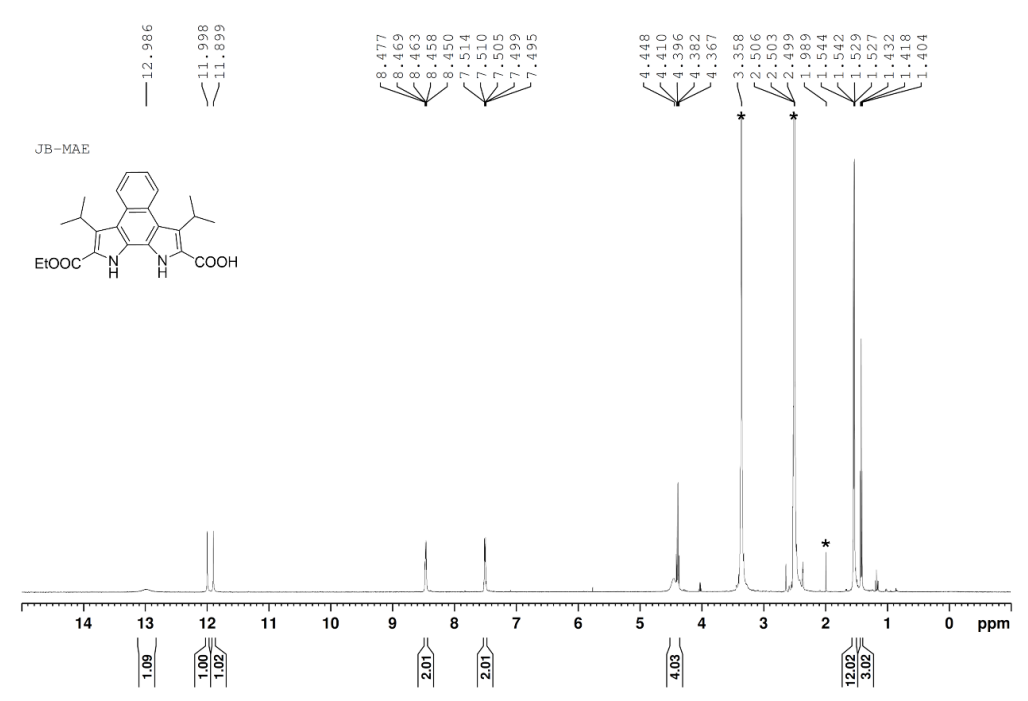


**Figure 3.21**: <sup>1</sup>H NMR spectrum of **JB-3.1** in DMSO-*d*<sub>6</sub> recorded at 25 °C (\*Asterisk indicates water and residual solvent impurity).

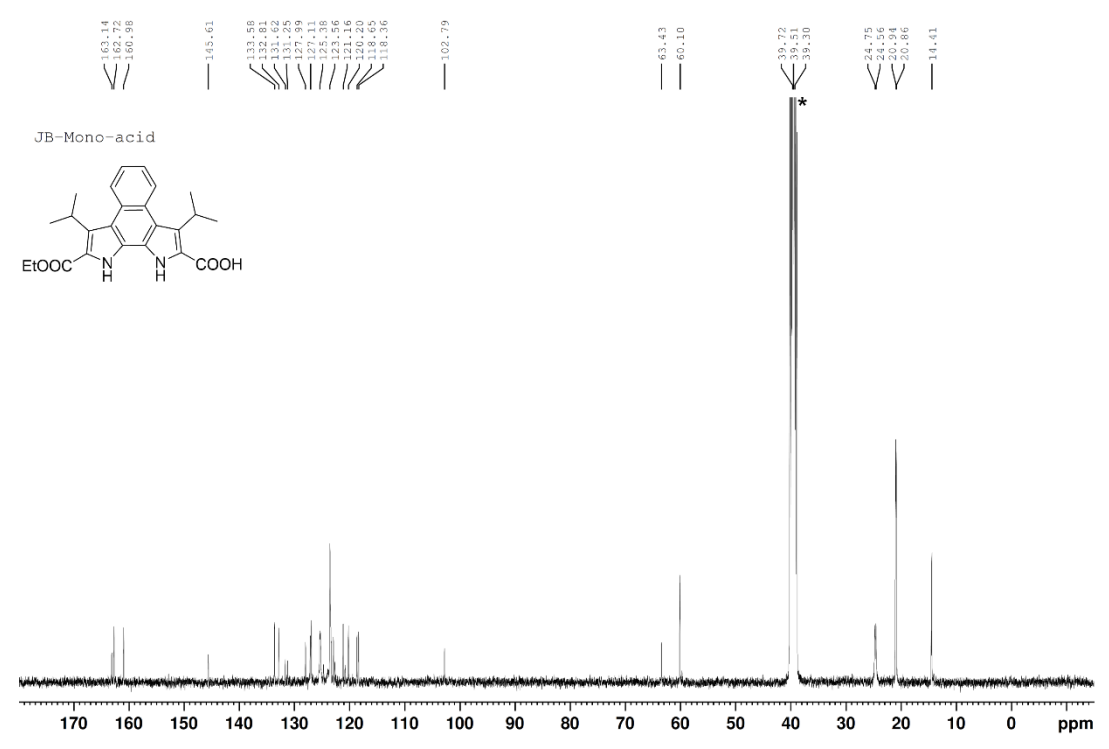


**Figure 3.22.**  $^{13}$ C NMR spectrum of **JB-3.1** in DMSO- $d_6$  recorded at 25 °C (\*Asterisk indicates residual solvent impurity.

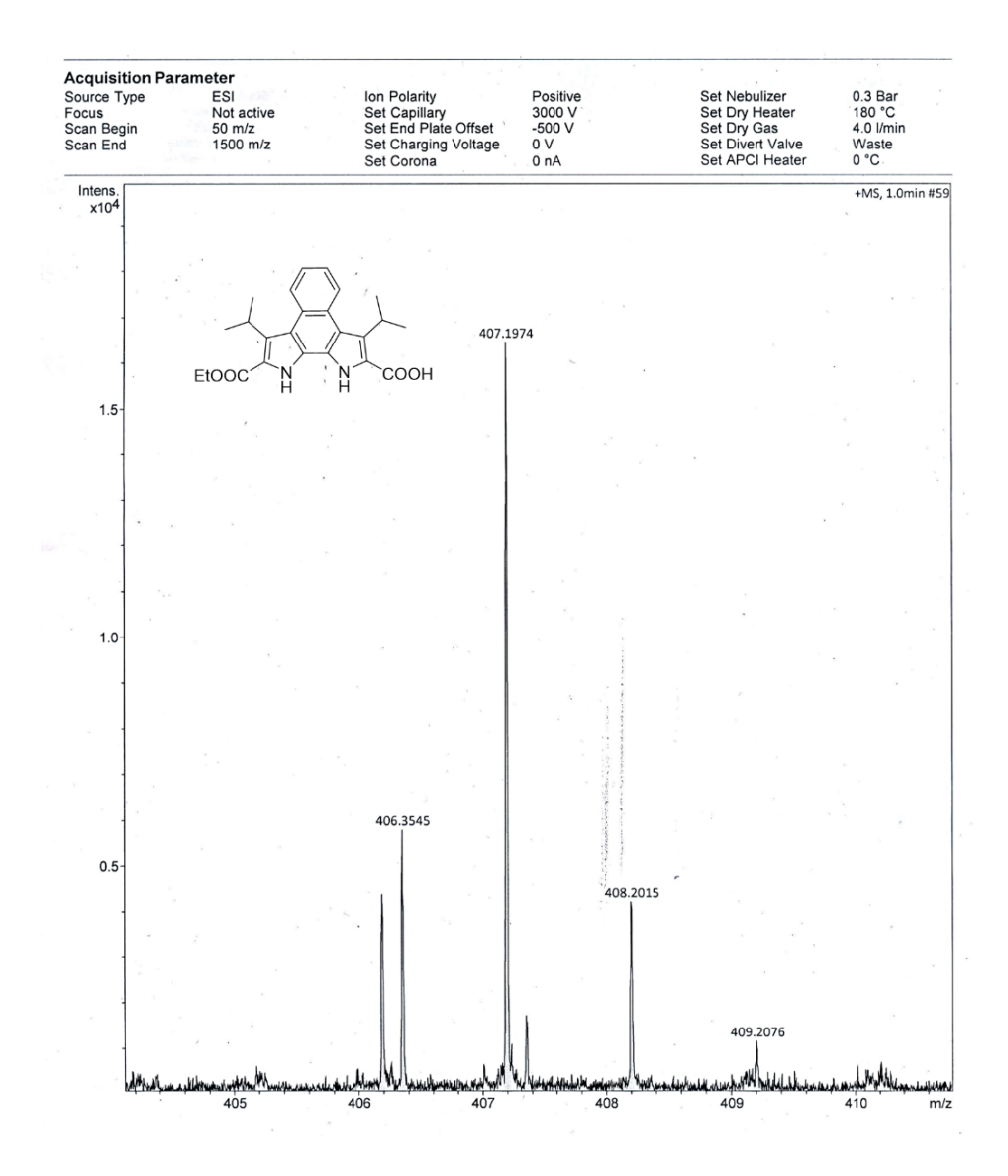


**Figure 3.23.** HR-ESI mass spectrum of **JB-3.1**; m/z calculated for  $C_{24}H_{27}N_2O_4$  [M+H]<sup>+</sup> 407.1971 found 407.1974.

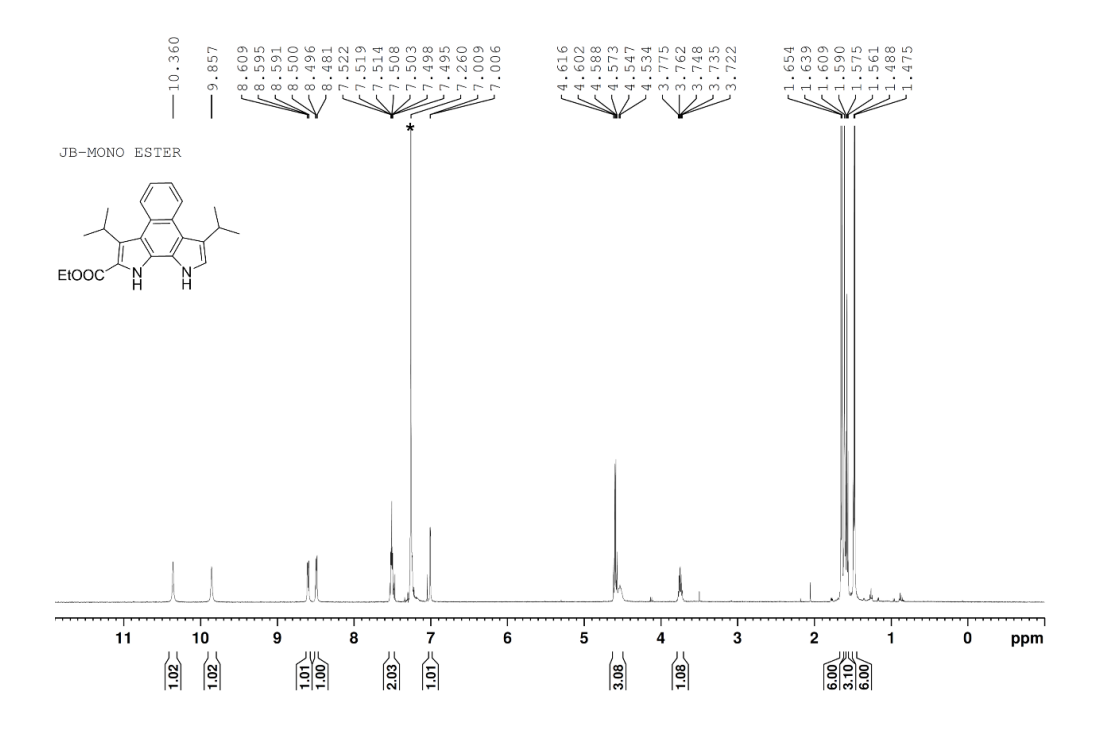


**Figure 3.24.** <sup>1</sup>H NMR spectrum of **JB-3.2** in CDCl<sub>3</sub> recorded at 25 °C (\*Asterisk indicates residual solvent impurity).

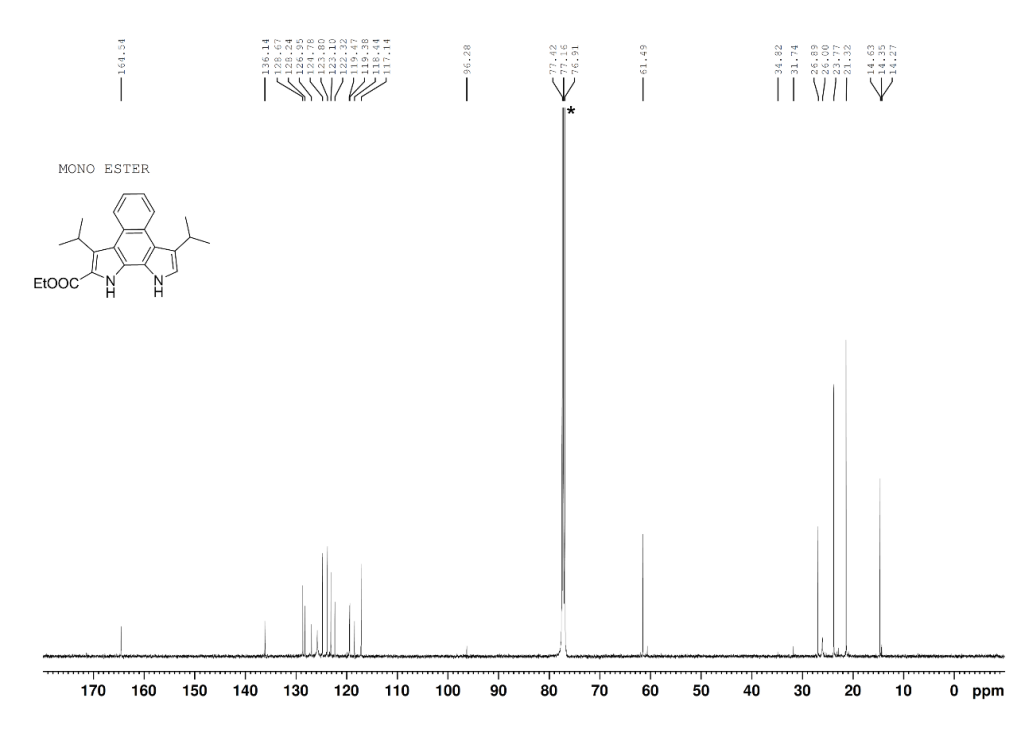


**Figure 3.25** <sup>13</sup>C NMR spectrum of **JB-3.2** in CDCl<sub>3</sub> recorded at 25 °C (\*Asterisk indicates residual solvent impurity).

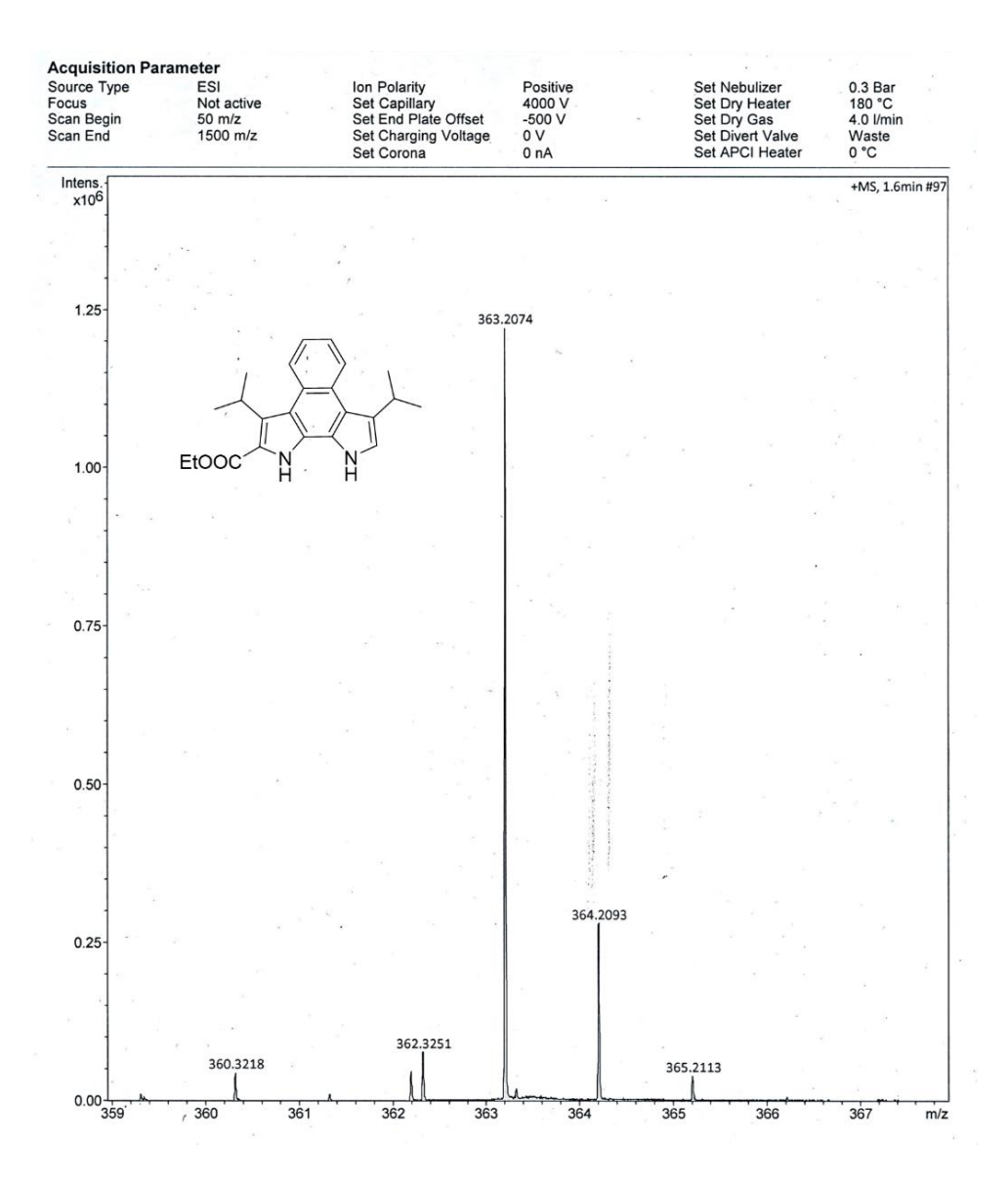


**Figure 3.26** HR-ESI mass spectrum of **JB-3.2**; m/z calculated for  $[M+H]^+$   $C_{23}H_{27}N_2O_2$  363.2073, found 363.2074.

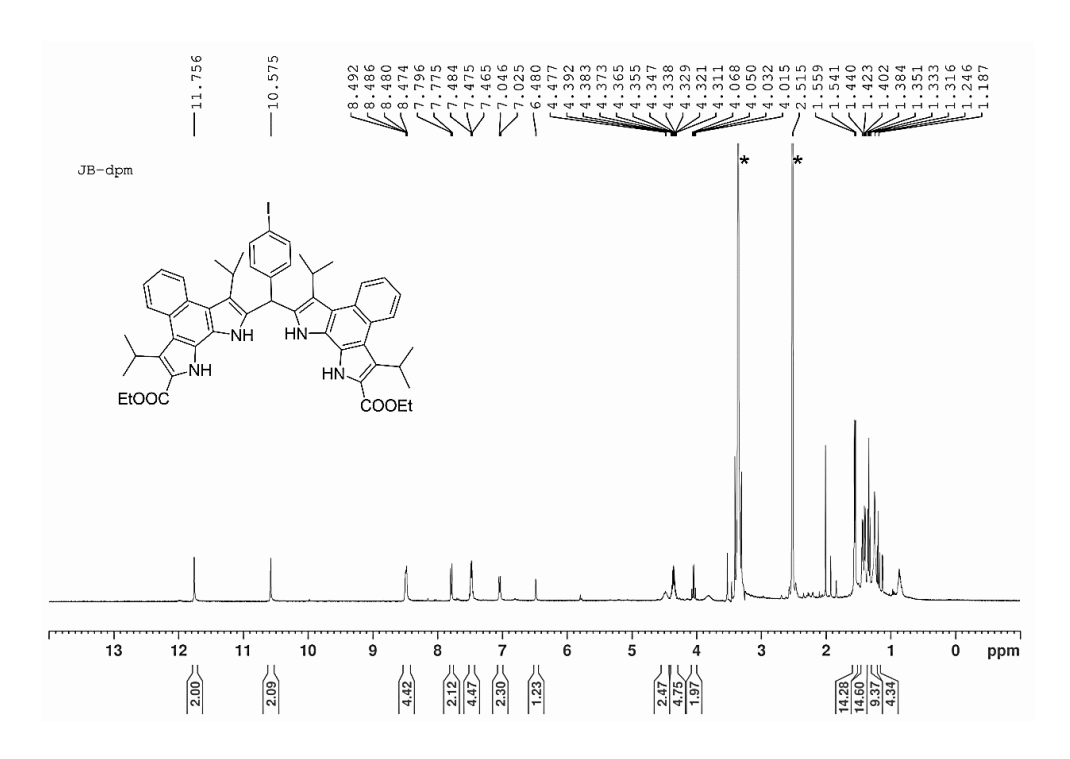


**Figure 3.27**  $^{1}$ H NMR spectrum of **JB-3.3** in DMSO- $d_6$  recorded at 25  $^{\circ}$ C (\*Asterisk indicates residual solvent impurity).

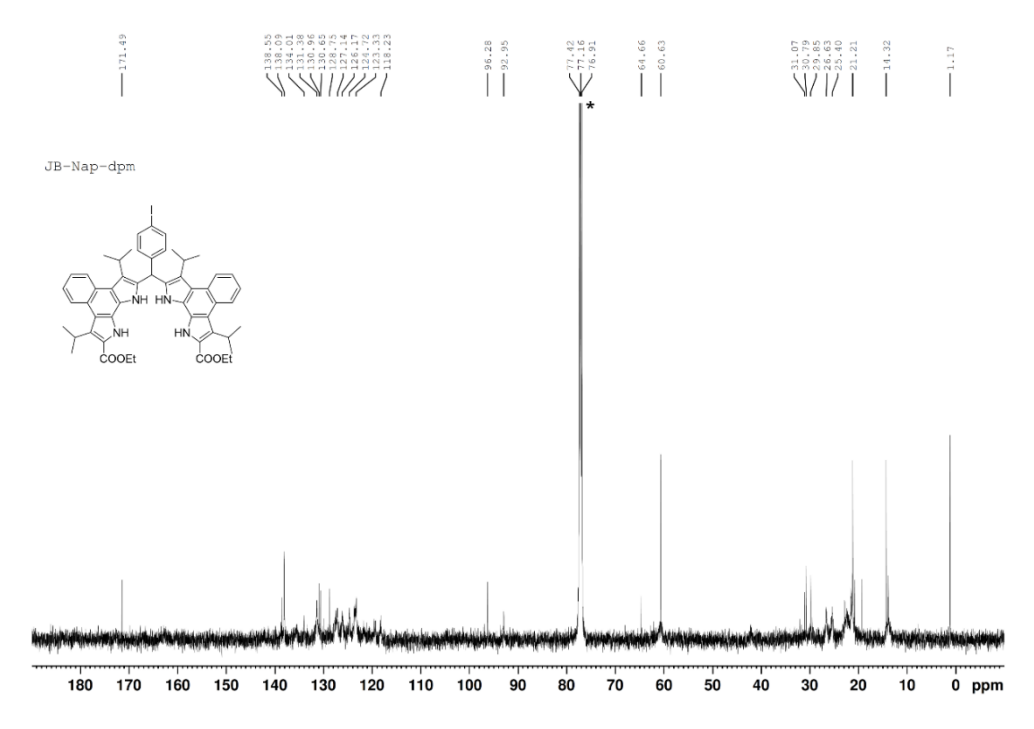


**Figure 3.28** <sup>13</sup>C NMR spectrum of **JB-3.3** in CDCl<sub>3</sub> recorded at 25 °C (\*Asterisk indicates residual solvent impurity).

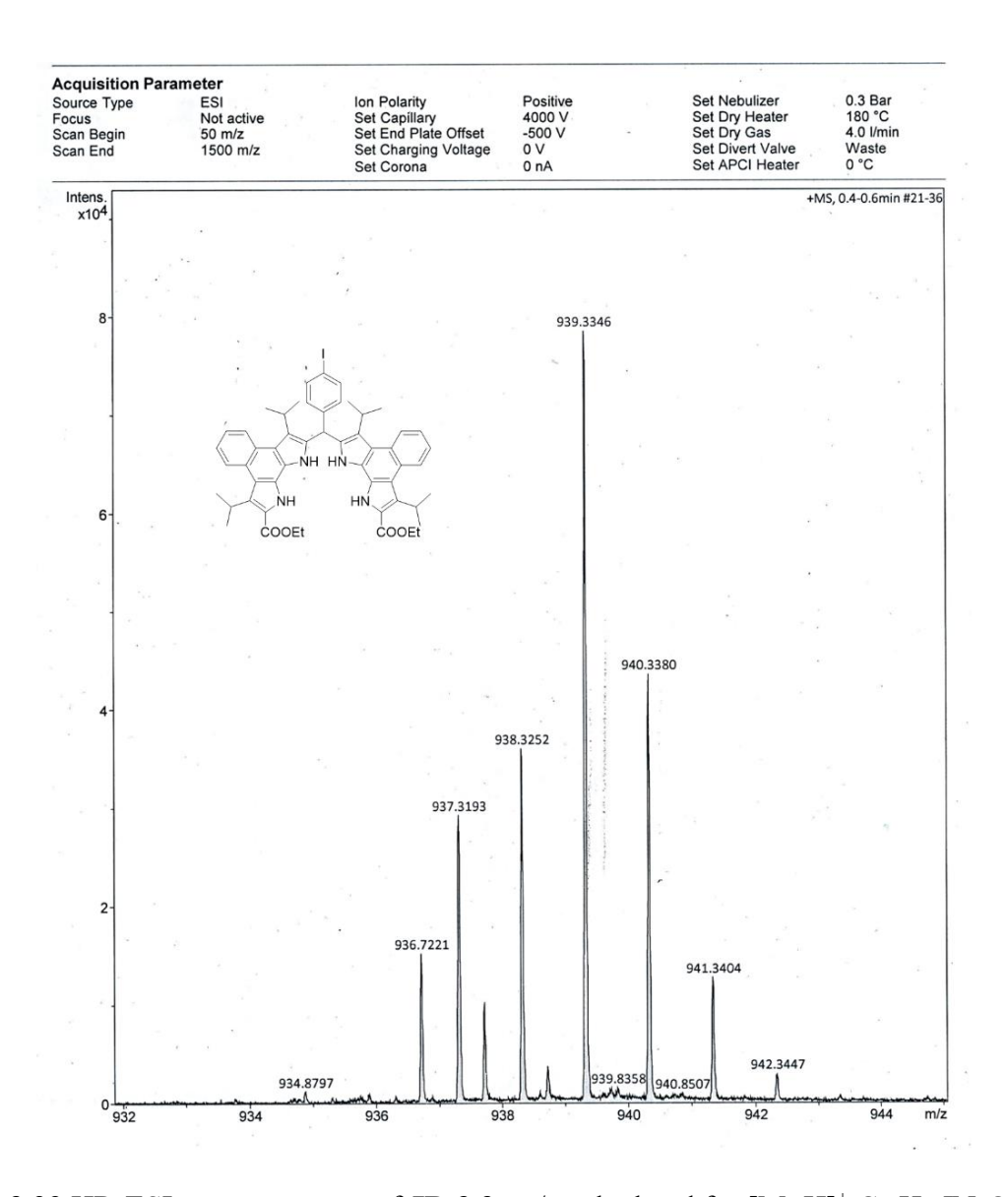


**Figure 3.29** HR-ESI mass spectrum of **JB-3.3**; m/z calculated for  $[M+H]^+$   $C_{53}H_{56}IN_4O_4$  939.3346, found 939.3346.

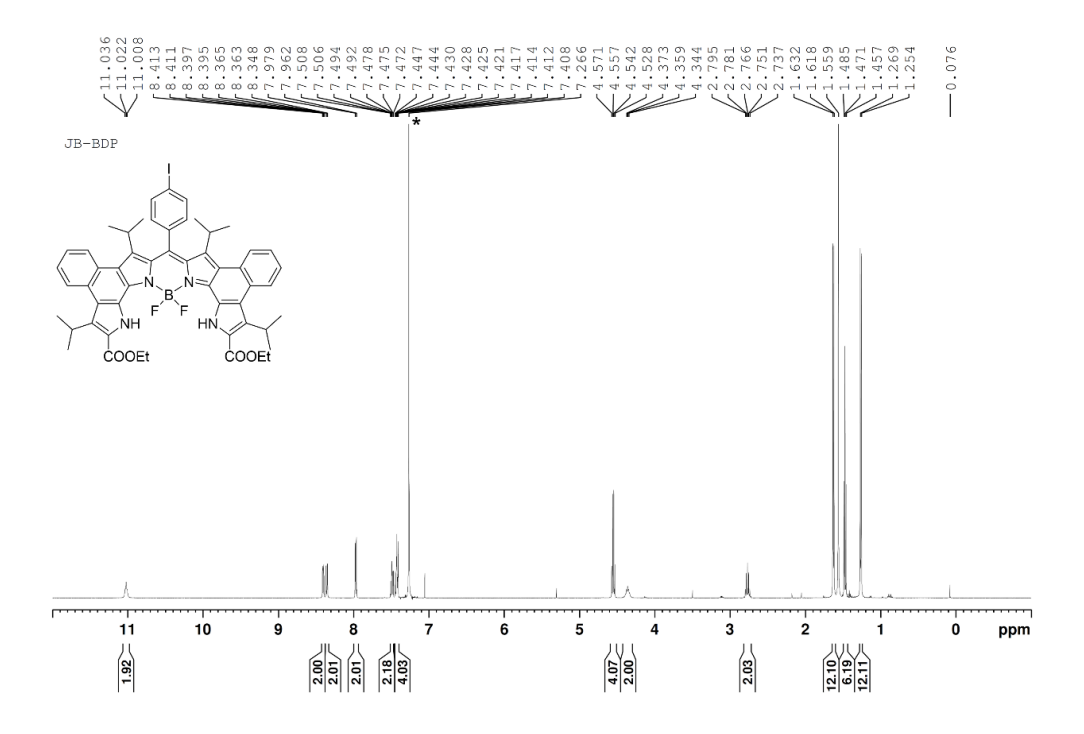
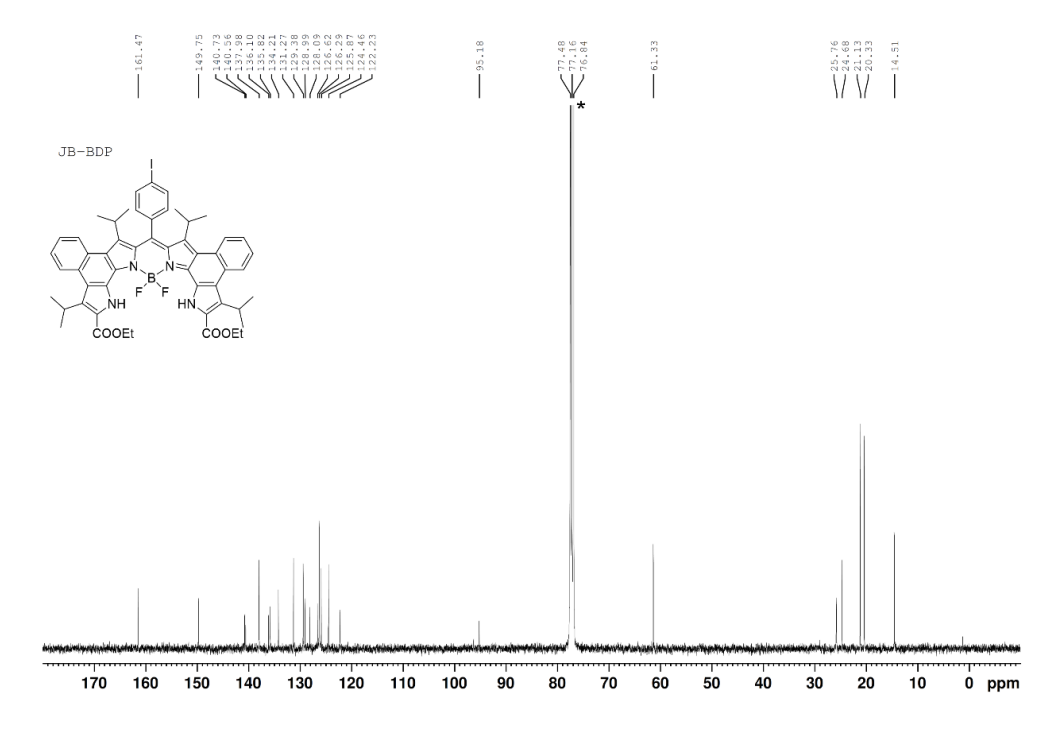
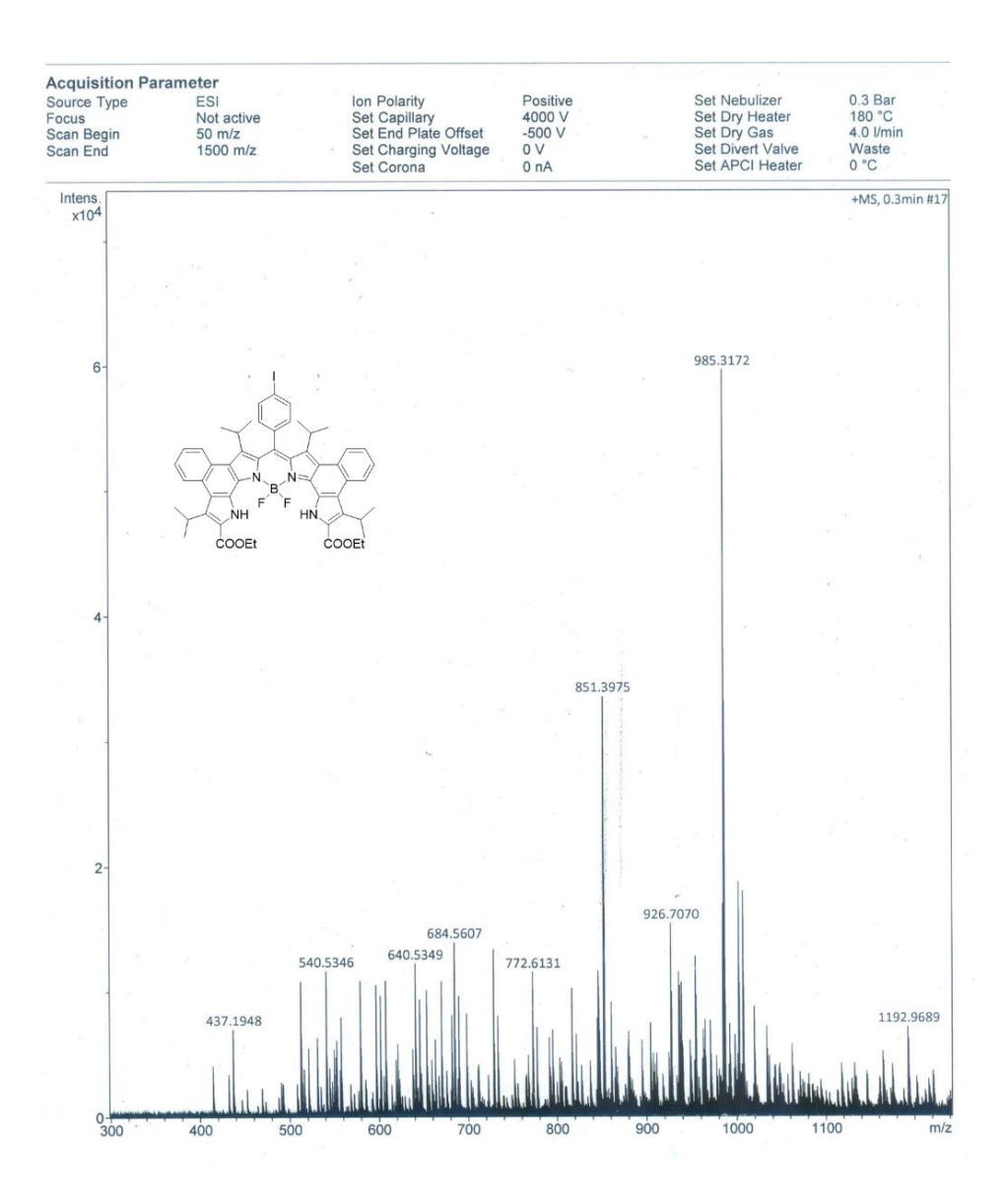


Figure 3.30  $^{1}$ H NMR spectrum of JB-3.4 in CDCl<sub>3</sub> recorded at 25  $^{\circ}$ C (\*Asterisk indicates residual solvent impurity).



**Figure 3.31**  $^{13}$ C NMR spectrum of **JB-3.4** in CDCl<sub>3</sub> recorded at 25  $^{\circ}$ C (\*Asterisk indicates residual solvent impurity).



**Figure 3.32** HR-ESI mass spectrum of **JB3.4**; m/z calculated for  $[M+H]^+$   $C_{53}H_{53}BF_2IN_4O_4$  985.3173, found 985.3172.

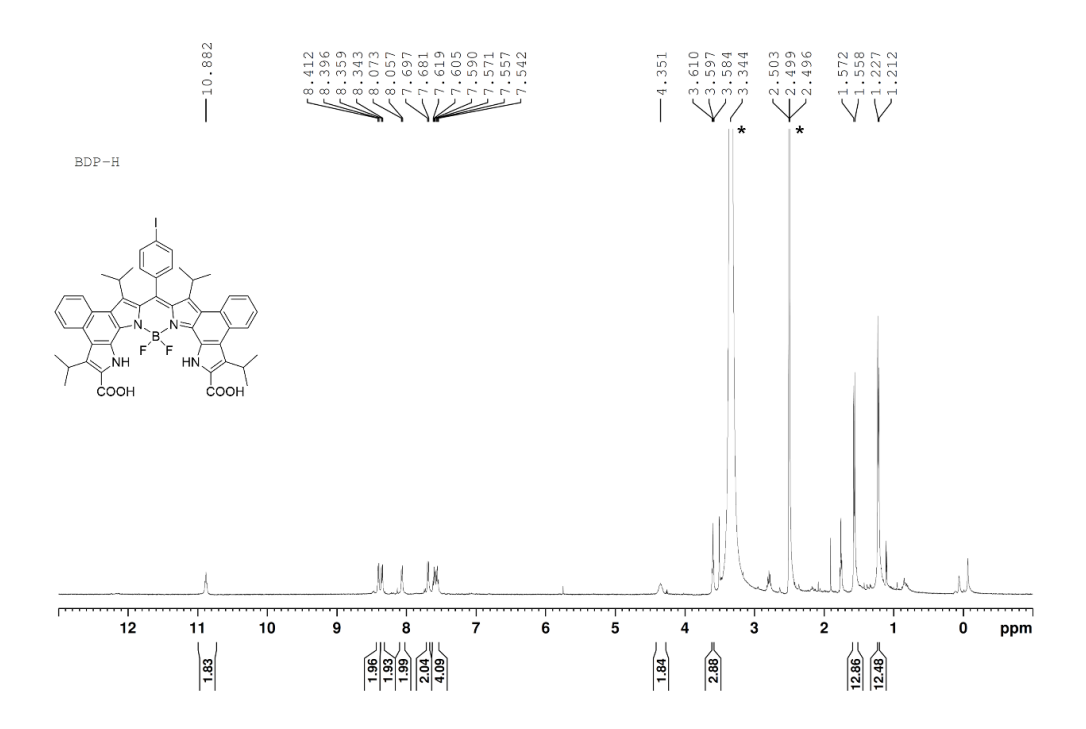


**Figure 3.33** <sup>1</sup>H NMR spectrum of **JB-3.5** in THF- $d_8$  recorded at 25 °C (\*Asterisk indicates residual solvent impurity).

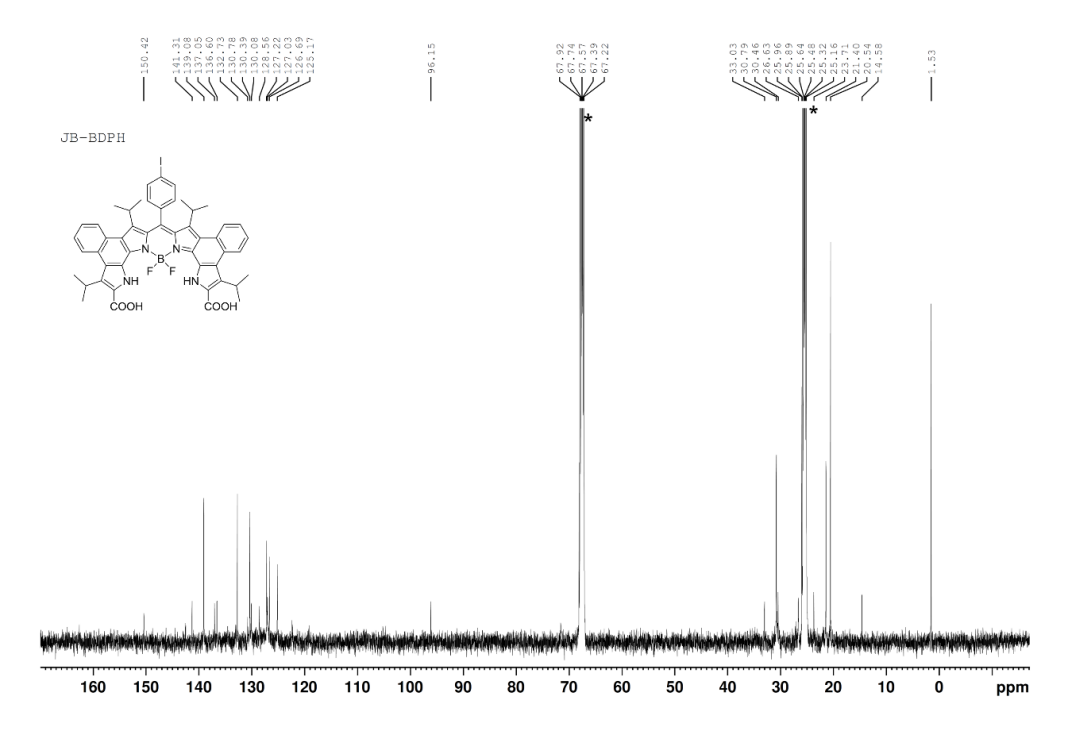


**Figure 3.34**  $^{13}$ C NMR spectrum of **JB-3.5** in THF- $d_8$  recorded at 25  $^{\circ}$ C (\*Asterisk indicates residual solvent impurity).

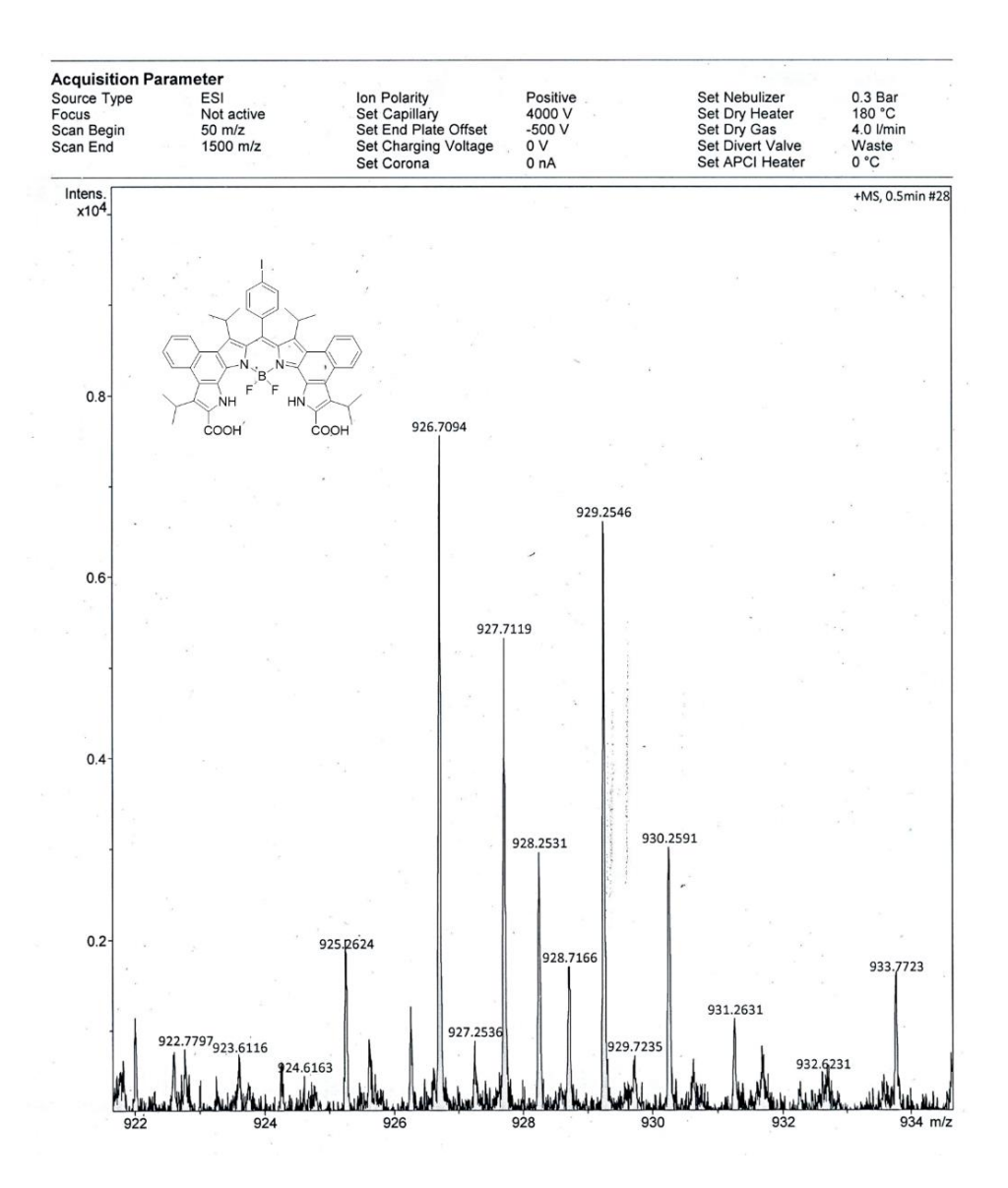


**Figure 3.35** HR-ESI mass spectrum of **JB-3.5**; m/z calculated for  $[M+H]^+$   $C_{49}H_{45}BF_2IN_4O_4$  929.2547, found 929.2546.

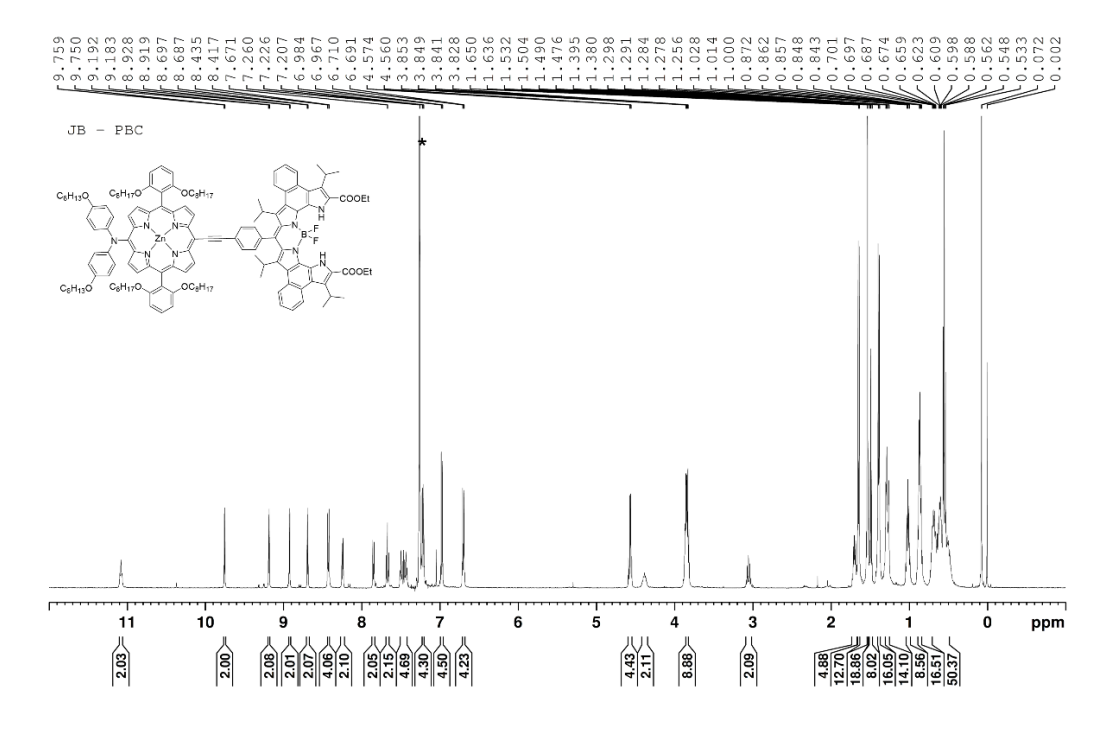


**Figure 3.36** <sup>1</sup>H NMR spectrum of **JB-3.6** in CDCl<sub>3</sub> recorded at 25 °C (\*Asterisk indicates residual solvent impurity).

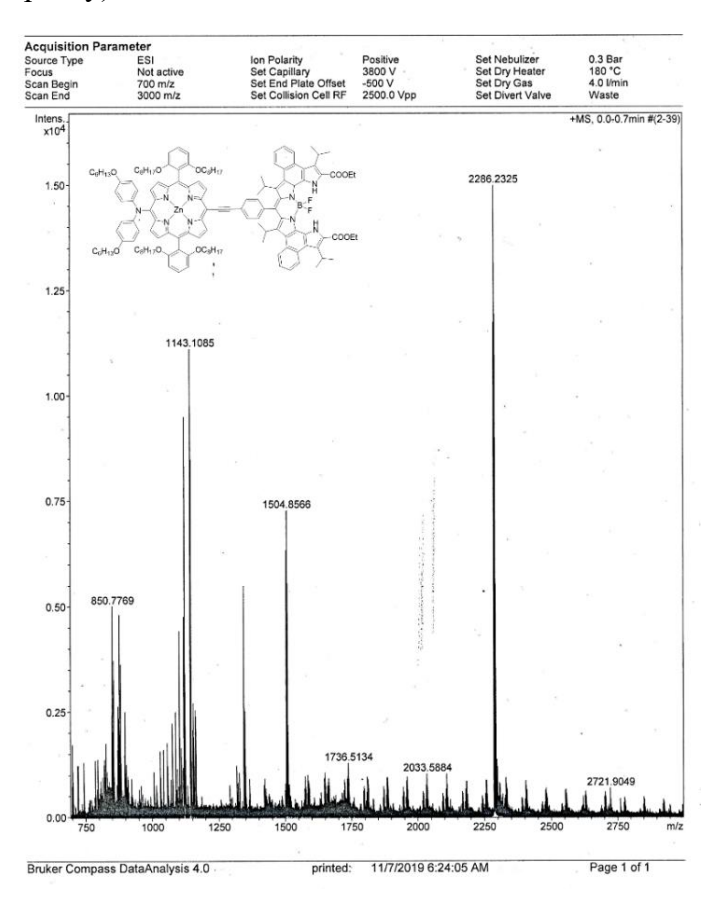


**Figure 3.37** HR-ESI mass spectrum of **JB-3.6**; m/z calculated for  $[M+H]^+$   $C_{143}H_{170}BF_2N_9O_{10}Zn$  2286.2379, found 2286.2325.

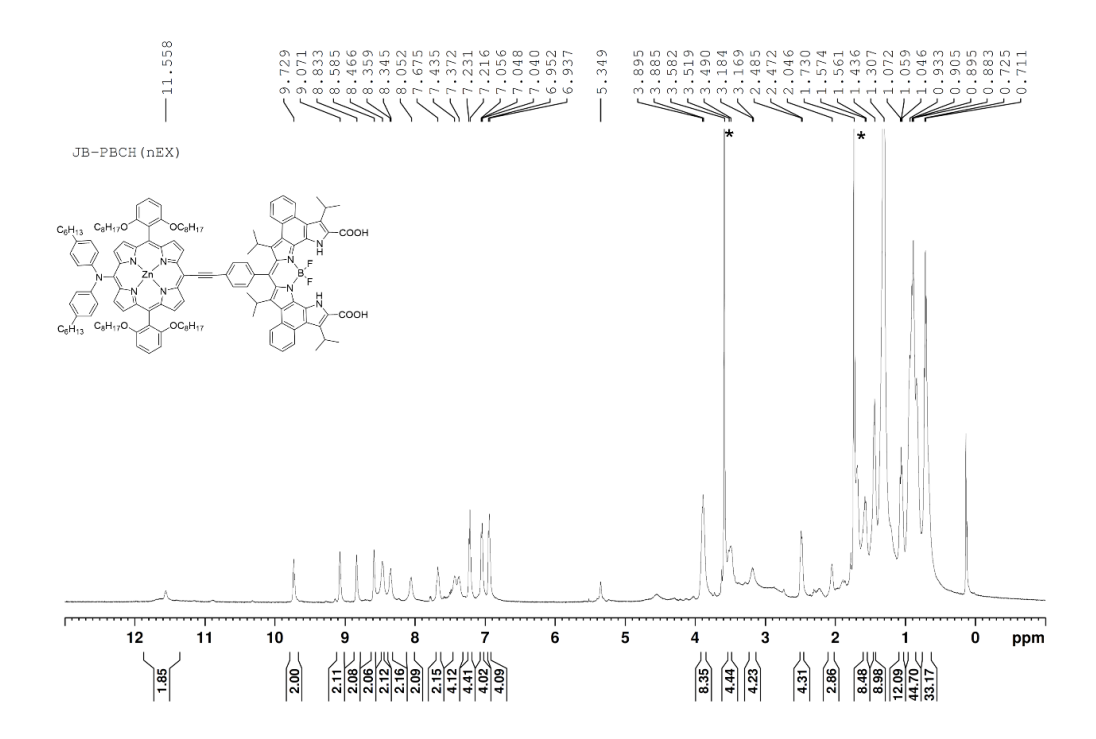


**Figure 3.38** <sup>1</sup>H NMR spectrum of **JB-1** in THF- $d_8$  recorded at 25 °C (\*Asterisk indicates water and residual solvent impurity).

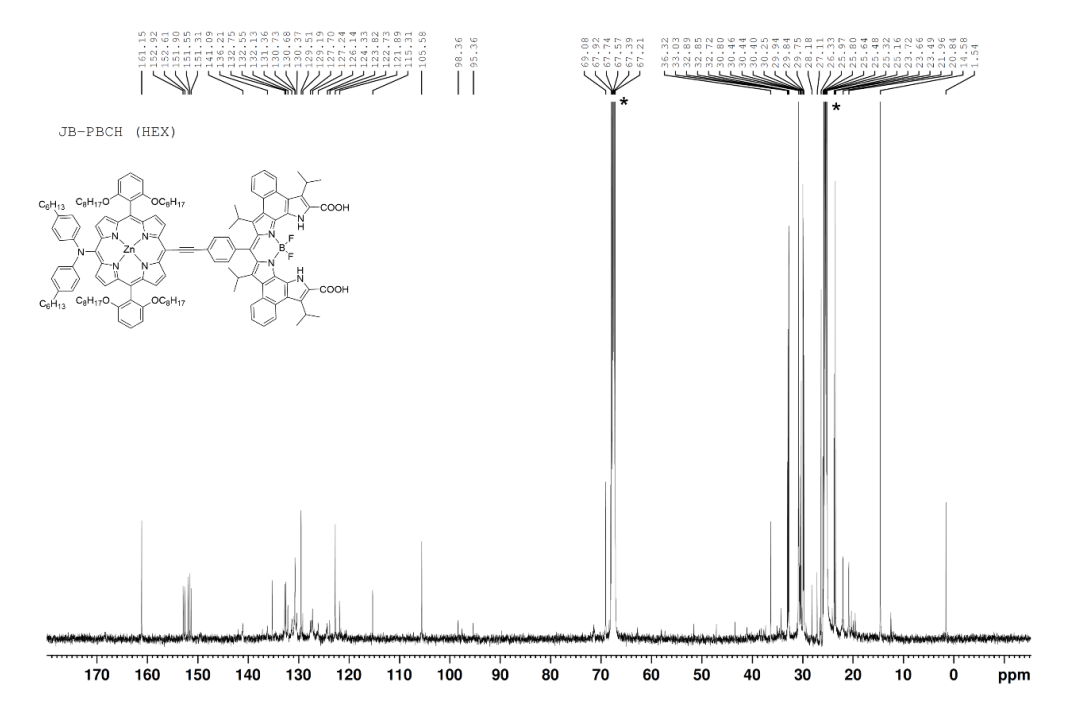


**Figure 3.39**  $^{13}$ C NMR spectrum of **JB-1** in THF- $d_8$  recorded at 25  $^{\circ}$ C (\*Asterisk indicates residual solvent impurity).

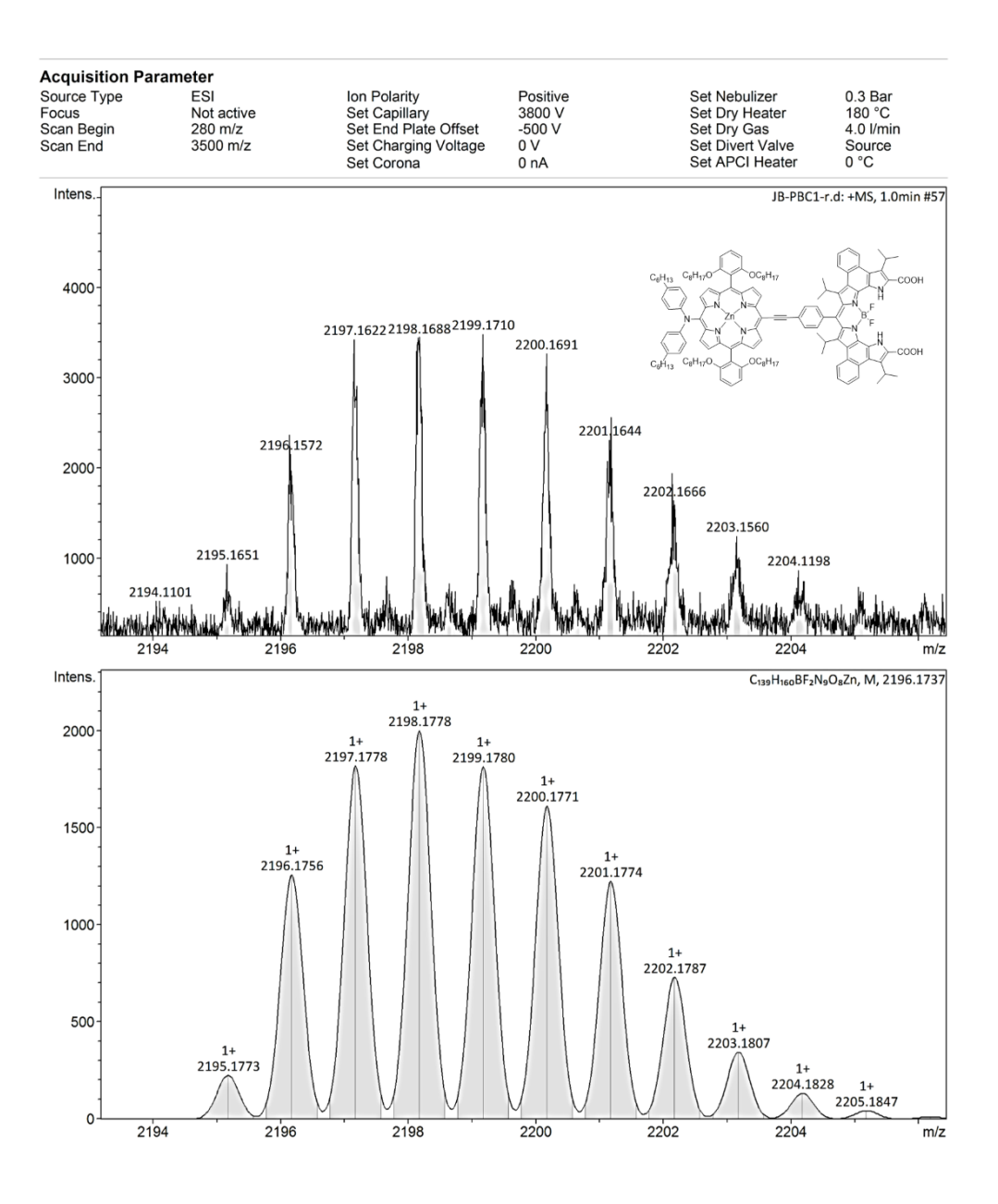


**Figure 3.40** HR-ESI mass spectrum of **JB-1**; m/z calculated for [M]  $C_{139}H_{160}BF_2N_9O_8Zn$  2198.1778, found 2198.1710.

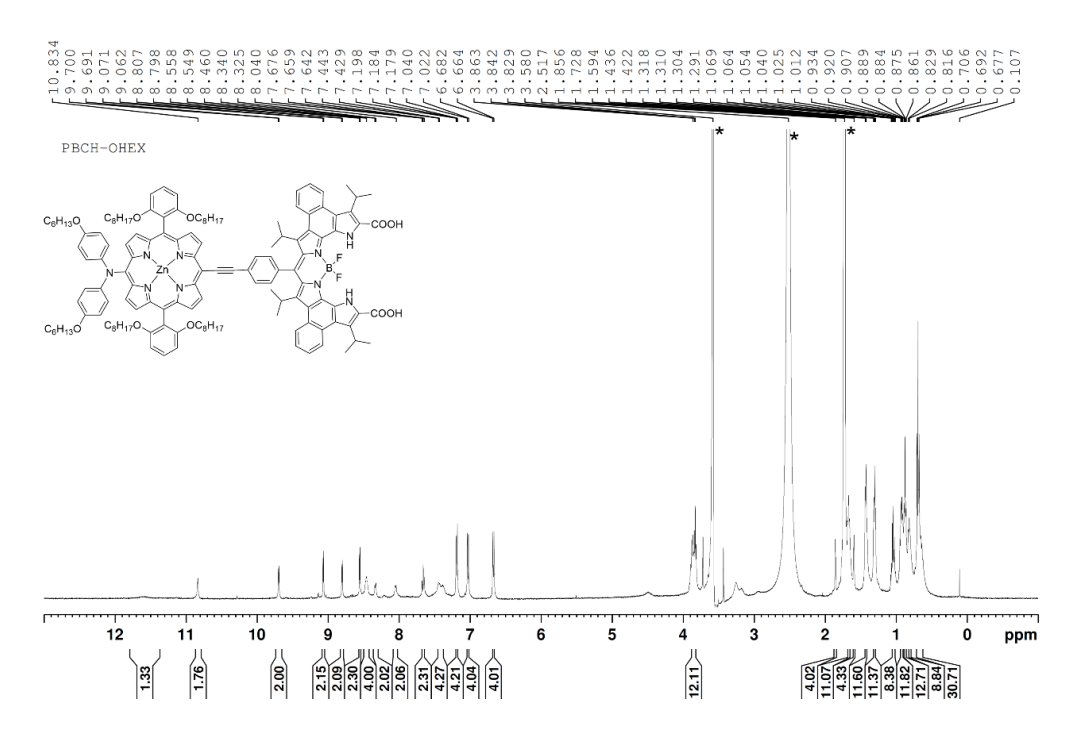


**Figure 3.41** <sup>1</sup>H NMR spectrum of **JB-2** in THF- $d_8$  recorded at 25 °C (\*Asterisk indicates residual solvent impurity).

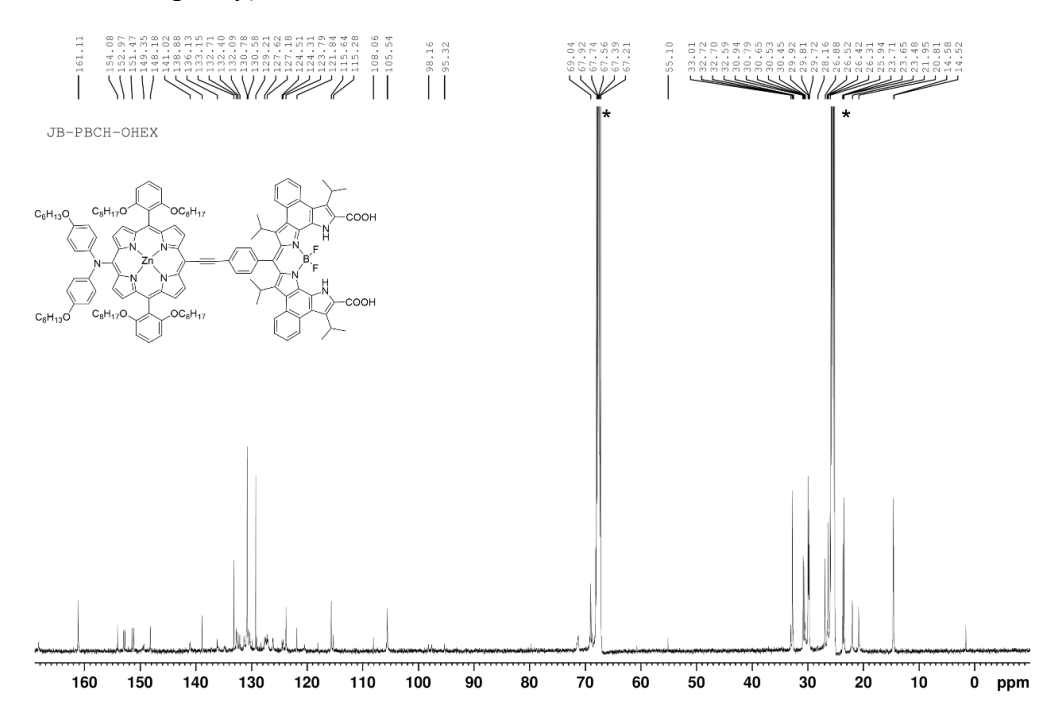


**Figure 3.42**  $^{13}$ C NMR spectrum of **JB-2** in THF- $d_8$  recorded at 25  $^{\circ}$ C (\*Asterisk indicates residual solvent impurity).

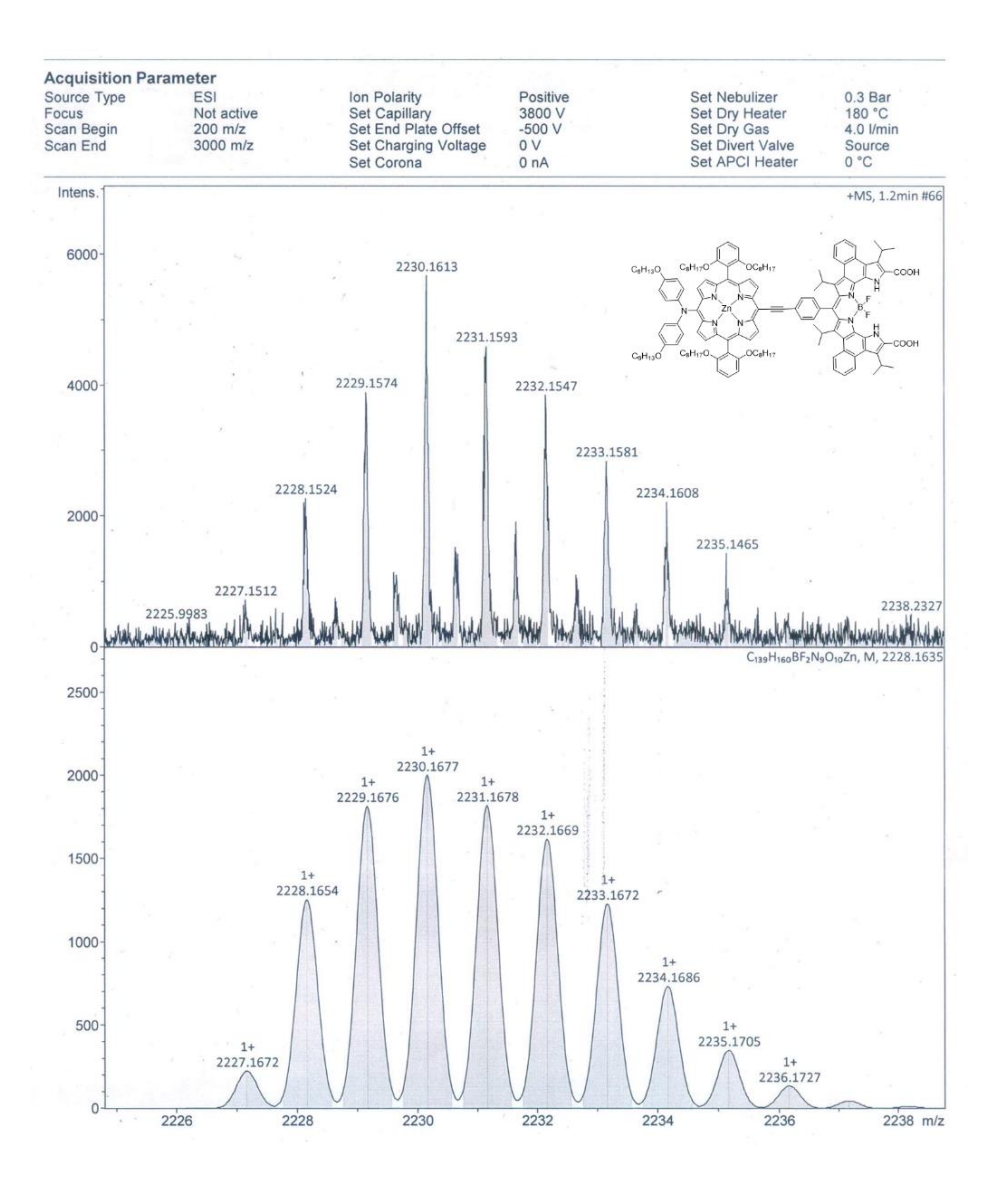


**Figure 3.43** HR-ESI mass spectrum of **JB-2**; m/z calculated for  $[M+H]^+C_{139}H_{161}BF_2N_9O_{10}Zn$  2230.1677, found 2230.1613.

## 3.8. Computational Studies

Optimized coordinates of Porphyrin-BODIPY Conjugates JB-1 and JB-2.

**Table 3.4.** Coordinates of the optimized structure of **JB-1**.

Tag	Symbol	Х	Υ	Z
1	С	6.396335	-7.10374	-0.7496
2	С	7.715801	-7.56282	-0.73841
3	С	8.753849	-6.66647	-0.52336
4	С	8.528139	-5.28629	-0.3333
5	С	7.189306	-4.79772	-0.52277
6	С	6.147546	-5.74195	-0.65019
7	С	9.581443	-4.34384	0.047158
8	С	9.291538	-2.95678	0.083118
9	С	8.000466	-2.45773	-0.22551

<b>T</b>				
10	С	6.951431	-3.35685	-0.55979
11	С	10.94623	-4.49314	0.466111
12	С	11.43294	-3.18451	0.662652
13	N	10.41279	-2.28865	0.446779
14	N	7.567069	-1.18021	-0.3259
15	С	6.221396	-1.19358	-0.70025
16	С	5.84543	-2.56622	-0.96142
17	С	6.367824	7.239375	-0.23626
18	С	7.685996	7.68657	-0.13956
19	С	8.713328	6.758479	-0.05321
20	С	8.476511	5.368752	-0.0357
21	С	7.120598	4.901735	-0.17614
22	С	6.107449	5.876207	-0.26914
23	С	9.570603	4.402689	0.028361
24	С	9.287472	3.053133	-0.27937
25	С	7.965147	2.569191	-0.39043
26	С	6.852034	3.457278	-0.27942
27	С	10.97433	4.477702	0.31506
28	С	11.4783	3.180733	0.086362
29	N	10.44728	2.35588	-0.27725
30	N	7.555127	1.284078	-0.49456
31	С	6.158057	1.271055	-0.47902
32	С	5.695354	2.635547	-0.29562
33	С	5.490531	0.028454	-0.65043
34	С	4.249551	3.018861	-0.02087
35	С	11.75691	5.655689	0.868594
36	С	4.739089	-3.12983	-1.85146
37	С	12.80313	2.559295	0.226928
38	С	-0.24795	-0.06475	-0.36479
39	С	-9.66631	-0.33415	2.770068
40	С	-8.63975	-0.43505	3.661794
41	С	-7.40917	-0.31851	2.913039
42	N	-7.70313	-0.14058	1.582997
43	С	-9.07181	-0.14674	1.466616
44	С	-9.08789	0.40358	-3.26432
45	С	-9.99041	0.321328	-2.24557
46	С	-9.2337	0.12416	-1.03065
47	N	-7.8923	0.094331	-1.32519
48	C	-7.77201	0.266474	-2.68275
49	С	-9.78957	-0.0051	0.259952
50	С	-3.01654	0.189902	-2.71724
51	С	-4.04116	0.189902	-3.60989
52	С	-5.27252	0.240168	-2.85322
53	N	-4.97369	0.107132	-2.83322
54	C	-3.61117	0.107132	-1.31374
55	С			
		-6.56155	0.320606	-3.40547
56 57	C	-3.58993	-0.40016	3.344758
57		-2.68927	-0.30805	2.326294
58	C	-3.44836	-0.1815	1.103858
59	N	-4.78548	-0.19666	1.38849

60	С	-4.90873	-0.32998	2.755326
61	С	-6.11562	-0.39391	3.471128
62	С	-2.88321	-0.05634	-0.19325
63	С	-6.66166	0.48227	-4.89377
64	С	-6.02258	-0.56129	4.959232
65	С	-6.62928	1.759933	-5.48326
66	С	-6.72451	1.914137	-6.87415
67	С	-6.85357	0.77937	-7.67246
68	С	-6.88958	-0.49972	-7.12101
69	С	-6.79303	-0.64307	-5.72908
70	С	-5.93953	-1.84272	5.535398
71	С	-5.85356	-2.003	6.926169
72	С	-5.85195	-0.8704	7.7379
73	С	-5.93348	0.412312	7.199895
74	С	-6.01883	0.561738	5.807856
75	0	-6.81538	-1.84542	-5.08643
76	0	-6.50342	2.800944	-4.61106
77	0	-5.95168	-2.88098	4.650966
78	N	-11.2225	0.00941	0.354549
79	С	-1.46459	-0.06198	-0.28584
80	С	11.66692	-5.79704	0.770215
81	0	-6.10077	1.767935	5.177374
82	С	-6.95711	-3.02604	-5.85878
83	С	-6.46179	4.119851	-5.12983
84	С	-5.86859	-4.20341	5.155601
85	С	-6.11209	2.946886	5.965159
86	Н	5.567973	-7.79952	-0.84971
87	Н	7.935466	-8.61803	-0.87535
88	Н	9.765234	-7.04773	-0.52405
89	Н	5.119468	-5.40414	-0.64436
90	Н	10.48776	-1.28945	0.604164
91	Н	5.545889	7.945719	-0.3136
92	Н	7.91502	8.748571	-0.15109
93	H	9.732356	7.119686	-0.04024
94	H	5.084896	5.562482	-0.38962
95	Н	10.5461	1.376949	-0.51902
96	H	3.708901	2.085483	0.114012
97	H	11.0434	6.464788	1.033385
98	H	5.115543	-4.11848	-2.1246
99	H	-10.7263	-0.37599	2.973553
100	H	-8.70531	-0.5825	4.730427
101	H	-9.29032	0.551515	-4.31558
102	Н	-11.0671	0.381181	-2.30882
102	H	-1.95444	0.188633	-2.91695
103	H	-3.97655	0.390863	-4.68415
104	Н	-3.387	-0.50408	4.401191
		-1.61029	-0.32134	2.385769
106 107	H			-7.3309
	•	-6.70053	2.895922	
108	H	-6.92802	0.894742	-8.75053
109	Н	-6.9902	-1.36369	-7.76641

110	Н	-5.79003	-2.98767	7.372812
111	Н	-5.78559	-0.99039	8.815998
112	Н	-5.92951	1.274398	7.85554
113	Н	10.8943	-6.56661	0.798117
114	Н	-6.95551	-3.85024	-5.14336
115	Н	-7.9023	-3.03271	-6.41745
116	Н	-6.12199	-3.15327	-6.56031
117	Н	-6.3577	4.77605	-4.26393
118	Н	-5.60357	4.264428	-5.79932
119	Н	-7.3853	4.372536	-5.66741
120	Н	-5.89308	-4.85654	4.281506
121	Н	-4.93255	-4.36866	5.705313
122	Н	-6.71794	-4.44104	5.809729
123	Н	-6.18723	3.775011	5.258268
124	Н	-5.18845	3.051766	6.549638
125	Н	-6.97421	2.970867	6.64468
126	С	12.73211	-2.57329	0.941462
127	В	8.45457	0.060133	-0.26965
128	F	9.456368	-0.01186	-1.26145
129	F	9.110879	0.136059	0.973329
130	Zn	-6.33828	-0.03408	0.033147
131	C	12.6712	-6.19814	-0.32929
132	Н	13.48488	-5.47164	-0.40192
133	Н	13.10777	-7.17941	-0.10627
134	H	12.18166	-6.25903	-1.30836
135	C	12.29613	-5.83624	2.178918
136	Н	13.13965	-5.15189	2.277849
137	H	11.5515	-5.58328	2.94196
138	H	12.65812	-6.85056	2.386881
139	C	4.634376	-2.38687	-3.19914
140	Н	4.222415	-1.38295	-3.09503
141	H	5.616314	-2.30872	-3.67788
142	H	3.973966	-2.94742	-3.87207
143	C	3.35505	-3.3714	-1.21746
144	Н	3.438745	-3.84671	-0.23341
145	H	2.785908	-2.45009	-1.09417
145	Н	2.772098	-4.03822	-1.86454
147	С	3.531735	3.715176	-1.80434
147	Н	3.529474	3.066775	-2.08101
149	Н	2.488099	3.913383	-0.92945
150	Н	3.98483	4.660277	-0.92943
151	С	4.080281	3.74282	1.335508
152	Н	4.447825	3.104705	2.146593
153	Н	4.608895	4.694909	1.403885
154	Н	3.015419	3.933357	1.514883
155	С	12.82492	6.168604	1
				-0.11778
156	Н	13.3176	7.060933	0.287279
157	Н	13.58987	5.405811	-0.28724
158	Н	12.37935	6.434891	-1.08355
159	С	12.36245	5.354583	2.256343

160	Н	11.58609	5.027178	2.957119
161	Н	13.13086	4.581635	2.196121
162	Н	12.82193	6.264283	2.662294
163	0	12.88798	-1.37162	1.112435
164	0	13.78658	-3.42509	0.953159
165	0	12.72503	1.243259	-0.10339
166	0	13.83769	3.085712	0.594453
167	Н	14.56487	-2.86823	1.143669
168	Н	13.54005	0.790652	0.177954
169	С	3.35452	-0.487	0.531994
170	С	1.967964	-0.48397	0.63003
171	С	1.169551	-0.06393	-0.45626
172	С	1.819444	0.359122	-1.63587
173	С	3.207777	0.384327	-1.71326
174	С	3.999324	-0.03753	-0.63404
175	Н	3.953385	-0.81814	1.37524
176	Н	1.486528	-0.81716	1.544066
177	Н	1.222092	0.683334	-2.48219
178	Н	3.687346	0.742884	-2.6189
179	С	-11.8633	1.146152	0.91302
180	С	-13.0326	1.022339	1.684347
181	С	-11.318	2.427781	0.736083
182	С	-13.6351	2.147905	2.240128
183	Н	-13.465	0.04105	1.85122
184	С	-11.9249	3.541229	1.3138
185	Н	-10.4149	2.54873	0.14711
186	С	-13.0984	3.431484	2.069628
187	Н	-14.5373	2.020562	2.835065
188	H	-11.4758	4.52071	1.162716
189	С	-11.9547	-1.11293	-0.11309
190	C	-13.2135	-0.96354	-0.72238
191	C	-11.4171	-2.40563	-0.00968
192	C	-13.9072	-2.07507	-1.1929
193	Н	-13.6439	0.02676	-0.83045
194	С	-12.1182	-3.50524	-0.50137
195	Н	-10.4465	-2.54639	0.454166
196	C	-13.3789	-3.36993	-1.09469
197	Н	-14.8777	-1.92789	-1.66277
198	H	-11.6734	-4.49405	-0.41074
199	C	-14.1513	-4.57086	-1.58903
200	Н	-13.4829	-5.40292	-1.83578
200	H	-14.8587	-4.93632	-0.83174
201	H	-14.7353	-4.33195	-2.48522
202	C	-13.7733	4.648531	2.65828
203	Н	-14.2822	4.409633	3.599097
204	Н	-14.2822	5.448488	2.859943
		-13.0324		<u> </u>
206	Н	-14.5515	5.059631	1.976933

 Table 3.5. Coordinates of the optimized structure of JB-2.

Tag	Symbol	X	Υ	Z
1	С	-6.66313	7.129692	0.552568
2	С	-7.98237	7.578637	0.652959
3	С	-9.01957	6.657572	0.707939
4	С	-8.7933	5.265817	0.644142
5	С	-7.45584	4.82024	0.361734
6	С	-6.4144	5.772478	0.402663
7	С	-9.84462	4.269458	0.854392
8	С	-9.5556	2.898951	0.636275
9	С	-8.26741	2.464989	0.231581
10	С	-7.21951	3.410224	0.060648
11	С	-11.2061	4.339868	1.303317
12	C	-11.6925	3.017105	1.263656
13	N	-10.6748	2.175401	0.881728
14	N	-7.83665	1.22776	-0.10566
15	C	-6.4937	1.309376	-0.48137
16	C	-6.1173	2.706578	-0.48699
17	С	-6.65317	-7.06707	-1.5718
18	С	-7.971	-7.5246	-1.54295
19	С	-8.99556	-6.62749	-1.27813
20	С	-8.75593	-5.26375	-1.27813
21	С		-4.77901	-1.01141
	С	-7.40064		
22		-6.39049	-5.72041	-1.35937
23	С	-9.84735	-4.32509	-0.76151
24	С	-9.56441	-2.94211	-0.82123
25	С	-8.24232	-2.44615	-0.8546
26	С	-7.13007	-3.33985	-0.91985
27	С	-11.2485	-4.45037	-0.4795
28	C	-11.7521	-3.13328	-0.46369
29	N	-10.7227	-2.2568	-0.68114
30	N	-7.83081	-1.16387	-0.72467
31	С	-6.43362	-1.15412	-0.72046
32	С	-5.97195	-2.52929	-0.79711
33	С	-5.7651	0.098531	-0.6644
34	С	-4.52381	-2.95735	-0.61753
35	С	-12.0281	-5.709	-0.14174
36	С	-5.01401	3.424301	-1.2622
37	С	-13.074	-2.54681	-0.19903
38	С	-0.0243	0.116169	-0.40289
39	С	9.37691	-0.93751	2.60768
40	С	8.345161	-1.2271	3.450812
41	С	7.120164	-0.92015	2.749118
42	N	7.422485	-0.44398	1.496531
43	С	8.791583	-0.44292	1.383242
44	С	8.829935	1.174796	-3.09656
45	С	9.7277	0.866207	-2.11749
46	С	8.966768	0.38907	-0.98621
47	N	7.626998	0.419607	-1.28933

	1	T	<b>T</b>	T
48	С	7.512579	0.898381	-2.5719
49	С	9.518032	-0.03225	0.243864
50	С	2.757269	0.826919 -2.650	
51	С	3.786525	1.116751	-3.49554
52	С	5.014143	0.90265	-2.76131
53	N	4.708409	0.481722	-1.48421
54	С	3.345312	0.43202	-1.3917
55	С	6.305665	1.108941	-3.27248
56	С	3.298424	-1.03074	3.152352
57	С	2.403236	-0.70476	2.178086
58	С	3.169254	-0.32695	1.012758
59	N	4.504787	-0.42214	1.288847
60	С	4.620536	-0.85458	2.593135
61	С	5.823173	-1.09941	3.275412
62	С	2.611145	0.064968	-0.23287
63	С	6.413814	1.609496	-4.68279
64	С	5.72175	-1.60347	4.684899
65	С	6.591065	0.7114	-5.75205
66	С	6.696149	1.174431	-7.07199
67	С	6.622353	2.544359	-7.31533
68	С	6.447009	3.460361	-6.27999
69	С	6.34411	2.987047	-4.9636
70	С	5.751084	-0.70864	5.770986
71	С	5.657446	-1.17423	7.090844
72	С	5.534108	-2.54359	7.316967
73	С	5.502398	-3.45629	6.264593
	С			
74		5.597199	-2.98049	4.948567
75	0	6.176281	3.79506	-3.87779
76	0	6.647169	-0.60545	-5.40301
77	0	5.871738	0.607832	5.437159
78	N	10.94803	-0.04246	0.347035
79	С	1.192014	0.092662	-0.32683
80	С	-11.9233	5.567088	1.843116
81	0	5.579771	-3.78544	3.847706
82	С	6.094469	5.196011	-4.0798
83	С	6.840869	-1.57097	-6.42312
84	С	5.923241	1.570483	6.476785
85	С	5.447896	-5.18508	4.031966
86	Н	-5.835	7.832444	0.575903
87	Н	-8.20215	8.641158	0.709824
88	Н	-10.0308	7.032083	0.781602
89	Н	-5.38641	5.439853	0.342438
90	Н	-10.7494	1.164247	0.85629
91	Н	-5.8335	-7.74768	-1.78535
92	Н	-8.20217	-8.56695	-1.74421
93	Н	-10.015	-6.98536	-1.31926
94	Н	-5.36878	-5.38992	-1.43227
95	Н	-10.822	-1.25015	-0.73994
96	Н	-3.97829	-2.0651	-0.32153
97	Н	-11.3147	-6.53488	-0.13329

98	Н	-5.38907	4.447089	-1.34437
99	Н	10.43504	-1.04192	2.79754
100	Н	8.404116	-1.62041	4.455668
101	Н	9.03693	1.562786	-4.08379
102	Н	10.80394	0.946663	-2.15792
103	Н	1.695981	0.876337	-2.84953
104	Н	3.727413	1.446254	-4.52321
105	Н	3.089735	-1.36088	4.160121
106	Н	1.323878	-0.7195	2.230781
107	Н	6.832025	0.485762	-7.89688
108	Н	6.702828	2.90717	-8.33662
109	Н	6.39408	4.519731	-6.49916
110	Н	5.678199	-0.48801	7.928574
111	Н	5.460929	-2.90858	8.338004
112	Н	5.40708	-4.51527	6.470775
113	Н	-11.1499	6.319119	2.004285
114	Н	5.961998	5.631266	-3.08772
115	Н	7.013085	5.594178	-4.53079
116	Н	5.23702	5.464696	-4.71084
117	Н	6.860216	-2.53755	-5.91668
118	Н	6.019613	-1.55975	-7.15202
119	Н	7.792485	-1.41822	-6.94904
120	Н	6.029122	2.536976	5.981061
121	Н	5.002897	1.568894	7.075728
122	Н	6.784457	1.405929	7.137775
123	Н	5.452221	-5.61785	3.029964
124	Н	4.504698	-5.44002	4.532922
125	Н	6.286034	-5.59811	4.608746
126	C	-12.9904	2.365503	1.43701
127	В	-8.72584	-0.00162	-0.27086
128	F	-9.73568	0.251856	-1.22386
129	F	-9.37155	-0.30499	0.942657
130	Zn	6.06531	0.008565	0.002664
131	C	-12.9346	6.15983	0.841034
132	Н	-13.7488	5.45762	0.643426
133	H	-13.3695	7.084032	1.24098
134	H	-12.4514	6.397231	-0.11398
135	C	-12.5431	5.351152	3.239952
136	Н	-13.3856	4.658863	3.220195
137	H	-11.7932	4.966478	3.940188
138	H	-12.9041	6.31089	3.629278
139	C	-4.91789	2.946506	-2.72572
140	Н	-4.50852	1.940094	-2.81411
141	H	-5.90243	2.961533	-3.20528
142	H	-4.25918	3.621896	-3.28538
143	C	-3.62705	3.540715	-0.59994
144	Н	-3.70614	3.829532	0.454467
145	Н	-3.06208	2.609861	-0.64791
146	Н	-3.04264	4.311699	-1.11699
147	С	-3.82524	-3.42471	-1.91546
14/		-3.02324	-3.424/1	-1.51340

148	Н	-3.83177	-2.62397	-2.66054
149	Н	-2.77901	-3.67203	-1.70108
150	Н	-4.28689	-4.28689 -4.29565	
151	С	-4.33791	-3.91789	0.580682
152	Н	-4.6896	-3.43751	1.500314
153	Н	-4.87061	-4.86516	0.482902
154	Н	-3.27148	-4.14068	0.70537
155	С	-13.1064	-6.03353	-1.19462
156	Н	-13.5984	-6.9835	-0.95278
157	Н	-13.8703	-5.25141	-1.21662
158	Н	-12.6702	-6.12188	-2.19667
159	С	-12.6198	-5.66463	1.283382
160	Н	-11.8363	-5.46944	2.024321
161	Н	-13.3875	-4.89364	1.371641
162	Н	-13.0768	-6.6329	1.522249
163	0	-13.1464	1.152641	1.392031
164	0	-14.044	3.201648	1.606375
165	0	-12.9958	-1.19257	-0.28559
166	0	-14.1059	-3.13047	0.077411
167	H	-14.8217	2.61959	1.699665
168	Н	-13.8062	-0.79768	0.083061
169	С	-3.62002	0.372096	0.580134
170	С	-2.23279	0.344922	0.666379
171	C	-1.4431	0.139703	-0.4857
172	C	-2.10123	-0.04471	-1.72062
173	C	-3.4903	-0.05021	-1.79217
174	С	-4.27335	0.157951	-0.64662
175	Н	-4.21238	0.536585	1.475201
176	H	-1.74385	0.494646	1.623995
177	H	-1.50983	-0.20293	-2.61699
178	H	-3.97675	-0.22806	-2.74648
179	С	11.58746	0.911301	1.184479
180	С	12.734	0.587671	1.923445
181	С	11.06327	2.211163	1.310365
182	С	13.35053	1.527682	2.752656
183	Н	13.15554	-0.40974	1.849678
184	С	11.66018	3.142003	2.149925
185	Н	10.17975	2.487798	0.744469
186	С	12.81282	2.813419	2.876739
187	Н	14.23759	1.236494	3.30407
188	Н	11.25228	4.143302	2.248241
189	С	11.68982	-1.00331	-0.3914
190	С	11.17198	-2.29531	-0.59851
190	С	12.93697	-0.69452	-0.95213
191	С	11.87332	-3.23274	-1.3447
192	Н	10.21103	-3.23274	-1.3447
194	С	13.65609	-1.64148	-1.68509
195	Н	13.35679	0.296544	-0.8132
196	С	13.12496	-2.91916	-1.89216
197	Н	11.47077	-4.22806	-1.50584

198	Н	14.61875	-1.36167	-2.09818
199	0	13.73792	-3.91793	-2.59971
200	0	13.32883	3.806668	3.664989
201	С	14.4855	3.516814	4.428242
202	Н	14.72309	4.431239	4.975579
203	Н	14.30632	2.703477	5.144952
204	Н	15.33745	3.24738	3.788659
205	С	14.9993	-3.64326	-3.18081
206	Н	15.30205	-4.55944	-3.69188
207	Н	14.94046	-2.82471	-3.91149
208	Н	15.75059	-3.3892	-2.42013

# **CHAPTER 4**

# Carbazole and phenothiazine based porphyrin-BODIPY conjugates

#### 4.1 Introduction

With the consumption of fossil fuels and aggravated pollution problems, solar cells have been identified as possible clean alternative renewable energy sources. In this case, DSSC offers a cheap and convenient solution because of its low production cost, ease of fabrication and relatively high solar energy conversion efficiencies. Due to the pivotal role of sensitizer in DSSC, significant efforts have been put towards synthesizing potential dyes for DSSC.<sup>1</sup> Porphyrin has been one of the dyes that has been studied the most in the past decade.<sup>2</sup> D-π-A based dyes have achieved record-breaking power conversion efficiencies.<sup>3,4</sup>

It has been observed that electron donor moiety and its geometry in designing of a dye plays a very crucial role in electrochemical, optical and photovoltaic properties of the dye.<sup>5,6</sup> It was found that the HOMO, LUMO levels, and molar absorption ability of porphyrin molecules are greatly affected by the effect of various donors on the porphyrin sensitizers. As it has been discussed in the previous chapter, diarylamine based derivatives have played a vital role for donors in D-π-A based porphyrin dyes. Apart from them, carbazole and phenothiazine, being structurally comparable to the diarylamine unit except that the if the two phenyl rings are fused together through a 5-membered ring lead to a carbazole unit and 6-membered ring via a heteroatom such as S will lead to a phenothiazine moiety, are the most investigated donors for DSSC because of their strong electron donating capability.<sup>7-9</sup> In carbazole, the two phenyl groups would the force to lie in the same plane by the fusion, further extending the πconjugation leading to a rigid structure and finding applications as building blocks in various π-conjugated compounds. Its properties can also be tuned by easily functionalization at its 3, 6 and the five-membered ring 9(NH) positions and can make covalent bonds with other compounds. Carbazole unit is primarily absorbing in 300-400 nm wavelength range where porphyrin lacks absorption and is also helpful in covering the UV region of solar spectrum. Additionally, phenothiazine and carbazole are used as donor groups in the push-pull structure of β-substituted zinc dibenzoporphyrins containing tertiary arylamines and acrylic acid groups as the pull/anchoring groups. <sup>10</sup> For example, carbazole based dye ADEKA-1, a non-porphyrin dye achieved an efficiency of 12.5%. 11a

$$\begin{array}{c} \text{MeO} \\ \text{Si-OMe} \\ \text{OMe} \\ \\ \text{S} \\ \text{C}_6 \text{H}_{13} \\ \\ \text{C}_$$

Figure 4.1 Structure of ADEKA-1.

Yongshu Xie's group reported 10.45% efficiency for the dye **XW4**, in which a porphyrin dye containing the carbazole electron donor including an additional ethynylene bridge that will increase the wavelength range of light absorption, and further aid in suppressing dye aggregation by adding additional alkoxy chains.<sup>5</sup>

$$C_{12}H_{25}O$$
  $OC_{12}H_{25}$   $OC_{6}H_{13}$   $OC_{6}H_{13}$   $OC_{12}H_{25}$   $OC_{12}H_{25}$ 

Figure 4.2 Structure of XW4.

In an effort to change the electronic level of the carbazole unit, a series of di-chromophoric zinc porphyrin appended carbazole dyes (CZP1) with an efficiency of 6.23% were synthesised by Attila J. Mozer's group. These dyes have a porphyrin core and a carbazole unit with a diarylamine substitution attached in the meso-position through a phenylethenyl linkage. 11b

Figure 4.3 Structure of CZP1.

Meanwhile, phenothiazine was also a good choice for donor in DSSC because of its tunable structure with butterfly like geometry, excellent electron donating properties, low cost, low environmental pollution and its non-planar butterfly conformation, which helps suppressing the aggregation. This heterocyclic molecule simultaneously has a nitrogen atom with a lone electron pair and an electron-donating sulfur atom in the same six-member ring which enhance its electron-donating ability. It is also anticipated that the sulfur atom in phenothiazine have impacts on its electronic structures.

Yongshu Xie's group have utilised phenothiazine as a donor in a number of dyes viz. **XW36** ( $\eta$ =11.7%), <sup>8</sup> **XW43** ( $\eta$ =12.10%), <sup>12</sup> **XW51** ( $\eta$ =11.1%), <sup>13</sup> **XW53** ( $\eta$ =9.6%) <sup>14</sup> and **XW73**. Among them **XW73** achieved highest efficiency of 12.3% in which they have introduced the propeller-shaped tetraphenylethylene (TPE) moiety on the phenothiazine donor appended to porphyrin (**XW73**). <sup>15</sup>

$$C_6H_{13}O$$
 $C_6H_{13}O$ 
 $C_6$ 

Figure 4.4 Structure of XW73.

Lingamallu Giribabu's group attached phenothiazine donor at the meso-position of porphyrin via an ethynyl spacer in **LG5** sensitizer, here role of phenothiazine not only acts as a donor, additionally, because of its nonplanar nature phenothiazine is also aids in reducing the aggregation. In order to improve the optical properties of the sensitizer, an ethynyl-bridge was added between the phenothiazine and the porphyrin ring. Phenyl and thiophene were also used as  $\pi$ -spacers, while cyanoacrylic acid served as an anchoring group and achieved an impressive efficiency of 10.20%. <sup>16</sup>

$$C_8H_{17}O$$
 $OC_8H_{17}$ 
 $OC_8H_{17}$ 
 $OC_8H_{17}$ 
 $OC_8H_{17}$ 
 $OC_8H_{17}$ 
 $OC_8H_{17}$ 
 $OC_8H_{17}$ 

Figure 4.5 Structure of LG5.

#### 4.2 Research goal

In view of the importance of the strong electron donating abilities of both carbazole and phenothiazine, we would like to utilize both of them as donors replacing the diarylamine units in our previously reported dyes porphyrin-BODIPY conjugates (**JB-1** and **JB-2**). Carbazole moiety, with its extended π-conjugation and phenothiazine moiety, with its butterfly shaped structure should probably increase the electron donor capability along with reducing the aggregation. We have opted for the hexyl chains on the carbazole and phenothiazine donor substituted to N, as it has been reported that the donors containing alkyl chain bonded to carbazole nitrogen, had a significant impact on the electrochemical and photovoltaic properties of these sensitizers, as well as spectra of the TiO<sub>2</sub> films. It has been observed that the sensitizer with a hexyl chain has a greater overall conversion efficiency that with a butyl chain due to its slower charge recombination rate and faster electron injection from the dye to the conduction band of the conducting glass.<sup>17</sup>

Figure 4.6 Porphyrin-BODIPY conjugates JB-3 and JB-4.

These new porphyrin-BODIPY conjugates **JB-3** and **JB-4** with strong electron donating groups carbazole and phenothiazine with hexyl chains as donor are expected to cover the entire visible portion of the solar spectrum along with NIR region. This should result in much higher solar energy-to-electricity conversion efficiency ( $\eta$ ) and help make efficient solar cell.

#### 4.3 Results and discussion

#### 4.3.1 Synthesis

Scheme 4.1 Synthesis of porphyrin-BODIPY conjugates JB-3 and JB-4.

Bromodiarylporphyrin, **2.9** and boryl substituted carbazole **2.15** and phenothiazine **2.19** donor were prepared according to the reported literature approach and were discussed in detail chapter 2. The Suzuki coupling of boryl substituted carbazole **2.15** or phenothiazine **2.19**, in presence of Pd(PPh<sub>3</sub>)<sub>4</sub>, DPPF, NatOBu in toluene yielded the required donor appended porphyrin **JB-4.1** and **JB-4.2** followed by deprotection of TIPS in presence of TBAF in THF at room

temperature yielded **JB-4.3** and **JB-4.4**. BODIPY diacid **JB-3.5** was successfully attached to the donor appended porphyrin moieties **JB-4.3** and **JB-4.4** via Sonogashira coupling in presence of Pd<sub>2</sub>(dba)<sub>3</sub>, AsPh<sub>3</sub> and Et<sub>3</sub>N in THF leading to the formation of the desired porphyrin-BODIPY conjugates **JB-3** and **JB-4** in 42 and 43 % yield, respectively as shown in **Scheme 4.1**.<sup>18</sup>

## 4.3.2 UV-Vis-NIR and fluorescence spectroscopic studies

The photophysical studies of the porphyrin-BODIPY conjugates **JB-3** and **JB-4** were studied in THF solvent at room temperature as shown in **Figure 4.7.** As expected, BODIPY acceptor unit had a significant impact on the absorption spectra of the dyes, most evident being the lowest energy bands. The two dyes exhibited an intense but narrow Soret band appearing at 446 nm when compared to **YD2-o-C8** and multiple Q bands from 550 to 750 nm, albeit with decreasing intensity of around 50% compared to their previous compared

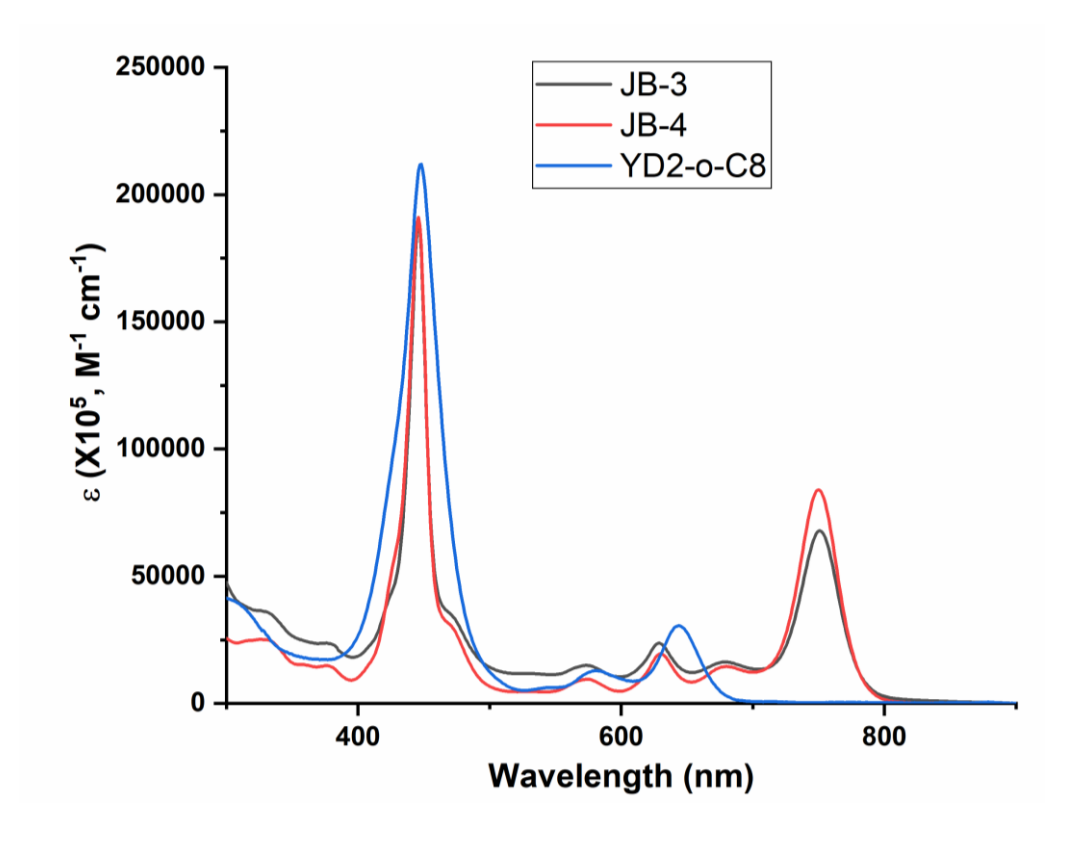
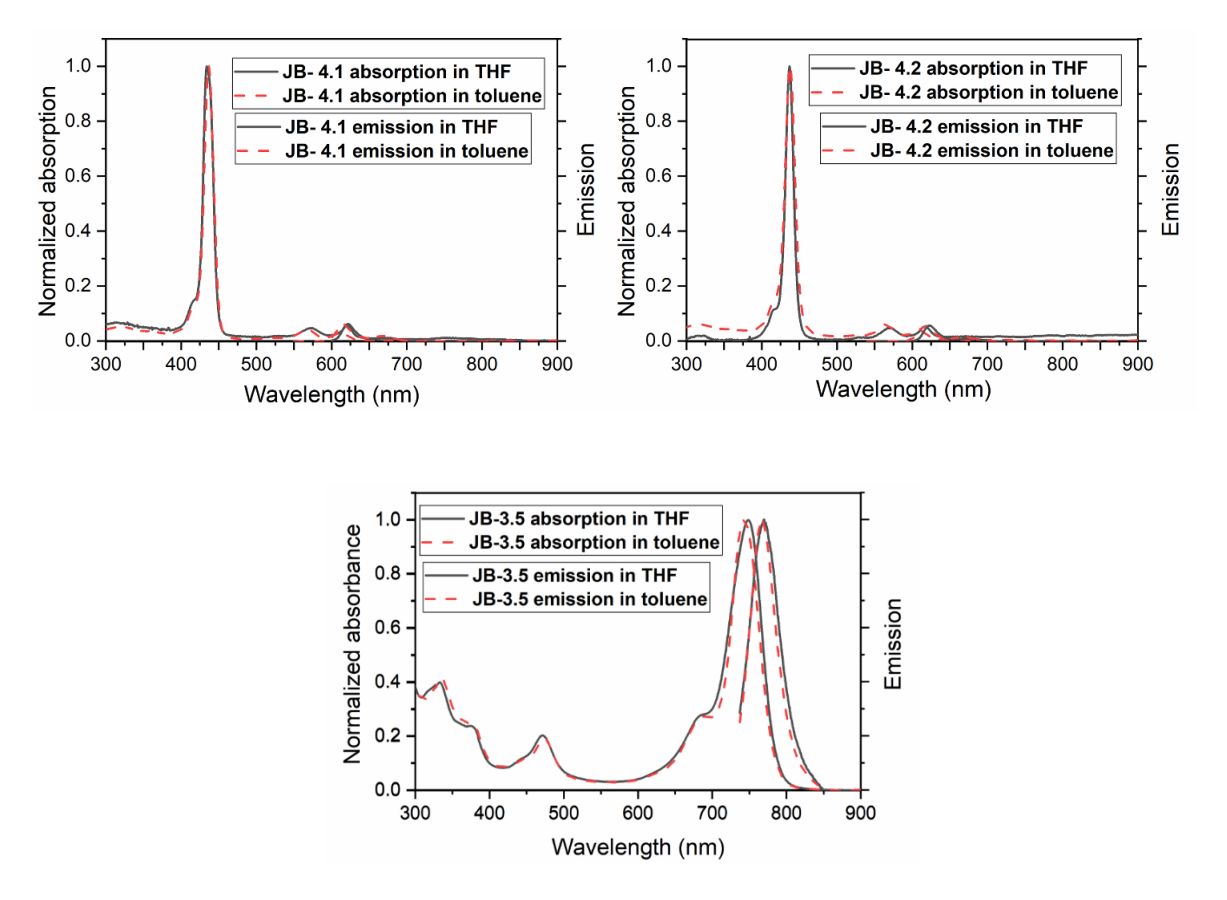


Figure 4.7 Absorption spectra of JB-3 and JB-4 in THF.

to their previous analogues **JB-1** and **JB-2**. Still, the absorption coefficient values of the dyes **JB-3** and **JB-4** are high enough to fulfill the requirement for dyes used in a DSSC. A non-zero absorption seen in the entire range of 300-800 nm from these new dyes along with their good

amount of absorption of solar flux in the NIR region make them panchromatic similar to their congeners **JB-1** and **JB-2** reported in chapter 3.

To understand the emission properties of the conjugates, first the emission of the individual moieties i.e., two donors (**JB-4.1** and **JB-4.2**) and BODIPY acceptor (**JB-3.5**) were checked in a polar solvent (THF) and a nonpolar solvent (toluene). The fluorescence spectra of the three units as shown in **Figure 4.8** have no significant change in their emission pattern in two different solvents.



**Figure 4.8** Fluorescence spectra of compounds **JB-4.1**, **JB-4.2** and **JB-3.5** excited at 434, 437 and 748 nm, respectively in THF (black solid line) and in toluene (dash red line).

But emission properties of the dyes JB-3 and JB-4 measured in THF solvent at room temperature by exciting at their respective Soret bands as shown in Figure 4.9(a) exhibit dual bands. The first band corresponds to the emission from the porphyrin unit and the second band is from the BODIPY acceptor indicating that probably in THF the molecule is behaving like independent moieties. The quantum yields of JB-3 and JB-4 in THF were found to be  $\phi_f$ = 0.015 for JB-3 and  $\phi_f$ = 0.020 for JB-4. Similar to the porphyrin-BODIPY conjugates JB-1 and JB-2, for the dyes JB-3 and JB-4 in toluene as shown in Figure 4.9(b), the emission band corresponding to the porphyrin is quenched leading to a minor band and the band emerging

from the BODIPY acceptor got intensified. The quantum yield was found to be  $\phi_f$ = 0.02 for **JB-3** and  $\phi_f$ = 0.021 for **JB-4**. This type of phenomena with an altered emission in different solvents is probably due to the intramolecular charge transfer transition process occurring from donor appended porphyrin to BODIPY acceptor moiety as discussed in previous chapter.

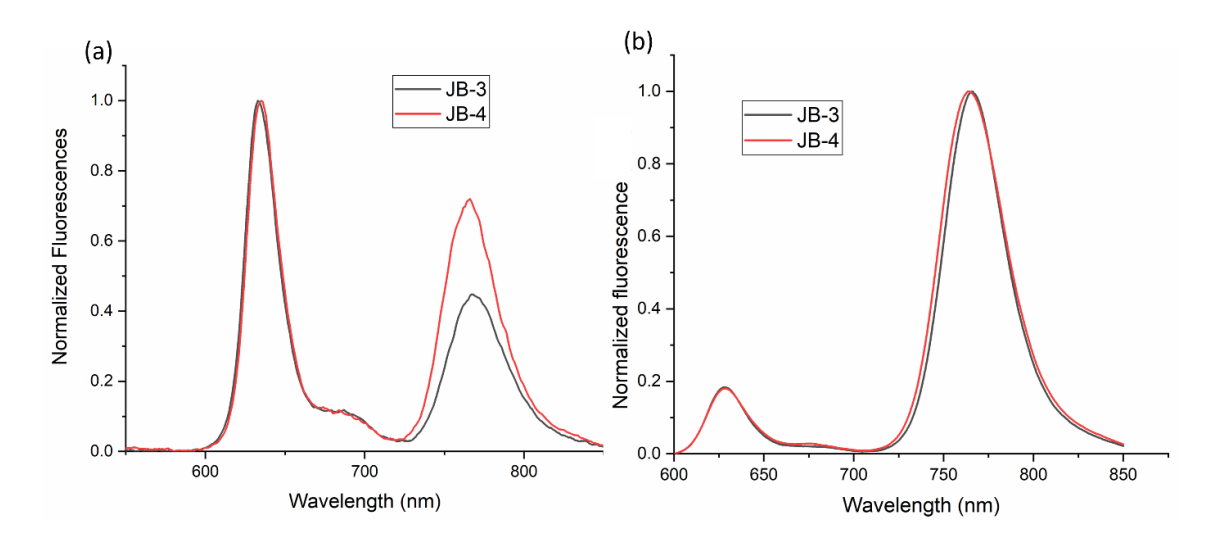


**Figure 4.9** Fluorescence spectra of dyes **JB-3** and **JB-4**, excited at their respective Soret bands at 446 nm (a) in THF (b) in toluene.

Fluorescence studies of the porphyrin-BODIPY conjugates excited at different wavelengths including BODIPY absorption band in THF and toluene leads to the same emission pattern, further confirming the role of BODIPY as acceptor in this case also, as shown in **Figure 4.10** and **4.11**.

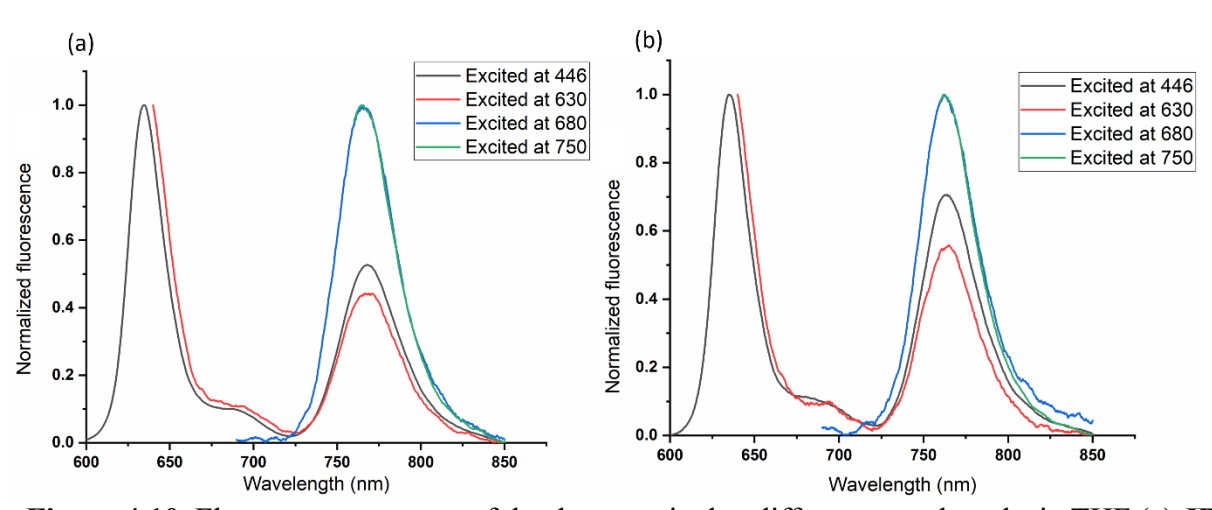
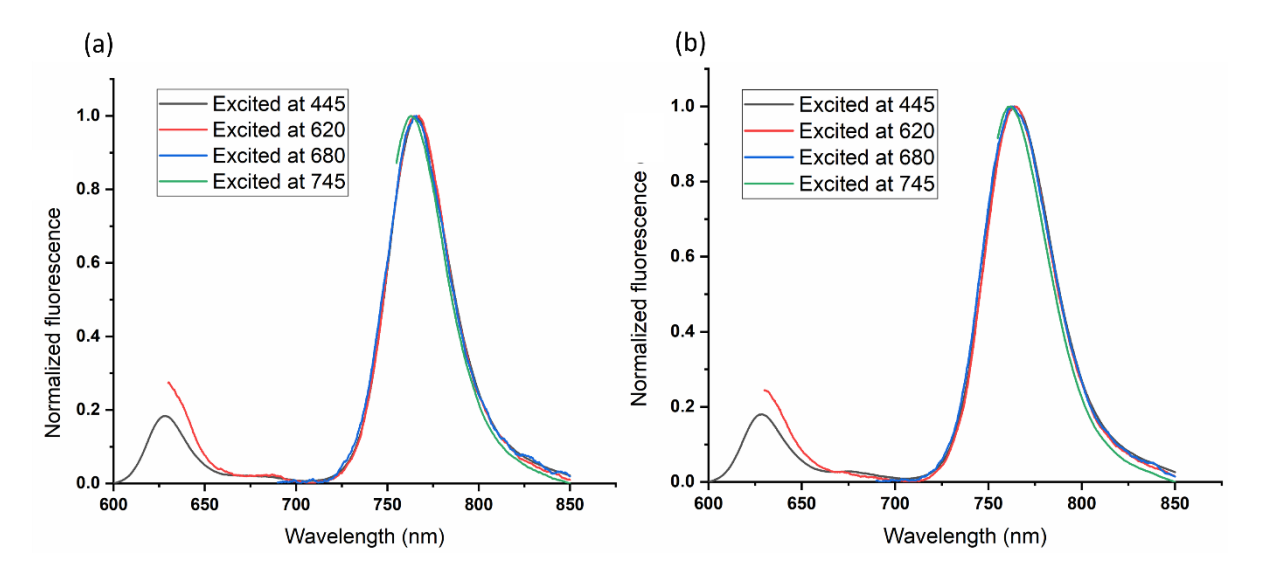
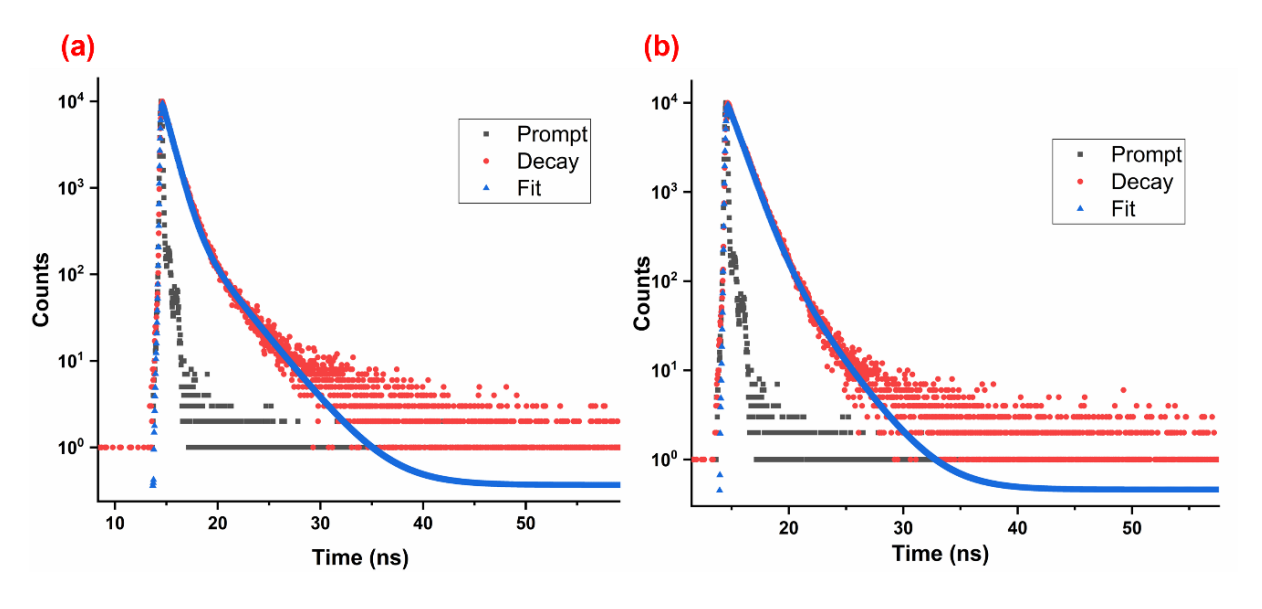


Figure 4.10. Fluorescence spectra of the dyes, excited at different wavelengths in THF (a) JB-3 (b) JB-4.



**Figure 4.11.** Fluorescence spectra of the dyes, excited at different wavelengths in toluene (a) **JB-3** (b) **JB-4**.

Photoluminescence decay as shown in **Figure 4.9** was measured using time-correlated single-photon counting with a picosecond pulsed diode laser ( $\lambda_{exc}$ =405 nm). Decay profile of **JB-3** and **JB-4** were found to be both tri-exponential with an average lifetime of 2.4 and 2.06 ns, respectively.



**Figure 4.12** Fluorescence decay profile of: a) **JB-3**; b) **JB-4** recorded in chloroform ( $\lambda_{exc}$ = 405 nm).

#### 4.3.3. DFT Calculations

We have carried out quantum mechanical calculations using Gaussian 09 program provided by CMSD facility of the University of Hyderabad. 19 All calculations were carried out by density functional theory (DFT) with Becke's three-parameter hybrid exchange functional and the Lee-Yang-Parr correlation functional (B3LYP) was used. LANL2DZ basis set was used for Zn and 6-31G basis set was used for all other atoms in calculations and the molecular orbitals were visualized using Gauss view 5. The optimized structures were shown in **Figure 4.10.** The **Figure 4.11** clearly depicts that the porphyrin and BODIPY units of the dyes **JB-3** and **JB-4** are not in the same plane along with that the butterfly structure of phenothiazine which is advantageous for reducing dye aggregation. Porphyrin and BODIPY exhibit a dihedral angle of 60.89° for **JB-3** and 77.86° for **JB-4**, which is again advantageous for reducing dye aggregation.

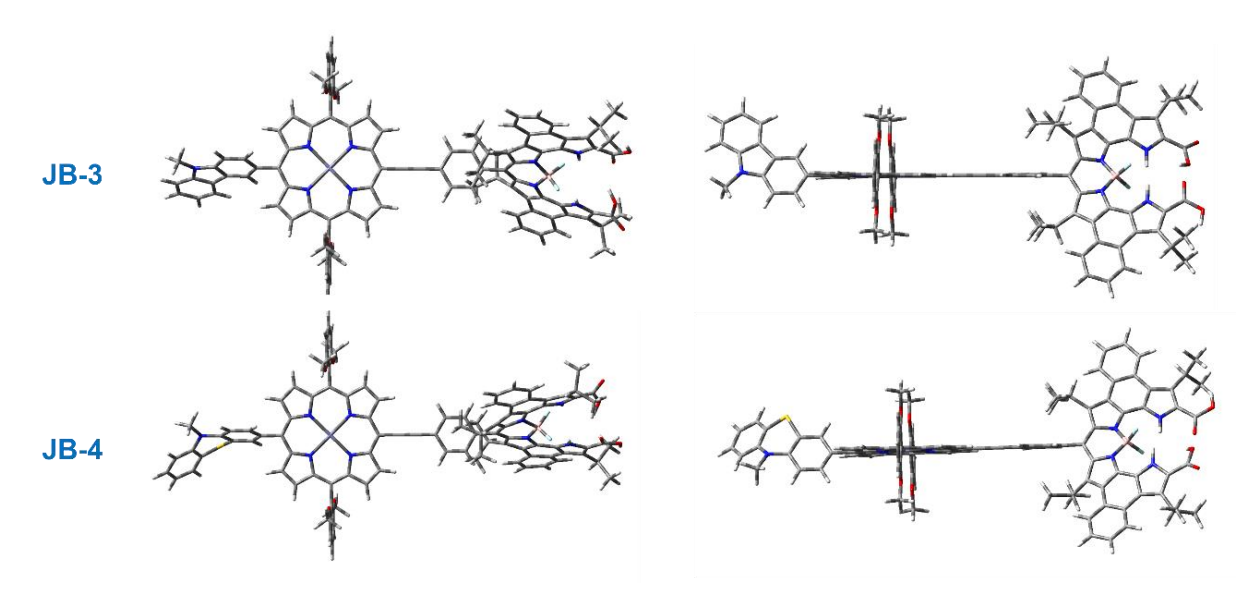
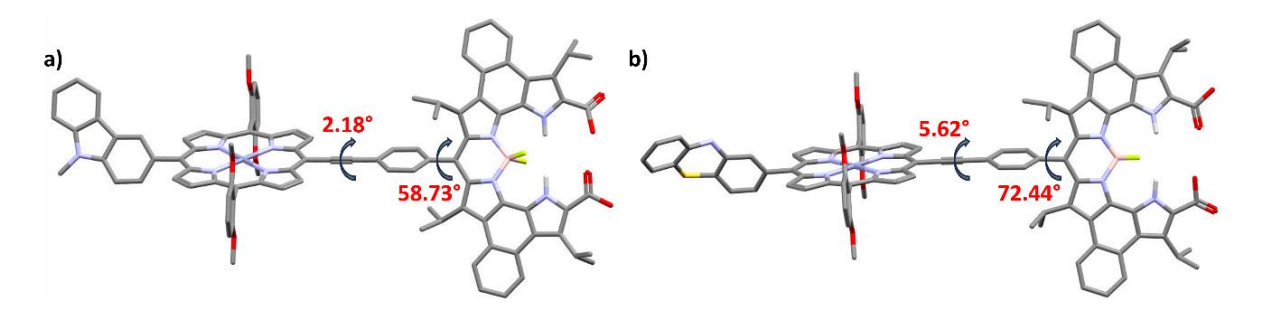
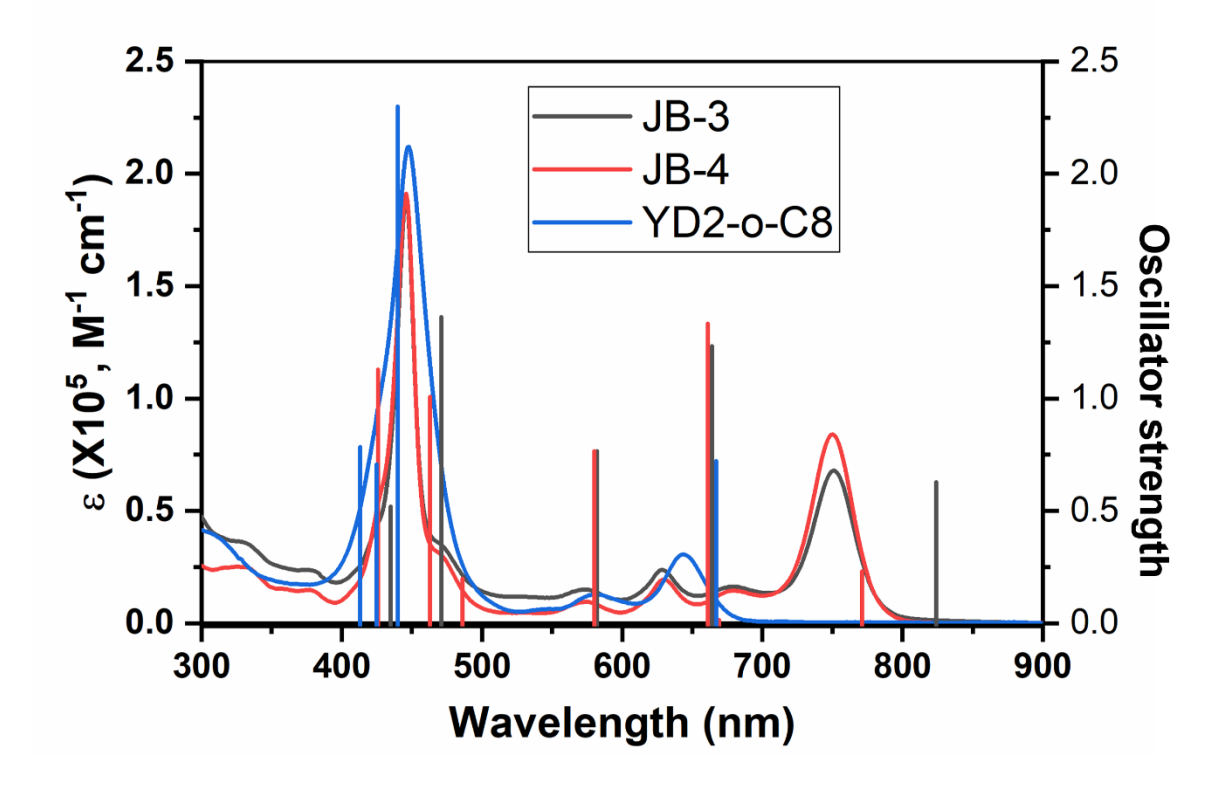


Figure 4.13. Different views of DFT optimized structures of dyes JB-3 and JB-4.



**Figure 4.14.** DFT optimized structures of dyes (a) **JB-3** and (b) **JB-4** with dihedral angle between porphyrin, phenyl and BODIPY planes.

To understand further insight, we have done TD-DFT calculations in THF solvent using PCM model and the results were analysed using GaussSum programme<sup>20</sup> and simulated the theoretical absorption spectra for both the **JB-3** and **JB-4**. The vertical electronic transitions and the steady state absorption spectra were found to be very similar (**Figure 4.12**). The donor bands around 400-450 nm observed are probably attributed to the phenothiazine and carbazole appended porphyrin.



**Figure 4.15.** Theoretical (vertical bars) and experimental (continuous lines) UV-Vis-NIR absorption spectra of **JB-3** (black) and **JB-4** (red) in THF.

The frontier orbital diagrams as shown in **Figure 4.13 and 4.14** further revealed that HOMO levels are primarily localized over carbazole and phenothiazine donor moieties and extending up to the porphyrin segment implying the significant contribution of the new donors viz carbazole and phenothiazine substituted porphyrins. LUMO coefficient is completely absent on porphyrin, which was not observed in the case of previously reported much accomplished porphyrin dyes such as **YD2-o-C8** and **SM315**. <sup>16,17</sup> On the other hand, LUMO lies completely on the acceptor BODIPY unit, which implies HOMO to LUMO photoexcitation will involve charge transfer from the donor substituted porphyrin to BODIPY unit. A well separated electron density distribution of HOMO and LUMO levels may indicate smooth electron transfers from

the donor to the acceptor via the porphyrin bridge, resulting in an efficient electron injection into TiO<sub>2</sub> conduction band. Computational HOMO-LUMO energy gap was found to be 1.80 and 1.83 eV for the sensitizers **JB-3** and **JB-4**, respectively.

**Table 4.2:** Selected transitions, oscillator strength, symmetry calculated (H = HOMO, L = LUMO) from DFT analysis for **JB-3** and **JB-4**.

Dye	Wavelength (nm)	Oscillator Strength	Major Contribution
JB-3	824	0.41	H→L (99%)
	664	0.79	H-2→L (100%)
	582	0.49	H→L+1 (78%)
	471	0.87	H-9→L (64%)
	435	0.34	H-12→L (30%), H-3→L+2 (10%)
JB-4	771	0.15	H→L (95%)
	669	0.02	H-1→L (92%)
	661	0.86	H-2→L (100%)
	580	0.49	H→L+1 (80%)
	486	0.13	H-1→L+2 (82%), H→ L+2 (11%)
	463	0.65	H-8→L (83%)
	426	0.73	H-15→L (61%), H-11→L (14%)

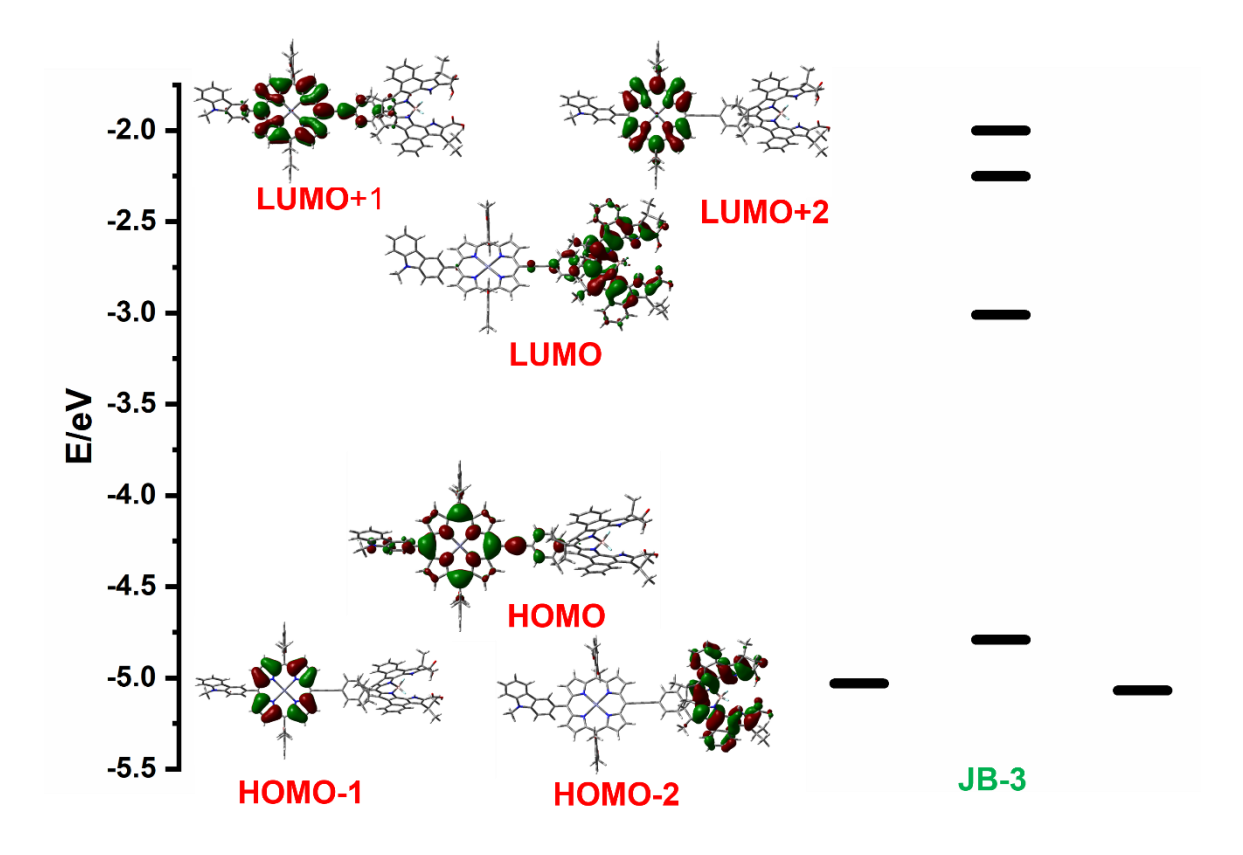


Figure 4.16. Delocalized electron densities of selected MOs of JB-3 with energy level diagram.

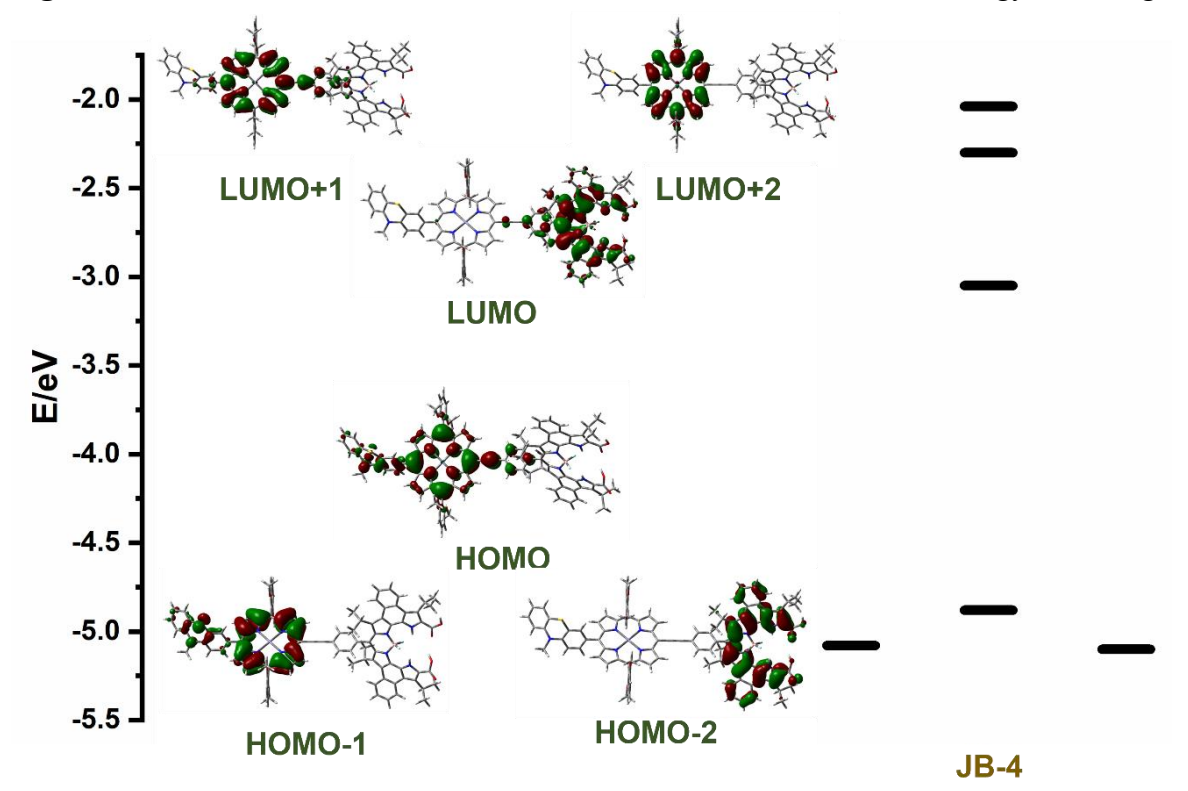


Figure 4.17. Delocalized electron densities of selected MOs of JB-4 with energy level diagram.

#### 4.3.4 Electrochemical studies

The electrochemical properties of porphyrin-BODIPY conjugates, **JB-3** and **JB-4** were recorded by measuring CV and DPV in THF solvent using tetrabutylammonium hexafluorophosphate as supporting electrolyte, a glassy carbon working electrode, an Ag/AgCl reference electrode and Pt wire auxiliary electrode and the corresponding data were shown in **Figure 4.15** with potential details in **Table 4.3**. The first oxidations for the formation of the porphyrin cation radical  $E_{Ox}/HOMO$  level of **JB-3** and **JB-4** are found to be quasi reversible undergoing displayed two very close one electron oxidations. Both the dyes exhibit more positive potentials than the redox potential of the  $I^-/I_3^-$  couple, demonstrating the feasibility of the dye regeneration. In addition, energy level of LUMO, ( $E_{LUMO}$ ) calculated from the equation  $E_{LUMO} = E_{ox} - E_{0-0}$  for **JB-3** and **JB-4** are found to be -0.58 and -0.55 V, respectively, which are higher than that of conduction band edge ( $E_{CB}$ ) of TiO<sub>2</sub> indicating the workable electron injection from the excited sensitizer to the conduction band of TiO<sub>2</sub> as shown in **Figure 4.16**.

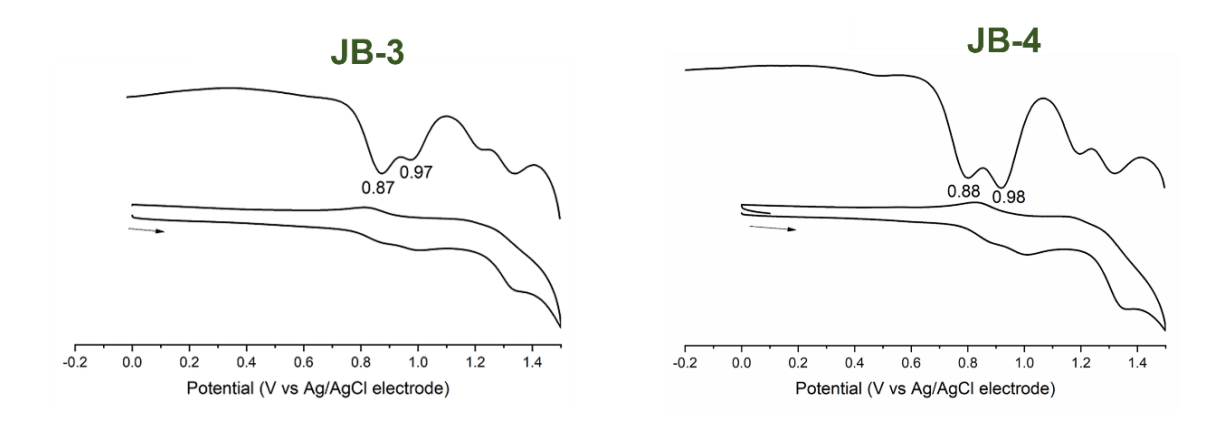


Figure 4.18. CV (below) and DPV (above) of JB-3 and JB-4 in THF measured at 298K.

**Table 4.3:** Absorption spectral and electrochemical data for JB-3 and JB-4.

Dye	Absorption	Emission	$E_{0-0}$	Oxidation	Reduction	$E_{LUMO}=E_{0}$	$E_{ec}$
	$\lambda_{\text{max}}/\text{nm}$ ( $\epsilon/10^5$	in nm	in	$E_{ox}$ (from	E <sub>Red</sub> (from	$_{0}$ - $E_{\mathrm{HOMO}}$	in V
	M <sup>-1</sup> cm <sup>-1</sup> )		eV	DPV) vs.	DPV) vs.	in V	
	·			NHE in V	NHE in V		
JB-3	446 (1.90), 750 (0.677)	633, 768	1.66	1.08	-0.41	-0.58	1.48
JB-4	446 (1.91), 750 (0.839)	635, 766	1.64	1.09	-0.43	-0.55	1.52

### 4.4 Conclusion

In conclusion we have successfully incorporated carbazole and phenothiazine moieties endowed with hexyl chains as electron-donating groups by replacing the diarylamine donor of the previously synthesized porphyrin-BODIPY conjugate. The newly prepared dyes **JB-3** and **JB-4** also displayed a significant red shifted and intense lowest energy bands having non-zero absorption beyond 800 nm much like their previous congeners. The TDDFT calculations also further revealed a well separated HOMO and LUMO located on donor and anchoring group, respectively increasing the chances of charge separation processes as well as dye regeneration and charge injection capabilities.

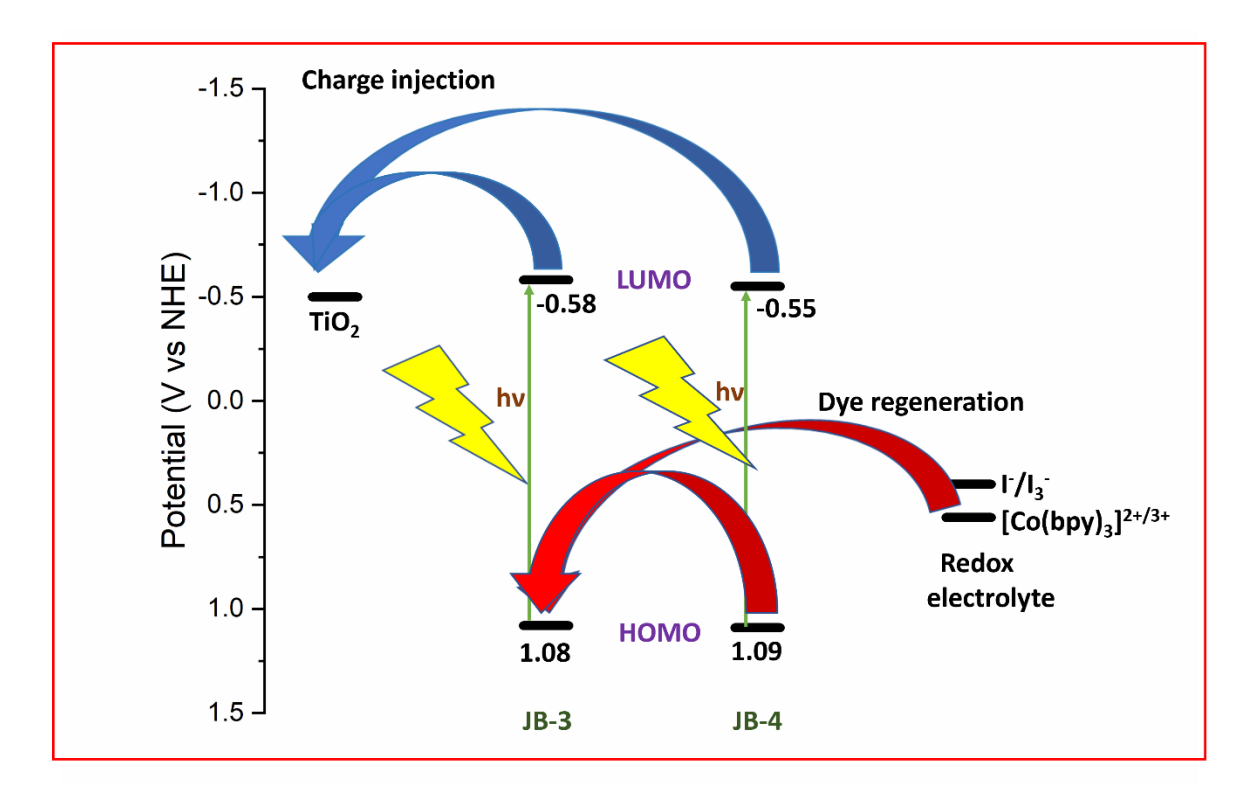


Figure 4.19. The electron transfer processes in DSSC.

#### 4.5 Synthetic routes for JB-3 and JB-4:

Synthesis of [5,15-bis(2,6-bis(octyloxy)phenyl)-10-(9-hexyl-9H-carbazol-3-yl)-20-((triisopropylsilyl)ethynyl) porphyrinato] Zinc (II) (JB-4.1): JB-4.1 was prepared by addition of a degassed solution of boryl carbazole 2.15 (0.073 g, 0.19 mmol) in toluene (5 mL) to the Schlenk tube containing compound 2.9 (0.050 g, 0.038 mmol), Pd(PPh<sub>3</sub>)<sub>4</sub> (0.0053 g, 0.0046 mmol) and NaOtBu (0.019 g, 0.19 mmol). The mixture was refluxed for 2 h. The solvent was removed under reduced pressure and the residue was purified by column chromatography (silica gel) using 30% DCM/hexanes as eluent. The product was recrystallized from MeOH/hexane to give the product JB-4.1 (37.9 mg, 67%) as a purple powder.

Melting point: >300°C; FTIR: 2930, 2958, 1631, 1461 cm<sup>-1</sup>; <sup>1</sup>H NMR (CDCl<sub>3</sub>, 500 MHz)  $\delta_H$  9.72 (d, J=4.5 Hz, 2H), 8.93 (d, J=4.4 Hz, 2H), 8.88 (s, 1H), 8.84-8.76 (m, 4H), 8.29-8.13 (m, 2H), 7.72-7.64 (m, 4H), 7.58-7.53 (m, 1H), 6.98 (d, J=8.5 Hz, 4H), 4.54 (t, J=6.9, 1H), 3.82 (t, J=6.2 Hz, 8H), 2.14-2.09 (m, 1H), 1.62-1.56 (m, 2H), 1.45-1.44 (m, 20H), 0.97-0.93 (m, 10H), 0.80-0.76 (m, 8H), 0.62-0.38 (m, 50H). <sup>13</sup>C NMR (CDCl<sub>3</sub>, 125 MHz)  $\delta_C$  160.1, 152.6, 151.1, 150.5, 149.5, 143.3, 141.4, 140.0, 134.5, 133.9, 132.2, 131.8, 131.0, 130.8, 130.7, 129.8, 127.3, 126.4, 125.9, 127.3, 126.4, 125.9, 123.1, 119.0, 114.5, 105.5, 68.9, 32.0, 31.8, 31.4, 29.8, 29.5, 29.3, 28.7, 27.3, 25.3, 22.8, 22.2, 19.2, 14.2, 13.8, 12.1. HRMS: m/z calcd for [M+H]<sup>+</sup> C<sub>93</sub>H<sub>124</sub>N<sub>5</sub>O<sub>4</sub>SiZn 1467.8748, found 1467.8705.

[5,15-bis(2,6-bis(octyloxy)phenyl)-10-ethynyl-20-(9-hexyl-9H-carbazol-3-yl) porphyrinato] Zinc (II) (JB-4.3): To a solution of porphyrin JB-4.1 (23 mg, 0.015 mmol) in dry THF (3 mL) was added TBAF (78 μL, 1M in THF). The solution was stirred at room temperature for 30 min under nitrogen atmosphere. The mixture was quenched with water and then extracted with DCM. The organic layer was dried over anhydrous Na<sub>2</sub>SO<sub>4</sub> and the solvent was removed under reduced pressure and used as it is.

Synthesis of [3-(10,20-bis(2,6-bis(octyloxy)phenyl)-15-((triisopropylsilyl)ethynyl)-10-hexyl-10H-phenothiazine) porphyrinatol Zinc (II) (JB-4.2): Compound JB-4.2 was prepared by addition of a degassed solution of boryl phenothiazine 2.19 (0.079 g, 0.19 mmol) in toluene (5 mL) to the Schlenk tube containing compound 2.9 (0.050 g, 0.023 mmol), Pd(PPh<sub>3</sub>)<sub>4</sub> (0.053 g, 0.0046 mmol) and NaOtBu (0.019 g, 0.193 mmol). The mixture was refluxed for 2 h. The solvent was removed under reduced pressure and the residue was purified by column chromatography (silica gel) using 30% DCM/hexanes eluent. The product was recrystallized from MeOH/hexane to give the product JB-4.2 (37.6 mg, 65%) as a purple powder.

Melting point: >300°C; FTIR: 2914, 2953, 1599, 1457 cm<sup>-1</sup>; <sup>1</sup>H NMR (CDCl<sub>3</sub>, 500 MHz)  $\delta_{\rm H}$  9.72 (d, J=4.1 Hz, 2H), 8.93 (d, J=4.6 Hz, 2H), 8.87-8.77 (m, 4H), 7.95 (s, 2H),7.68 (t, J=8.3 Hz, 2H), 7.25-7.13 (m, 3H), 7.07-6.95 (m, 6H), 4.09 (s, 2H), 3.82 (t, J=6.2 Hz, 8H), 2.06 (s, 2H), 1.63-1.58 (m, 2H), 1.45-1.44 (m, 20H), 0.97-0.93 (m, 10H), 0.79-0.75 (m, 8H), 0.59-0.37 (m, 50H). <sup>13</sup>C NMR (CDCl<sub>3</sub>, 100 MHz)  $\delta_{\rm C}$  160.1, 152.6 151.1, 150.5, 149.6, 132.2, 131.8, 131.0, 130.7, 129.8, 127.8, 127.4, 126.4, 122.6, 121.4, 115.6, 114.5, 113.3, 105.5, 96.2, 68.8, 32.0, 31.7, 31.4, 31.3, 29.8, 29.5, 28.7, 27.2, 27.0, 25.3, 22.8, 22.3, 19.2, 19.1, 14.2, 13.9, 12.1. HRMS: m/z calcd for [M+H]<sup>+</sup> C<sub>93</sub>H<sub>124</sub>N<sub>5</sub>O<sub>4</sub>SiZn 1499.8468, found 1499.8467.

Synthesis of 3-(10,20-bis(2,6-bis(octyloxy)phenyl)-15-ethynyl)-10-hexyl-10H-phenothiazine porphyrinato] Zinc (II) (JB-4.4): To a solution of porphyrin JB-4.2 (20 mg, 0.013 mmol) in dry THF (3 mL) was added TBAF (65 μL, 1M in THF). The solution was stirred at room temperature for 30 min under nitrogen atmosphere. The mixture was quenched with water and then extracted with DCM. The organic layer was dried over anhydrous Na<sub>2</sub>SO<sub>4</sub> and the solvent was removed under reduced pressure and used as it is.

Synthesis of JB-3: The JB-4.3 (21 mg, 0.016) and BODIPY JB-3.6 (10 mg, 0.0107 mmol) were taken in a Schlenk tube and dissolved in a mixture of dry THF (5 mL) and Et<sub>3</sub>N (0.4 mL) and the solution was degassed with dinitrogen for 10 min, Pd<sub>2</sub>(dba)<sub>3</sub> (3 mg, 0.0032 mmol) and AsPh<sub>3</sub> (6.6 mg, 0.022 mmol) were added to the mixture. The solution was refluxed for 4 h under nitrogen atmosphere. The solvent was removed under reduced pressure. The residue was purified by recrystallization from CH<sub>3</sub>OH/hexane to give JB-3 (10 mg, 42%) as a green solid.

Melting point: >233°C (decompose); FTIR: 2923, 2845, 1612, 1461 cm<sup>-1</sup>; <sup>1</sup>H NMR (THF  $d_8$ , 500 MHz)  $\delta_{\rm H}$  11.55 (s, 2H), 9.79 (d, J=4.8 Hz, 2H), 8.90 (d, J=4.4 Hz, 2H), 8.65 (d, J=6.8 Hz, 2H), 8.51 (s, 1H), 8.45 (d, J=4.9 Hz, 4H), 8.35 (d, J=5.9 Hz, 3H), 8.06-8.03 (m, 2H), 7.82 (d, J=7.4 Hz, 2H), 7.70-7.61 (m, 4H), 7.47 (s br, 3H), 7.42 (t, J=7 Hz, 2H), 7.36 (d, J=7.1 Hz, 2H), 7.06 (d, J=8.4 Hz, 4H), 4.51 (s, 2H), 3.91-3.84 (m, 8H), 3.50 (s br, 4H), 3.17 (s br, 4H), 2.48 (s br, 4H), 2.04 (s, 2H), 1.57 (s br, 8H), 1.44 (s br, 8H), 1.66 (d, J=6.9 Hz, 12H), 1.43 (d, J=7 Hz, 12H), 1.06-0.83 (m, 42H), 0.75-0.63 (m, 33H). <sup>13</sup>C NMR (THF- $d_8$ , 125 MHz) δ<sub>C</sub> 161.3, 152.9, 152.2, 151.4, 151.3, 150.6, 141.1, 136.2, 134.7, 133.8, 133.1, 132.8, 132.1, 131.7, 131.6, 131.4, 130.9, 130.6, 130.3, 129.7, 129.2, 128.3, 128.2, 127.6, 127.4, 127.2, 126.9, 126.1, 124.3, 124.1, 122.4, 122.1, 120.5, 118.6, 116.6, 115.5, 111.8, 105.8, 105.7, 71.6, 69.2, 57.9, 57.3, 51.6, 47.1, 44.0, 43.4, 40.1, 38.5, 37.8, 37.3, 35.0, 33.0, 32.6, 31.5, 30.8, 30.4, 29.9, 26.5, 23.7, 23.4,

21.9, 20.9, 14.5. HRMS: m/z calcd for  $[M+H]^+$   $C_{133}H_{146}BF_2N_9O_8Zn$  2113.0759, found 2113.0795.

Synthesis of JB-4: The JB-4.4 (20 mg, 0.014) and BODIPY JB-3.6 (9.2 mg, 0.0099 mmol) were dissolved in a mixture of dry THF (5 mL) and Et<sub>3</sub>N (0.4 mL) and the solution was degassed with dinitrogen for 10 min, Pd<sub>2</sub>(dba)<sub>3</sub> (2.7 mg, 0.0029 mmol) and AsPh<sub>3</sub> (6 mg, 0.0198 mmol) were added to the mixture. The solution was refluxed for 4 h under nitrogen atmosphere. The solvent was removed under reduced pressure. The residue was purified by recrystallization from CH<sub>3</sub>OH/hexane to give JB-4 (20 mg, 43%) as a green solid.

Melting point: >254 °C(decompose); FTIR: 2916, 2934, 1595, 1457 cm<sup>-1</sup>; <sup>1</sup>H NMR (THF  $d_8$ , 500 MHz)  $\delta_{\rm H}$  11.55 (s, 2H), 9.79 (d, J=3.8 Hz, 2H), 8.88 (s br, 2H), 8.84 (d, J=4.1 Hz, 1H), 8.76 (d, J=4.1 Hz, 1H), 8.71-8.65 (m, 2H), 8.57 (d, J=4.1 Hz, 1H), 8.45 (d, J=6.1 Hz, 4H), 8.35 (s, 2H), 8.05 (d, J=5.6 Hz, 2H), 7.99 (d, J=6.7 Hz, 1H), 7.89 (d, J=9 Hz, 1H), 7.74-7.66 (m, 4H), 7.45-7.28 (m, 6H), 7.07 (d, J=7.2 Hz, 4H), 4.56 (s, 2H), 3.88 (d, J=6.1, 8H), 1.67 (d, J=6.2 Hz, 12H), 1.43 (d, J=6.7 Hz, 12H), 1.05-0.81 (m, 42H), 0.75-0.61 (m, 33H). <sup>13</sup>C NMR (THF- $d_8$ , 125 MHz)  $\delta_{\rm C}$  161.2, 152.9, 152.1, 151.3, 150.3, 138.8, 136.8, 134.4, 133.8, 133.0, 132.7, 132.1, 131.9, 131.6, 131.5, 130.6, 130.4, 129.1, 128.3, 127.6, 127.2, 122.5, 122.2, 115.4, 114.1, 105.7, 71.5, 69.1, 62.7, 51.5, 48.5, 47.0, 34.4, 34.2, 33.0, 32.6, 30.8, 30.6, 30.4, 29.9, 29.8, 28.1, 27.7, 27.4, 26.4, 25.9, 23.7, 23.4, 20.7, 14.6, 14.5. HRMS: m/z calcd for [M+H]<sup>+</sup> C<sub>133</sub>H<sub>146</sub>BF<sub>2</sub>N<sub>9</sub>O<sub>8</sub>SZn 2145.0477, found 2145.0496.

#### 4.6 References

- Grätzel, M. Recent Advances in Sensitized Mesoscopic Solar Cells. Acc. Chem. Res., 2009, 42, 1788.
- 2. Li, L. L.; Diau, E. W. G. Porphyrin-Sensitized Solar Cells. *Chem. Soc. Rev.*, **2013**, 42, 291.
- 3. Yella, A.; Lee, H.-W.; Tsao, H. N.; Yi, C.; Chandiran, A. K.; Nazeeruddin, M. K.; Diau, E. W.-G.; Yeh, C.-Y.; Grätzel, M. Porphyrin-Sensitized Solar Cells with Cobalt (II/III)—Based Redox Electrolyte Exceed 12 Percent Efficiency. *Science*, **2011**, *334*, 629.
- 4. Mathew, S.; Yella, A.; Gao, P.; Humphry-Baker, R.; Curchod, B. F.; Ashari-Astani, N.; Tavernelli, I.; Rothlisberger, U.; Nazeeruddin, M. K.; Grätzel, M. Dye-sensitized solar cells with 13% efficiency achieved through the molecular engineering of porphyrin sensitizers, *Nat. Chem.*, **2014**, *6*, 242.
- 5. Wang, Y.; Chen, B.; Wu, W.; Li, X.; Zhu, W.; Tian, H.; Xie, Y. Efficient Solar Cells Sensitized by Porphyrins with an Extended Conjugation Framework and a Carbazole Donor: From Molecular Design to Cosensitization. *Angew. Chem. Int. Ed.*, **2014**, *53*, 10779.
- Kumar, R.; Sudhakar, V.; Prakash, K.; Krishnamoorthy, K.; Sankar, M. Tuning the Photovoltaic Performance of DSSCs by Appending Various Donor Groups on trans-Dimesityl Porphyrin Backbone. ACS Appl. Energy Mater., 2018, 1, 2793.
- 7. Chen, J.; Ko, S.; Liu, L.; Sheng, Y.; Han, H.; Li, X. The effect of porphyrins suspended with different electronegative moieties on the photovoltaic performance of monolithic porphyrin-sensitized solar cells with carbon counter electrodes. *New J. Chem.*, **2015**, *39*, 2889.
- 8. Lu, Y.; Song, H.; Li, X.; Ågren, H.; Liu, Q.; Zhang, J.; Zhang, X.; Xie, Y. Multiply Wrapped Porphyrin Dyes with a Phenothiazine Donor: A High Efficiency of 11.7% Achieved through a Synergetic Coadsorption and Cosensitization Approach. *ACS Appl. Mater. Interfaces*, **2019**, *11*, 5046.
- 9. T. Higashino and H. Imahori, Porphyrins as excellent dyes for dye-sensitized solar cells: recent developments and insights. *Dalton Trans.*, **2015**, *44*, 448.
- 10. Hu, Y.; Alsaleh, A.; Trinh, O.; D'Souza, F.; Wang, H. J. Mater. Chem. A., 2021, 9, 27692.

- (a) Kakiage, K.; Aoyama, Y.; Yano, T.; Otsuka, T.; Kyomen, T.; Unno, M.; Hanaya, M. *Chem. Commun.*, 2014, 50, 6379. (b) Zhao, L.; Wagner, P.; Elliott, A. B. S.; Griffith, M. J.; Clarke, T. M.; Gordon, K. C.; Mori, S.; Mozer, A. J. Enhanced performance of dye-sensitized solar cells using carbazole-substituted di-chromophoric porphyrin dyes. *J. Mater. Chem. A.*, 2014, 2, 16963.
- 12. Lu, Y.; Liu, Q.; Luo, J.; Wang, B.; Feng, T.; Zhou, X.; Liu, X.; Xie, Y. Solar Cells Sensitized with Porphyrin Dyes Containing Oligo (Ethylene Glycol) Units: a High Efficiency Beyond 12%. *ChemSusChem*, **2019**, 10.1002/cssc.201900139.
- 13. Zeng, K.; Tang, W.; Li, C.; Chen, Y.; Zhao, S.; Liu, Q.; Xie, Y. Systematic optimization of the substituents on the phenothiazine donor of doubly strapped porphyrin sensitizers: an efficiency over 11% unassisted by any cosensitizer or coadsorbent. *J. Mater. Chem. A.*, **2019**, *7*, 20854.
- 14. Chen, Y.; Zeng, K.; Li, C.; Liu, X.; Xie, Y. A new type of multibenzyloxy-wrapped porphyrin sensitizers for developing efficient dye-sensitized solar cells. 10.1142/S1088424619501281.
- 15. Zou, J.; Tang, Y.; Baryshnikov, G.; Yang, Z.; Mao, R.; Feng, W.; Guan, J.; Li, C.; Xie, Y. Porphyrins containing a tetraphenylethylene substituted phenothiazine donor for fabricating efficient dye sensitized solar cells with high photovoltages, *J. Mater. Chem. A.*, **2022**, *10*, 1320.
- 16. Krishna, N. V.; Krishna, J. S. V.; Singh, S. P.; Han, L.; Giribabu, L.; Bedja, I. M.; Gupta, R. K.; Islam, A. Donor-π–Acceptor Based Stable Porphyrin Sensitizers for Dye-Sensitized Solar Cells: Effect of π-Conjugated Spacers. J. Phys. Chem. C., 2017, 121, 6464.
- 17. Xue, X.; Zhang, W.; Zhang, N.; Ju, C.; Peng, X.; Yang, Y.; Liang, Y.; Feng, Y.; Zhang, B. Effect of the length of the alkyl chains in porphyrin meso-substituents on the performance of dye-sensitized solar cells. *RSC Adv.*, **2014**, *4*, 8894.
- 18. Bania, J.; Sahoo, S. S.; Kishore, M. V. N.; Panda, P. K. Porphyrin-BODIPY Conjugates as photosensitizers with absorption up to near infrared region for dye-sensitized solar-cells (DSSC). Indian Patent Application No.: 202341027215; May 05, 2023.
- 19. Gaussian 09, (Revision C.01), Frisch, M. J. et al. Gaussian, Inc., Wallingford CT, 2010.
- 20. O'Boyle, N. M.; Tenderholt, A. L.; Langner, K. M. A library for package-independent computational chemistry algorithms, *J. Comp. Chem.*, **2008**, *29*, 839.

# 4.7 <sup>1</sup>H NMR, <sup>13</sup>C NMR and HRMS spectra

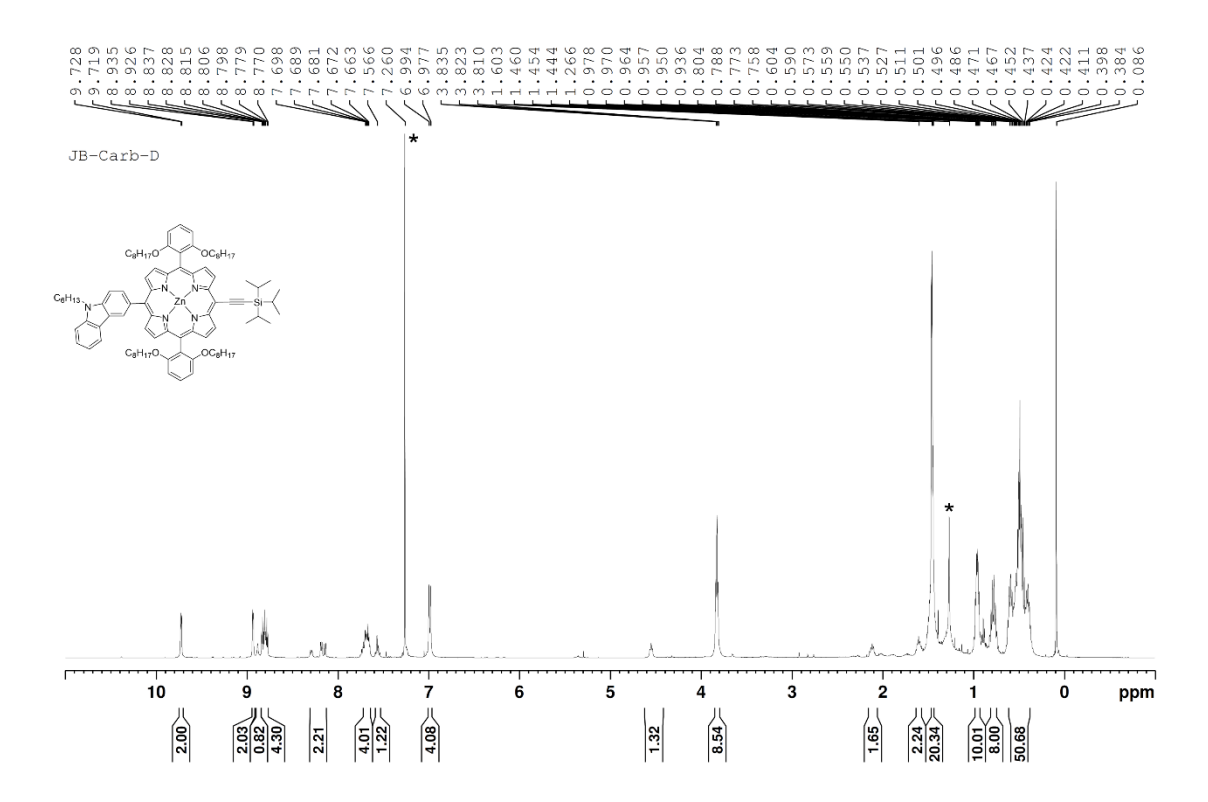


**Figure 4.20.** <sup>1</sup>H NMR spectrum of **JB-4.1** in CDCl<sub>3</sub> recorded at 25 °C (\*Asterisk indicates residual solvent impurity).

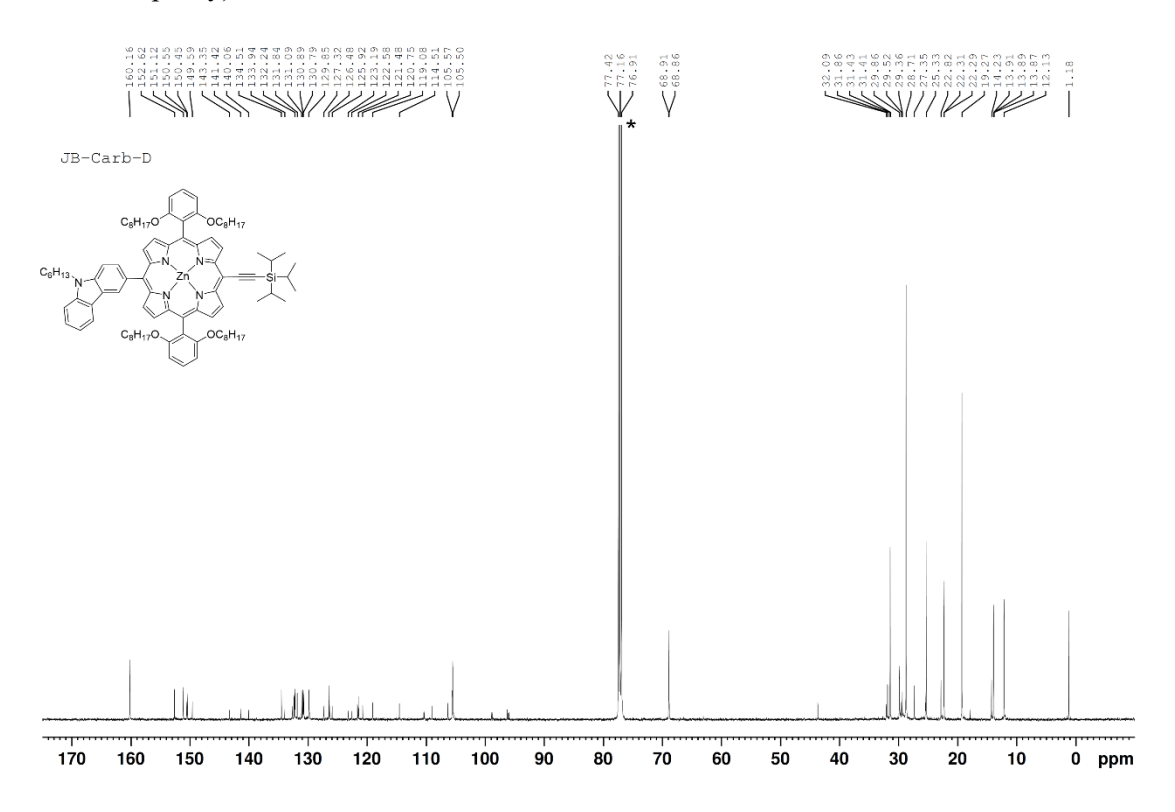


**Figure 4.21** <sup>13</sup>C NMR spectrum of **JB-4.1** in CDCl<sub>3</sub> recorded at 25 °C (\*Asterisk indicates residual solvent impurity).

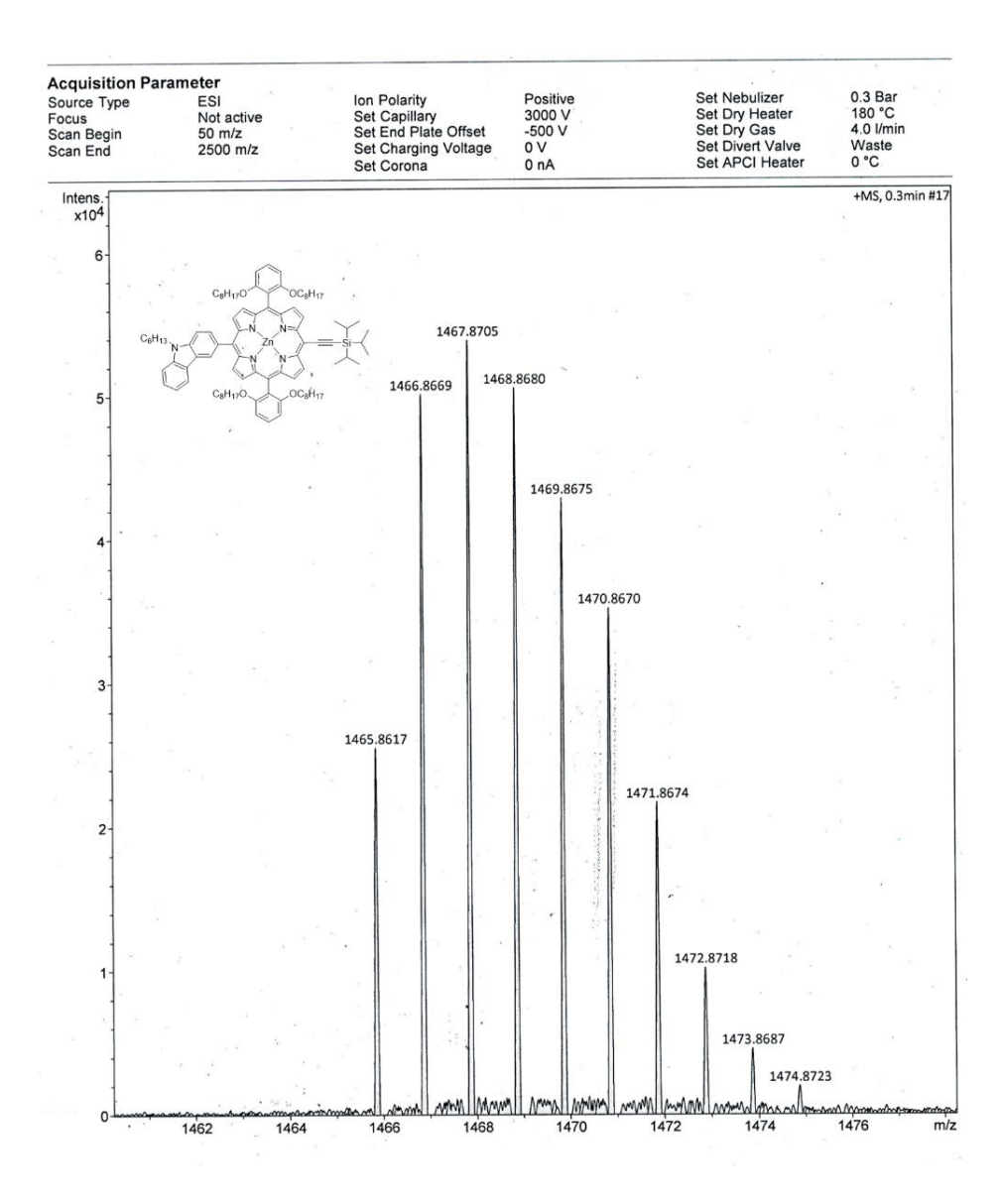


**Figure 4.22.** HRMS spectrum of **JB-4.1**  $[M+H]^+$   $C_{93}H_{124}N_5O_4SiZn$  1467.8748, found 1467.8705.

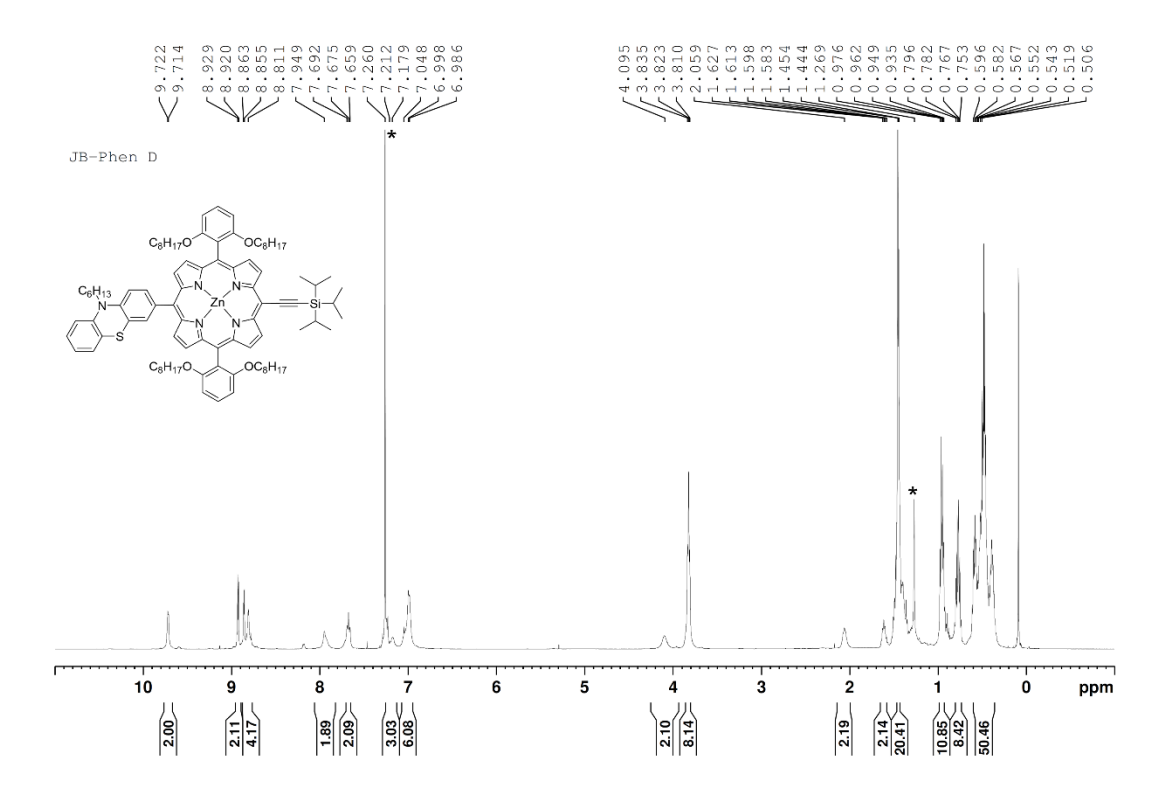


**Figure 4.23** <sup>1</sup>H NMR spectrum of **JB-4.2** in CDCl<sub>3</sub> recorded at 25 °C (\*Asterisk indicates residual solvent impurity).

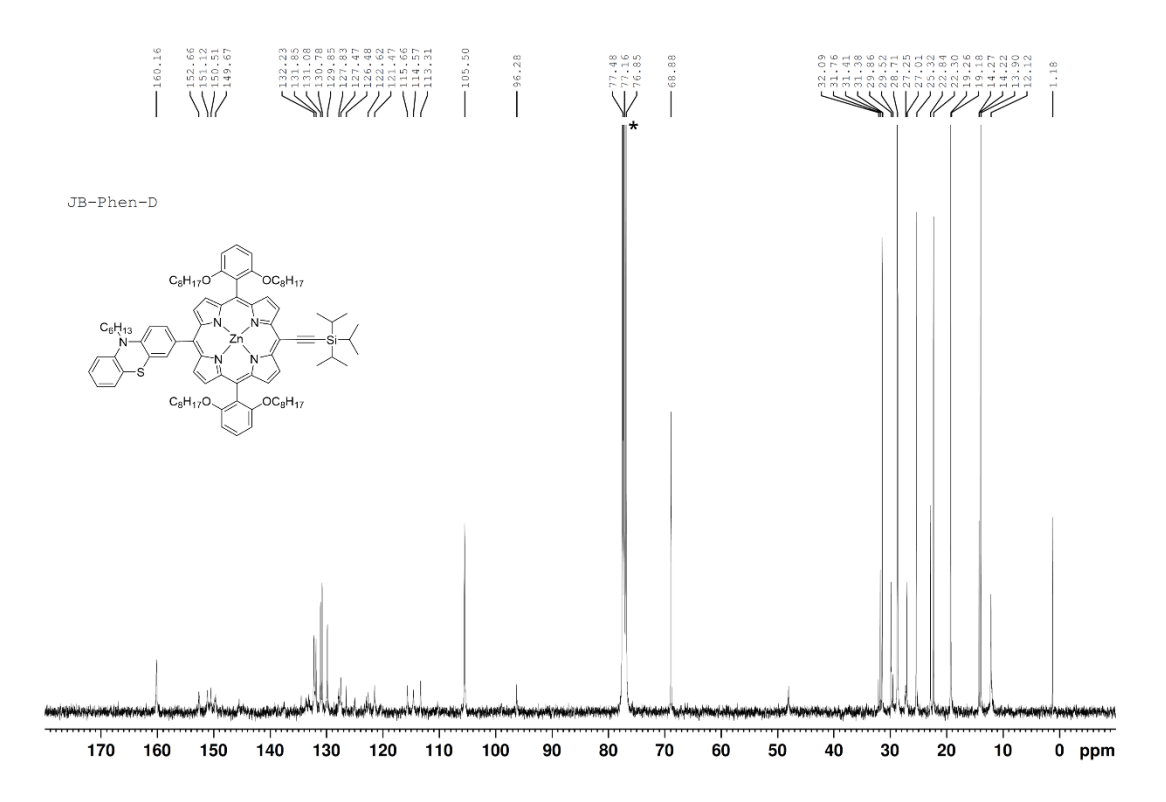


**Figure 4.24.** <sup>13</sup>C NMR spectrum of **JB-4.2** in CDCl<sub>3</sub> recorded at 25 °C (\*Asterisk indicates residual solvent impurity).

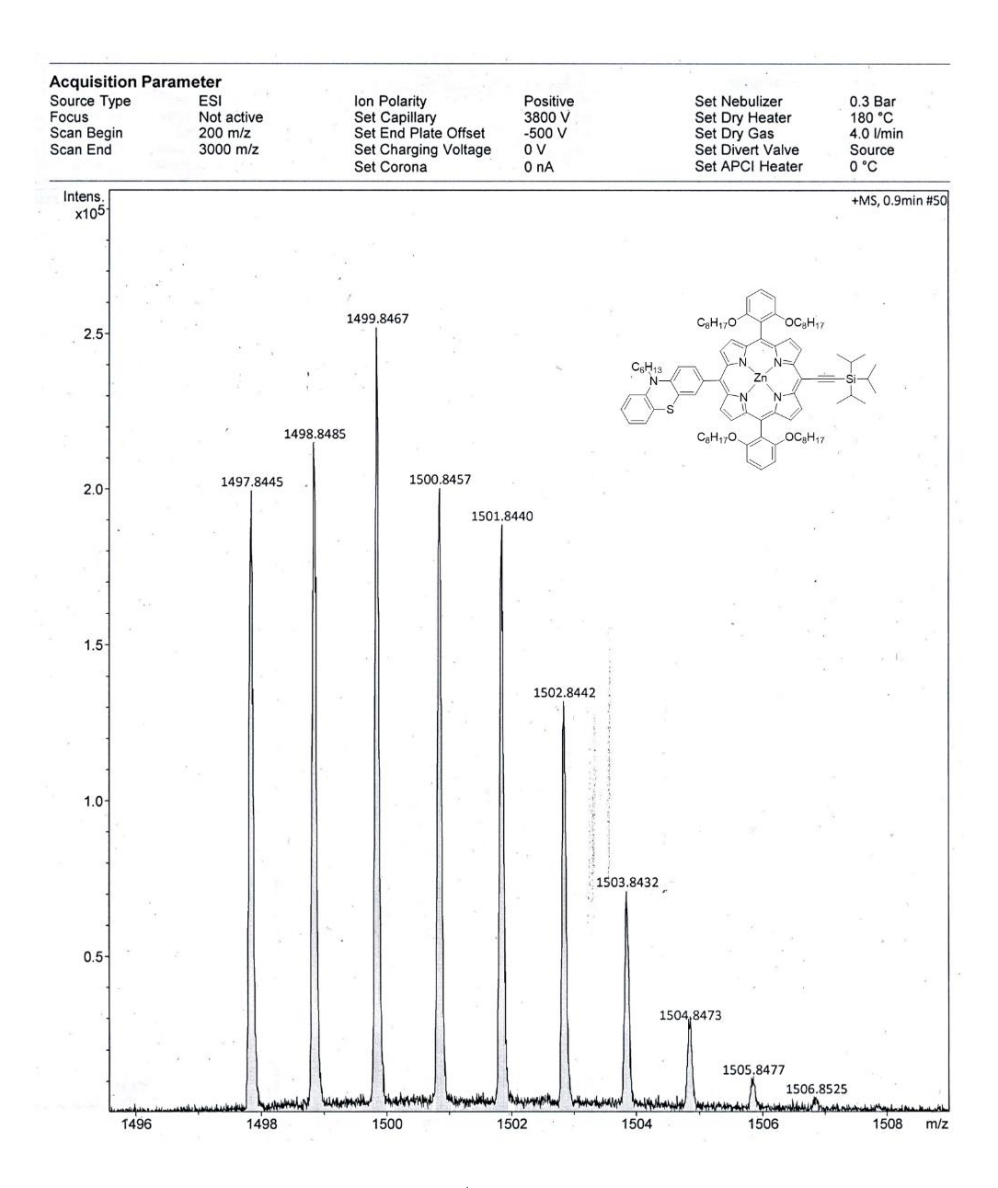


**Figure 4.25.** HRMS spectrum of **JB-4.2** [M+H]<sup>+</sup> C<sub>93</sub>H<sub>124</sub>N<sub>5</sub>O<sub>4</sub>SiZn 1499.8468, found 1499.8467.

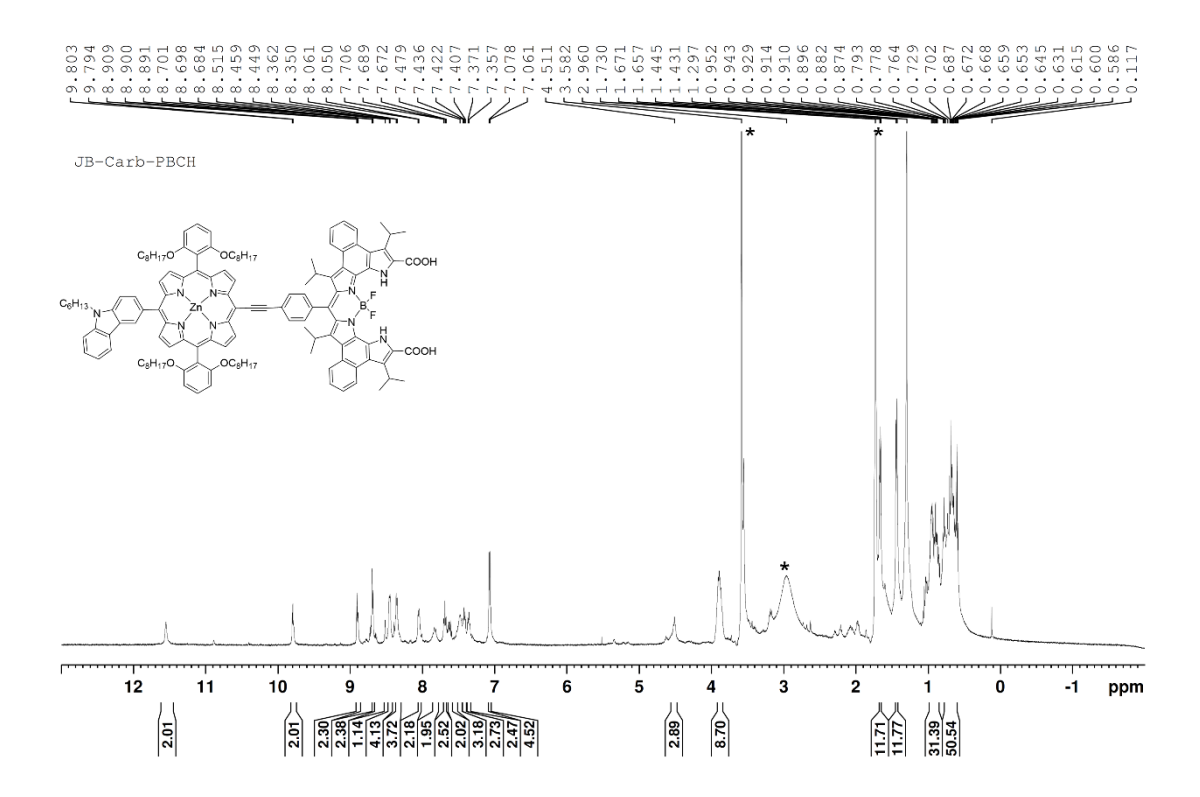


**Figure 4.26.** <sup>1</sup>H NMR spectrum of **JB-3** in THF- $d_8$  recorded at 25 °C (\*Asterisk indicates residual solvent impurity and water).

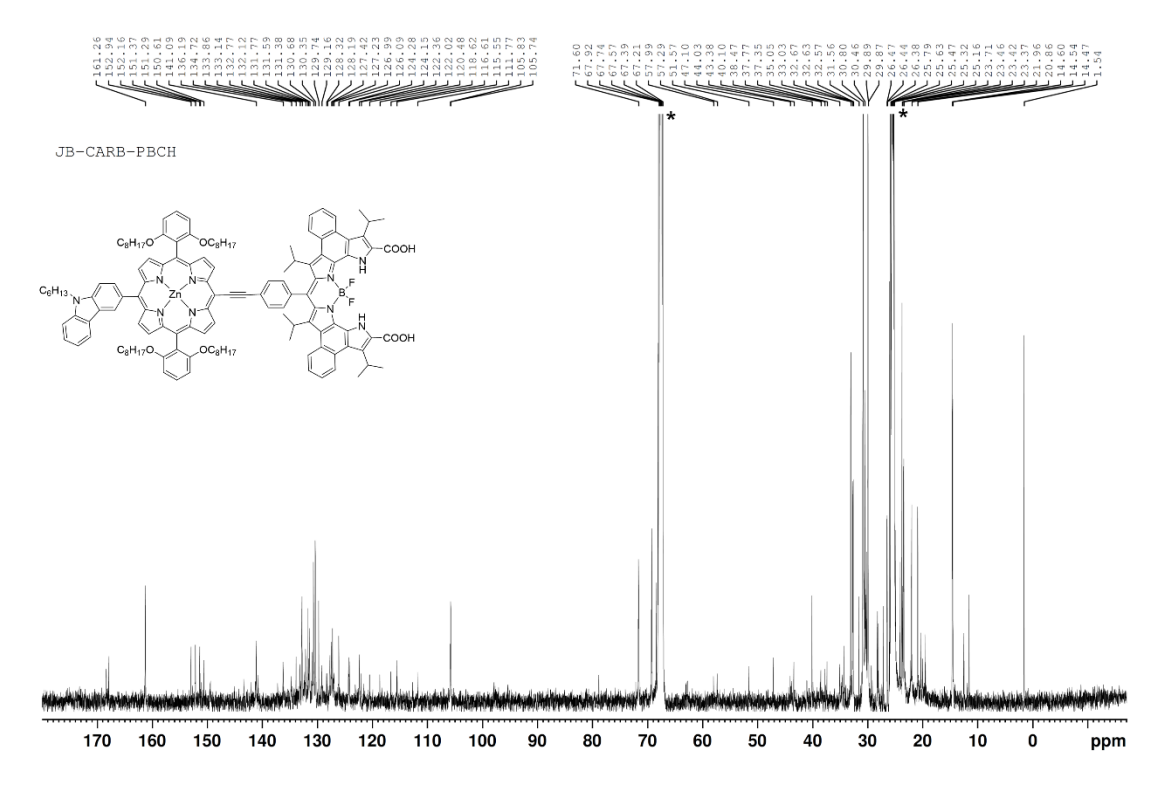


**Figure 4.27.** <sup>13</sup>C NMR spectrum of **JB-3** in THF-*d*<sub>8</sub> recorded at 25 °C (\*Asterisk indicates residual solvent impurity).

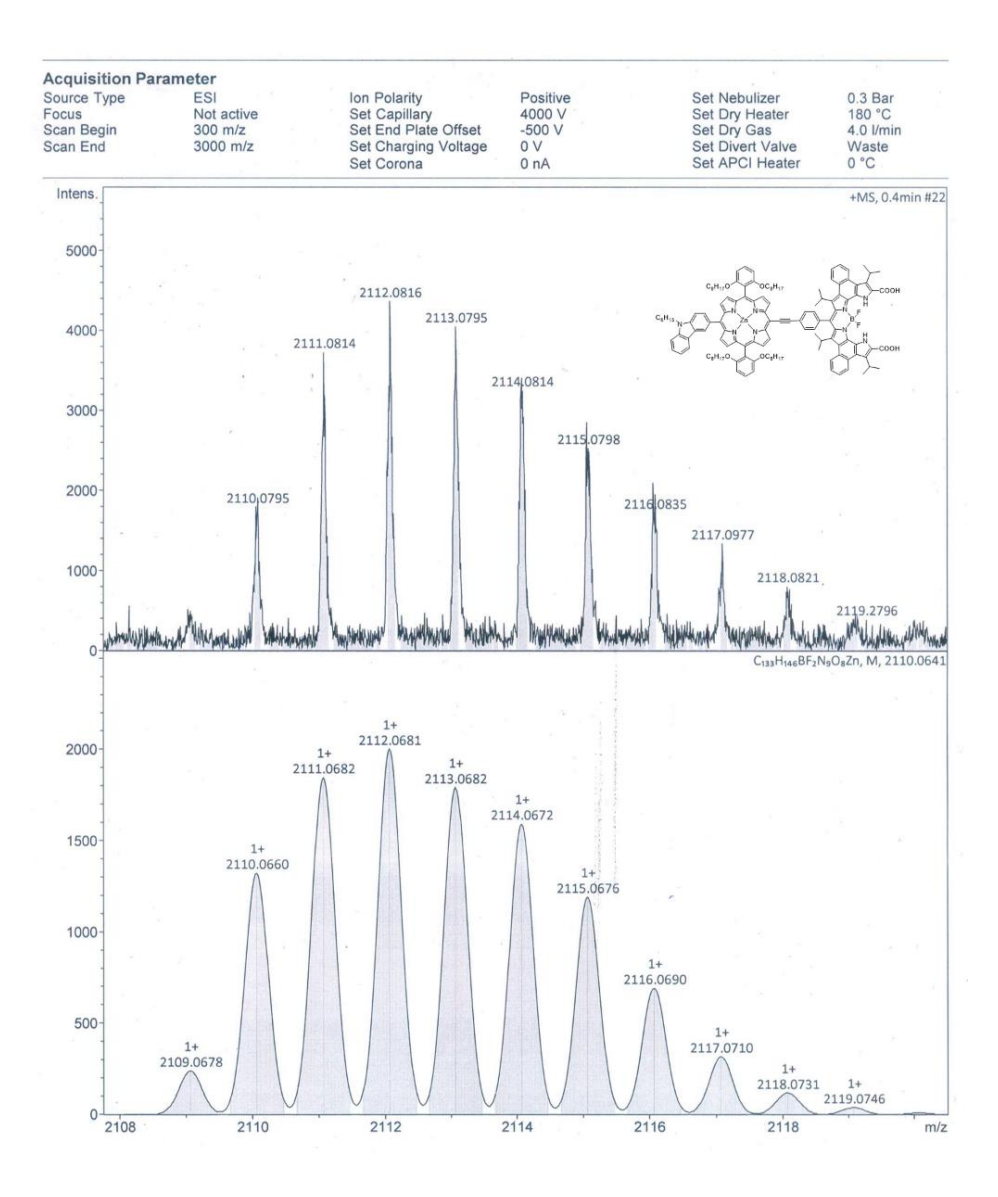


**Figure 4.28.** HRMS spectrum of **JB-3** [M+H] $^+$  C<sub>133</sub>H<sub>146</sub>BF<sub>2</sub>N<sub>9</sub>O<sub>8</sub>Zn 2113.0759, found 2113.0795.

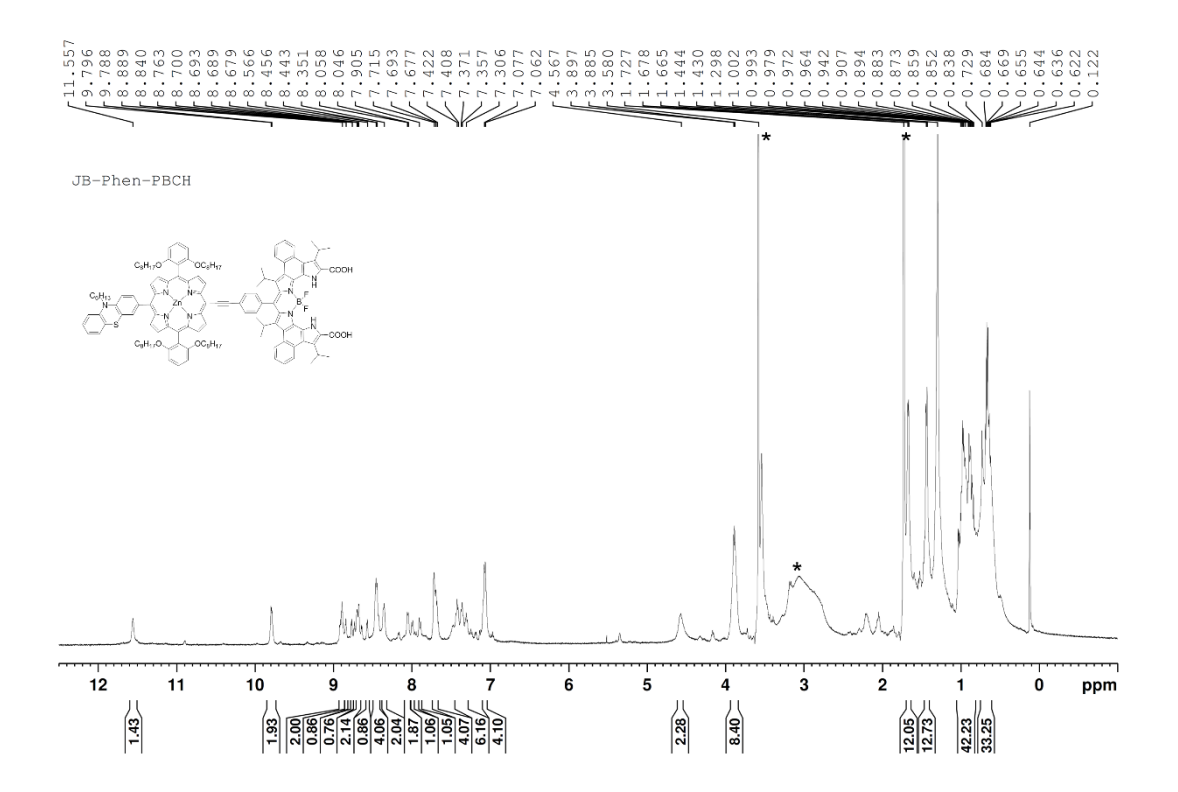


**Figure 4.29** <sup>1</sup>H NMR spectrum of **JB-4** in THF- $d_8$  recorded at 25 °C (\*Asterisk indicates residual solvent impurity and water).

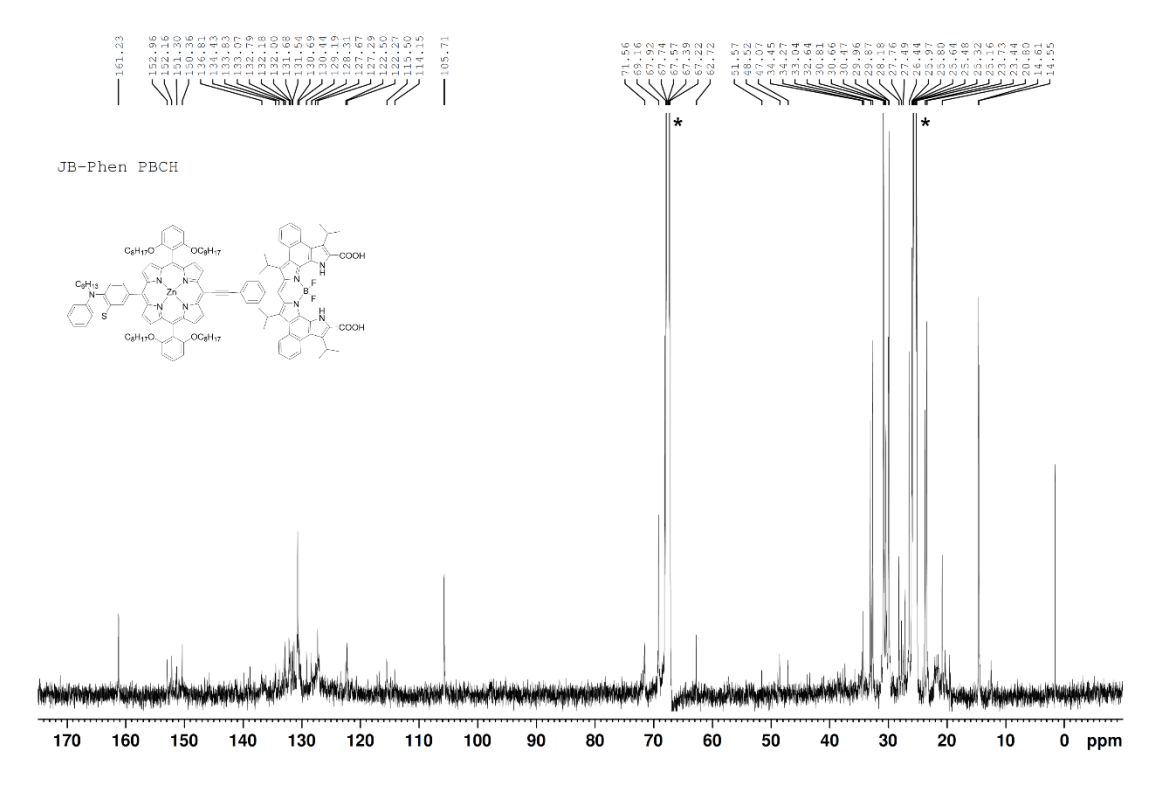


**Figure 4.30**  $^{13}$ C NMR spectrum of **JB-4** in THF- $d_8$  recorded at 25  $^{\circ}$ C (\*Asterisk indicates residual solvent impurity).

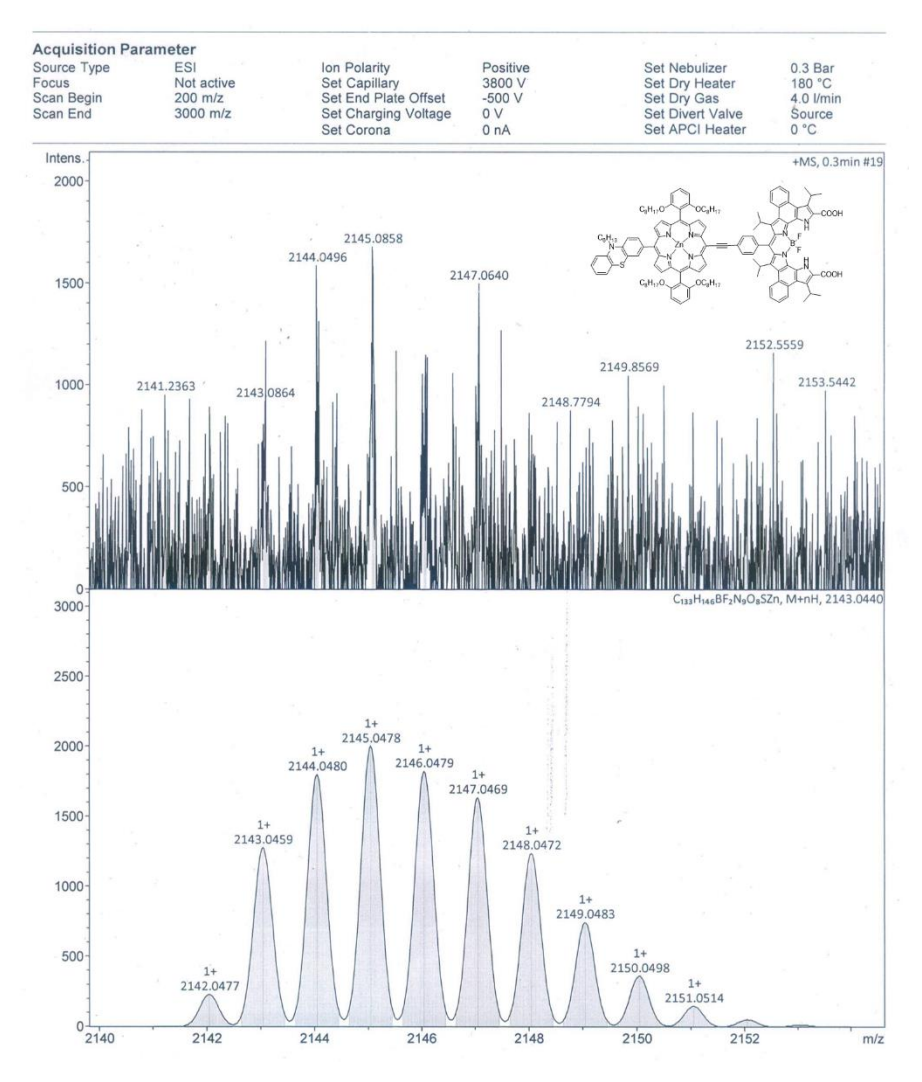


**Figure 4.3** HRMS spectrum of **JB-4**  $[M+H]^+$   $C_{133}H_{146}BF_2N_9O_8SZn$  2145.0477, found 2145.0496.

# 4.8 Computational Studies

Optimized coordinates of Porphyrin-BODIPY Conjugates JB-3 and JB-4.

Table 4.4 Coordinates of the optimized structure of JB-3.

Tag	Symbol	Х	Υ	Z
1	С	9.772929	1.695478	1.796085
2	С	8.795704	2.484815	2.321208
3	С	7.53623	1.968777	1.846368
4	N	7.753202	0.879254	1.036679
5	С	9.117975	0.695232	0.984978
6	С	8.878523	-3.11464	-1.82452
7	С	9.833768	-2.33596	-1.24553
8	С	9.145971	-1.32731	-0.47336
9	N	7.784362	-1.49558	-0.60146
10	С	7.60048	-2.58316	-1.42196
11	С	9.785568	-0.31993	0.273905

12	С	2.871871	-2.33866	-1.38473
13	С	3.845488	-3.12844	-1.91351
14	С	5.112016	-2.58054	-1.48764
15	N	4.894272	-1.46434	-0.70383
16	С	3.537224	-1.30336	-0.63242
17	С	6.360696	-3.10818	-1.83188
18	С	3.766705	2.564788	2.118469
19	С	2.815036	1.790326	1.530636
20	С	3.508953	0.746033	0.817419
21	N	4.861587	0.886687	0.970388
22	С	5.048363	1.998957	1.7676
23	С	6.281719	2.509444	2.185026
24	С	2.869214	-0.27326	0.072222
25	С	6.381804	-4.32245	-2.71262
26	С	6.267481	3.723188	3.066606
27	С	1.4494	-0.26066	0.02713
28	С	6.395253	-5.6141	-2.15471
29	С	6.41558	-6.75276	-2.97305
30	С	6.423066	-6.58985	-4.35656
31	С	6.41078	-5.32564	-4.94162
32	С	6.3903	-4.19374	-4.11391
33	С	6.324866	5.014699	2.510992
34	С	6.312201	6.15295	3.330033
35	С	6.242226	5.989833	4.711744
36	C	6.184845	4.725762	5.294448
37	C	6.19796	3.594265	4.466116
38	С	0.230608	-0.24832	-0.01225
39	С	-1.1874	-0.23211	-0.05906
40	C	-1.90148	-1.2221	-0.76926
41	C	-3.29167	-1.21876	-0.79291
42	C	-4.02343	-0.20899	-0.1485
43	C	-3.31237	0.798856	0.529196
44	С	-1.9254	0.777742	0.596921
45	C	-5.50652	-0.17361	-0.15145
46	C	-6.14388	0.948932	-0.74589
47	C	-6.28286	-1.1966	0.483497
48	N	-7.47634	1.209271	-0.40759
49	C	-7.83152	2.403024	-0.92977
50	C	-6.74653	2.961444	-1.66167
51	C	-5.70227	2.007594	-1.63746
52	С	-5.99014	-2.4023	1.233845
53	С	-7.2276	-3.09864	1.369253
54	С	-8.22189	-2.25586	0.8187
55	N	-7.6715	-1.13234	0.311438
56	C	-9.09494	3.030771	-0.93602
57	C	-9.34024	4.197019	-1.69218
58	С	-8.20959	4.884294	-2.318
59	С	-6.90659	4.274296	-2.316
	С		1	-2.28453
60	L	-8.32024	6.178953	-2.80405

61	С	-7.22583	6.857164	-3.38356
62	С	-5.95904	6.272132	-3.3339
63	С	-5.80867	5.011021	-2.77374
64	С	-7.64101	-4.35362	2.009257
65	С	-9.04612	-4.6283	2.199944
66	С	-10.041	-3.75532	1.576563
67	С	-9.59072	-2.59672	0.908493
68	С	-6.72124	-5.32474	2.461131
69	С	-7.11301	-6.4471	3.177937
70	С	-8.46139	-6.63329	3.484535
71	С	-9.40115	-5.73903	2.992746
72	N	-10.2643	2.622156	-0.3667
73	С	-11.2705	3.482496	-0.73485
74	С	-10.7471	4.463913	-1.59424
75	С	-11.473	-3.77841	1.430381
76	С	-11.81	-2.59595	0.733864
77	N	-10.6577	-1.93138	0.419633
78	С	-4.60851	2.004126	-2.70535
79	С	-3.19291	2.465596	-2.30613
80	С	-4.56666	0.680249	-3.49502
81	С	-4.75806	-2.8437	2.019289
82	С	-3.79994	-3.80042	1.276009
83	С	-3.98346	-1.73172	2.750524
84	С	-12.4131	-4.90897	1.820279
85	С	-13.2058	-4.62343	3.114592
86	С	-13.3088	-5.39146	0.65678
87	С	-11.5368	5.523977	-2.34299
88	С	-12.8387	4.993805	-2.97562
89	С	-11.8058	6.766223	-1.46845
90	В	-8.46821	0.132778	-0.00362
91	F	-9.37722	-0.09785	-1.06265
92	F	-9.23143	0.537023	1.116429
93	Zn	6.325802	-0.29784	0.174919
94	0	6.37832	-2.91222	-4.58009
95	С	6.387894	-2.69915	-5.98234
96	0	6.385678	-5.65894	-0.79141
97	С	6.39764	-6.92561	-0.15385
98	0	6.390342	5.059634	1.149381
99	С	6.451356	6.326206	0.514068
100	0	6.147398	2.312722	4.93027
101	С	6.077219	2.100051	6.330766
102	С	-12.6139	3.332607	-0.12614
103	0	-13.359	4.267306	0.080023
104	0	-12.969	2.091011	0.291394
105	С	-13.0179	-1.8408	0.338787
106	0	-12.9321	-0.82114	-0.32582
107	0	-14.2336	-2.26167	0.749355
108	Н	10.83927	1.773087	1.949014
109	H	8.90999	3.333883	2.979858
	1			

110	Н	9.019705	-3.96539	-2.47577
111	Н	10.90616	-2.42535	-1.33861
112	Н	1.800469	-2.43575	-1.48675
113	Н	3.727189	-4.00396	-2.5359
114	Н	3.6243	3.441225	2.734461
115	Н	1.741019	1.903191	1.568711
116	Н	6.425254	-7.74809	-2.54603
117	Н	6.438893	-7.46964	-4.99444
118	Н	6.417601	-5.22924	-6.0204
119	Н	6.355611	7.148162	2.904882
120	Н	6.232163	6.869352	5.35008
121	Н	6.131444	4.629303	6.371915
122	Н	-1.35113	-1.9978	-1.29255
123	Н	-3.82219	-1.99647	-1.3341
124	Н	-3.86346	1.587677	1.031891
125	Н	-1.39578	1.549497	1.1465
126	Н	-9.27543	6.684463	-2.84575
127	Н	-7.35675	7.85462	-3.79403
128	Н	-5.08792	6.807951	-3.70067
129	Н	-4.80956	4.607541	-2.67269
130	Н	-5.67255	-5.2159	2.229668
131	Н	-6.36552	-7.16371	3.506684
132	Н	-8.78219	-7.4772	4.08893
133	Н	-10.4391	-5.89761	3.251424
134	Н	-10.3148	1.885554	0.33029
135	Н	-10.6272	-1.10007	-0.16258
136	Н	-4.96823	2.742282	-3.42807
137	Н	-2.63413	2.736261	-3.21013
138	Н	-3.21728	3.343262	-1.65064
139	Н	-2.63297	1.683129	-1.79425
140	Н	-3.9174	0.801031	-4.3706
141	Н	-5.56472	0.403386	-3.85047
142	Н	-4.16992	-0.14583	-2.9024
143	Н	-5.19745	-3.43071	2.831388
144	Н	-3.14938	-4.30762	1.999036
145	Н	-4.34076	-4.56629	0.709816
146	Н	-3.15711	-3.26161	0.579002
147	Н	-3.38015	-2.18803	3.544586
148	Н	-4.66675	-1.01665	3.221239
149	Н	-3.3028	-1.18251	2.102053
150	Н	-11.7795	-5.7699	2.036984
151	Н	-13.8252	-5.48544	3.387598
152	Н	-12.5268	-4.4087	3.946706
153	Н	-13.8752	-3.75577	3.034253
154	Н	-13.8825	-6.27103	0.97073
155	Н	-12.6918	-5.67709	-0.20111
156	Н	-14.0251	-4.64556	0.299916
157	Н	-10.9119	5.830987	-3.18723
158	Н	-13.267	5.765369	-3.62642
· · · · · · · · · · · · · · · · · · ·	1	1		1

159	Н	-12.6456	4.106628	-3.58944
160	Н	-13.5859	4.74242	-2.22073
161	Н	-12.3155	7.541827	-2.05318
162	Н	-10.8741	7.191944	-1.07732
163	Н	-12.441	6.494242	-0.6214
164	Н	6.37606	-1.61622	-6.11712
165	Н	7.292005	-3.11279	-6.44812
166	Н	5.502138	-3.13419	-6.46367
167	Н	6.386697	-6.71787	0.917546
168	Н	5.512417	-7.51949	-0.41702
169	Н	7.302078	-7.4959	-0.40359
170	Н	7.347036	6.88625	0.813443
171	Н	6.496957	6.118479	-0.5564
172	Н	5.559605	6.92975	0.728587
173	Н	6.046709	1.017327	6.464509
174	Н	6.958422	2.504545	6.845927
175	Н	5.170807	2.544381	6.7626
176	Н	-12.5289	1.358331	-0.17998
177	Н	-14.1443	-3.02582	1.340233
178	С	15.64415	3.353409	-1.81282
179	С	16.86493	2.77647	-1.42306
180	С	16.90778	1.58577	-0.69993
181	С	15.69176	0.976532	-0.37694
182	С	14.44895	1.550511	-0.75645
183	С	14.43524	2.746625	-1.48216
184	Н	15.64596	4.282943	-2.37482
185	Н	17.79707	3.269135	-1.68631
186	Н	17.85808	1.156782	-0.39645
187	Н	13.49243	3.197124	-1.78151
188	С	14.08098	-0.39355	0.416159
189	С	13.36173	-1.41943	1.035981
190	С	11.97162	-1.37321	0.971938
191	С	11.28305	-0.32927	0.313998
192	С	12.01943	0.694407	-0.29317
193	С	13.41617	0.672386	-0.24655
194	Н	13.85886	-2.22731	1.564541
195	Н	11.39291	-2.15684	1.452107
196	Н	11.49837	1.499987	-0.80311
197	С	16.46754	-1.05388	0.904331
198	Н	16.10374	-2.08368	0.948682
199	Н	17.36489	-1.0421	0.279466
200	Н	16.73983	-0.73186	1.918497
201	N	15.45376	-0.20692	0.314949

Table 4.5. Coordinates of the optimized structure of JB-4.

	Tag	Symbol	Χ	Υ	Z
ſ	1	С	6.546714	-6.70304	-2.63772
Γ	2	С	7.862117	-7.1969	-2.75268

3	С	8.940036	-6.38932	-2.3785
4	С	8.75976	-5.06245	-1.90035
5	С	7.425403	-4.50981	-1.93413
6	С	6.342585	-5.37854	-2.24195
7	С	9.864718	-4.23418	-1.40095
8	С	9.618322	-2.87125	-1.04515
9	С	8.307486	-2.31689	-1.09766
10	С	7.221612	-3.09695	-1.60223
11	С	11.26654	-4.48768	-1.15941
12	С	11.82556	-3.24061	-0.76591
13	N	10.80671	-2.29607	-0.68259
14	N	7.856934	-1.05902	-0.78434
15	С	6.478232	-0.97489	-1.08685
16	С	6.091404	-2.22677	-1.71699
17	С	6.668768	6.987905	1.869249
18	С	7.993489	7.370282	2.153298
19	С	9.023633	6.440834	1.988653
20	С	8.783286	5.110095	1.557075
21	С	7.42348	4.720356	1.236419
22	С	6.405794	5.693255	1.412772
23	С	9.880089	4.157626	1.355538
24	С	9.58891	2.938148	0.6773
25	С	8.268932	2.52498	0.388571
26	С	7.149869	3.367951	0.703777
27	С	11.29395	4.139498	1.660701
28	С	11.79328	2.936288	1.089094
29	N	10.75124	2.25064	0.500821
30	N	7.845018	1.318376	-0.10709
31	С	6.429271	1.329611	-0.15051
32	С	5.977284	2.605925	0.402523
33	С	5.750434	0.190265	-0.67696
34	С	4.520889	2.952784	0.689682
35	С	12.10537	5.122858	2.494317
36	С	4.945807	-2.53082	-2.69039
37	С	13.1062	2.270152	1.027957
38	С	-0.01559	0.066448	-0.29924
39	С	-9.43096	-1.04123	2.880856
40	С	-8.37822	-1.49291	3.642222
41	С	-7.1549	-1.1687	2.925921
42	N	-7.47641	-0.52046	1.736284
43	С	-8.86767	-0.42471	1.685615
44	С	-8.95293	1.781644	-2.5586
45	С	-9.84604	1.356591	-1.60237
46	С	-9.07501	0.716162	-0.54349
47	N	-7.71952	0.772687	-0.87
48	С	-7.62181	1.418409	-2.09999
49	С	-9.6223	0.15454	0.636406
50	С	-2.85312	1.228214	-2.31878
51	С	-3.90285	1.679161	-3.08407
52	С	-5.1286	1.385453	-2.355
	l			

53	N	-4.80381	0.755084	-1.14978
54	С	-3.42144	0.651231	-1.10886
55	С	-6.4258	1.69805	-2.80206
56	С	-3.32263	-1.52088	3.162048
57	С	-2.43266	-1.08932	2.206904
58	С	-3.21342	-0.49805	1.129506
59	N	-4.56335	-0.57458	1.438008
60	С	-4.66042	-1.19971	2.685022
61	С	-5.85169	-1.481	3.379271
62	С	-2.6629	0.071774	-0.05292
63	С	-6.55173	2.392346	-4.12948
64	С	-5.73129	-2.16954	4.710092
65	С	-6.54184	3.803951	-4.21613
66	С	-6.65905	4.466048	-5.4587
67	С	-6.78736	3.699422	-6.6277
68	С	-6.80107	2.296383	-6.5803
69	С	-6.68321	1.653368	-5.32785
70	С	-5.7324	-3.5804	4.803314
71	С	-5.61965	-4.23572	6.049793
72	С	-5.50474	-3.46271	7.215977
73	С	-5.50055	-2.06003	7.162081
74	С	-5.6145	-1.42377	5.9059
75	0	-6.68641	0.267537	-5.17123
76	0	-6.40965	4.469996	-2.99867
77	0	-5.85263	-4.2533	3.588006
78	С	-1.23973	0.065722	-0.18801
79	С	11.95995	-5.84664	-1.18024
80	0	-5.62079	-0.03935	5.742143
81	С	-6.80239	-0.57774	-6.35103
82	С	-6.39183	5.92611	-2.98555
83	С	-5.86506	-5.70919	3.583221
84	С	-5.50577	0.813602	6.916886
85	Н	5.695945	-7.34085	-2.86313
86	Н	8.041767	-8.20669	-3.11274
87	Н	9.9363	-6.79466	-2.48078
88	Н	5.325124	-5.02549	-2.13781
89	Н	10.95102	-1.31282	-0.47079
90	Н	5.852128	7.695898	1.984455
91	Н	8.219965	8.381186	2.482221
92	Н	10.03934	6.765754	2.165163
93	Н	5.385982	5.445441	1.173121
94	Н	10.86784	1.373101	0.001712
95	Н	3.94104	2.050633	0.510148
96	Н	11.41746	5.876084	2.886079
97	Н	5.2921	-3.41531	-3.23342
98	Н	-10.4854	-1.12542	3.098468
99	Н	-8.42148	-2.00469	4.592805
100	Н	-9.16906	2.302886	-3.48006
101	Н	-10.9191	1.478717	-1.60256
102	Н	-1.79722	1.274695	-2.54204
	1	1	·	·

103	Н	-3.85916	2.163975	-4.04879
104	Н	-3.10225	-2.0087	4.10066
105	Н	-1.35475	-1.15813	2.220868
106	Н	-6.65126	5.548718	-5.51949
107	Н	-6.87803	4.20176	-7.58784
108	Н	-6.90144	1.724842	-7.49638
109	Н	-5.62115	-5.31798	6.115925
110	Н	-5.41751	-3.95979	8.179129
111	Н	-5.41085	-1.48347	8.076055
112	Н	11.1641	-6.59533	-1.19467
113	Н	-6.77304	-1.60083	-5.97133
114	Н	-7.75269	-0.40386	-6.87462
115	Н	-5.96359	-0.41524	-7.04203
116	Н	-6.28201	6.199014	-1.93437
117	Н	-5.54249	6.319507	-3.56117
118	Н	-7.33044	6.339748	-3.37944
119	Н	-5.96639	-5.98868	2.532893
120	Н	-4.92791	-6.1172	3.986265
121	Н	-6.71685	-6.10233	4.155036
122	Н	-5.53548	1.834123	6.530646
123	Н	-4.55521	0.643783	7.441319
124	Н	-6.34465	0.65462	7.608491
125	С	13.17439	-2.74099	-0.52825
126	В	8.6758	0.060043	-0.20699
127	F	9.860431	0.274778	-1.06888
128	F	9.238061	-0.30378	1.078769
129	Zn	-6.14185	0.10835	0.289091
130	С	12.82343	-6.05933	-2.45285
131	Н	13.6586	-5.35294	-2.47336
132	Н	13.23255	-7.07884	-2.46696
133	Н	12.22898	-5.91645	-3.36516
134	С	12.75277	-6.15262	0.118621
135	Н	13.63516	-5.51824	0.217913
136	Н	12.1175	-6.01575	1.003407
137	Н	13.0856	-7.19954	0.100929
138	С	4.819029	-1.44365	-3.79133
139	Н	4.451083	-0.49436	-3.40082
140	Н	5.787839	-1.26671	-4.27534
141	Н	4.11267	-1.78591	-4.55997
142	С	3.568177	-2.91533	-2.0906
143	Н	3.6751	-3.60928	-1.24691
144	Н	3.012447	-2.04603	-1.73815
145	Н	2.961016	-3.40911	-2.86191
146	С	3.924418	4.001896	-0.29445
147	Н	3.878329	3.580856	-1.30546
148	Н	2.900251	4.255238	0.009042
149	Н	4.500848	4.927465	-0.3634
150	С	4.270221	3.25597	2.196218
151	H	4.521502	2.372408	2.796741
152	H	4.848588	4.093283	2.59091
	<u> </u>	1.0.0000		

153         H         3.204912         3.47399         2.349636           154         C         13.17802         5.858726         1.646589           155         H         13.69366         6.610513         2.259474           156         H         13.92782         5.150913         1.277463           157         H         12.72506         6.368815         0.786104           158         C         12.73998         4.446407         3.740731           159         H         11.97529         3.939159         4.343301           160         H         13.50251         3.718278         3.451287           161         H         13.21883         5.209537         4.369649           162         O         13.4418         -1.5822         -0.12687	
155         H         13.69366         6.610513         2.259474           156         H         13.92782         5.150913         1.277463           157         H         12.72506         6.368815         0.786104           158         C         12.73998         4.446407         3.740731           159         H         11.97529         3.939159         4.343301           160         H         13.50251         3.718278         3.451287           161         H         13.21883         5.209537         4.369649           162         O         13.4418         -1.5822         -0.12687	
156       H       13.92782       5.150913       1.277463         157       H       12.72506       6.368815       0.786104         158       C       12.73998       4.446407       3.740731         159       H       11.97529       3.939159       4.343301         160       H       13.50251       3.718278       3.451287         161       H       13.21883       5.209537       4.369649         162       O       13.4418       -1.5822       -0.12687	
157         H         12.72506         6.368815         0.786104           158         C         12.73998         4.446407         3.740731           159         H         11.97529         3.939159         4.343301           160         H         13.50251         3.718278         3.451287           161         H         13.21883         5.209537         4.369649           162         O         13.4418         -1.5822         -0.12687	
158       C       12.73998       4.446407       3.740731         159       H       11.97529       3.939159       4.343301         160       H       13.50251       3.718278       3.451287         161       H       13.21883       5.209537       4.369649         162       O       13.4418       -1.5822       -0.12687	
159     H     11.97529     3.939159     4.343301       160     H     13.50251     3.718278     3.451287       161     H     13.21883     5.209537     4.369649       162     O     13.4418     -1.5822     -0.12687	
160     H     13.50251     3.718278     3.451287       161     H     13.21883     5.209537     4.369649       162     O     13.4418     -1.5822     -0.12687	
161     H     13.21883     5.209537     4.369649       162     O     13.4418     -1.5822     -0.12687	
162 O 13.4418 -1.5822 -0.12687	
163 O 14.20343 -3.62082 -0.83369	
164 O 12.95187 1.083109 0.328495	
165 O 14.1936 2.648863 1.503147	
166 H 15.06835 -3.1842 -0.65946	
167         H         13.6893         0.433698         0.340526	
168 C 3.623295 -0.59721 0.384553	
169 C 2.228172 -0.61365 0.508894	
170 C 1.407312 0.076896 -0.42343	
171 C 2.043889 0.785146 -1.47819	
172 C 3.440506 0.816925 -1.58057	
173 C 4.252995 0.129128 -0.65398	
174 H 4.234901 -1.13336 1.10515	
175 H 1.761619 -1.16305 1.321582	
176 H 1.434452 1.31828 -2.20214	
177 H 3.905444 1.391209 -2.37711	
178 C -11.1177 0.171546 0.787643	
179 C -11.9298 -0.60521 -0.06276	
180 C -13.3347 -0.62575 0.072628	
181 C -13.9375 0.171308 1.07263	
182 C -13.1396 0.979022 1.896095	
183 C -11.7384 0.972955 1.769898	
184 C -16.326 -0.50212 -0.25733	
185 C -15.4632 -1.22876 -1.1113	
186 C -15.9847 -1.75787 -2.3137	
187 H -15.3259 -2.31249 -2.98008	
188 C -17.3357 -1.57406 -2.65324	
189 C -18.1819 -0.83102 -1.8099	
190 C -17.6654 -0.28921 -0.61619	
191 H -11.462 -1.21617 -0.83242	
192 H -13.6104 1.605681 2.649349	
193 H -11.1318 1.595605 2.420678	
193     H     -11.1318     1.595605     2.420678       194     H     -17.7195     -1.9995     -3.57716       195     H     -19.2247     -0.6744     -2.0708	
193     H     -11.1318     1.595605     2.420678       194     H     -17.7195     -1.9995     -3.57716       195     H     -19.2247     -0.6744     -2.0708       196     H     -18.3103     0.286077     0.043579	
193       H       -11.1318       1.595605       2.420678         194       H       -17.7195       -1.9995       -3.57716         195       H       -19.2247       -0.6744       -2.0708         196       H       -18.3103       0.286077       0.043579         197       S       -15.7492       0.083849       1.393353	
193     H     -11.1318     1.595605     2.420678       194     H     -17.7195     -1.9995     -3.57716       195     H     -19.2247     -0.6744     -2.0708       196     H     -18.3103     0.286077     0.043579	

## **CHAPTER 5 Conclusion**

#### 5.1 Summary

The thesis entitled "Intense NIR Absorbing Porphyrin based Dyes with BODIPY as Acceptor: Potential Photosensitizers for Dye Sensitized Solar Cells" which consists of five chapters. The first chapter provides brief overview about the porphyrin, detailing its synthetic methodologies and applications specially emphasizing its role in Dye Sensitized Solar Cells. The second chapter deals with materials and methods employed during the course of the research work. Subsequently, there are two chapters, which provides detail information about the synthesis, photophysical properties, electrochemical aspects and DFT calculations of porphyrin-BODIPY conjugates. Finally, the current chapter provides overall summary of the research work carried out.

#### 5.1.1 Introduction

Dependence on solar energy, as the most available greener source of renewable energy, received much attention due to the fast diminishing of non-renewable energy sources. Though dominated by the devices comprising silicon-based materials for the long time, DSSC, first introduced by Grätzel et al., have shown promising features including ease of fabrication, low-cost production and wide tunability of the photosensitizers. In this aspect, porphyrins due to their intense absorption in the visible region, high molar extinction coefficients and tunable electrochemical properties have enriched their presence in DSSC, offering promising features of thin film generation. Even though a number of D-π-A based porphyrin dyes including **YD2-***o*-C8 and SM315, reported by Grätzel and coworkers reached an efficiency upto 13%, hut they lack significant absorption in the NIR region which contains significant flux of photons from sunlight. We have employed highly efficient NIR active naphthobipyrrole based BODIPY that our group had reported as an acceptor, in an effort to conquer the NIR region.

#### 5.1.2 Synthesis and characterization

As the porphyrin dyes with D- $\pi$ -A structure have shown higher efficiencies, we have opted for the hexyl/hexyloxy groups appended diarylamine/carbazole/phenothiazine moieties as donor because of their stronger electron donating capability and bisoctyloxyphenyl substituted porphyrin as the  $\pi$ -bridge. The BODIPY unit enacting as an acceptor was conjugated with this donor substituted porphyrin moiety to give novel porphyrin-BODIPY conjugates **JB1** - **JB4**. The synthesis of porphyrin-BODIPY conjugates achieved in two parts – a donor substituted porphyrin moiety and an acceptor located BODIPY unit. The donor substituted porphyrins can be further split into two, comprising the synthesis of ethyne linked bromodiarylporphyrin and different donors viz diarylamine, carbazole and phenothiazine. The condensation of

dipyromethane with 2,6-bisoctyloxybenzaldehyde, prepared as per the reported procedure<sup>3</sup>, yielded the diaryl porphyrin. It was subjected to bromination, ethynylation and further bromination in a sequence to yield the ethyne-linked bromodiarylporphyrin. The Buchwald-Hartwig coupling of 4-hexyloxy aniline and 4-hexyloxy bromobenzene yielded the diarylamine-donor which was further coupled with the substituted porphyrin to give the donor substituted porphyrin moieties. Similarly, carbazole and phenothiazine were initially substituted with hexyl chain on nitrogen followed by bromination and borylation, which was further coupled via Suzuki coupling with substituted porphyrin to yield the donor substituted porphyrins units.

The BODIPY diacid part was obtained from the hydrolysis of naphthobipyrrole-substituted BODIPY ester, which was in turn prepared from the corresponding dipyrromethane through oxidation and treatment with boron trifluoride etherate, where the dipyromethane was in turn synthesized from the condensation of naphthobipyrrole monoester with 4-iodobenzaldehyde. The BODIPY diacid was attached to the donor substituted porphyrin moieties via Sonogashira coupling, which then led to the formation of porphyrin-BODIPY conjugates **JB-1** - **JB-4** in good yields.

All the porphyrin-BODIPY conjugates were well characterized by their melting points, IR, NMR and mass spectral analysis.

#### 5.1.3 Photophysical properties

All the porphyrin-BODIPY conjugates displayed absorption well beyond 800 nm with an intense and broad Soret band and with an intensified and red shift of the Q-bands. The Soret band of **JB-1** and **JB-2** looks much broadened when compared to **YD2-o-C8**, while the same is not in case of **JB-3** and **JB-4** which displayed narrowed Soret bands compared to **YD2-o-C8**. The Q-bands appeared in the range of 670 to 750 nm with a huge red shift when compared to **YD2-o-C8** illustrating the effect of the naphthobipyrrole based BODIPY acceptor moiety. The comparative absorption spectra of porphyrin-BODIPY conjugates **JB-1 - JB-4** with **YD2-o-C8** were studied in THF solvent at room temperature as shown in **Figure 5.1**.

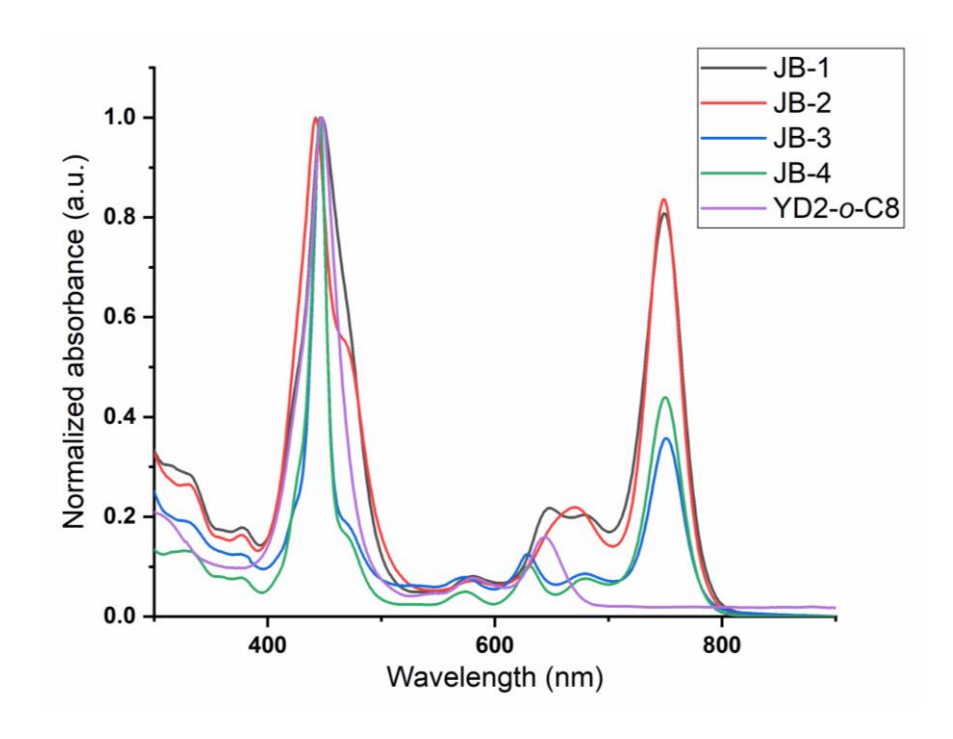


Figure 5.1 Absorption spectra of JB-1 - JB-4 in comparison with YD2-o-C8 in THF.

Further, a high molar extinction coefficient of around 1.9 lakh (Soret band) and with the last Q-bands coming almost 80% as intense as Soret band in case of **JB-1** and **JB-2**, and around 50% in case of **JB-3** and **JB-4**, along with a non-zero absorption in the entire range of 300-800 nm making them panchromatic with a significant absorption of photons in the NIR region of sunlight. These porphyrin-BODIPY conjugates displayed two emission peaks on excitation at their respective Soret bands as shown in **Figure 5.2**.

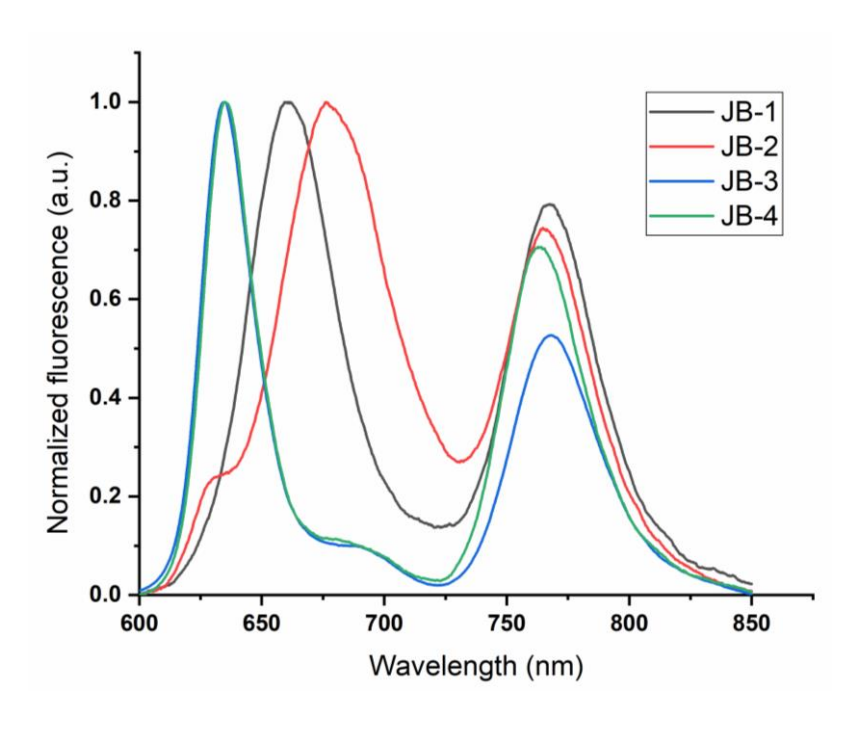


Figure 5.2. Fluorescence spectra of dyes JB-1 - JB-4 in THF.

#### **5.1.4 Electrochemical studies**

The electrochemical studies of porphyrin-BODIPY conjugates done using a silver chloride reference electrode revealed a quasi-reversible single electron oxidation for the formation of the porphyrin cation radical  $E_{Ox}$  level for **JB-1** and **JB-2** with values of 1.02 and +0.98 V (vs NHE), respectively, whereas **JB-3** and **JB-4** displayed two very close one electron quasi reversible oxidations with values of 1.08 and 1.09 V (vs NHE) (**Table 5.1**). The energy levels of HOMO and LUMO calculated according to the literature with the equations ( $E_{ox} = E_{HOMO}$  and  $E_{LUMO} = E_{0-0} - E_{HOMO}$ ) with respect to NHE electrode further indicate a facile dye regeneration and electron injection.

Table 5.1 The electrochemical data for JB-1-4.

Dye	E <sub>0-0</sub> in eV	Oxidation E <sub>ox</sub> (from DPV) vs. NHE in V	Reduction E <sub>Red</sub> (from DPV) vs. NHE in V	E <sub>LUMO</sub> =E <sub>0-0</sub> - E <sub>HOMO</sub> in V	E <sub>ec</sub> in V
JB-1	1.64	1.02	-0.4	-0.62	1.42
JB-2	1.64	0.98	-0.55	-0.66	1.53
JB-3	1.66	1.08	-0.41	-0.58	1.48
JB-4	1.64	1.09	-0.43	-0.55	1.52

#### 5.1.5 DFT calculations

The DFT studies clearly revealed that the porphyrin and BODIPY moieties are not in the same plane. To understand further insight, we performed TD-DFT calculations using Becke's three-parameter hybrid exchange functional and the Lee-Yang-Parr correlation functional (B3LYP) was used. LANL2DZ basis set was used for Zn and 6-31G basis set was used for all other atoms in calculations and the molecular orbitals were visualized using Gauss view 5. Electronic spectra were calculated using TD-DFT in THF solvent using PCM model. The result of TD-DFT was analyzed using GaussSum program. The TD-DFT studies revealed that the simulated absorption spectra were found to be very similar with the steady state absorption spectra with the vertical electronic transitions coincide well with the steady state absorption spectra. The frontier orbital diagrams with energy level diagram as shown in **Figure 5.3** revealed the significant contribution of substituted porphyrin as a donor since the electron density of HOMO

remained only on the donor substituted porphyrins in case of **JB-1** and **JB-2** and on only donor in case of **JB-3** and **JB-4**. The electron density of porphyrin is completely absent in case of LUMO, which was not observed in the case of previous reports of porphyrin dyes such as **YD2-** *o*-**C8** and **SM315**. Since the LUMO lies completely on the acceptor BODIPY unit, which may probably increase the electron injection efficiency.

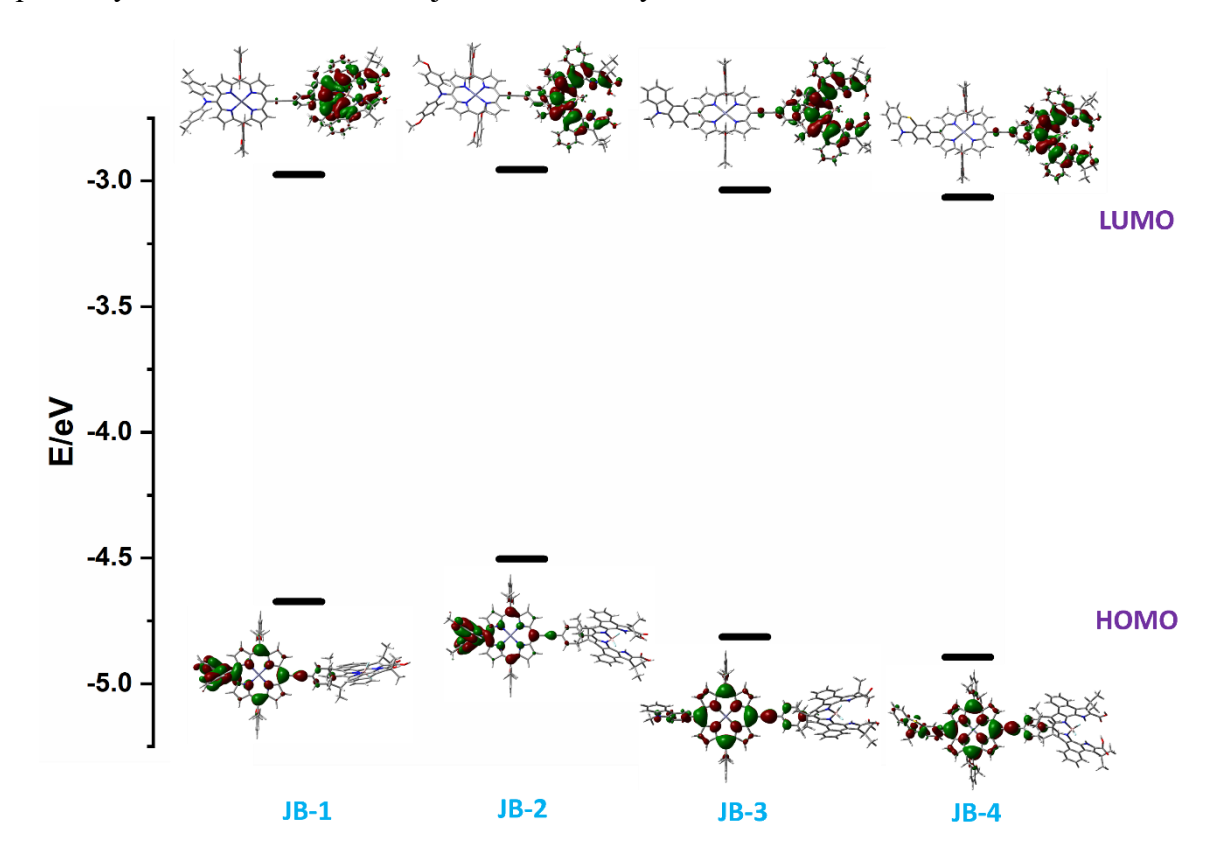


Figure 5.3. Frontier molecular orbitals with energy levels for JB-1-4.

Overall, we have synthesized four porphyrin-BODIPY conjugates **JB-1-4** with full characterization, which displayed a panchromatic absorption beyond 800 nm and well suited electrochemical potentials for their probable application in DSSC. Their possible application in solar cell application will be taken up in future.

#### **5.2 References**

- 1. O'Regan, B.; Grätzel, M. Nature 1991, 353, 737.
- 2. Urbani, M.; Grätzel, M.; Nazeeruddin, M. K., and Torres, T. *Chem. Rev.*, **2014**, 114, 12330.
- 3. Yella, A.; Lee, H.-W.; Tsao, H. N.; Yi, C.; Chandiran, A. K.; Nazeeruddin, M. K.; Diau, E. W.-G.; Yeh, C.-Y.; Grätzel, M. *Science*, **2011**, *334*, 629.
- 4. Mathew, S.; Yella, A.; Gao, P.; Humphry-Baker, R.; Curchod, B. F.; Ashari-Astani, N.; Tavernelli, I.; Rothlisberger, U.; Nazeeruddin, M. K.; Grätzel, M. *Nat. Chem.*, **2014**, 6, 242.
- 5. Sarma, T.; Panda, P. K.; Setsune, J.-i. Chem. Commun., 2013, 49, 9806.

#### **Research Publications (Thesis)**

- Bania, J.; Sahoo, S. S.; Kishore, M. V. N.; Panda, P. K. Porphyrin-BODIPY
  Conjugates as Photosensitizers with Absorption up to Near Infrared Region for DyeSensitized Solar Cells (DSSC). Indian Patent Application No.: 202341027215; April
  12, 2023.
- 7. Bania, J.; Sahoo, S. S.; Kishore, M. V. N.; Panda, P. K. Intense NIR Absorbing Porphyrin based Dyes with BODIPY as Acceptor. *New J. Chem.*, **2023**, *47*, 16327-16331.https://doi.org/10.1039/D3NJ02995F
- 8. Bania, J.; Sahoo, S. S.; Kishore, M. V. N.; Panda, P. K. Carbazole and Phenothiazine based Panchromatic Porphyrin-BODIPY Conjugates. (*Manuscript under preparation*).

#### **Conference presentations**

- Poster presentation on "A Panchromatic Porphyrin-BODIPY Conjugate for DSSC", CHEMFEST-2020, School of Chemistry, University of Hyderabad, Hyderabad, 27-28<sup>th</sup> February, 2020.
- Oral presentation on "A Novel Porphyrin-BODIPY Conjugate with Panchromatic Absorption for DSSC" in Virtual Conference Recent Advances in Bis and Tetra-Pyrrolic Molecular Materials, Department of Chemistry, Central University of Kerala, Kerala, 24-26<sup>th</sup> August, 2020.
- 3. Oral presentation on "Novel Porphyrin-Bodipy Conjugate with Panchromatic Absorption for Dye Sensitized Solar Cell Application", National Seminar on Recent Advances in Materials Chemistry (RAMC-2021), P. G. Department of Chemistry & Centre of Excellence in Advanced Materials and Applications, Utkal University, Bhubaneswar, 8-9<sup>th</sup> March, 2021.
- Oral presentation on "A Panchromatic Porphyrin-BODIPY Conjugate for DSC Application", CHEMFEST-2021, School of Chemistry, University of Hyderabad, Hyderabad, 19-20<sup>th</sup> March, 2021.
- Poster presentation on "A Novel Panchromatic Porphyrin-BODIPY Conjugate for DSC Application", 11th International Conference on Porphyrins and Phthalocyanines (ICPP-11) Virtual Meeting, 28 June to 3 July 2021.
- Poster presentation on "Novel Panchromatic Porphyrin BODIPY Conjugates for Application in Dye Sensitized Solar Cells", ACS CRSI poster session (online), 27th CRSI National Symposium Chemistry, Kolkata, 26-29<sup>th</sup> September, 2021.

# Intense NIR Absorbing Porphyrin based Dyes with BODIPY as Acceptor: Potential Photosensitizers for DyeSensitized Solar Cells

by Jyotsna Bania

Librarian

UNIVERSITY OF HYDERABAD Central University P.O.

HYDERABAD-500 046

Submission date: 12-Sep-2023 03:13PM (UTC+0530)

**Submission ID: 2163992305** 

File name: jb-submitted.pdf (465.34K)

Word count: 10793
Character count: 58795

Intense NIR Absorbing Porphyrin based Dyes with BODIPY as Acceptor: Potential Photosensitizers for Dye-Sensitized Solar Cells

**ORIGINALITY REPORT** 

28%

6%

27%

3%

SIMILARITY INDEX

**INTERNET SOURCES** 

**PUBLICATIONS** 

STUDENT PAPERS

**PRIMARY SOURCES** 

Jyotsna Bania, Sipra Sucharita Sahoo, Nanda Kishore M V, Pradeepta Panda. "Intense NIR Absorbing Porphyrin based Dyes with BODIPY as Acceptor", New Journal of Chemistry, 2023

15% fraction /223

Publication

Prof. Pradeepta K. Panda
School of Chemistry
University of Hyderabad
Hyderabad - 500 046.

Jyotsna Bania, Sipra S. Sahoo, M. V. Nanda Kishore, Pradeepta K. Panda. "Intense NIR absorbing porphyrin based dyes with BODIPY as the acceptor", New Journal of Chemistry, 2023

Publication

istina.ipmnet.ru

1 %

Anup Rana, Sipra Sucharita Sahoo, Pradeepta K. Panda. "β-Octaalkoxyporphyrins: Versatile fluorometric sensors towards nitrated explosives", Journal of Porphyrins and Phthalocyanines, 2019

1%

Publication

5	Maxence Urbani, Michael Grätzel, Mohammad Khaja Nazeeruddin, Tomás Torres. "Meso-Substituted Porphyrins for Dye- Sensitized Solar Cells", Chemical Reviews, 2014 Publication	1 %
6	Anders Hagfeldt, Gerrit Boschloo, Licheng Sun, Lars Kloo, Henrik Pettersson. "Dye- Sensitized Solar Cells", Chemical Reviews, 2010 Publication	1 %
7	Tamanna K. Khan, Martin Bröring, Sanjay Mathur, Mangalampalli Ravikanth. "Boron dipyrrin-porphyrin conjugates", Coordination Chemistry Reviews, 2013 Publication	1 %
8	Hafsah Klfout, Adam Stewart, Mahmoud Elkhalifa, Hongshan He. "BODIPYs for Dye- Sensitized Solar Cells", ACS Applied Materials & Interfaces, 2017 Publication	<1%
9	www.researchgate.net Internet Source	<1%
10	Yi Hu, Ajyal Alsaleh, Oanh Thi Phuong Trinh, Francis D'Souza, Hong Wang. "β- Functionalized Push-Pull Opp- Dibenzoporphyrins as Sensitizers for Dye-	<1%

### Sensitized Solar Cells: The Push Group Effect", Journal of Materials Chemistry A, 2021

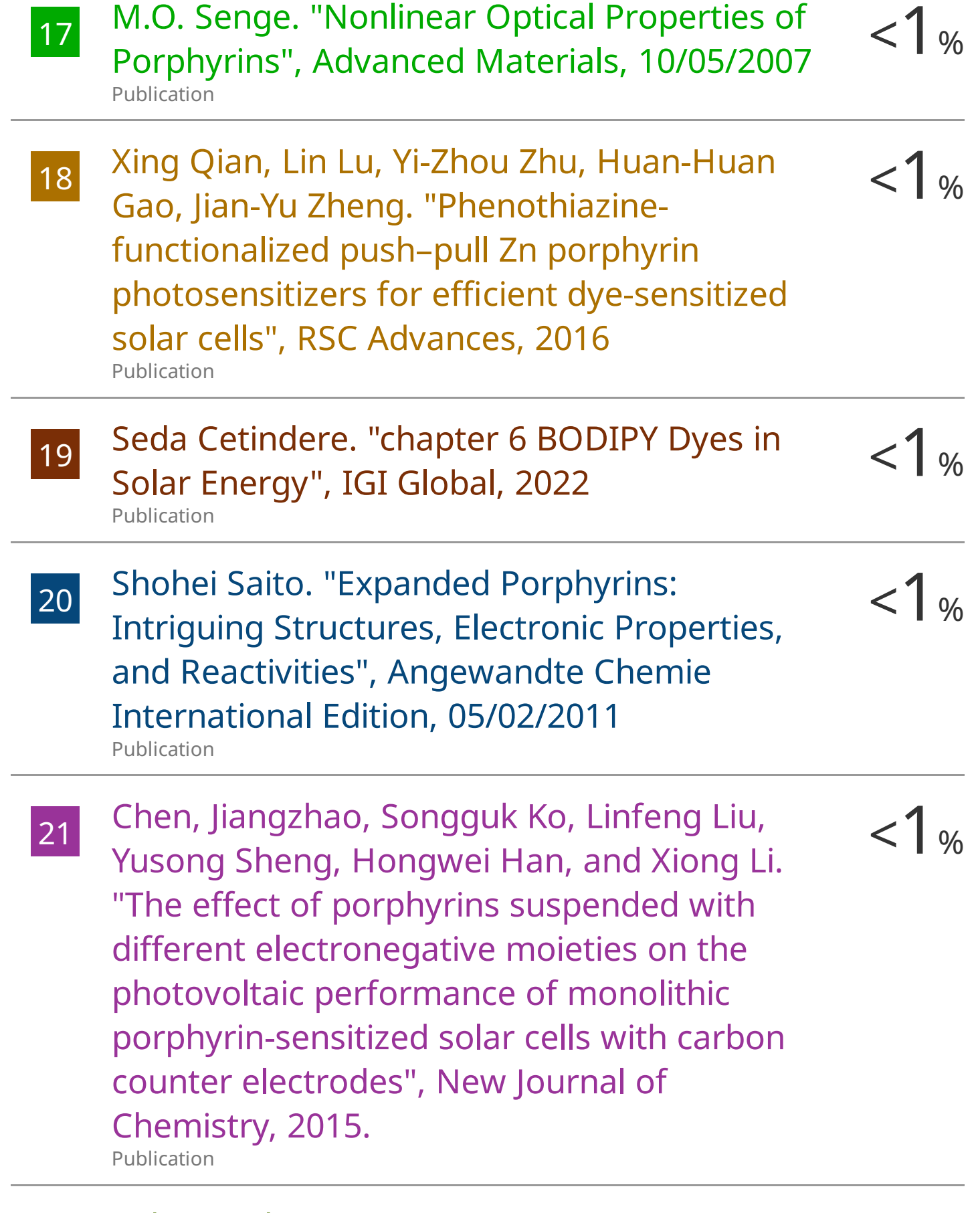
Publication

11	Rita Giovannetti. "Chapter 17 The Use of Spectrophotometry UV-Vis for the Study of Porphyrins", IntechOpen, 2012	<1%
12	repository.dl.itc.u-tokyo.ac.jp Internet Source	<1%
13	Submitted to University of Hyderabad, Hyderabad Student Paper	<1%
14	Singh, Surya Prakash, and Thumuganti Gayathri. "Evolution of BODIPY Dyes as Potential Sensitizers for Dye-Sensitized Solar Cells: Sensitizers for Dye-Sensitized Solar Cells", European Journal of Organic Chemistry, 2014.	<1%
15	Yi Hu, Ajyal Alsaleh, Oanh Trinh, Francis D'Souza, Hong Wang. " β-Functionalized push–pull -dibenzoporphyrins as sensitizers for dye-sensitized solar cells: the push group	<1%

www.freepatentsonline.com
Internet Source

effect ", Journal of Materials Chemistry A,

2021
Publication



23	pyridyl)methyliden]-@a(or @b)- aminonaphthalene: Single crystal X-ray structure of di-chloro-N-[{(2- pyridyl)methyliden}-@b- aminonaphthalene]palladium(II), Pd(@b- NaiPy)Cl"2, spectra and DFT, TD-DFT study", Polyhedron, 20070920 Publication	<1%
24	munin.uit.no Internet Source	<1%
25	"N4-Macrocyclic Metal Complexes", Springer Science and Business Media LLC, 2006 Publication	<1%
26	Narra Vamsi Krishna, Jonnadula Venkata Suman Krishna, Surya Prakash Singh, Lingamallu Giribabu et al. "Donor- $\pi$ -Acceptor Based Stable Porphyrin Sensitizers for Dye-Sensitized Solar Cells: Effect of $\pi$ -Conjugated Spacers", The Journal of Physical Chemistry C, 2017 Publication	<1%
	Susmita Das Tanay Dehnath Amrita Basu	1

Susmita Das, Tanay Debnath, Amrita Basu, Deepanwita Ghosh, Abhijit Kumar Das, Gary A. Baker, Amitava Patra. "Efficient White-Light Generation from Ionically Self-Assembled

<1%

#### Triply-Fluorescent Organic Nanoparticles", Chemistry – A European Journal, 2016

Publication

28	docksci.com Internet Source	<1%
29	www.mdpi.com Internet Source	<1%
30	Submitted to 7996 Student Paper	<1%
31	Submitted to National University of Singapore  Student Paper	<1%

Exclude quotes On Exclude bibliography On

Exclude matches < 14 words